

Conformational switching of a foldamer in a multi-component system by pH-filtered selection between competing non-covalent interactions

Julien Brioche,^a Sarah J. Pike,^a Sofja Tshepelevitsh,^b Ivo Leito,^b Gareth A. Morris,^a Simon J. Webb,^{a,c} and Jonathan Clayden^{a*}

^a School of Chemistry, University of Manchester. Oxford Rd., Manchester M13 9PL, UK; clayden@man.ac.uk

^b Institute of Chemistry, University of Tartu, Ravila 14a, Tartu 50411, Estonia

^c Manchester Institute of Biotechnology, University of Manchester, 131 Princess St., Manchester M1 7DN, UK

Supplementary Information

Table of Contents

General experimental method	S-3
Preparation of foldamers F2-F7, F5Me ⁺ and F6Me ⁺	S-4
Investigation of the HA-F interaction (Table 1)	S-14
Estimation of the helical excess	S-34
Titration studies of F with HA	S-40
Dilution studies for systems HA \leftrightarrow F	S-49
Influence of MeOH-d ₃ on HA4 \leftrightarrow F4 system	S-54
Influence of HCl on F4 in CDCl ₃ at 296 K	S-55
Estimation of the binding constants for the systems HA1 \leftrightarrow F4, HA4 \leftrightarrow F4 and HA6 \leftrightarrow F4	S-56
Estimation of relative pKa values of acids in 1,2-dichloroethane	S-64
VT ¹³ C NMR experiments of F4 with 0.5 equiv. of HA1 and F4 with 0.5 equiv. of HA4	S-66
Line shapes simulation of the ¹³ C NMR spectra	S-67
Switching induction ON and OFF experiments by the use of acid or base (Figure 4)	S-70
Absolute screw sense induction in F4* induced by (S)-HA1, (S)-HA4 and (S)-HA6 (Figure 5a-c)	S-72
Conformational switching experiments of foldamer F4* (Three-component system: Figure 6)	S-73
Conformational switching experiments of foldamer F4* (Four-component system: Figure 7)	S-75
Conformational switching experiments of foldamer F4* (Four-component system: Figure 8)	S-78
NMR spectra of new compounds	S-81

I. General experimental method

• All reactions were carried out in oven-dried glassware under an atmosphere of nitrogen using standard anhydrous techniques. All reagents were obtained from commercially available sources and used without further purification. Anhydrous dichloromethane was obtained by distillation from calcium hydride. Other anhydrous reaction solvents were obtained from standard anhydrous solvent engineering system. Flash column chromatography was carried out using Aldrich silica gel 60 Å, 230-400 Mesh. Thin layer chromatography (TLC) was performed using commercially available precoated plates (Macherey-Nagel, POLYGRAM®. SIL G/UV254) and visualized with UV light at 254 nm; phosphomolybdic acid dip was used to reveal the products. All products were dried on a rotary evaporator followed by connection to a high vacuum system to remove any residual solvent.

• All ^1H , ^{19}F and ^{13}C nuclear magnetic resonance spectra were obtained using Bruker Ultrashield 300, 400 or 500 MHz spectrometers. Chemical shifts (δ) are quoted in parts per million (ppm) and coupling constants (J) are quoted in Hz. ^1H -NMR were referenced to the residual deuterated solvent peak (CDCl_3 , 7.24 ppm and MeOH-d_4 (= CD_3OD), 3.31 ppm). ^{13}C -NMR were referenced to the carbon resonance of the solvent (CDCl_3 , 77.23; MeOH-d_4 , 49.15 ppm). Multiplicities are denoted as s (singlet), d (doublet), t (triplet), q (quartet), spt (septet) and m (multiplet) or denoted as br (broad), or some combination of these, where appropriate. Exchangeable protons (NH, OH) are reported only where observed. Infra-red spectra were recorded on a Thermo Scientific Nicolet iS5 FTIR Spectrometer. Only absorption maxima (λ max) of interest are reported and quoted in wavenumbers (cm^{-1}). Low and high resolution mass spectra were recorded by staff at the University of Manchester. Electrospray (ES) spectra were recorded on a Waters Platform II and high resolution mass spectra (HRMS) were recorded on a Thermo Finnigan MAT95XP and are accurate to ± 0.001 Da. Melting points were determined on a Gallenkamp apparatus and are uncorrected. Optical rotation measurements were taken on an AA-100 polarimeter at $+20$ °C with the solvent and concentration stated.

• The following abbreviations have been used: Aib = aminoisobutyric acid, DIPEA = N,N-diisopropylethylamine, EDC·HCl = N-(3-dimethylaminopropyl)-1N'-ethylcarbodiimide, EtOAc = Ethyl acetate, HOBT = 1-hydroxybenzotriazole, MeOH = Methanol, TRIPHAT = [Tetrabutylammonium] [Δ -tris(tetrachloro-1,2-benzenediolato)phosphate(V)]; BINPHAT = [Tetrabutylammonium][[(Λ ,R)-(1,1'-binaphthalene-2,2'-diolato)(bis(tetrachloro-1,2-benzenediolato)phosphat(V))].

$\text{N}_3\text{Aib}_4\text{O}^t\text{Bu}$,¹ $\text{N}_3\text{Aib}_4\text{OH}$,¹ $\text{H}_2\text{NAib}_4\text{O}^t\text{Bu}$,¹ 2-amino-1,1-di(3-fluorophenyl)ethanol,² $\text{N}_3\text{Aib}_4\text{Aib}^{**}\text{OMe}$ (**F0**),³ $\text{H}_2\text{NAib}_4\text{Aib}^{**}\text{OMe}$ (**F1**),³ Z-L(α Me)ValOH⁴ and N-triflyl phosphoramidate **HA6**⁵ were prepared according previously reported procedures.

NB: Phosphoric acids **HA2-5** (purchased from Aldrich) and N-triflyl phosphoramidate **HA6** were dissolved in CH_2Cl_2 , washed with an aqueous solution of HCl (2 N), water, dried over NaSO_4 and evaporated to dryness prior their use in all the experiments described in this study.

[1] Clayden, J.; Castellanos, A.; Solà, J.; Morris G. A. *Angew. Chem. Int. Ed.* **2009**, *48*, 5962–5965.

[2] Pike, S. J.; De Poli, M.; Zawodny, W.; Raftery, J.; Webb, S. J.; Clayden, J. *Org. Biomol. Chem.* **2013**, *11*, 3168–3176.

[3] Solà, J.; Fletcher, S. P.; Castellanos, A.; Clayden, J. *Angew. Chem. Int. Ed.* **2010**, *49*, 6836–6839.

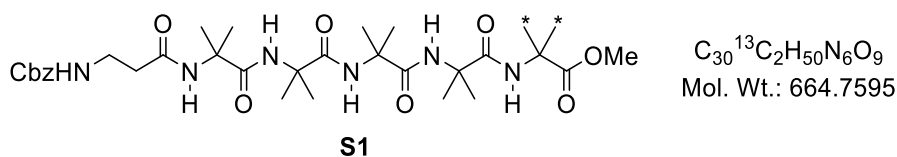
[4] Pengo, P.; Broxterman, Q. B.; Kaptein, B.; Pasquato, L.; Scrimin, P. *Langmuir* **2003**, *19*, 2521–2524.

[5] Rueping, M.; Nachtsheim, B. J.; Koenigs, R. M.; Ieawsuwan, W. *Chem. Eur. J.* **2010**, *16*, 13116–13126.

II. Preparation of foldamers F2-F7, F5Me⁺ and F6Me⁺

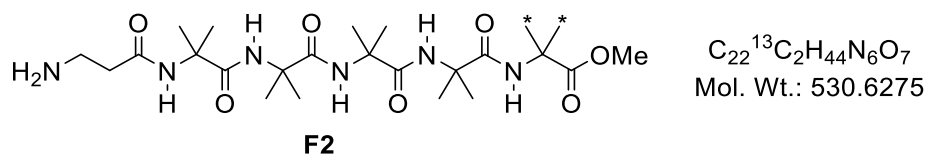
• Synthesis of foldamer F2

Step 1: Z-β-Ala-Aib₄Aib**OMe (S1)



To a solution Z-β-Ala-OH (64 mg, 0.30 mmol) in CH₂Cl₂ (2 mL) at 0 °C were added successively 1-Hydroxybenzotriazole hydrate (41 mg, 0.30 mmol) and EDC-HCL (58 mg, 0.30 mmol). The cold bath was removed and the reaction mixture was stirred for a further 45 min. After this time, DIPEA (160 μL, 0.90 mmol) and H₂NAib₄Aib**OMe **F1** (70 mg, 0.15 mmol) were added to the reaction mixture. After 12 h stirring at RT, the reaction was diluted with CH₂Cl₂ and water. The layers were separated and the organic phase was washed two times with a saturated solution of NaHCO₃, brine, dried over MgSO₄, filtered and concentrated under reduced pressure. The crude residue was purified by flash chromatography on silica gel (gradient starting from 98:2 to 90:10 / CH₂Cl₂:MeOH) to give **S1** (72 mg, 72%) as a white solid; **M.p.** = 247-248 °C; **¹H NMR (400 MHz, CDCl₃ + 2% MeOH-d₃)** δ 7.64 (s, 1H, NH), 7.45 (s, 1H, NH), 7.43 (s, 1H, NH), 7.34-7.26 (m, 6H, 5^{Ar}CH and NH), 6.99 (s, 1H, NH), 5.84 (br s, 1H, NH), 5.04 (s, 2H, -OCH₂Ph), 3.62 (s, 3H, OCH₃), 3.47-3.37 (m, 2H, CbzHNCH₂-), 2.45-2.38 (m, 2H, CbzNCH₂CH₂-), 1.48 (dd, 6H, ¹J_{C-H} = 129.1 and ³J_{C-H} = 4.1 Hz, 2*¹³CH₃), 1.44 (s, 6H, 2*CH₃), 1.40 (s, 6H, 2*CH₃), 1.36 (s, 6H, 2*CH₃), 1.35 (s, 6H, 2*CH₃); **¹³C NMR (100 MHz, CDCl₃ + 2% MeOH-d₃)** (C(¹³CH₃)₂ signal is not observed), δ 175.9 (CO), 175.4 (CO), 175.0 (CO), 174.7 (CO), 174.3 (CO), 172.5 (CO), 157.2 (CO), 136.3 (C), 128.7 (2*CH), 128.5 (CH), 128.3, (2*CH), 67.1 (CH₂), 57.0 (C), 56.9 (C), 56.8 (C), 56.7 (C), 52.2 (OCH₃), 37.7 (CH₂), 36.9 (CH₂), 25.7-24.2 (8*CH₃ and 2*¹³CH₃); **FTIR (ν_{max} cm⁻¹)**. 3280, 2944, 2934, 1727, 1651, 1537, 1455, 1435, 1383, 1361, 1264, 1234, 1147. **HRMS** calcd for C₃₀¹³C₂H₅₀N₆O₉Na [M+Na]⁺: 687.3604. Found 687.3572.

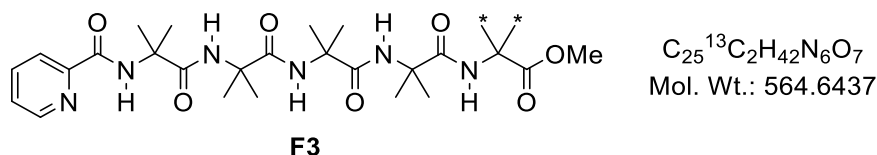
Step 2: β-Ala-Aib₄Aib**OMe (F2)



To a solution of Z-β-Ala-Aib₄Aib**OMe **S1** (55 mg, 0.08 mmol) in MeOH (15 mL) at RT and under inert atmosphere was added Pd/C (6.0 mg, 0.006 mmol, 10 Wt%). The atmosphere was purged with hydrogen and the reaction was stirred for 12 h under hydrogen (1 atm). After this time, the reaction was filtered through a Celite (MeOH) and the filtrate was concentrated under reduced pressure. The crude residue was dissolved in CH₂Cl₂, washed with aqueous saturated solution of NaHCO₃, brine, dried over MgSO₄, filtered and concentrated under reduced pressure to give **F2** (30 mg, 70%) as a white solid; **M.p.** = 194-195 °C; **¹H NMR (400 MHz, CDCl₃)** δ 7.91 (s, 1H, NH), 7.87 (s, 1H, NH), 7.73 (s, 1H, NH), 7.52 (s, 1H, NH), 7.49 (s, 1H, NH), 3.65 (s, 3H, OCH₃), 3.05 (br s, 1H, H₂NCH₂-), 2.39 (br s, 1H, H₂NCH₂-), 2.12 (br s, 4H, H₂NCH₂CH₂- and

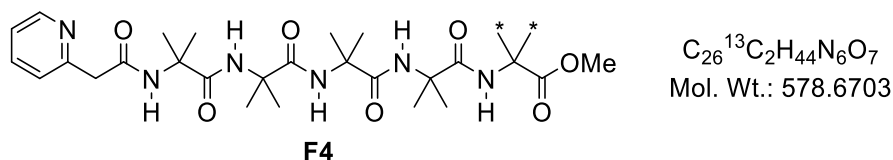
NH_2), 1.49 (br d, 6H, $^1J_{C-H} = 129.2$ Hz, $2*^{13}CH_3$), 1.47 (s, 6H, $2*CH_3$), 1.43 (s, 9H, $3*CH_3$), 1.38 (s, 6H, $2*CH_3$), 1.22 (br s, 3H, CH_3); ^{13}C NMR (100 MHz, $CDCl_3$) δ 175.9 (CO), 175.5 (CO), 175.4 (CO), 175.0 (CO), 174.7 (CO), 173.8 (CO), 57.05 (C), 56.96 (2C), 56.7 (C), 55.9 (t, $C(^{13}CH_3)_2$, $J_{C-C} = 36.6$ Hz), 52.3 (OCH₃), 39.1 (CH₂), 38.3 (CH₂), 25.7-24.5 ($8*CH_3$ and $2*^{13}CH_3$); FTIR (ν_{max} cm^{-1}). 3289, 2983, 2925, 1731, 1644, 1532, 1455, 1435, 1382, 1360, 1304, 1263, 1224, 1147. HRMS calcd for $C_{22}^{13}C_2H_{44}N_6O_7Na$ [M+Na]⁺: 553.3236. Found 553.3246.

• Synthesis of foldamer 2-Pyridine-Aib₄Aib**OMe (F3)



To a solution of $H_2NAib_4Aib^{**}OMe$ **F1** (25 mg, 0.05 mmol) and 2-picolinic acid (13 mg, 0.11 mmol) in CH_2Cl_2 (0.5 mL) at RT were added successively DIPEA (40 μ L, 0.22 mmol), 1-Hydroxybenzotriazole hydrate (15 mg, 0.11 mmol) and EDC-HCl (21 mg, 0.11 mmol). After 12 h stirring at RT, the reaction was diluted with CH_2Cl_2 and water. The layers were separated and the organic phase was washed two times with a saturated solution of $NaHCO_3$, brine, dried over $MgSO_4$ and concentrated under reduced pressure. The crude residue was purified by flash chromatography on silica gel (gradient starting from 98:2 to 95:5 / CH_2Cl_2 :MeOH). The purified product was dissolved in CH_2Cl_2 , washed with aqueous saturated solution of $NaHCO_3$, brine, dried over $MgSO_4$, filtered and concentrated under reduced pressure to give **F3** (24 mg, 85%) as a white solid; **M.p.** = 241-242 °C; 1H NMR (400 MHz, $CDCl_3$) δ 8.69 (br d, 1H, $J = 4.9$ Hz, ^{Ar}CH), 8.41 (s, 1H, NH), 8.20 (br d, 1H, $J = 7.8$ Hz, ^{Ar}CH), 7.99 (ddd, apparent td, 1H, $J = 7.8$ and 1.6 Hz, ^{Ar}CH), 7.69 (s, 1H, NH), 7.62 (br dd, 1H, $J = 7.8$ and 4.9 Hz, ^{Ar}CH), 7.37 (s, 1H, NH), 7.28 (s, 1H, NH), 6.43 (s, 1H, NH), 3.63 (s, 3H, OCH₃), 1.58 (s, 6H, $2*CH_3$), 1.49 (s, 6H, $2*CH_3$), 1.48 (dd, 6H, $^1J_{C-H} = 129.2$ and $^3J_{C-H} = 4.3$ Hz, $2*^{13}CH_3$), 1.45 (s, 6H, $2*CH_3$), 1.39 (s, 6H, $2*CH_3$); ^{13}C NMR (100 MHz, $CDCl_3$) δ 175.7 (CO), 174.8 (CO), 174.2 (CO), 173.9 (CO), 173.6 (CO), 165.0 (CO), 148.7 (C), 148.7 (CH), 138.1 (CH), 127.4 (CH), 122.5 (CH), 57.2 (C), 57.1 (C), 57.0 (C), 56.8 (C), 55.8 (t, $C(^{13}CH_3)_2$, $J_{C-C} = 36.6$ Hz), 52.1 (OCH₃), 25.7-24.6 ($8*CH_3$ and $2*^{13}CH_3$); FTIR (ν_{max} cm^{-1}). 3303, 2986, 2945, 1738, 1652, 1527, 1463, 1455, 1434, 1384, 1224. HRMS calcd for $C_{25}^{13}C_2H_{43}N_6O_7$ [M+H]⁺: 565.3255. Found 565.3247.

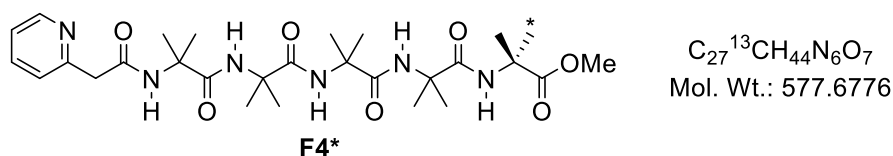
• Synthesis of foldamer 2-Pyridine-CH₂-Aib₄Aib**OMe (F4)



To a solution of $H_2N-Aib_4Aib^{**}OMe$ **F1** (100 mg, 0.22 mmol) and 2-pyridylacetic acid hydrochloride (76 mg, 0.44 mmol) in CH_2Cl_2 (2 mL) at RT were added successively DIPEA (230 μ L, 1.31 mmol), 1-Hydroxybenzotriazole hydrate (59 mg, 0.44 mmol) and EDC-HCl (83 mg, 0.44 mmol). After 12 h stirring at RT, the reaction was diluted with CH_2Cl_2 and water. The layers were separated and the organic phase was

washed two times with a saturated solution of NaHCO₃, brine, dried over MgSO₄ and concentrated under reduced pressure. The crude residue was purified by flash chromatography on silica gel (gradient starting from 98:2 to 95:5 / CH₂Cl₂:MeOH). The purified product was dissolved in CH₂Cl₂, washed with aqueous saturated solution of NaHCO₃, brine, dried over MgSO₄, filtered and concentrated under reduced pressure to give **F4** (95 mg, 75%) as a white solid; **M.p.** = 261-262 °C; **¹H NMR (400 MHz, CDCl₃)** δ 8.47 (br d, 1H, *J* = 4.3 Hz, ^{Ar}CH), 7.67 (ddd, apparent td, 1H, *J* = 7.7 and 1.5 Hz, ^{Ar}CH), 7.41 (s, 1H, NH), 7.34 (s, 1H, NH), 7.27-7.16 (m, 4H, 2*^{Ar}CH and 2*NH), 7.11 (s, 1H, NH), 3.73 (s, 2H, CH₂), 3.60 (s, 3H, OCH₃), 1.48 (dd, 6H, ¹J_{C-H} = 128.9 and ³J_{C-H} = 4.1 Hz, 2*¹³CH₃), 1.43 (s, 6H, 2*CH₃), 1.41 (s, 6H, 2*CH₃), 1.33 (s, 12H, 4*CH₃); **¹³C NMR (100 MHz, CDCl₃)** (C(¹³CH₃)₂ signal is not observed) δ 175.8 (CO), 174.9 (CO), 174.4 (CO), 173.9 (CO), 173.8 (CO), 170.1 (CO), 155.5 (C), 149.2 (CH), 137.8 (CH), 124.6 (CH), 122.8 (CH), 57.4 (C), 57.1 (C), 56.9 (C), 56.8 (C), 52.2 (OCH₃), 45.4 (CH₂), 25.8-24.5 (8*CH₃ and 2*¹³CH₃); **FTIR (ν_{max} cm⁻¹)** 3282, 2984, 2941, 1732, 1667, 1641, 1537, 1463, 1435, 1381, 1221. **HRMS** calcd for C₂₆¹³C₂H₄₅N₆O₇ [M+H]⁺: 579.3411. Found 579.3399.

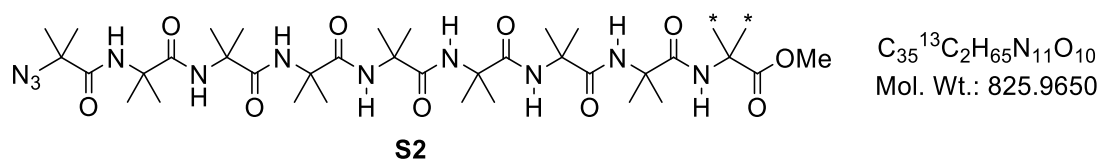
• **Synthesis of 2-Pyridine-CH₂-Aib₄Aib*OMe (F4*)**



To a solution of H₂NAib₄Aib*OMe **F1** (50 mg, 0.11 mmol) and 2-pyridylacetic acid hydrochloride (38 mg, 0.22 mmol) in CH₂Cl₂ (1 mL) at RT were added successively DIPEA (115 μL, 0.65 mmol), 1-Hydroxybenzotriazole hydrate (29 mg, 0.22 mmol) and EDC·HCl (42 mg, 0.22 mmol). After 12 h stirring at RT, the reaction was diluted with CH₂Cl₂ and water. The layers were separated and the organic phase was washed two times with a saturated solution of NaHCO₃, brine, dried over MgSO₄ and concentrated under reduced pressure. The crude residue was purified by flash chromatography on silica gel (gradient starting from 98:2 to 95:5 / CH₂Cl₂:MeOH). The purified product was dissolved in CH₂Cl₂, washed with aqueous saturated solution of NaHCO₃, brine, dried over MgSO₄, filtered and concentrated under reduced pressure to give **F4*** (42 mg, 67%) as a white solid; **M.p.** = 261-262 °C; **¹H NMR (400 MHz, CDCl₃)** δ 8.51 (br dd, 1H, *J* = 4.9 and 2.3 Hz, ^{Ar}CH), 7.71 (ddd, apparent td, 1H, *J* = 7.7 and 1.9 Hz, ^{Ar}CH), 7.46 (s, 1H, NH), 7.39 (s, 1H, NH), 7.29 (s, 1H, NH), 7.27-7.24 (m, 4H, 2*^{Ar}CH and 2*NH), 7.14 (s, 1H, NH), 3.77 (s, 2H, CH₂), 3.65 (s, 3H, OCH₃), 1.48 (d, 3H, ¹J_{C-H} = 129.2 Hz, ¹³CH₃), 1.48 (d, 3H, ³J_{C-H} = 4.6 Hz, CH₃(C)¹³CH₃), 1.47 (s, 6H, 2*CH₃), 1.46 (s, 6H, 2*CH₃), 1.38 (br s, 12H, 4*CH₃); **¹³C NMR (100 MHz, CDCl₃)** δ 175.8 (CO), 174.9 (CO), 174.4 (CO), 173.9 (CO), 173.8 (CO), 170.1 (CO), 155.5 (C), 149.3 (CH), 137.8 (CH), 124.6 (CH), 122.8 (CH), 57.4 (C), 57.1 (C), 56.9 (C), 56.8 (C), 55.9 (d, CH₃(C)¹³CH₃), *J*_{C-C} = 36.3 Hz), 52.2 (OCH₃), 45.5 (CH₂), 25.4-24.8 (9*CH₃ and ¹³CH₃); **FTIR (ν_{max} cm⁻¹)** 3270, 2986, 2930, 1732, 1668, 1642, 1537, 1467, 1436, 1383, 1223. **HRMS** calcd for C₂₇¹³C₁H₄₅N₆O₇ [M+H]⁺: 578.3378. Found 578.3369.

• Synthesis of foldamer F4'

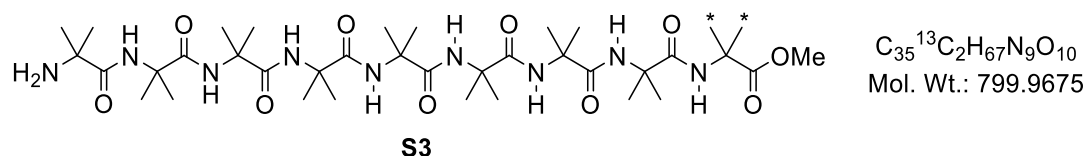
Step 1: N₃Aib₈Aib**OMe (S2)



(a) *Azlactone formation*: To solution of N₃Aib₄OH (167 mg, 0.43 mmol) in CH₂Cl₂ (2 mL) at 0 °C was added EDC-HCl (167 mg, 0.87 mmol). The cold bath was removed and the reaction was stirred at rt for 5 h. After this time, the reaction was diluted with CH₂Cl₂ and H₂O. The layers were separated and the organic phase was washed with H₂O, saturated solution of NaHCO₃, brine, dried over MgSO₄, filtered and concentrated under reduced pressure to give the corresponding crude azlactone residue (140 mg, 87%) which was used in the next step without further purification.

(b) *Azlactone ring-opening*: Crude step (a) (104 mg, 0.28 mmol), H₂NAib₄Aib**OMe **F1** (100 mg, 0.22 mmol), triethylamine (40 μL, 0.28 mmol) and MeCN (1.5 mL) were heated at 90 °C in a sealed tube under argon for 3 days. After this time, the reaction was diluted with CH₂Cl₂, washed with an aqueous solution of KHSO₄ (5 Wt%), a saturated aqueous solution of NaHCO₃, brine, dried over MgSO₄, filtered and concentrated under reduced pressure. The crude residue was purified by flash chromatography on silica gel (gradient starting from 60:40 to 80:20 / EtOAc:CH₂Cl₂) to give **S2** (115 mg, 63%) as a white solid; **M.p.** = 287-288 °C; **¹H NMR (400 MHz, CDCl₃)** δ 7.61 (s, 1H, NH), 7.56 (s, 1H, NH), 7.55 (s, 1H, NH), 7.49 (s, 1H, NH), 7.45 (s, 1H, NH), 7.34 (s, 1H, NH), 6.94 (s, 1H, NH), 6.16 (s, 1H, NH), 3.66 (s, 3H, OCH₃), 1.53 (s, 6H, 2*CH₃), 1.51 (dd, 6H, ¹J_{C-H} = 128.7 and ³J_{C-H} = 4.8 Hz, 2*¹³CH₃), 1.50 (s, 6H, 2*CH₃), 1.48 (s, 6H, 2*CH₃), 1.47 (s, 6H, 2*CH₃), 1.46 (s, 6H, 2*CH₃), 1.45 (s, 6H, 2*CH₃), 1.44 (s, 6H, 2*CH₃), 1.41 (s, 6H, 2*CH₃); **¹³C NMR (100 MHz, CDCl₃)** (C(¹³CH₃)₂ signal is not observed), δ 175.9 (CO), 175.8 (CO), 175.5 (CO), 175.4 (CO), 175.1 (CO), 174.4 (CO), 174.2 (CO), 173.5 (CO), 173.4 (CO), 64.2 (C), 57.1 (C), 57.05 (C), 56.99 (C), 56.86 (3*C), 56.8 (C); 52.2 (OCH₃), 25.6-24.7 (14*CH₃ and 2*¹³CH₃), 24.6 (2* CH₃) **FTIR (ν_{max} cm⁻¹)** 3300, 2983, 2942, 2111, 1729, 1656, 1530, 1455, 1382, 1226. **HRMS** calcd for C₃₅¹³C₂H₆₆N₁₁O₁₀ [M+H]⁺: 826.5056. Found 826.5058.

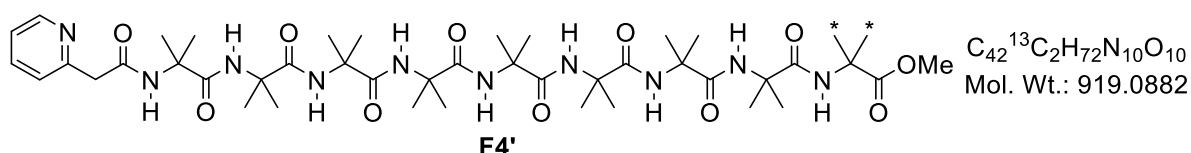
Step 2: H₂NAib₈Aib**OMe (S3)



To a solution of N₃Aib₈Aib**OMe **S2** (100 mg, 0.12 mmol) in MeOH (15 mL) at RT and under inert atmosphere was added Pd/C (10 mg, 0.009 mmol, 10 Wt%). The atmosphere was purged with hydrogen and the reaction was stirred for 12 h under hydrogen (1 atm). After this time, the reaction was filtered through a Celite (MeOH) and the filtrate was concentrated under reduced pressure. The crude residue was

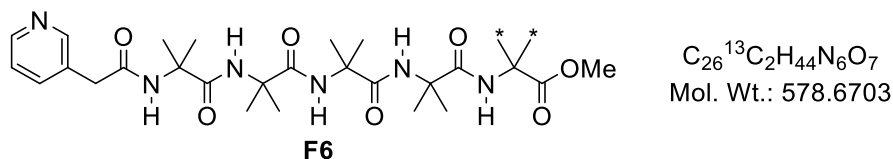
dissolved in CH₂Cl₂, washed with aqueous saturated solution of NaHCO₃, brine, dried over MgSO₄, filtered and concentrated under reduced pressure to give **S3** (75 mg, 78%) as a white solid; **M.p.** = 295-296 °C; **¹H NMR (400 MHz, CDCl₃)** δ 8.27 (s, 1H, NH), 7.83 (s, 1H, NH), 7.63 (s, 1H, NH), 7.59 (s, 2H, 2*NH), 7.44 (s, 1H, NH), 7.34 (s, 1H, NH), 6.25 (s, 1H, NH), 3.66 (s, 3H, OCH₃), 1.53 (s, 6H, 2*CH₃), 1.51 (dd, 6H, ¹J_{C-H} = 129.3 and ³J_{C-H} = 4.4 Hz, 2*¹³CH₃), 1.48-1.43 (m, 30H, 10*CH₃), 1.40 (s, 6H, 2*CH₃), 1.36 (s, 6H, 2*CH₃); **¹³C NMR (100 MHz, CDCl₃)** (C(¹³CH₃)₂ signal is not observed), δ 178.9 (CO), 175.94 (CO), 175.89 (CO), 175.6 (2*CO), 175.1 (CO), 174.49 (CO), 174.47 (CO), 174.1 (CO), 57.01 (C), 56.98 (C), 56.83 (2*C), 56.79 (C), 56.7 (C), 56.4 (C), 55.0 (C), 52.2 (OCH₃), 29.1 (2*CH₃), 25.6-24.7 (14*CH₃ and 2*¹³CH₃); **FTIR (ν_{max} cm⁻¹)** 3291, 2983, 2939, 1729, 1655, 1534, 1450, 1534, 1382, 1227. **HRMS** calcd for C₃₅¹³C₂H₆₈N₉O₁₀ [M+H]⁺: 800.5151. Found 800.5146.

Step 3: 2-Pyridine-CH₂-Aib₈Aib**OMe (F4')



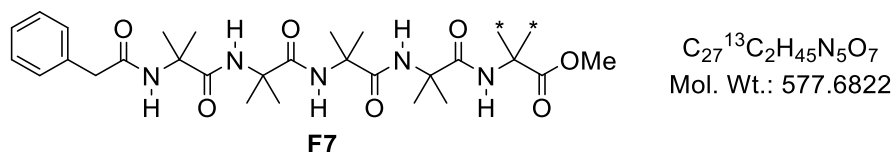
To a solution of H₂NAib₈Aib**OMe **S3** (40 mg, 0.05 mmol) and 2-pyridylacetic acid hydrochloride (17 mg, 0.10 mmol) in CH₂Cl₂ (1 mL) at RT were added successively DIPEA (55 μL, 0.30 mmol), 1-Hydroxybenzotriazole hydrate (13 mg, 0.10 mmol) and EDC-HCl (19 mg, 0.10 mmol). After 12 h stirring at RT, the reaction was diluted with CH₂Cl₂ and water. The layers were separated and the organic phase was washed two times with a saturated solution of NaHCO₃, brine, dried over MgSO₄ and concentrated under reduced pressure. The crude residue was purified by flash chromatography on silica gel (gradient starting from 98:2 to 90:10 / CH₂Cl₂:MeOH). The purified product was dissolved in CH₂Cl₂, washed with aqueous saturated solution of NaHCO₃, brine, dried over MgSO₄, filtered and concentrated under reduced pressure to give **F4'** (30 mg, 65%) as a white solid; **M.p.** > 300 °C; **¹H NMR (400 MHz, CDCl₃)** δ 8.46 (br d, 1H, J = 4.9 Hz, ^{Ar}CH), 7.71 (ddd, apparent td, 1H, J = 7.8 and 1.6 Hz, ^{Ar}CH), 7.68-7.55 (m, 5H, 2*^{Ar}CH and 3*NH), 7.55 (s, 1H, NH), 7.48 (s, 1H, NH), 7.43 (s, 1H, NH), 7.38 (s, 1H, NH), 7.27 (s, 1H, NH), 7.25 (s, 1H, NH), 3.81 (s, 2H, CH₂), 3.64 (s, 3H, OCH₃), 1.49 (dd, 6H, ¹J_{C-H} = 129.3 and ³J_{C-H} = 4.4 Hz, 2*¹³CH₃), 1.48 (s, 6H, 2*CH₃), 1.47 (s, 6H, 2*CH₃), 1.47-1.44 (m, 24H, 8*CH₃), 1.39 (s, 6H, 2*CH₃), 1.36 (s, 6H, 2*CH₃); **¹³C NMR (100 MHz, CDCl₃)** (C(¹³CH₃)₂ signal is not observed), δ 176.13 (CO), 176.07 (CO), 175.9 (2*CO), 175.8 (CO), 175.3 (CO), 175.0 (CO), 174.7 (CO), 174.6 (CO), 170.5 (CO), 155.9 (C), 149.2 (CH), 137.7 (CH), 124.6 (CH), 122.7 (CH), 57.3 (C), 56.9 (C), 56.8-56.6 (6*C), 52.1 (OCH₃), 45.3 (CH₂), 29.9 (2*CH₃), 25.6-24.6 (14*CH₃ and 2*¹³CH₃); **FTIR (ν_{max} cm⁻¹)** 3303, 2984, 2936, 1727, 1652, 1532, 1467, 1455, 1435, 1381, 1227. **HRMS** calcd for C₄₂¹³C₂H₇₃N₁₀O₁₀ [M]⁺: 919.5522. Found 919.5524.

• Synthesis of foldamer 3-Pyridine-CH₂-Aib₄Aib**OMe (F6)



To a solution of H₂N-Aib₄Aib**OMe (30 mg, 0.06 mmol) and 3-pyridylacetic acid hydrochloride (23 mg, 0.13 mmol) in CH₂Cl₂ (1 mL) at RT were added successively DIPEA (70 μL, 0.39 mmol), 1-Hydroxybenzotriazole hydrate (18 mg, 0.13 mmol) and EDC-HCl (25 mg, 0.13 mmol). After 12 h stirring at RT, the reaction was diluted with CH₂Cl₂ and water. The layers were separated and the organic phase was washed two times with a saturated solution of NaHCO₃, brine, dried over MgSO₄ and concentrated under reduced pressure. The crude residue was purified by flash chromatography on silica gel (gradient starting from 98:2 to 95:5 / CH₂Cl₂:MeOH). The purified product was dissolved in CH₂Cl₂, washed with aqueous saturated solution of NaHCO₃, brine, dried over MgSO₄, filtered and concentrated under reduced pressure to give **F6** (14 mg, 38%) as a white solid; **M.p.** = 253-254 °C; **¹H NMR (400 MHz, CDCl₃)** δ 8.70-8.41 (m, 2H, ^{Ar}CH), 7.90 (s, 1H, NH), 7.74 (br d, 1H, *J* = 7.8 Hz, ^{Ar}CH), 7.54 (s, 1H, NH), 7.45 (s, 1H, NH), 7.42 (s, 1H, NH), 7.30-7.24 (br m, 1H, ^{Ar}CH), 6.63 (s, 1H, NH), 3.65 (s, 3H, OCH₃), 3.64 (s, 2H, CH₂), 1.48 (dd, 6H, ¹*J*_{C-H} = 128.7 and ³*J*_{C-H} = 4.8 Hz, 2*¹³CH₃), 1.47 (s, 6H, 2*CH₃), 1.44 (s, 6H, 2*CH₃), 1.34 (s, 6H, 2*CH₃), 1.27 (s, 6H, 2*CH₃); **¹³C NMR (100 MHz, CDCl₃)** (^{Ar}C and CH₃(C)¹³CH₃) signals are not observed), δ 176.1 (CO), 175.5 (CO), 174.84 (CO), 174.77 (CO), 174.5 (CO), 171.6 (CO), 150.2 (CH), 148.3 (CH), 137.4 (CH), 123.8 (CH), 57.2 (C), 57.0 (C), 56.8 (C), 56.6 (C), 52.4 (OCH₃), 40.2 (CH₂), 26.1-24.5 (8*CH₃ and 2*¹³CH₃); **FTIR (ν_{max} cm⁻¹)** 3290, 2984, 2930, 1730, 1643, 1532, 1455, 1434, 1382, 1222. **HRMS** calcd for C₂₆¹³C₂H₄₅N₆O₇ [M+H]⁺: 579.3417. Found 579.3416.

• Synthesis of foldamer 2-Pyridine-CH₂-Aib₄Aib**OMe (F7)

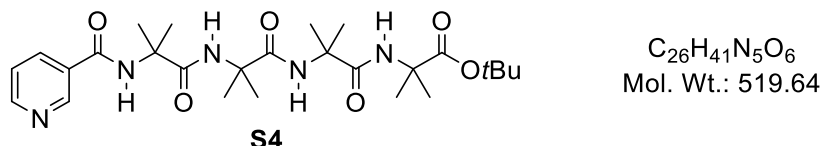


To a solution of H₂NAib₄Aib**OMe **F1** (30 mg, 0.06 mmol) and phenylacetic acid (18 mg, 0.13 mmol) in CH₂Cl₂ (1 mL) at RT were added successively DIPEA (70 μL, 0.39 mmol), 1-Hydroxybenzotriazole hydrate (18 mg, 0.13 mmol) and EDC-HCl (25 mg, 0.13 mmol). After 12 h stirring at RT, the reaction was diluted with CH₂Cl₂ and water. The layers were separated and the organic phase was washed two times with a saturated solution of NaHCO₃, brine, dried over MgSO₄, filtered and concentrated under reduced pressure. The crude residue was purified by flash chromatography on silica gel (gradient starting from 98:2 to 95:5 / CH₂Cl₂:MeOH) to give **F7** (30 mg, 79%) as a white solid; **M.p.** = 273-274 °C; **¹H NMR (400 MHz, MeOH-d₄)** (partially exchange NH signals were omitted for clarity) δ 7.41-7.23 (m, 5H, ^{Ar}CH), 3.67 (s, 3H, CH₃), 3.56 (s, 2H, CH₂), 1.48 (dd, 6H, ¹*J*_{C-H} = 129.0 Hz and ³*J*_{C-H} = 4.3 Hz, 2*¹³CH₃), 1.46 (s, 12H, 2*CH₃), 1.32 (s, 6H, 2*CH₃),

1.28 (s, 6H, 2*CH₃); ¹³C NMR (100 MHz, MeOH-d₄) (C(¹³CH₃)₂ signal is not observed), δ 177.0 (2*CO), 176.9 (2*CO), 176.6 (CO), 174.0 (CO), 137.2 (C), 130.4 (2*CH), 129.7 (2*CH), 128.1 (CH), 57.9 (2*C), 57.7 (C), 57.6 (C), 52.7 (OCH₃), 43.6 (CH₂), 26.0-24.9 (8*CH₃ and 2*¹³CH₃); FTIR (ν_{max} cm⁻¹) 3253, 2984, 2937, 1732, 1673, 1654, 1642, 1532, 1455, 1380, 1228. HRMS calcd for C₂₇¹³C₂H₄₆N₅O₇ [M+H]⁺: 578.3459. Found 578.3451.

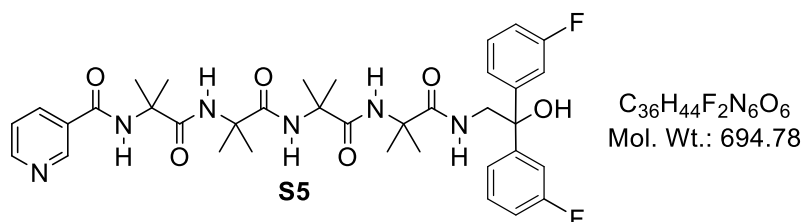
• **Synthesis of foldamer F5Me+**

Step 1: 3-Pyridine-Aib₄O^tBu (S4)



To a solution of nicotinic acid (0.18 g, 1.5 mmol) and HOBT (0.49 g, 3.7 mmol) in dry CH₂Cl₂ (15 mL) at 0 °C was added EDC·HCl (0.70 g, 3.7 mmol) and the reaction mixture was stirred at this temperature for 10 min. The reaction mixture was allowed to warm to room temperature, after which time H₂NAib₄O^tBu (0.60 g, 1.5 mmol) and DIPEA (0.64 mL, 3.7 mmol) were successively added and the resulting solution stirred at room temperature for 18 h. The solution was then diluted with CH₂Cl₂ (30 mL) and the organic layer washed with 5% KHSO₄ (2 × 8 mL), sat. NaHCO₃ (2 × 8 mL) and brine (8 mL), dried over MgSO₄, filtered and concentrated under reduced pressure. The resulting residue was purified by flash column chromatography (SiO₂, 4 → 6 % MeOH in CHCl₃) to give the desired product as a white solid (0.52 g, 69%); **M.p.** = 213-214 °C; ¹H NMR (300 MHz, CDCl₃) δ 9.09 (1H, s, PyH), 8.76 (1H, d, J = 4.4 Hz, PyH), 8.23 (1H, d, J = 8.0 Hz, PyH), 7.47 - 7.41 (2H, m, PyH + NH), 7.34 (1H, br, s, NH), 7.31 (1H, br, s, NH), 6.60 (1H, br, s, NH), 1.63 (6H, s, 2 × CH₃, Aib), 1.53 (6H, s, 2 × CH₃, Aib), 1.44 (6H, s, 2 × CH₃, Aib), 1.42 (6H, s, 2 × CH₃, Aib), 1.40 (9H, s, 3 × CH₃, O^tBu); ¹³C NMR (100 MHz, CDCl₃) δ 174.0 (CO), 173.6 (CO), 173.2 (CO), 172.5 (CO), 164.7 (CO), 148.8 (Py), 148.3 (Py), 137.8 (Py), 127.1 (Py), 122.4 (Py), 79.8 (αC, O^tBu), 57.0 (αC, Aib), 56.9 (αC, Aib), 56.8 (αC, Aib), 56.0 (αC, Aib), 27.9 (CH₃, O^tBu), 25.5 (CH₃, Aib), 25.4 (CH₃, Aib), 25.2 (CH₃, Aib), 24.7 (CH₃, Aib); FTIR (ν_{max} cm⁻¹) 3324, 2984, 2937, 1725, 1651, 1592, 1533, 1469, 1455, 1384, 1365, 1310, 1257, 1147. HRMS calcd for C₂₆H₄₂N₅O₆ [M+H]⁺: 520.3130. Found 520.3119.

Step 2: 3-Pyridine-Aib₄-2-amino-1,1-di(3-fluorophenyl)ethanol (S5)



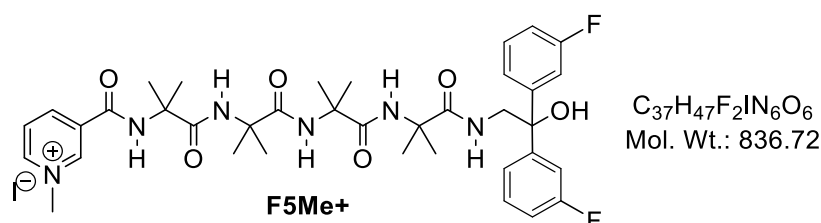
(a) *Boc deprotection*: To a solution of 3-Pyridine-Aib₄O^tBu (0.350 g, 0.67 mmol) in CH₂Cl₂ (7 mL) was added trifluoroacetic acid (7 mL) and the reaction mixture was stirred at ambient temperature overnight. After this time, the excess solvent was removed under reduced pressure and 3-PyridineAib₄OH (0.23 g,

0.50 mmol) isolated as a white solid after recrystallization from Et₂O and used in the next step without further purification.

(b) *Azlactone formation*: To a solution of 3-Pyridine-Aib₄OH (0.23 g, 0.5 mmol) in dry CH₂Cl₂ (5 mL) was added EDC·HCl (0.19 g, 1.0 mmol) and the resulting colourless solution was left stirring at ambient temperature overnight. After this time, the resulting solution was diluted with CH₂Cl₂ (5 mL) and washed with sat. NaHCO₃ (2 × 3 mL) and the brine (3 mL). The organic washings were dried over MgSO₄, filtered and concentrated under reduced pressure to give the corresponding azlactone as a white solid (0.26 g, 0.57 mmol), which was used in the next step without further purification.

(c) *Azlactone ring-opening*: To a solution of crude step (b) (0.26 g, 0.57 mmol) in acetonitrile (3 mL) was added 2-amino-1,1-di(3-fluorophenyl)ethanol (0.17 g, 0.69 mmol) and NEt₃ (0.096 mL, 0.69 mmol) and the reaction mixture was refluxed for 72 h. The excess solvent was removed under reduced pressure and the resulting residue subjected to column chromatography (SiO₂) (5 → 10 % MeOH in CHCl₃) to give the desired product as a white solid (0.24 g, 51% over 3 steps); **M.p.** = 217-220 °C; **¹H NMR (300 MHz, CDCl₃/MeOH-d₄:1/9)**: δ 9.09 (1H, dd, *J* = 1.6 Hz, ⁴*J* = 0.4 Hz, PyH), 8.73 (1H, dd, *J* = 4.0 Hz, ⁴*J* = 1.4 Hz, PyH), 8.35 (1H, dt, *J* = 6.4 Hz, ⁴*J* = 1.6 Hz, PyH), 7.76 (1H, br, s, NH), 7.58 (1H, dd, *J* = 4.0 Hz, ⁴*J* = 0.4 Hz, PyH), 7.33 – 7.23 (8H, m, ArH + 2 × NH), 6.95 – 6.93 (2H, m, ArH), 4.03 (2H, s, CH₂), 1.54 (6H, s, 2 × CH₃), 1.43 (6H, s, 2 × CH₃), 1.36 (6H, s, 2 × CH₃), 1.34 (6H, s, 2 × CH₃); **¹³C NMR (100 MHz, CDCl₃)** δ 176.8 (CO), 174.9 (CO), 173.6 (CO), 173.5 (CO), 165.1 (CO), 164.5 (Py), 161.2 (Ar), 148.61 (Py), 148.58 (Py), 147.9 (d, *J* = 32 Hz, Ar), 137.9 (Py), 129.5 (d, *J* = 44 Hz, Ar), 127.4 (Py), 122.3 (d, *J* = 48 Hz, Ar), 114.0 (d, *J* = 36 Hz, Ar), 113.7 (d, *J* = 28 Hz, Ar), 78.3 (CH₂), 57.3 (αC, Aib), 57.2 (αC, Aib), 57.0 (αC, Aib), 56.8 (αC, Aib), 49.8 (αC), 25.5 (CH₃, Aib), 25.2 (CH₃, Aib), 25.13 (CH₃, Aib), 25.10 (CH₃, Aib); **¹⁹F NMR (376 MHz, CDCl₃/MeOH-d₄:1/9)** δ 113.6; **FTIR (ν_{max} cm⁻¹)** 3305, 2929, 2872, 1650, 1612, 1591, 1539, 1484, 1445, 1385, 1363, 1269, 1229, 1170, 1128, 1058. **HRMS** calcd for C₃₆H₄₅N₆O₆F₂ [M+H]⁺: = 695.3363. Found 695.3354.

Step 3: 3-Methylpyridinium-Aib₄-2-amino-1,1-di(3-fluorophenyl)ethanol iodide (F5Me+)

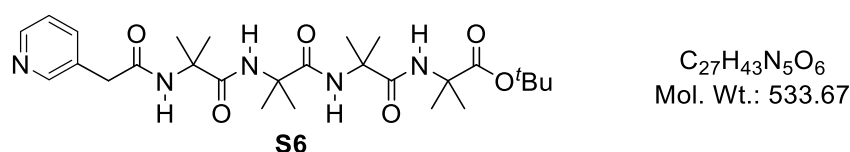


To a solution of 3-PyridineAib₄-2-amino-1,1-di(3-fluorophenyl)ethanol (0.034 mg, 0.049 mmol) and K₂CO₃ (0.068 g, 0.49 mmol) in acetone (2 mL) was added iodomethane (0.061 mL, 0.98 mmol) and the resulting bright yellow solution refluxed for 48 h. After this time, the resulting solution was filtered and washed with acetone (5 mL) and the solution concentrated (approx. 2 mL) under reduced pressure. The desired product was isolated as a bright yellow solid upon the addition of Et₂O (4 mL) and collected by filtration (0.026 g, 75%); **M.p.** = 196-197 °C; **¹H NMR (300 MHz, CDCl₃/MeOH-d₄: 1/1)** δ 9.44 (1H, s, PyH), 9.08 – 9.03 (2H, m, 2 × PyH), 8.24 (1H, t, *J* = 4.0 Hz, NH), 7.61 (1H, s, br, NH), 7.41 (1H, s, br, NH), 7.40 – 7.32 (1H, m, PyH), 7.29 –

7.20 (6H, m, ArH), 6.95 – 6.90 (2H, m, ArH), 4.50 (3H, s, br, N⁺CH₃), 4.01 (2H, d, J = 4.0 Hz, CH₂), 1.56 (6H, s, 2 × CH₃), 1.40 (6H, s, 2 × CH₃), 1.36 (6H, s, 2 × CH₃), 1.32 (6H, s, 2 × CH₃); ¹³C NMR (75 MHz, MeOH-d₄) δ 177.2 (CO), 176.6 (CO), 175.5 (CO), 165.4 (CO), 163.5 (CO), 163.0 (Py), 149.1 (d, J = 28 Hz, Ar), 148.7 (Ar), 147.1 (Py), 144.9 (Py), 135.3 (Py), 130.9 (d, J = 36 Hz, Ar), 129.0 (Py), 123.2 (d, J = 12 Hz, Ar), 114.8 (d, J = 84 Hz, Ar), 114.4 (d, J = 92 Hz, Ar), 78.7 (CH₂), 58.9 (αC), 58.16 (αC, Aib), 58.13 (αC, Aib), 58.11 (αC, Aib), 58.03 (αC, Aib), 29.5 (N⁺CH₃), 25.7 (CH₃, Aib), 25.4 (CH₃, Aib), 25.3 (CH₃, Aib), 25.1 (CH₃, Aib); ¹⁹F NMR (376 MHz, CDCl₃/MeOH-d₄:1/1) δ 113.5; FTIR (ν_{max} cm⁻¹) 3396, 2479, 2072, 1657, 1591, 1473, 1422, 1381, 1364, 1228, 1119, 1090. HRMS calcd for C₃₇H₄₇N₆O₆F₂ [M]⁺: 709.3520. Found 709.3524.

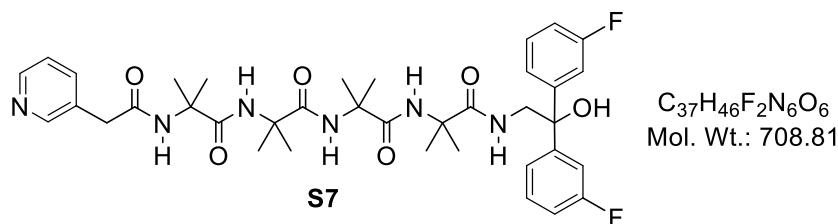
• **Synthesis of foldamer F6Me+**

Step 1: 3-Pyridine-CH₂Aib₄O^tBu (S6)



To a solution of 3-pyridineacetic acid (0.15 g, 1.1 mmol) and HOBt (0.37 g, 2.7 mmol) in dry CH₂Cl₂ (11 mL) at 0 °C was added EDC·HCl (0.52 g, 2.7 mmol) and the reaction mixture was stirred at this temperature for 10 min. The reaction mixture was allowed to warm to room temperature, after which time, H₂NAib₄O^tBu (0.45 g, 1.1 mmol) and DIPEA (0.48 mL, 2.7 mmol) were successively added and the resulting solution stirred at room temperature for 18 h. The solution was then diluted with CH₂Cl₂ (22 mL) and the organic layer washed with 5% KHSO₄ (2 × 5 mL), sat. NaHCO₃ (2 × 5 mL) and brine (5 mL), dried over MgSO₄, filtered and concentrated under reduced pressure. The resulting residue was purified by flash column chromatography (SiO₂, 5 → 8 % MeOH in CHCl₃) to give the desired product as a white solid (0.43 g, 73%); **M.p.** = 190-191 °C; ¹H NMR (300 MHz, CDCl₃) δ 8.52 (1H, d, J = 4.2 Hz, PyH), 7.72 (1H, dt, J = 7.7 Hz, ⁴J = 1.8 Hz, PyH), 7.38 (1H, br, s, NH), 7.29 – 7.25 (3H, m, 2 x PyH + NH), 7.14 (1H, br, s, NH), 7.11 (1H, br, s, NH), 3.78 (2H, s, CH₂), 1.49 (6H, s, 2 x CH₃, Aib), 1.44 (6H, s, 2 x CH₃, Aib), 1.41 (15H, s, 5 x CH₃, Aib + O^tBu), 1.36 (6H, s, 2 x CH₃, Aib); ¹³C NMR (100 MHz, CDCl₃) δ 174.0 (CO), 173.8 (CO), 173.7 (CO), 172.9 (CO), 169.8 (CO), 155.5 (Py), 149.0 (Py), 137.5 (Py), 124.4 (Py), 122.5 (Py), 79.8 (αC, O^tBu), 57.2 (αC, Aib), 56.7 (αC, Aib), 56.6 (αC, Aib), 56.0 (αC, Aib), 45.3 (CH₂), 27.8 (CH₃, O^tBu), 25.3 (CH₃, 2 × Aib), 25.1 (CH₃, Aib), 24.7 (CH₃, Aib); FTIR (ν_{max} cm⁻¹) 3324, 2982, 2928, 2855, 1731, 1664, 1657, 1530, 1455, 1431, 1384, 1365, 1310, 1226, 1148. HRMS calcd for C₂₇H₄₄O₆N₅ [M+H]⁺: 534.3286. Found 534.3276.

Step 2: 3-Pyridine-CH₂-Aib₄-2-amino-1,1-di(3-fluorophenyl)ethanol (S7)

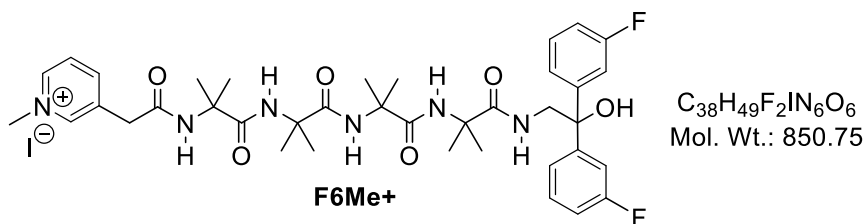


(a) *Boc deprotection*: To a solution of 3-Pyridine-CH₂-Aib₄O^tBu (0.20 g, 0.38 mmol) in CH₂Cl₂ (4 mL) was added trifluoroacetic acid (4 mL) and the reaction mixture was stirred at ambient temperature overnight. After this time, the excess solvent was removed under reduced pressure and 3-Pyridine-CH₂-Aib₄OH (0.16 g, 0.34 mmol) isolated as a white solid after recrystallization from Et₂O and used in the next step without further purification.

(b) *Azlactone formation*: To a solution of 3-Pyridine-CH₂-Aib₄OH (0.16 g, 0.34 mmol) in dry CH₂Cl₂ (3 mL) was added EDC-HCl (0.13 g, 0.68 mmol) and the resulting colourless solution was left stirring at ambient temperature overnight. After this time, the resulting solution was diluted with CH₂Cl₂ (5 mL) and washed with sat. NaHCO₃ (2 × 2 mL) and the brine (2 mL). The organic washings were dried over MgSO₄, filtered and concentrated under reduced pressure to give the corresponding azlactone as a white solid (0.11 g, 0.24 mmol), which was used in the next step without further purification.

(c) *Azlactone ring-opening*: To a solution of crude step (b) (0.11 g, 0.24 mmol) in acetonitrile (1.2 mL) was added 2-amino-1,1-di(3-fluorophenyl)ethanol (0.072 g, 0.29 mmol) and NEt₃ (0.040 mL, 0.29 mmol) and the reaction mixture was refluxed for 72 h. The excess solvent was removed under reduced pressure and the resulting residue subjected to column chromatography (SiO₂) (5 → 10 % MeOH in CHCl₃) to give the desired product as a white solid (0.088 g, 33% over 3 steps); **M.p.** = 202-204 °C; **¹H NMR (300 MHz, CDCl₃)** δ 8.54 (1H, d, *J* = 8.0 Hz, PyH), 7.84 (1H, t, *J* = 12.0 Hz, PyH), 7.55 (1H, t, *J* = 8.0 Hz, NH), 7.49 (1H, s, br, NH), 7.37 – 7.32 (2H, m, PyH + NH), 7.23 – 7.20 (8H, m, NH + 6 ArH + PyH), 6.88 – 6.83 (2H, m, ArH), 6.00 (1H, s, br, NH), 4.00 (2H, d, *J* = 8.0 Hz, CH₂), 3.82 (2H, s, PyCH₂), 1.45 (6H, s, 2 × CH₃), 1.39 (6H, s, 2 × CH₃), 1.28 (6H, s, 2 × CH₃), 1.27 (6H, s, 2 × CH₃); **¹³C NMR (75 MHz, CDCl₃/MeOH-d₄:1/1)** δ 177.2 (CO), 176.0 (CO), 174.9 (CO), 170.7 (CO), 164.2 (CO), 161.8 (Py), 155.8 (Ar), 148.9 (Py), 147.5 (d, *J* = 24 Hz, Ar), 137.9 (Py), 129.7 (d, *J* = 32 Hz, Ar), 125.2 (Py), 122.9 (Py), 122.2 (d, *J* = 12 Hz, Ar), 114.0 (d, *J* = 84 Hz, Ar), 113.8 (d, *J* = 88 Hz, Ar), 78.1 (CH₂), 57.3 (αC), 57.1 (αC, Aib), 56.9 (αC, Aib), 56.7 (αC, Aib), 53.7 (αC, Aib), 44.8 (CH₂), 25.3 (CH₃, Aib), 25.0 (CH₃, Aib), 24.8 (CH₃, Aib), 24.7 (CH₃, Aib); **¹⁹F NMR (376 MHz, CDCl₃/MeOH-d₄:1/1)** δ 113.7; **FTIR (ν_{max} cm⁻¹)**. 3310, 2986, 2476, 2070, 1651, 1591, 1536, 1440, 1385, 1364, 1230. **HRMS** calcd for C₃₇H₄₆N₆O₆F₂Na [M+Na]⁺: 731.3345. Found 731.3322.

Step 3: 3-Methylpyridinium-CH₂-Aib4-2-amino-1,1-di(3-fluorophenyl)ethanol iodide (F6Me⁺)



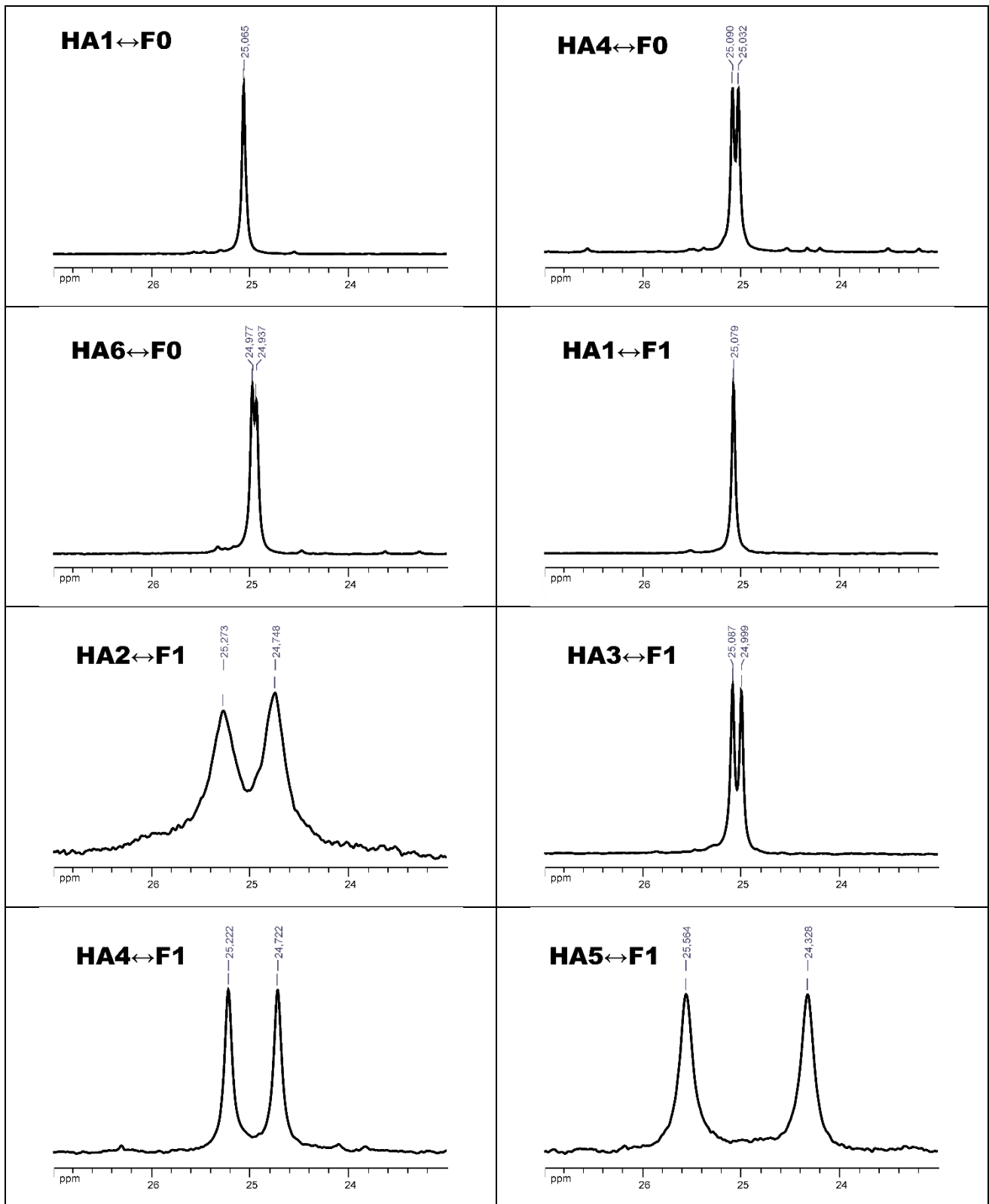
To a solution of foldamer **B6** (0.020 mg, 0.028 mmol) and K₂CO₃ (0.039 g, 0.28 mmol) in acetone (1 mL) was added methyl iodide (0.035 mL, 0.56 mmol) and the resulting bright yellow solution refluxed for 48 h. After this time, the resulting solution was filtered and washed with acetone (4 mL) and the solution concentrated (approx. 2 mL) under reduced pressure. The desired product was isolated as a bright yellow solid upon the addition of Et₂O (4 mL) and collected by filtration. (0.014 g, 69%); **M.p.** = 182-184 °C; **¹H NMR (300 MHz, MeOH-d₄)** δ 8.98 (1H, d, *J* = 4.0 Hz, PyH), 8.95 (1H, br, s, NH), 8.56 (1H, dt, *J* = 8.0 Hz, ⁴*J* = 1.2 Hz, PyH), 8.11 (1H, dd, *J* = 8.0 Hz, ⁴*J* = 1.2 Hz, PyH), 8.02 (1H, d, *J* = 7.6 Hz, ⁴*J* = 1.6 Hz, PyH), 7.51 (1H, br, s, NH), 7.42 – 7.18 (7H, m, 1 x NH + 6 x ArH), 6.95 – 6.91 (2H, m, 2 x ArH), 4.38 (3H, s, N⁺CH₃), 4.36 (2H, d, *J* = 8.0 Hz, CH₂), 3.98 (2H, s, CH₂), 1.46 (6H, s, 2 x CH₃), 1.35 (6H, s, 2 x CH₃), 1.29 (6H, s, 2 x CH₃), 1.25 (3H, s, CH₃), 1.10 (3H, s, CH₃); **¹³C NMR (75 MHz, MeOH-d₄)** δ 176.3 (CO), 175.68 (CO), 175.67 (CO), 171.6 (CO), 165.0 (CO), 164.1 (Py), 163.1 (Ar), 149.02 (Py), 148.97 (Py), 148.1 (Ar), 146.9 (Py), 130.7 (d, *J* = 28 Hz, Ar), 127.8 (Py), 123.1 (Ar), 114.7 (d, *J* = 68 Hz, Ar), 114.3 (d, *J* = 72 Hz, Ar), 70.5 (CH₂), 58.2 (αC), 58.0 (αC, Aib), 57.9 (αC, Aib), 57.8 (αC, Aib), 55.9 (αC, Aib), 46.9 (CH₂), 29.4 (CH₃, N⁺Me), 25.5 (CH₃, Aib), 25.3 (CH₃, Aib), 25.1 (CH₃, Aib), 25.0 (CH₃, Aib); **¹⁹F NMR (376 MHz, CDCl₃/MeOH-d₄:1/1)** δ 113.6; **FTIR (ν_{max} cm⁻¹)** 3455, 3322, 2985, 2935, 2476, 1658, 1590, 1520, 1472, 1441, 1383, 1364, 1230. **HRMS** calcd for C₃₈H₄₉N₆O₆F₂ [M]⁺: 723.3682. Found 723.3670.

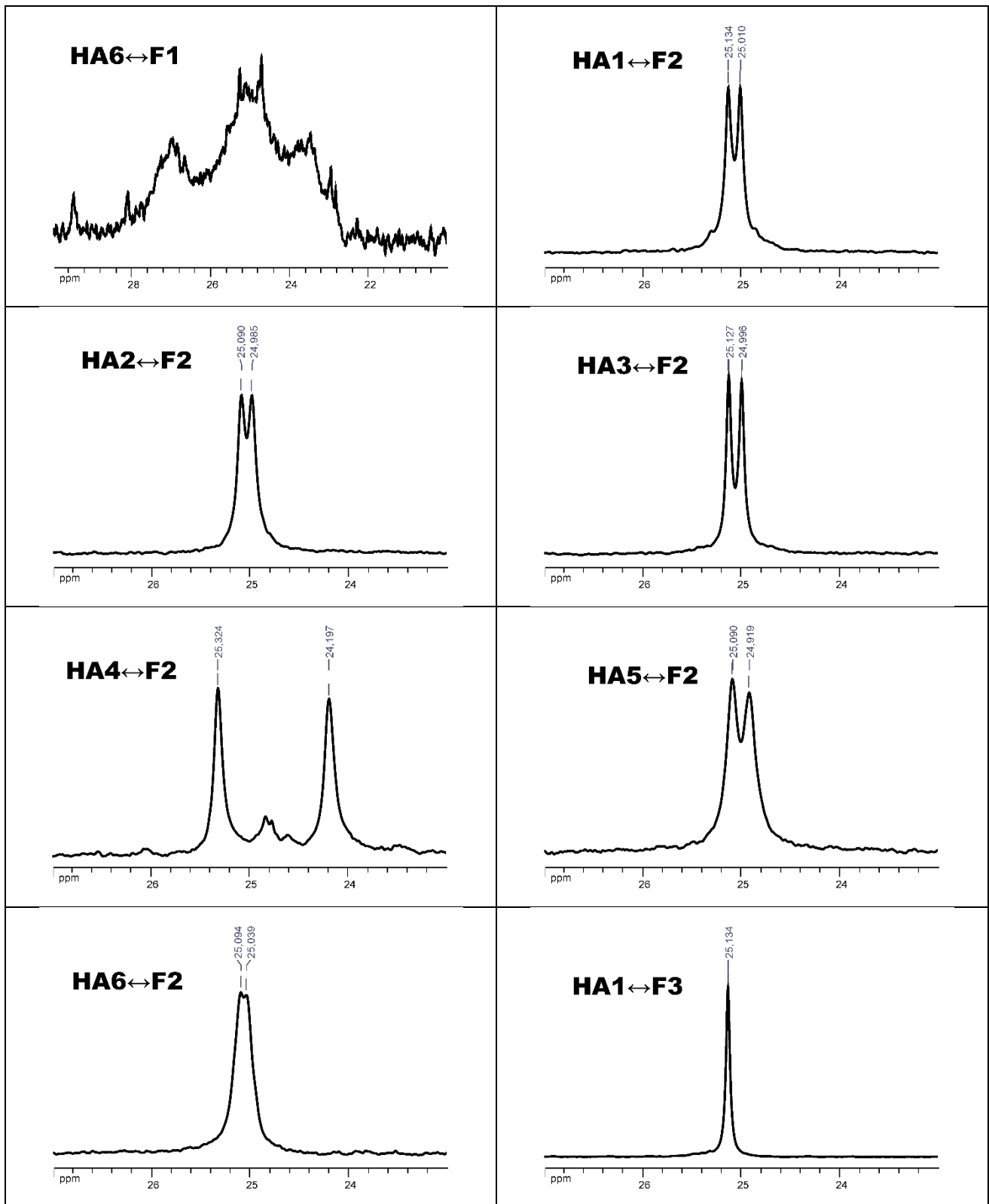
III. Investigation of the HA-F interaction (Table 1)

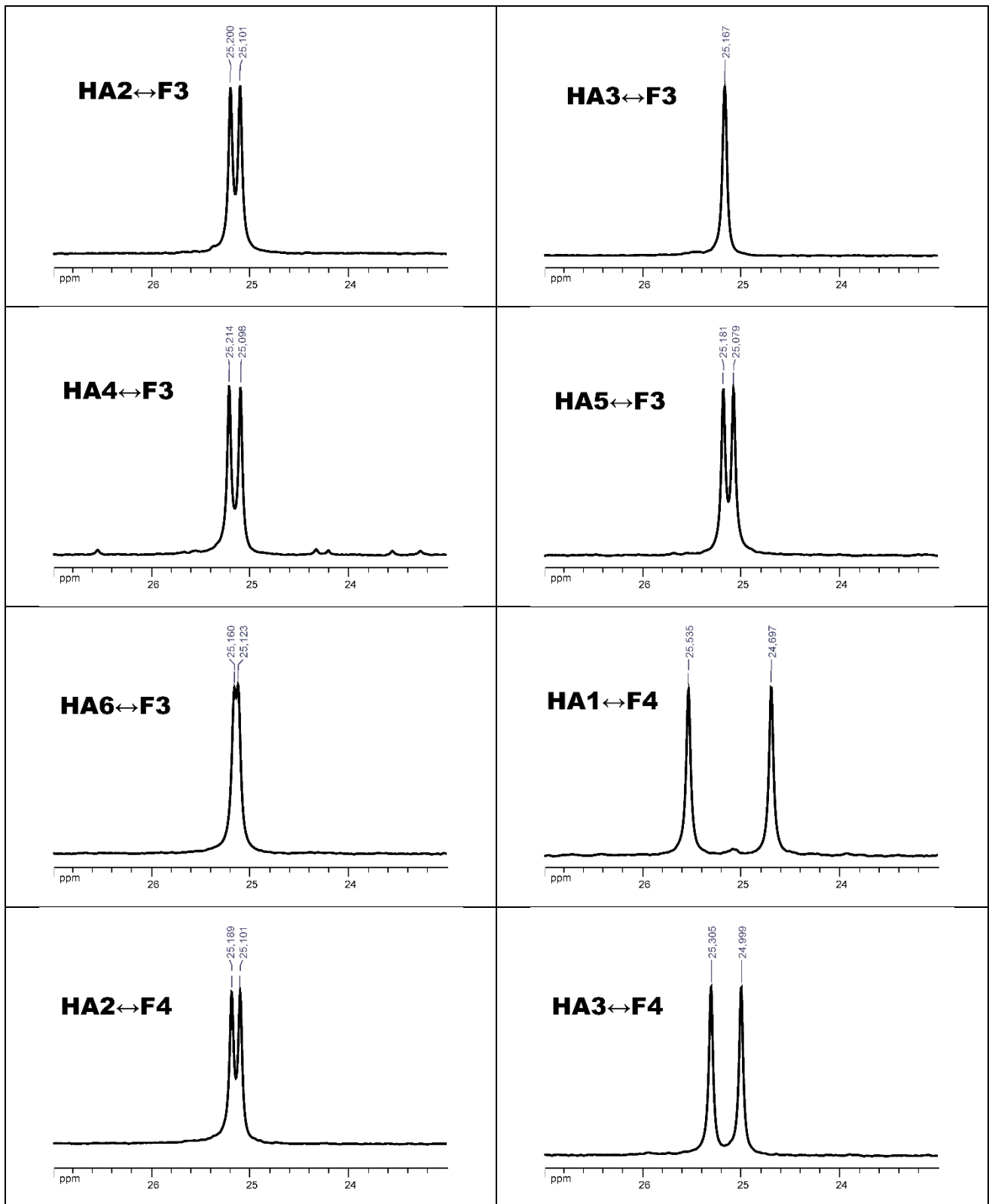
● Entries 1-6 and 9

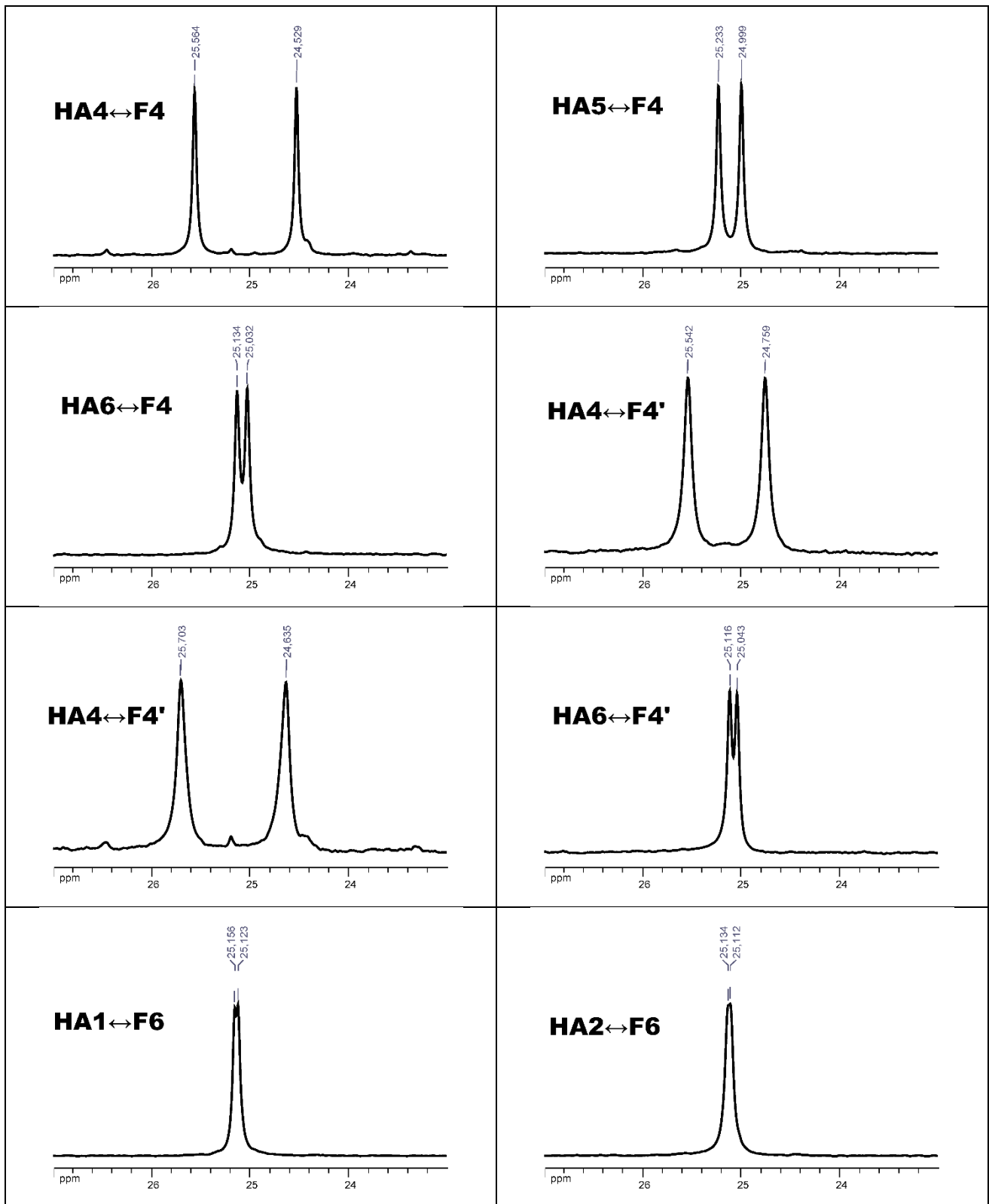
Procedure for the preparation of the NMR samples HA1↔F: A solution of **HA1** (0.0075 mmol, 0.5 mL, 15 mM) was added to foldamer **F** (0.005 mmol) which was directly weighed in an NMR tube. After vigorous shaking of the NMR tube for 1 min, ¹H and ¹³C spectra of the resultant solution were recorded at 296 K. The portions of the ¹³C NMR (CDCl₃, 100 MHz) spectra of **F** in the presence of **HA1** are shown in Table S1.

Procedure for the preparation of the NMR samples HA2-6↔F: **HA2, HA3, HA4, HA5** and **HA6** (0.006 mmol) and foldamer **F** (0.005 mmol) were directly weighed in an NMR tube to which CDCl₃ (0.5 mL) was added. After vigorous shaking of the NMR tube for 1 min, ¹H and ¹³C spectra of the resultant solution were recorded at 296 K. The portions of the ¹³C NMR (CDCl₃, 100 MHz) spectra of **F** in the presence of **HA2-6** are shown in Table S1.









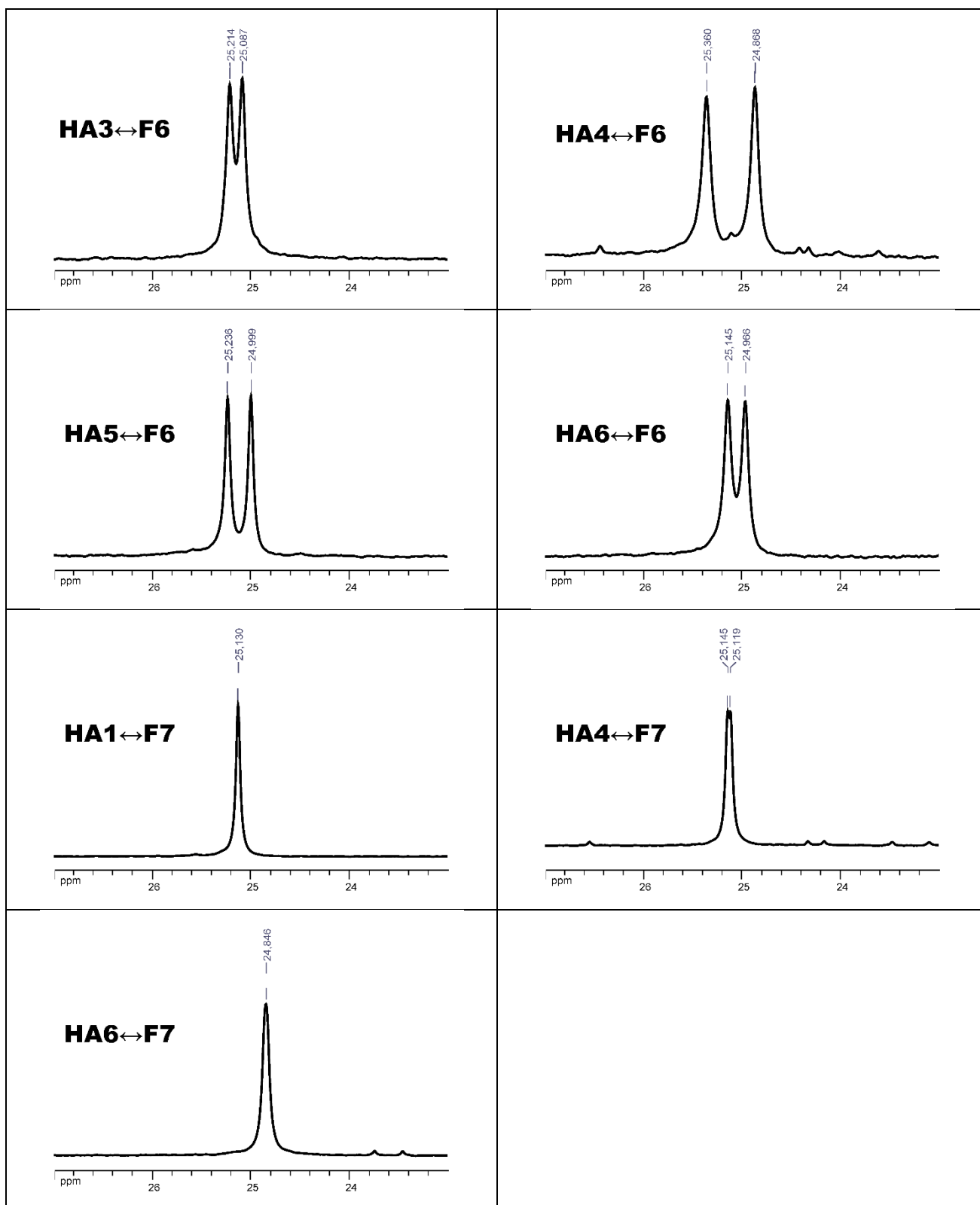


Table S1: Portions of the ^{13}C (100 MHz, CDCl_3) spectra of **F** in the presence of **HA** recorded at 296 K; **[F]** = 10 mM; **[HA1]** = 15 mM; **[HA2]**, **[HA3]**, **[HA4]**, **[HA5]** and **[HA6]** = 12 mM.

• **Entries 7 and 8**

Procedure for the titration of the foldamer (F5Me⁺ or F6Me⁺) with TRISPHAT or BINPHAT: To a solution of foldamer (F5Me⁺ or F6Me⁺) (0.008 M, 600 μ L) in CDCl₃/MeOH-d₄ the appropriate amount of TRISPHAT or BINPHAT (1 < number of equiv. < 10) was added and the solution transferred to an NMR tube. After vigorous shaking of the NMR tube for 30 seconds, ¹H and ¹⁹F spectra of the resultant solution were recorded at 296 K. The anisochronicity ($\Delta\delta$) of the ¹H and ¹⁹F NMR reporters are reported in Tables S2-4. The portions of the ¹H and ¹⁹F NMR spectra of F5Me⁺ and F6Me⁺ in the presence of TRISPHAT or BINPHAT are shown in Figures S1-23.

TRISPHAT (equiv.)	$\Delta\delta$ (ppb) of ¹ H NMR reporter	$\Delta\delta$ (ppb) of ¹⁹ F NMR reporter
1	0	5
3	30	15
6	30	15
8	40	20
10	40	19

Table S2. Titration experiment TRISPHAT \leftrightarrow F5Me⁺

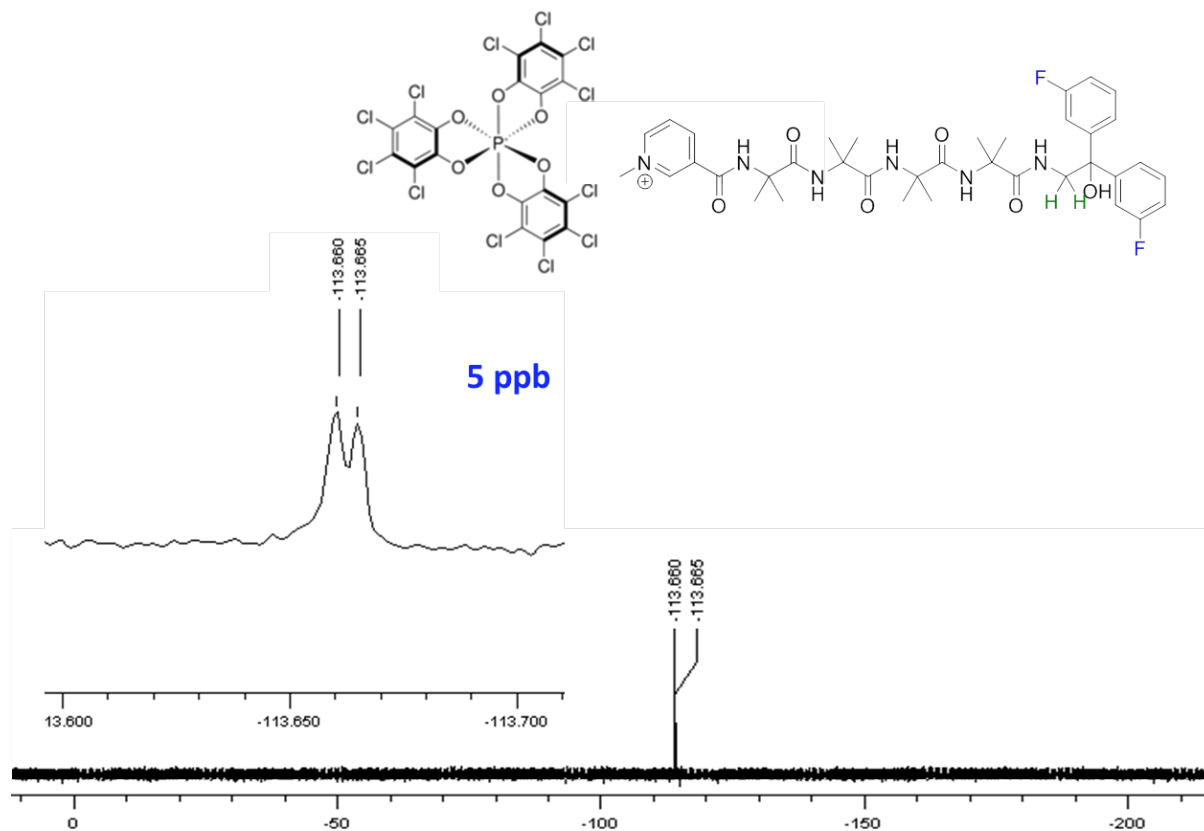


Figure S1. ¹⁹F NMR (376 MHz, CDCl₃/MeOH-d₄; 5/2, 296 K) spectrum of TRISPHAT \leftrightarrow F5Me⁺ (1:1). Iodide and tetrabutylammonium counter ions removed for clarity.

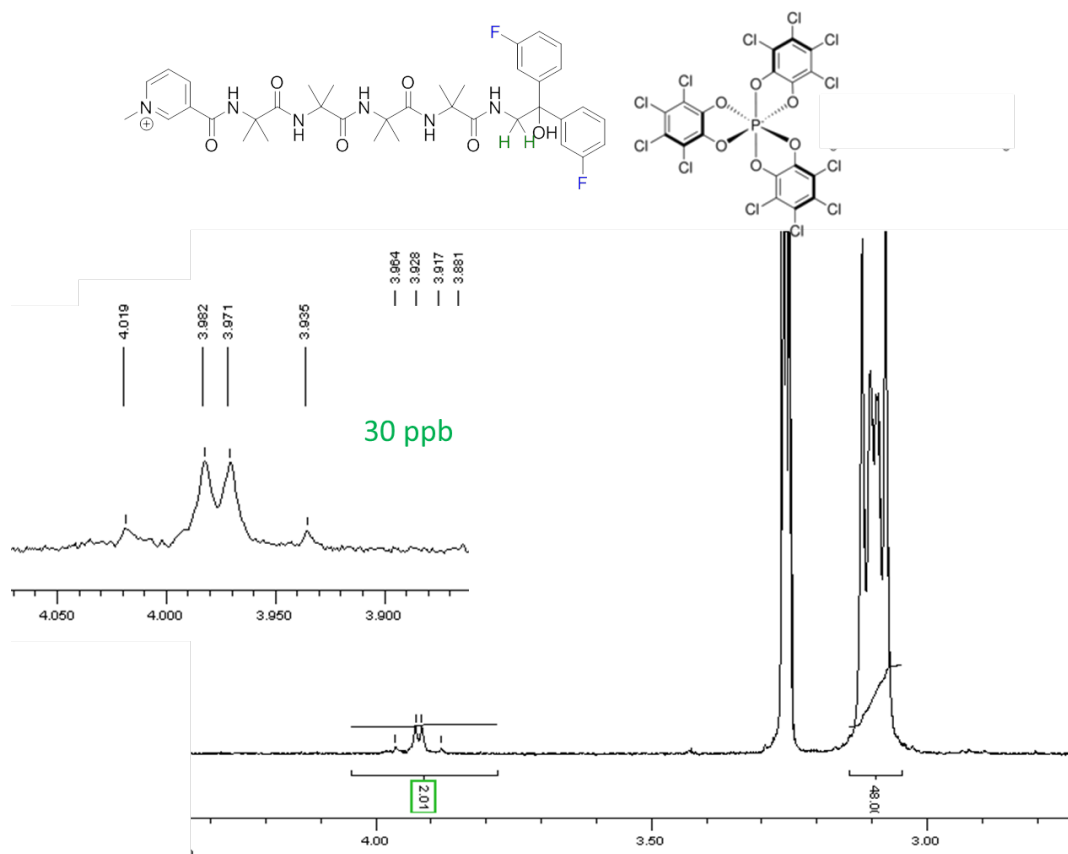


Figure S4. Partial ^1H NMR (400 MHz, $\text{CDCl}_3/\text{MeOH-d}_4$; 5/2, 296 K) spectrum of $\text{TRISPHAT} \leftrightarrow \text{F5Me}^+$ (6:1). Iodide and tetrabutylammonium counter ions removed for clarity.

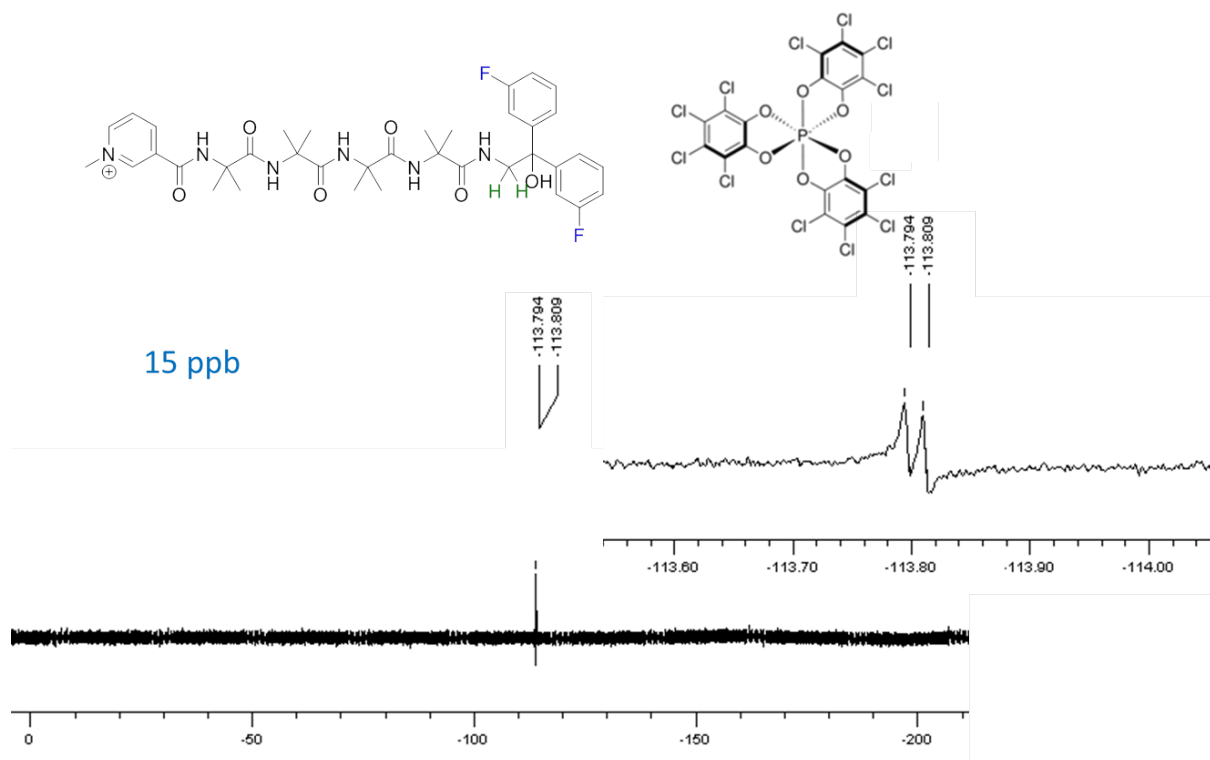


Figure S5. ^{19}F NMR (376 MHz, $\text{CDCl}_3/\text{MeOH-d}_4$; 5/2, 296 K) spectrum of $\text{TRISPHAT} \leftrightarrow \text{F5Me}^+$ (6:1). Iodide and tetrabutylammonium counter ions removed for clarity.

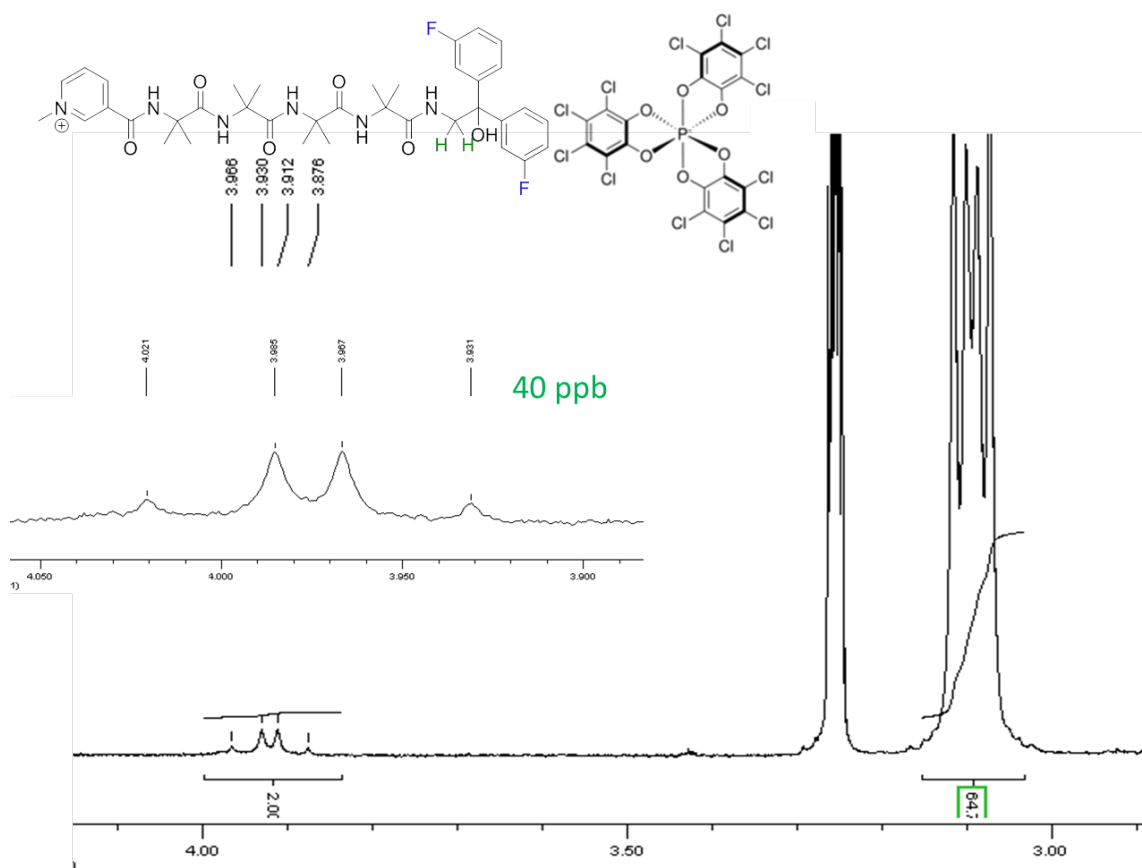


Figure S6. Partial ^1H NMR (400 MHz, $\text{CDCl}_3/\text{MeOH-d}_4$; 5/2, 296 K) spectrum of **TRISPHAT** ↔ **F5Me $^+$** (8:1). Iodide and tetrabutylammonium counter ions removed for clarity.

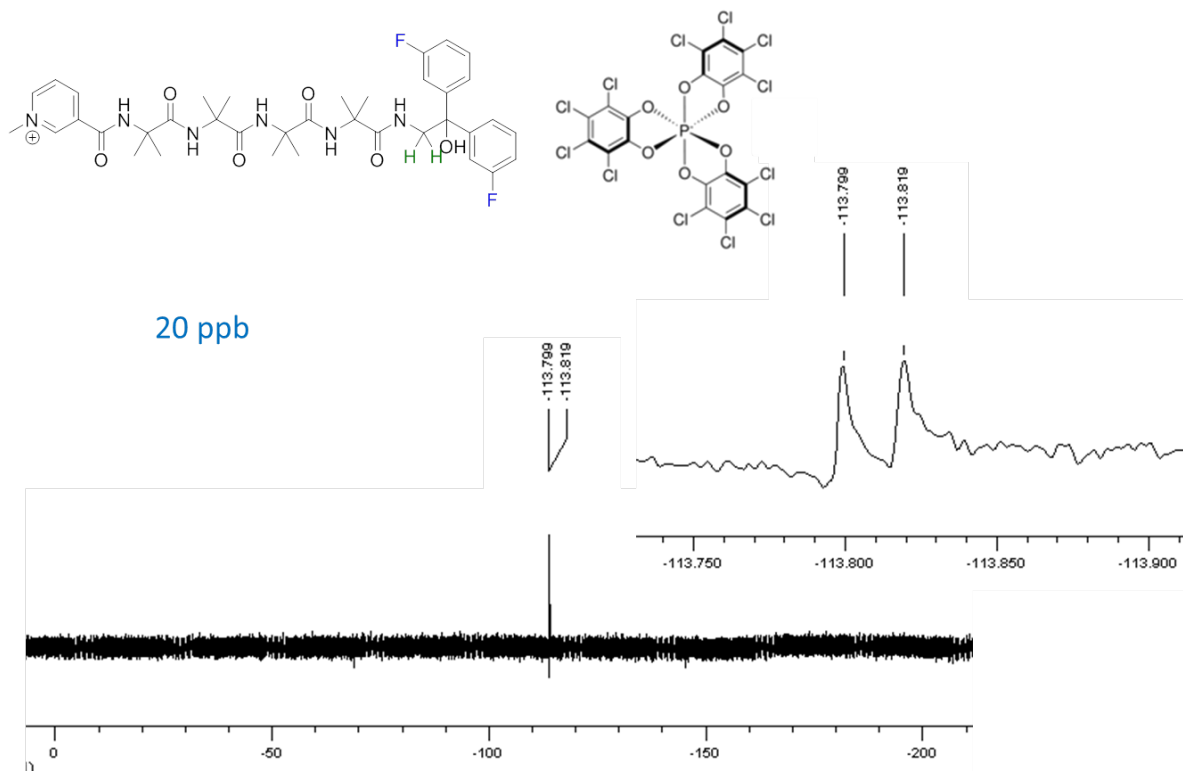


Figure S7. ^{19}F NMR (376 MHz, $\text{CDCl}_3/\text{MeOH-d}_4$; 5/2, 296 K) spectrum of **TRISPHAT** ↔ **F5Me $^+$** (8:1). Iodide and tetrabutylammonium counter ions removed for clarity.

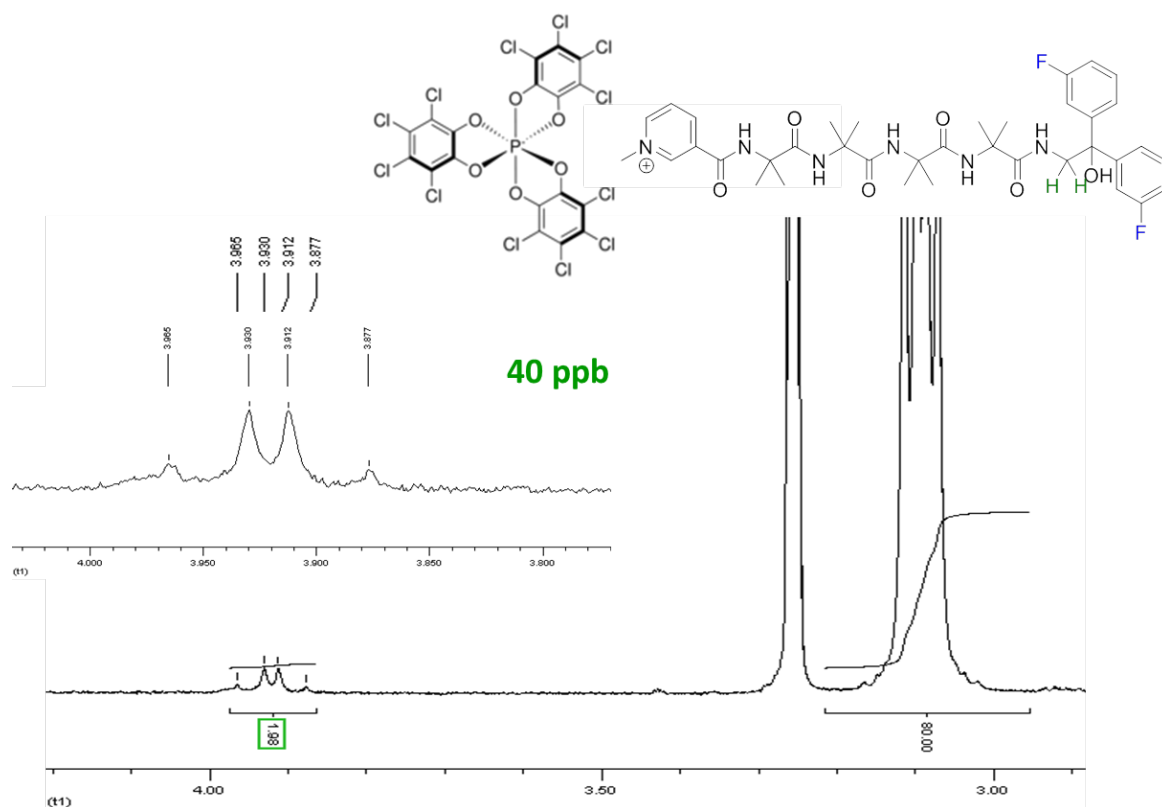


Figure S8. Partial ^1H NMR (400 MHz, $\text{CDCl}_3/\text{MeOH-d}_4$; 5/2, 296 K) spectrum of **TRISPHAT** \leftrightarrow **F5Me $^+$** (10:1). Iodide and tetrabutylammonium counter ions removed for clarity.

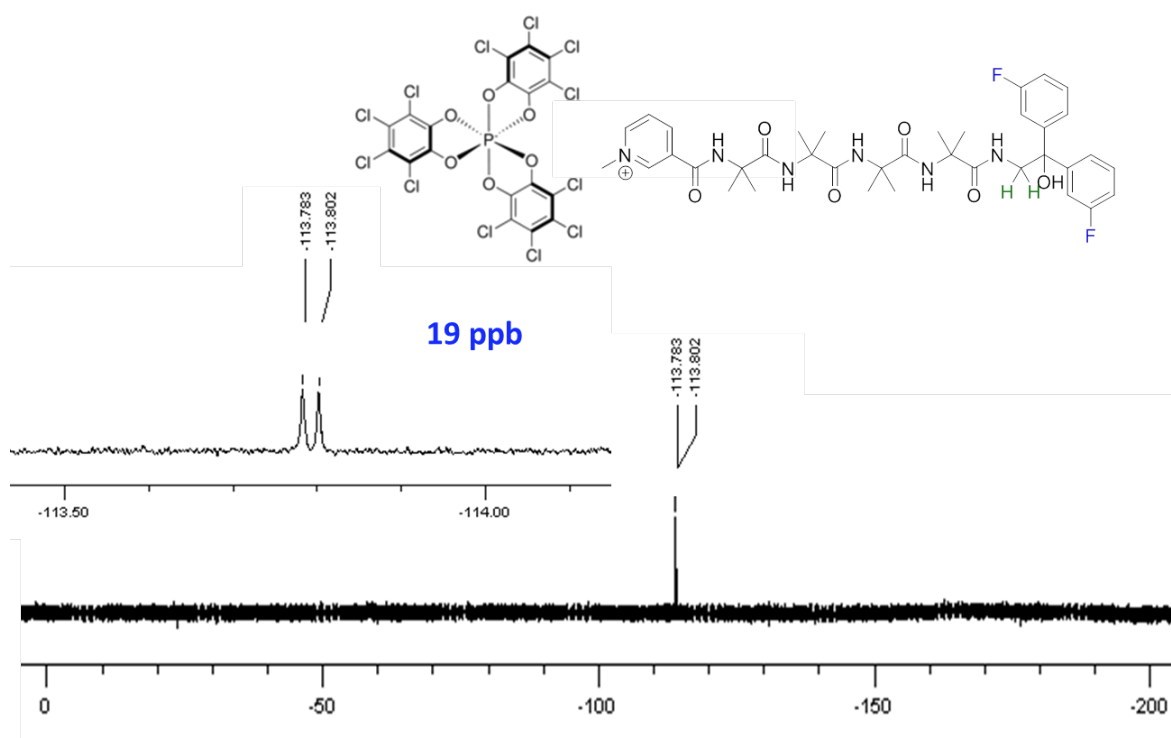


Figure S9. ^{19}F NMR (376 MHz, $\text{CDCl}_3/\text{MeOH-d}_4$; 5/2, 296 K) spectrum of **TRISPHAT** \leftrightarrow **F5Me $^+$** (10:1). Iodide and tetrabutylammonium counter ions removed for clarity.

BINPHAT (equiv.)	$\Delta\delta$ (ppb) of ^1H NMR reporter	$\Delta\delta$ (ppb) of ^{19}F NMR reporter
1	26	7
2	58	15
4	79	21
8	/	28

Table S3. Titration experiment $\text{BINPHAT} \leftrightarrow \text{F5Me}^+$

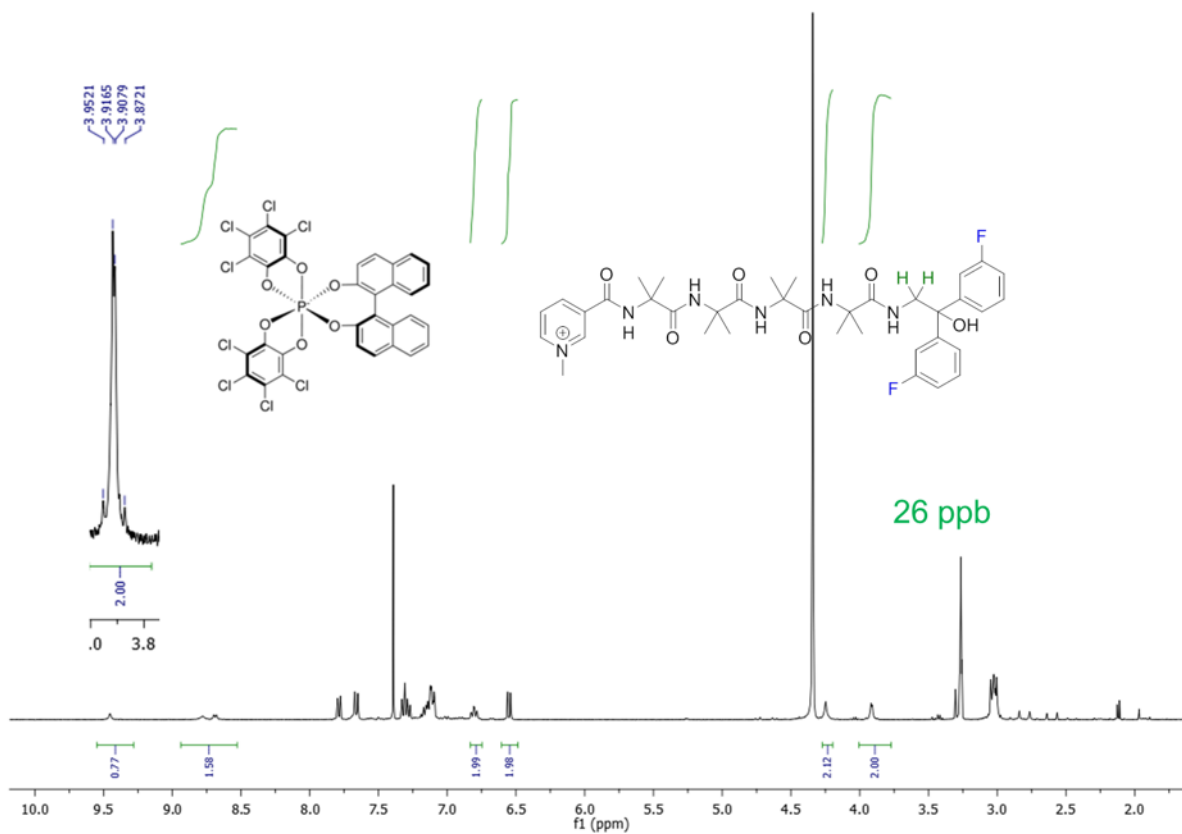


Figure S10. ^1H NMR (400 MHz, $\text{CDCl}_3/\text{MeOH-d}_4$; 5/2, 296 K) spectrum of $\text{BINPHAT} \leftrightarrow \text{F5Me}^+$ (1:1). Iodide and tetrabutylammonium counter ions removed for clarity.

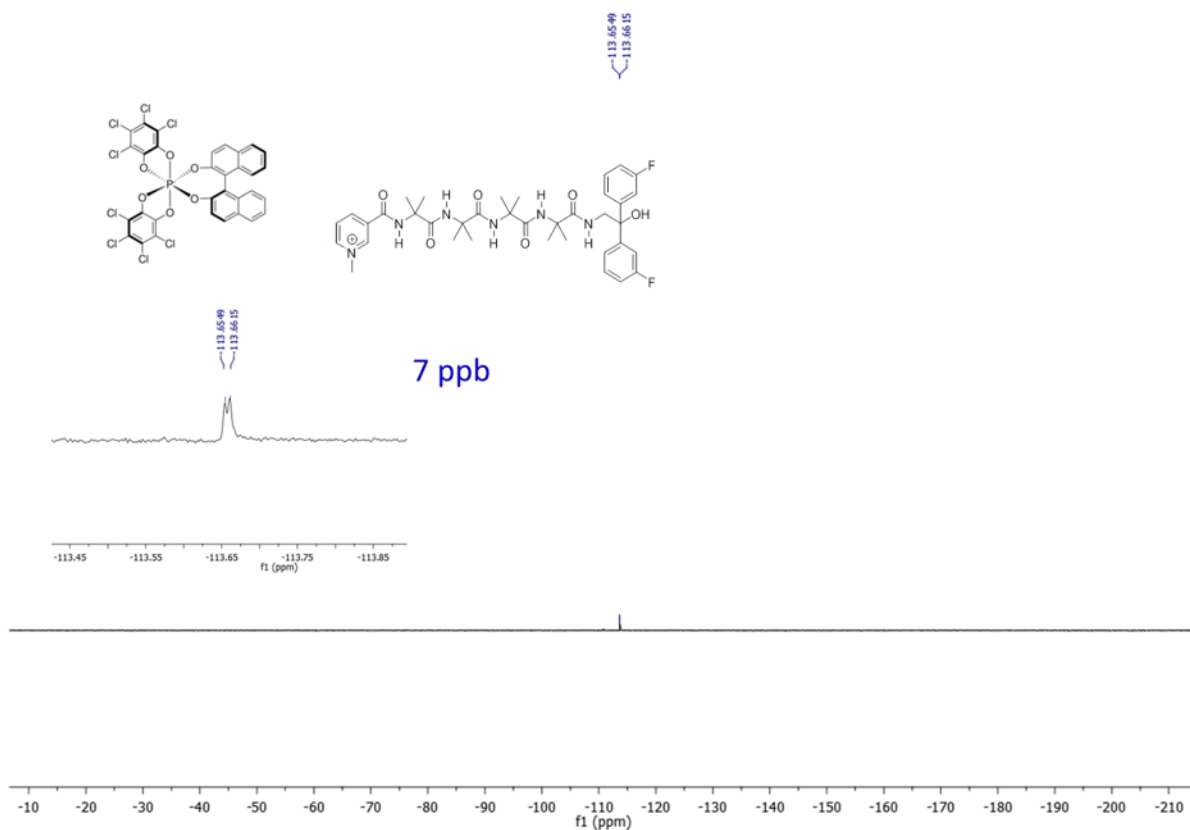


Figure S11. ^{19}F NMR (376 MHz, $\text{CDCl}_3/\text{MeOH-d}_4$; 5/2, 296 K) spectrum of $\text{BINPHAT} \leftrightarrow \text{F5Me}^+$ (1:1). Iodide and tetrabutylammonium counter ions removed for clarity.

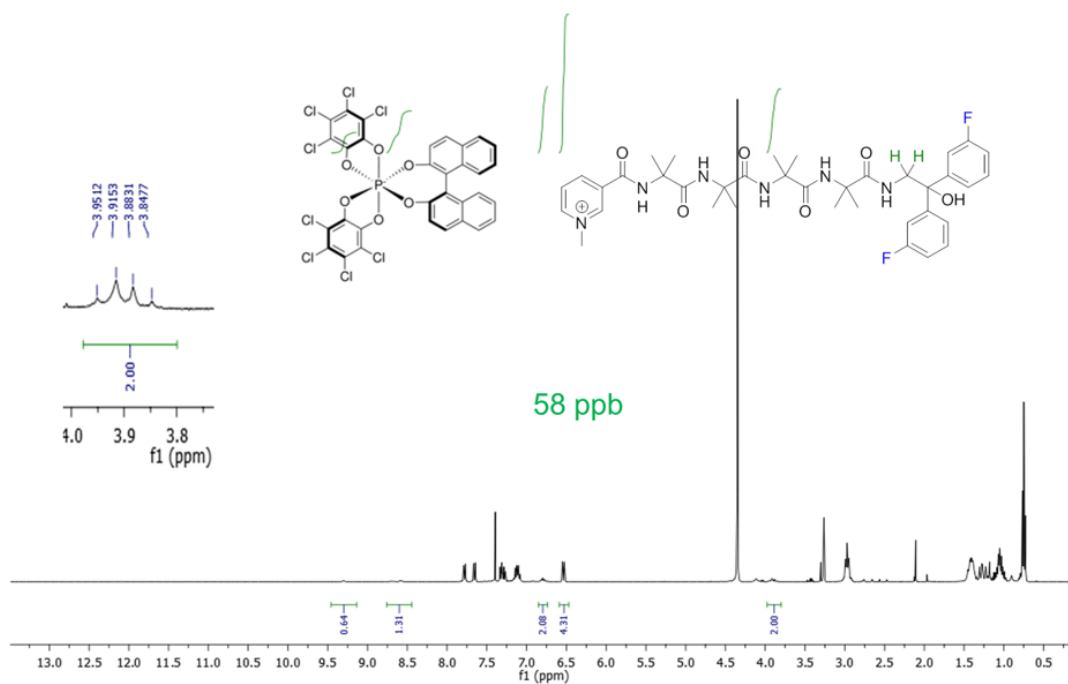


Figure S12. ^1H NMR (400 MHz, $\text{CDCl}_3/\text{MeOH-d}_4$; 5/2, 296 K) spectrum of $\text{BINPHAT} \leftrightarrow \text{F5Me}^+$ (2:1). Iodide and tetrabutylammonium counter ions removed for clarity.

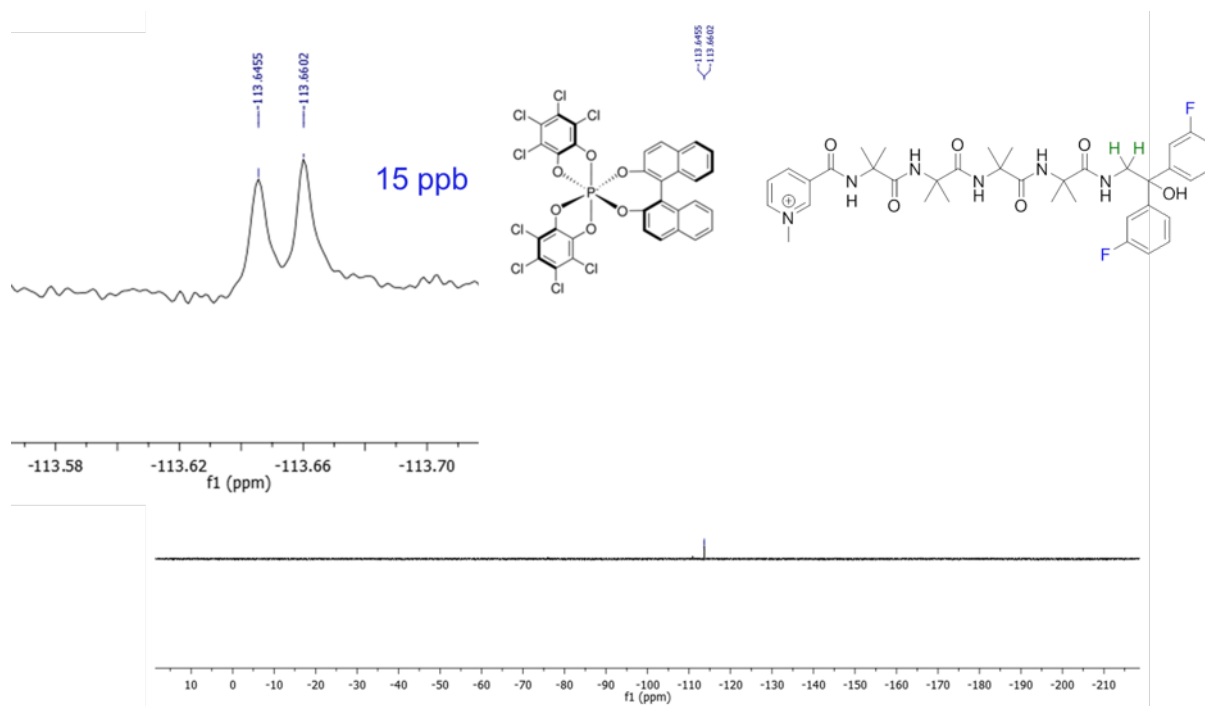


Figure S13. ^{19}F NMR (376 MHz, $\text{CDCl}_3/\text{MeOH-d}_4$; 5/2, 296 K) spectrum of BINPHAT ↔ F5Me⁺ (2:1). Iodide and tetrabutylammonium counter ions removed for clarity.

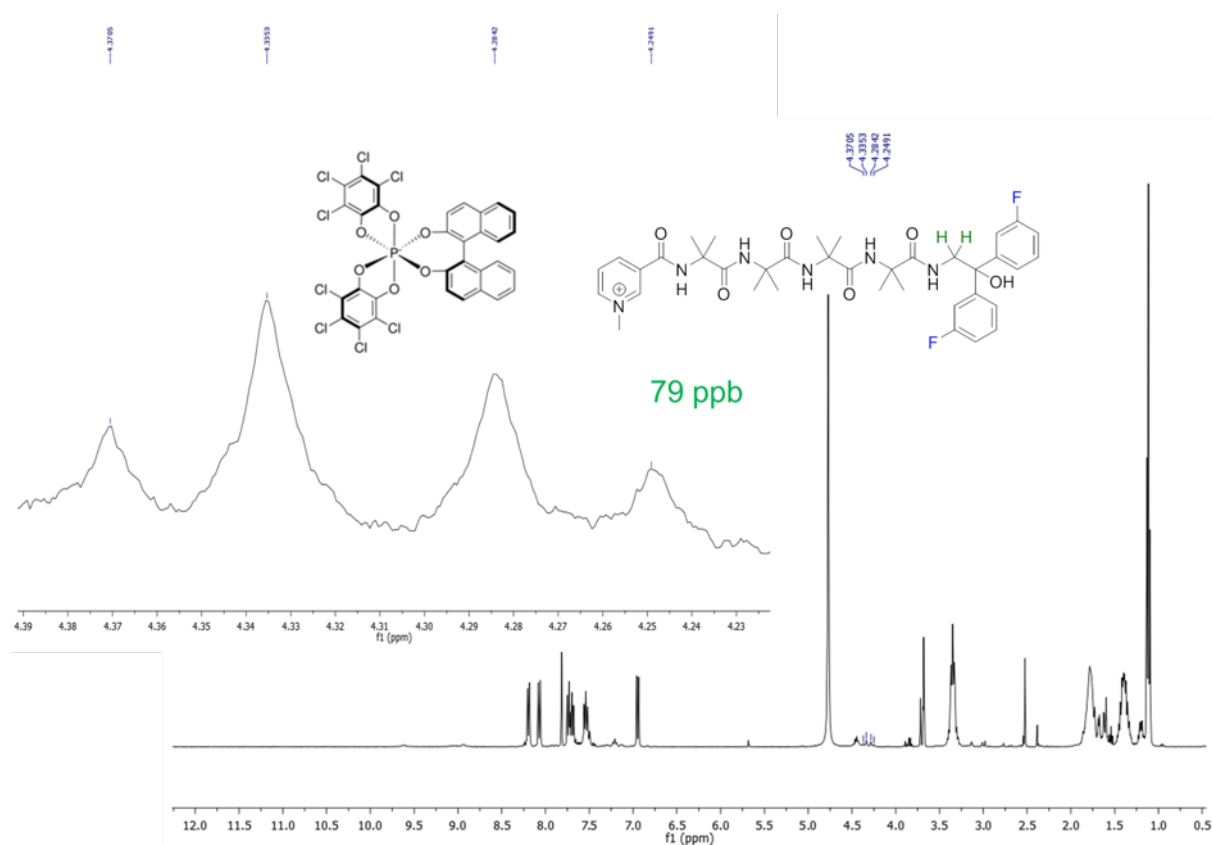


Figure S14. ^1H NMR (400 MHz, $\text{CDCl}_3/\text{MeOH-d}_4$; 5/2, 296 K) spectrum of BINPHAT ↔ F5Me⁺ (4:1). Iodide and tetrabutylammonium counter ions removed for clarity.

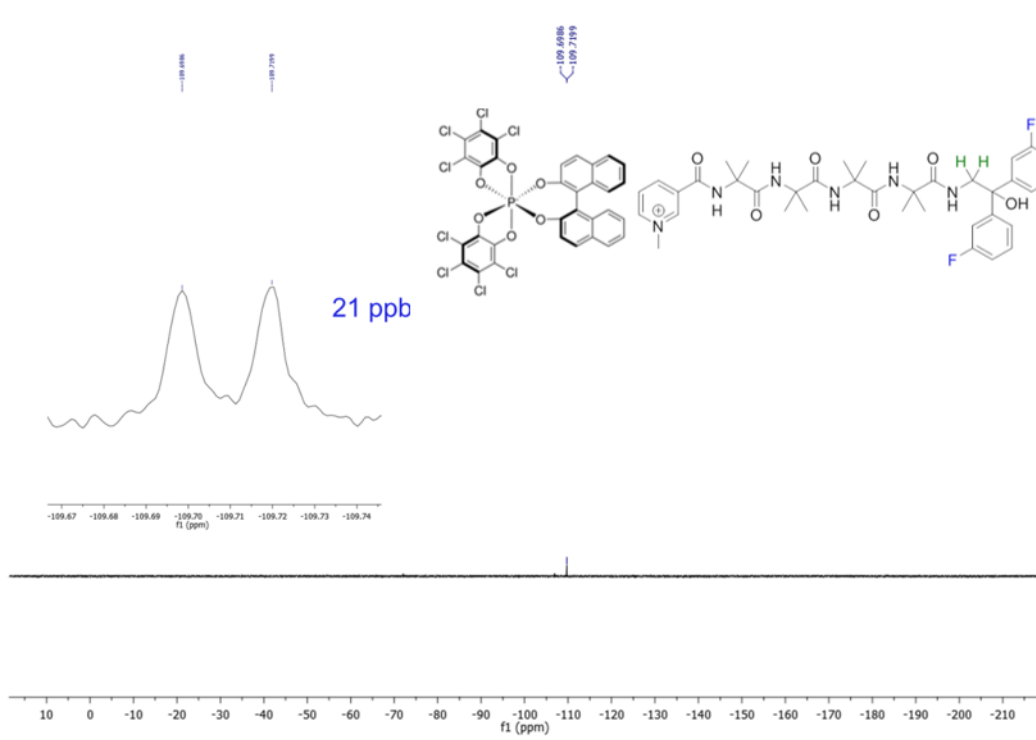


Figure S15. ^{19}F NMR (376 MHz, $\text{CDCl}_3/\text{MeOH-d}_4$; 5/2, 296 K) spectrum of $\text{BINPHAT} \leftrightarrow \text{F5Me}^+$ (4:1). Iodide and tetrabutylammonium counter ions removed for clarity.

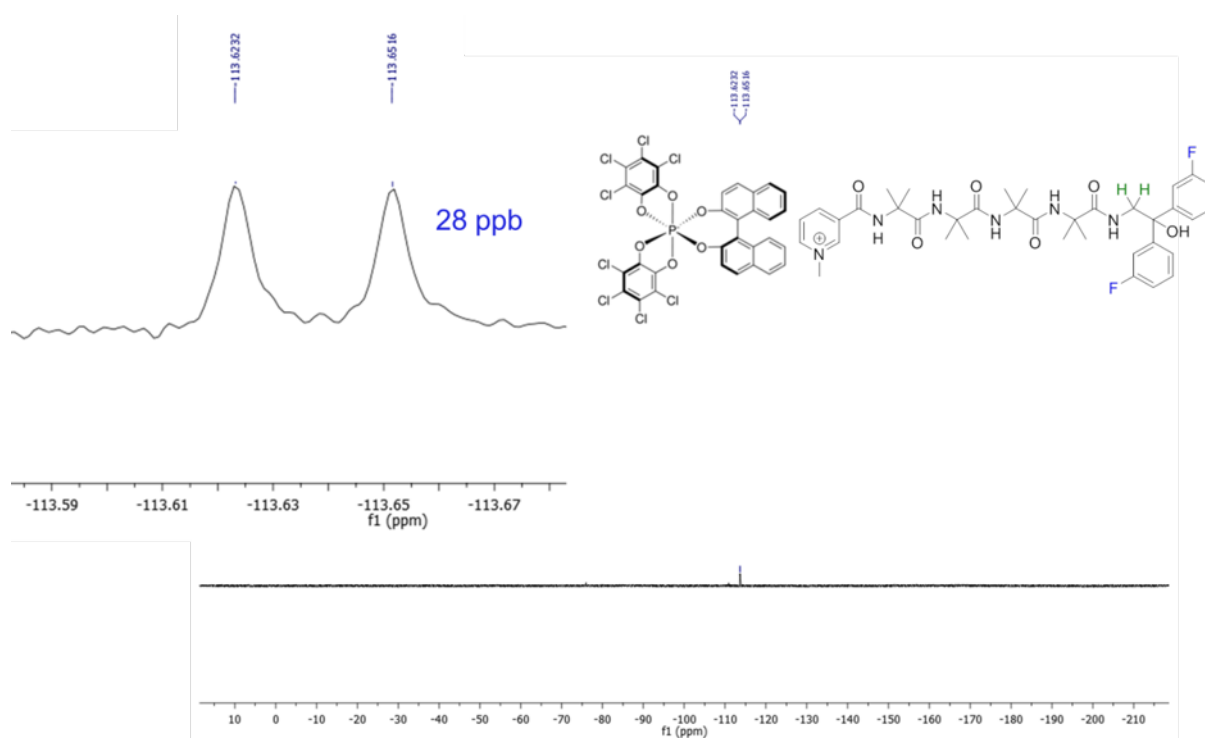


Figure S16. ^{19}F NMR (376 MHz, $\text{CDCl}_3/\text{MeOH-d}_4$; 5/2, 296 K) spectrum of $\text{BINPHAT} \leftrightarrow \text{F5Me}^+$ (8:1). Iodide and tetrabutylammonium counter ions removed for clarity.

TRISPHAT (equiv.)	$\Delta\delta$ (ppb) of ^1H NMR reporter	$\Delta\delta$ (ppb) of ^{19}F NMR reporter
6	0	0
10	/	0

Table S4. Titration experiment $\text{TRISPHAT} \leftrightarrow \text{F6Me}^+$

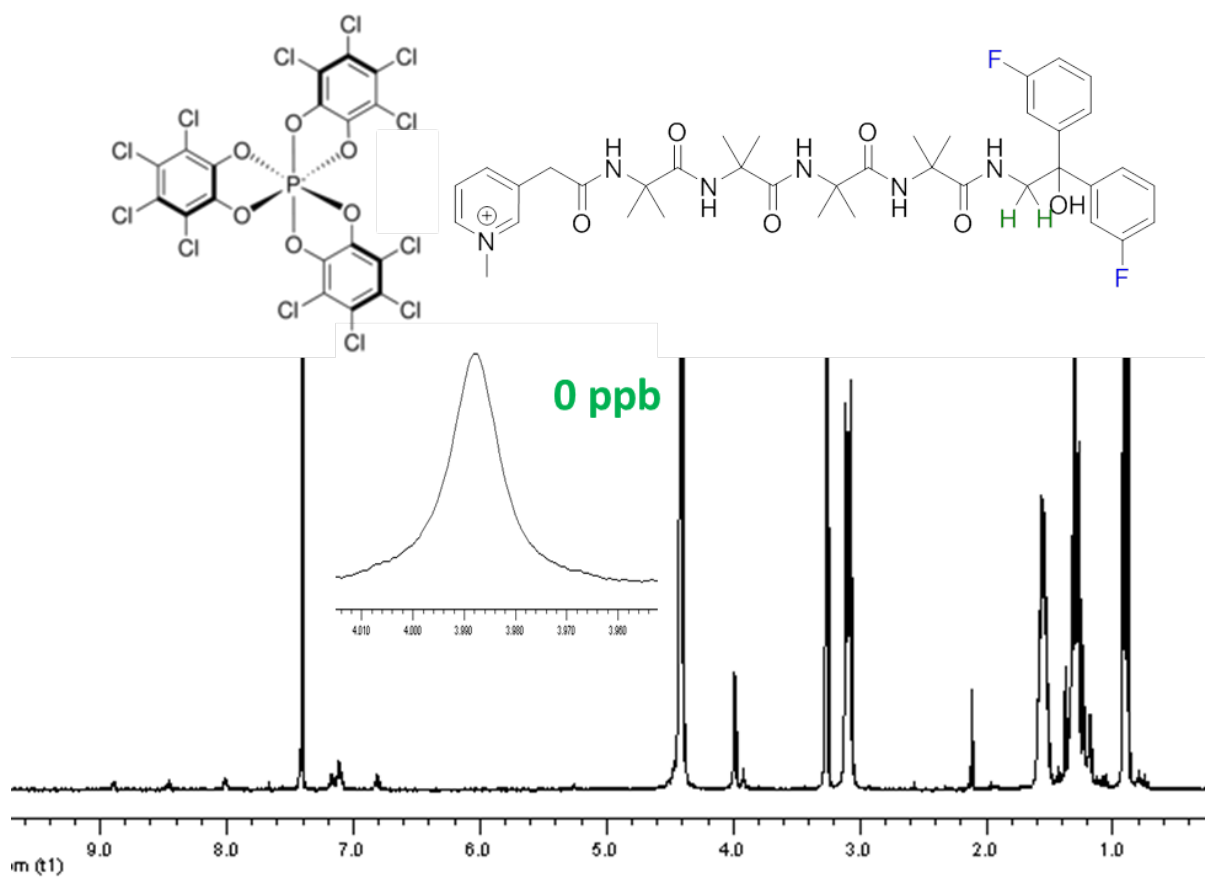


Figure S17. ^1H NMR (400 MHz, $\text{CDCl}_3/\text{MeOH-d}_4$; 5/2, 296 K) spectrum of $\text{TRISPHAT} \leftrightarrow \text{F6Me}^+$ (6:1). Iodide and tetrabutylammonium counter ions removed for clarity.

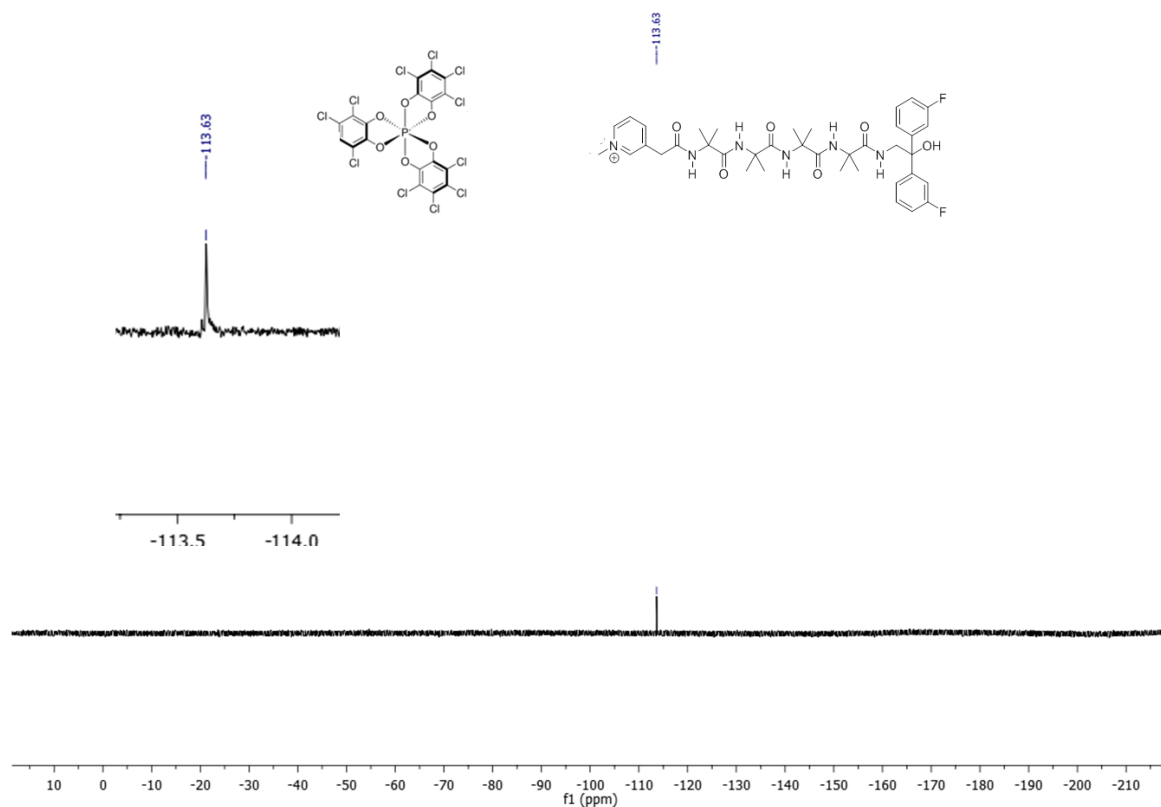


Figure S18. ^{19}F NMR (376 MHz, $\text{CDCl}_3/\text{MeOH-d}_4$; 5/2, 296 K) spectrum of **TRISPHAT** ↔ **F6Me⁺** (6:1). Iodide and tetrabutylammonium counter ions removed for clarity.

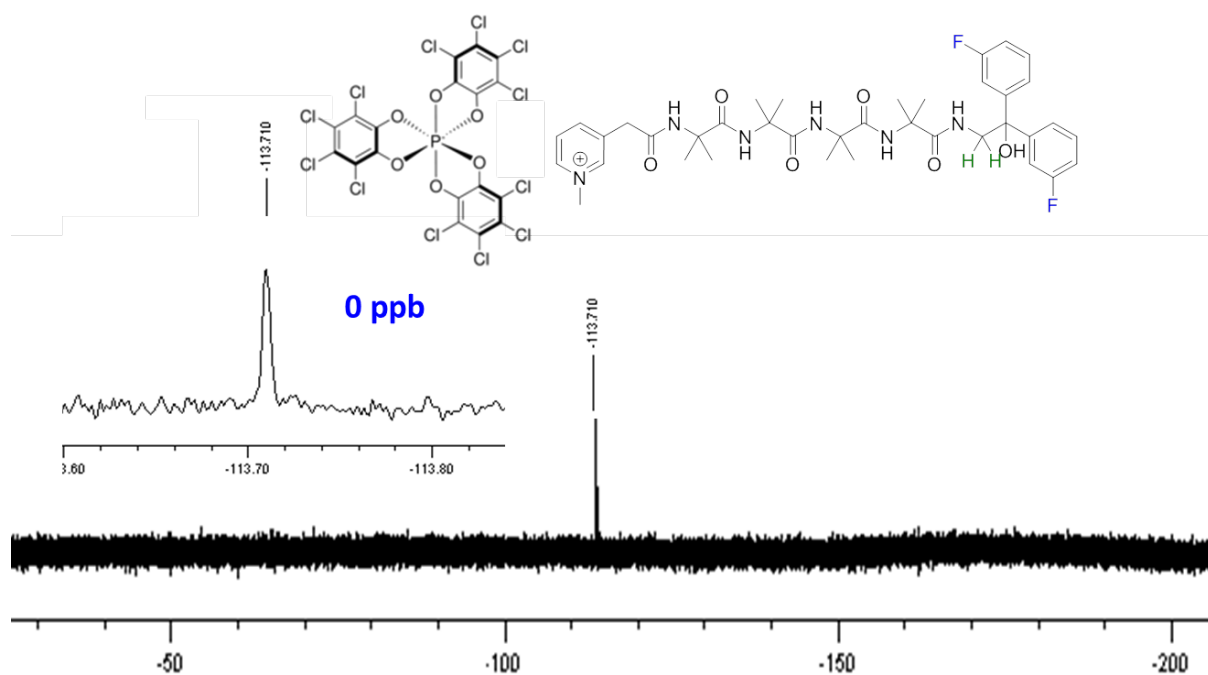


Figure S19. ^{19}F NMR (376 MHz, $\text{CDCl}_3/\text{MeOH-d}_4$; 5/2, 296 K) spectrum of **TRISPHAT** ↔ **F6Me⁺** (10:1). Iodide and tetrabutylammonium counter ions removed for clarity.

BINPHAT (equiv.)	$\Delta\delta$ (ppb) of ^1H NMR reporter	$\Delta\delta$ (ppb) of ^{19}F NMR reporter
1.5	0	8
2.5	0	9
4	36	12

Table S5. Titration experiment $\text{BINPHAT} \leftrightarrow \text{F6Me}^+$

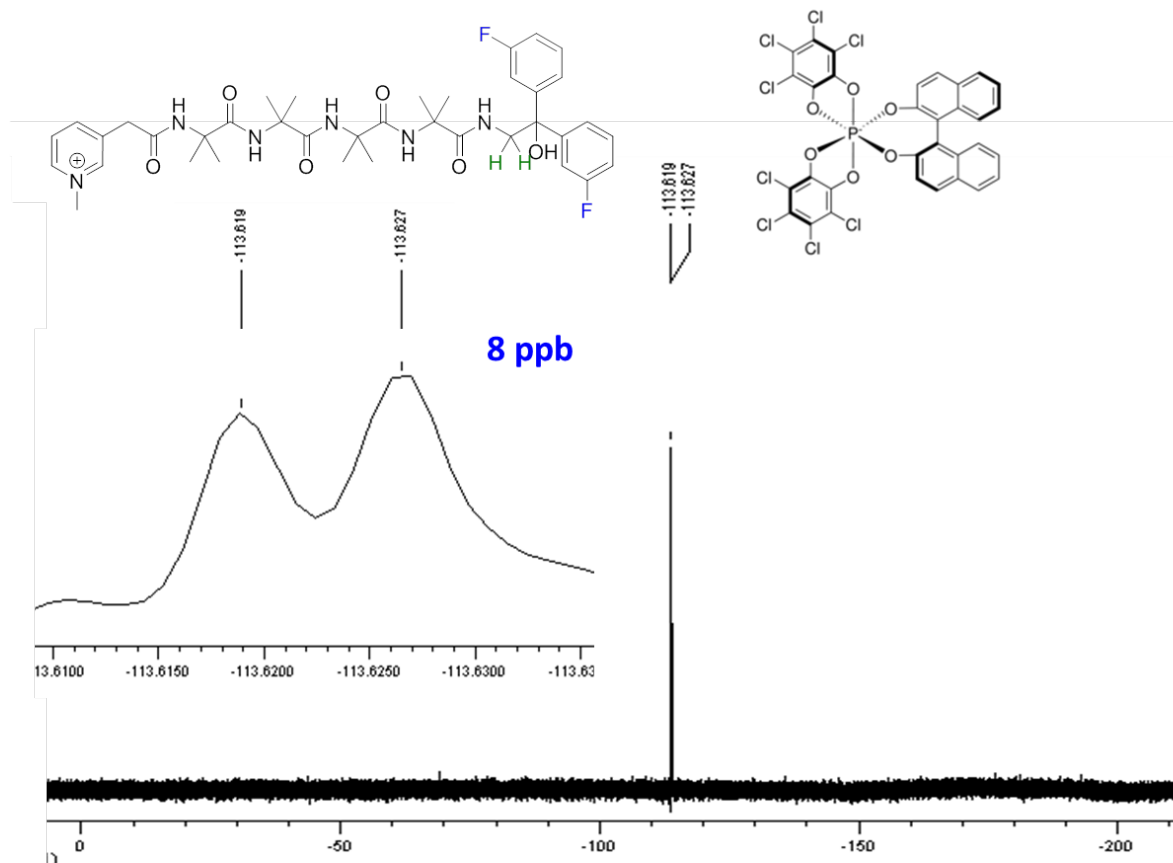


Figure S20. ^{19}F NMR (376 MHz, $\text{CDCl}_3/\text{MeOH-d}_4$; 5/2, 296 K) spectrum of $\text{BINPHAT} \leftrightarrow \text{F6Me}^+$ (1.5:1). Iodide and tetrabutylammonium counter ions removed for clarity.

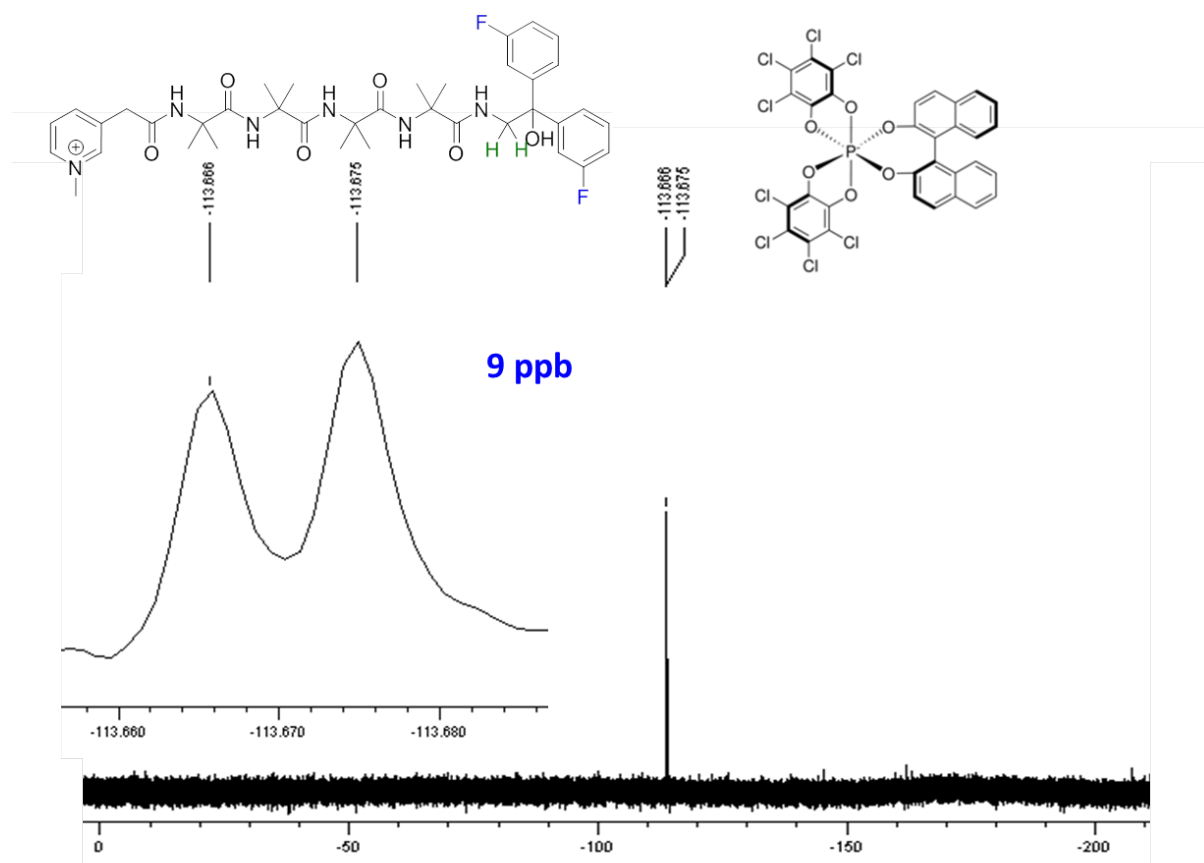


Figure S21. ^{19}F NMR (376 MHz, $\text{CDCl}_3/\text{MeOH-}d_4$; 5/2, 296 K) spectrum of $\text{BINPHAT} \leftrightarrow \text{F6Me}^+$ (2.5:1). Iodide and tetrabutylammonium counter ions removed for clarity.

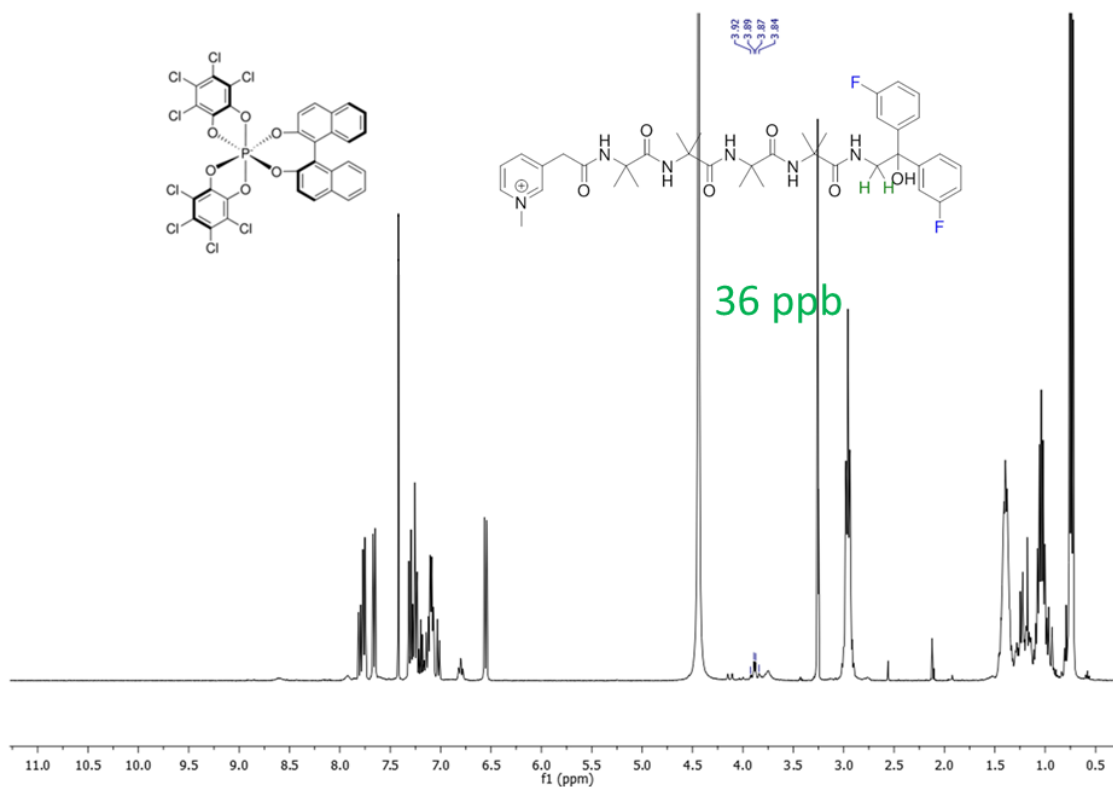


Figure S22. ^1H NMR (400 MHz, $\text{CDCl}_3/\text{MeOH-}d_4$; 5/2, 296 K) spectrum of $\text{BINPHAT} \leftrightarrow \text{F6Me}^+$ (2.5:1). Iodide and tetrabutylammonium counter ions removed for clarity.

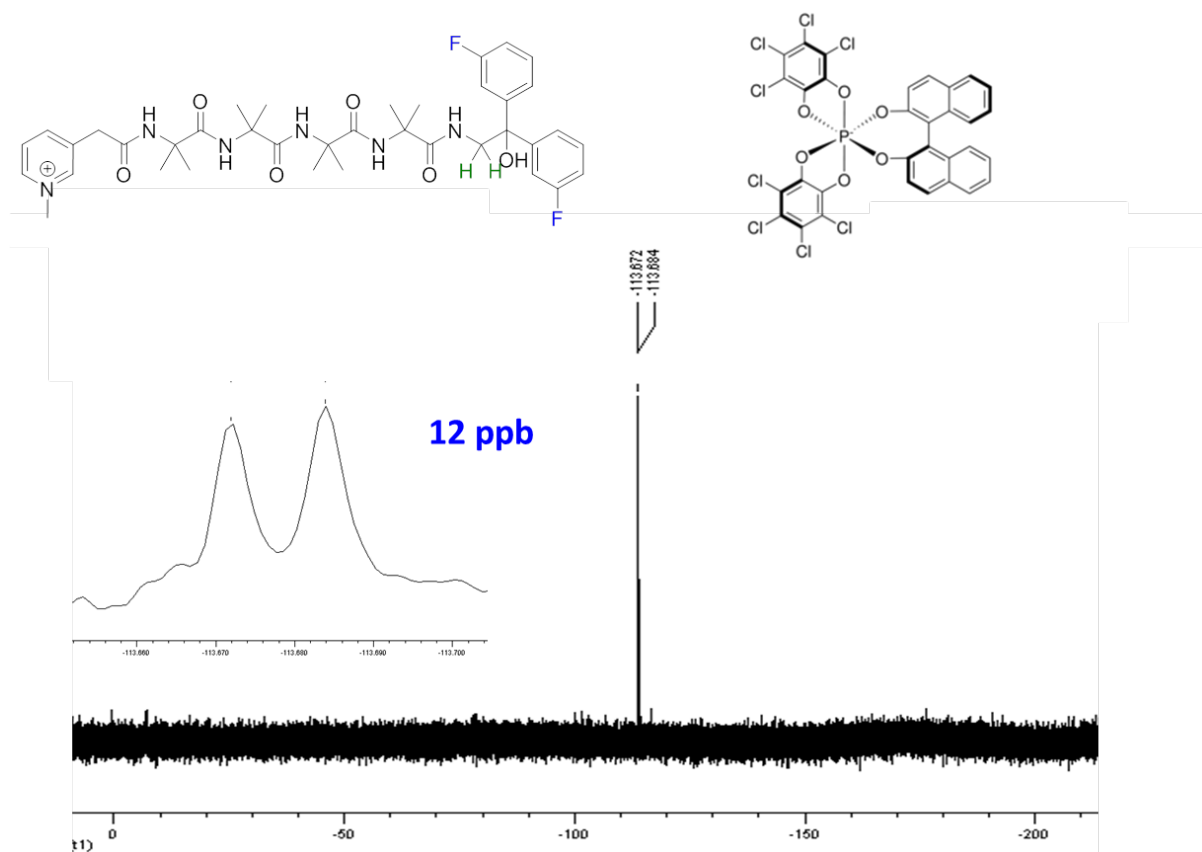
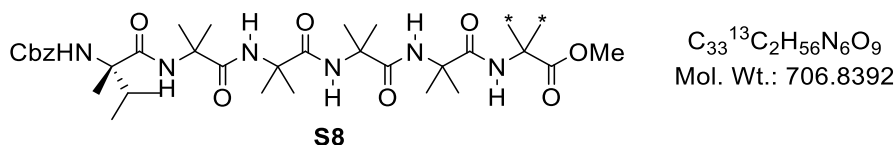


Figure S23. ¹⁹F NMR (400 MHz, CDCl₃/MeOH-d₄; 5/2, 296 K) spectrum of BINPHAT ↔ F6Me⁺ (4:1). Iodide and tetrabutylammonium counter ions removed for clarity.

IV. Estimation of the helical excess

• Synthesis of foldamer S9

Step 1: Z-L-(α Me)Val-Aib₄Aib**OMe (S8)

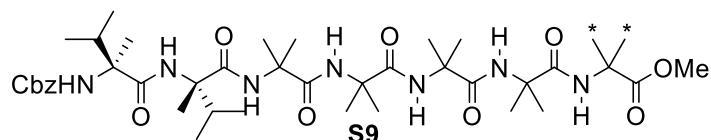


$C_{33}^{13}C_2H_{56}N_6O_9$
Mol. Wt.: 706.8392

(a) *Acid fluoride formation*: To a solution of Z-L-(α Me)ValOH (29 mg, 0.11 mmol) in CH_2Cl_2 (1 mL) at RT were added pyridine (9 μ L, 0.11 mmol) and fluoro-*N,N,N',N'*-tetramethylformamidinium hexafluorophosphate (43 mg, 0.16 mmol). After stirring for 3 h at RT, the reaction was diluted with CH_2Cl_2 and the organic phase was washed three times with ice-cold H_2O , dried over $MgSO_4$, filtered and concentrated under reduced pressure. The resulting acid fluoride crude material was used in the next step without further purification.

(b) *Amide bond formation*: To a solution of $H_2NAib_4Aib^{**}OMe$ **F1** (25 mg, 0.05 mmol) in CH_2Cl_2 (1.5 mL) at RT were added *N,N*-diisopropylethylamine (20 μ L, 0.11 mmol) and a solution of crude step (a) in CH_2Cl_2 (0.5 mL). The reaction was stirred at RT for 5 days. After this time, the reaction was diluted with CH_2Cl_2 , washed with an aqueous solution of $KHSO_4$ (5 Wt%), a saturated aqueous solution of $NaHCO_3$, brine, dried over $MgSO_4$, filtered and concentrated under reduced pressure. Before all solvent being removed, Et_2O was added and a white precipitate was formed. After filtration, the desired product **S8** (30 mg, 79%) was isolated as a white solid; $[\alpha]^{25}_D +38.0$ (c 1.0, $CHCl_3$); **M.p.** = 194-195 $^{\circ}C$; 1H NMR (400 MHz, $CDCl_3$) δ 7.60 (s, 1H, NH), 7.46 (s, 1H, NH), 7.44 (s, 1H, NH), 7.36-7.30 (m, 5H, ^{Ar}CH), 7.27 (s, 1H, NH), 6.32 (s, 1H, NH), 5.40 (s, 1H, NH), 5.16 (d, 1H, AB syst, $J_{AB} = 12.0$ Hz, CH_2), 5.01 (d, 1H, AB syst, $J_{AB} = 12.0$ Hz, CH_2), 3.64 (s, 3H, OCH_3), 1.96-1.87 (m, 1H, CH), 1.52 (dd, 3H, $^1J_{C-H} = 129.2$ and $^3J_{C-H} = 4.0$ Hz, $^{13}CH_3$), 1.50 (s, 3H, CH_3), 1.48 (dd, 3H, $^1J_{C-H} = 129.2$ and $^3J_{C-H} = 4.0$ Hz, $^{13}CH_3$), 1.47-1.37 (m, 21H, 7^*CH_3), 1.19 (s, 3H, CH_3), 0.96 (d, 3H, $J = 7.0$ Hz, CH_3), 0.93 (d, 3H, $J = 7.0$ Hz, CH_3); ^{13}C NMR (100 MHz, $CDCl_3$) ($C(^{13}CH_3)_2$ signal is not observed), δ 175.9 (CO), 175.3 (CO), 175.0 (CO), 174.2 (CO), 174.0 (CO), 172.9 (CO), 156.3 (CO), 136.2 (C), 128.95 (2^*CH), 128.89 (2^*CH), 128.4 (CH), 67.7 (CH_2), 63.2 (C), 57.02 (C), 56.97 (C), 56.83 (C), 56.80 (C), 52.1 (OCH_3), 35.7 (CH), 27.4 (CH_3), 27.0 (CH_3), 26.96 (CH_3), 26.85 (CH_3), 25.76 ($^{13}CH_3$), 24.5 ($^{13}CH_3$), 23.75 (CH_3), 23.70 (CH_3), 23.54 (CH_3), 23.49 (CH_3), 17.8 (CH_3), 17.5 (CH_3), 17.4 (CH_3); FTIR (ν_{max} cm^{-1}) 3304, 2980, 2937, 1724, 1703, 1651, 1527, 1453, 1381, 1263. HRMS calcd for $C_{33}^{13}C_2H_{57}N_9O_6$ $[M+H]^+$: 707.4249. Found 707.4245.

Step2: Z-L-(α Me)Val₂Aib₄AibOMe (S9)**



C₃₉¹³C₂H₆₇N₇O₁₀
Mol. Wt.: 819.9969

(a) *Cbz deprotection*: To a solution of Z-L-(α Me)ValAib₄Aib**OMe **S8** (30 mg, 0.04 mmol) in MeOH (5 mL) at RT and under inert atmosphere was added Pd/C (3 mg, 0.003 mmol, 10 Wt%). The atmosphere was purged with hydrogen and the reaction was stirred for 12 h under hydrogen (1 atm). After this time, the reaction was filtered through a Celite (MeOH) and the filtrate was concentrated under reduced pressure. The crude residue was dissolved in CH₂Cl₂, washed with aqueous saturated solution of NaHCO₃, brine, dried over MgSO₄, filtered and concentrated under reduced pressure to give H-L-(α Me)ValAib₄Aib**OMe (22 mg, 95%) as a white solid which was used in the next step without further purification.

(b) *Acid fluoride formation*: To a solution of Z-L-(α Me)ValOH (23 mg, 0.09 mmol) in CH₂Cl₂ (1 mL) at RT were added pyridine (7 μ L, 0.11 mmol) and fluoro-*N,N,N',N'*-tetramethylformamidinium hexafluorophosphate (36 mg, 0.13 mmol). After stirring for 3 h at RT, the reaction was diluted with CH₂Cl₂ and the organic phase was washed three times with ice-cold H₂O, dried over MgSO₄, filtered and concentrated under reduced pressure. The resulting acid fluoride crude material was used in the next step without further purification.

(c) *amide bond formation*: To a solution of H-L-(α Me)ValAib₄Aib**OMe (22 mg, 0.042 mmol) in CH₂Cl₂ (1.5 mL) at RT were added *N,N*-diisopropylethylamine (14 μ L, 0.083 mmol) and a solution of crude step (b) in CH₂Cl₂ (0.5 mL). The reaction was stirred at RT for 5 days. After this time, the reaction was diluted with CH₂Cl₂, washed with an aqueous solution of KHSO₄ (5 Wt%), a saturated aqueous solution of NaHCO₃, brine, dried over MgSO₄, filtered and concentrated under reduced pressure. The crude residue was purified by flash chromatography on silica gel (gradient starting from 70:30 to 40:60 / petroleum ether:EtOAc) to give **S9** (20 mg, 61%) as a white solid; [α]_D²⁵ +37.0 (c 1.0, CHCl₃); **M.p.** = 247-248 °C; **¹H NMR (400 MHz, CDCl₃)** δ 7.63 (br s, 2H, NH), 7.48 (s, 1H, NH), 7.40 (s, 1H, NH), 7.34-7.27 (br s, 6H, 5*^{Ar}CH and NH), 6.28 (s, 1H, NH), 5.15 (s, 1H, NH), 5.12 (d, 1H, AB syst, J_{AB} = 12.0 Hz, CH₂), 4.96 (d, 1H, AB syst, J_{AB} = 12.0 Hz, CH₂), 3.61 (s, 3H, OCH₃), 1.84-1.74 (m, 1H, CH), 1.62-1.56 (m, 1H, CH), 1.49 (dd, 3H, $^1J_{C-H}$ = 129.2 and $^3J_{C-H}$ = 4.0 Hz, ¹³CH₃), 1.48 (s, 3H, CH₃), 1.44 (dd, 3H, $^1J_{C-H}$ = 129.2 and $^3J_{C-H}$ = 4.0 Hz, ¹³CH₃), 1.45-1.35 (m, 24H, 8*CH₃), 1.33 (s, 3H, CH₃), 0.92 (d, 3H, J = 7.0 Hz, CH₃), 0.90 (d, 3H, J = 7.0 Hz, CH₃), 0.72 (d, 3H, J = 7.0 Hz, CH₃), 0.71 (d, 3H, J = 7.0 Hz, CH₃); **¹³C NMR (100 MHz, CDCl₃)** δ 175.9 (CO), 175.8 (CO), 175.2 (CO), 175.1 (CO), 174.4 (CO), 172.5 (2*CO), 156.4 (CO), 135.9 (C), 128.9 (3*CH), 128.8 (2*CH), 67.8 (CH₂), 63.6 (C), 62.5 (C), 57.05 (C), 56.96 (C), 56.87 (C), 56.77 (C), 55.9 (t, C(¹³CH₃)₂, J_{C-C} = 36.5 Hz), 52.1 (OCH₃), 36.2 (CH), 35.9 (CH), 28.0 (CH₃), 27.5 (CH₃), 27.4 (CH₃), 27.3 (CH₃), 25.9 (¹³CH₃), 24.3 (¹³CH₃), 23.1 (2*CH₃), 23.0 (CH₃), 22.9 (CH₃), 18.26 (CH₃), 18.22 (CH₃), 17.5 (CH₃), 17.4 (CH₃), 17.23 (CH₃), 17.17 (CH₃); **FTIR (ν_{max} cm⁻¹)** 3370, 2974, 2927, 1734, 1703, 1684, 1661, 1641, 1522, 1459, 1384, 1260. **HRMS** calcd for C₃₉¹³C₂H₆₈N₇O₁₀ [M+H]⁺: 820.5089. Found 820.5086.

• Dilution study of foldamer **S9** in CDCl₃ at 296 K

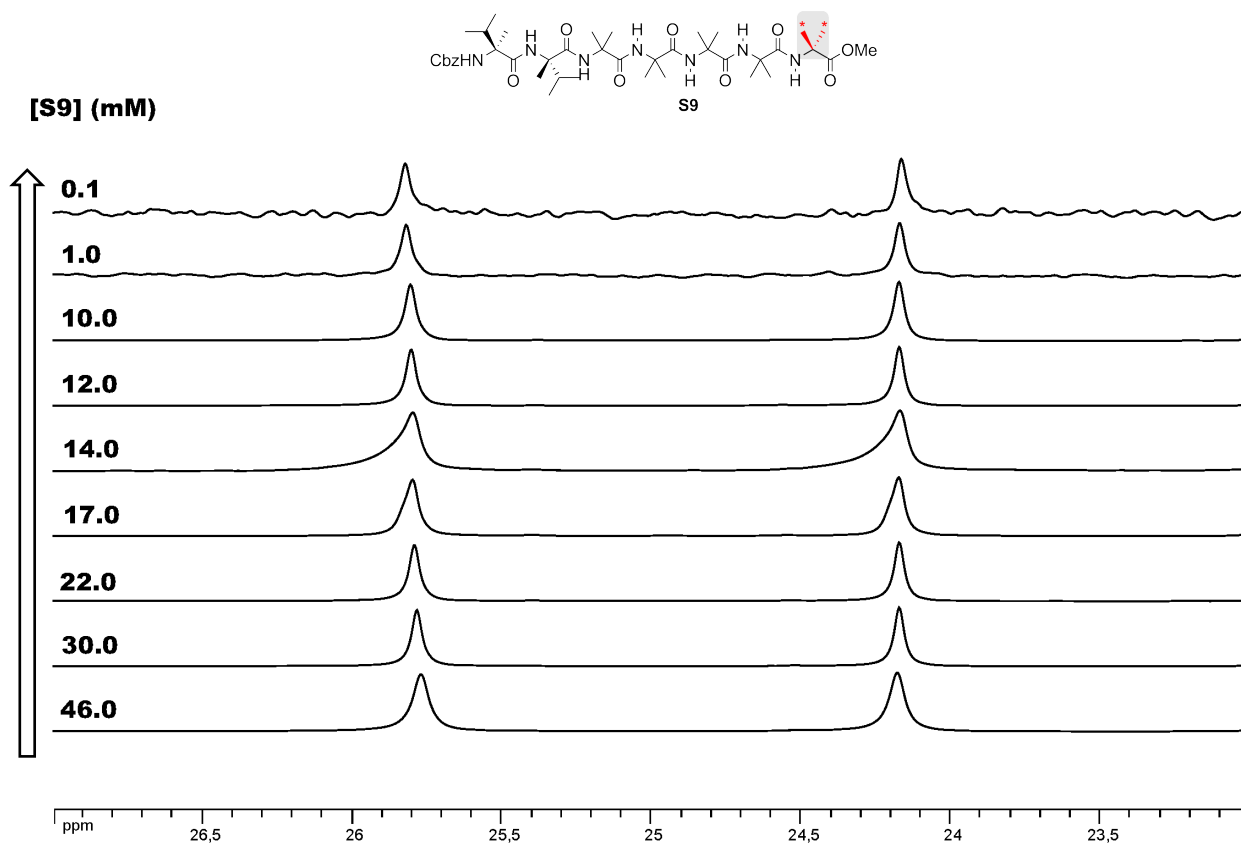


Figure S24. Dilution experiment: portions of the ¹³C NMR (100 MHz, CDCl₃) spectra of foldamer **S9** at 296 K; [S9] = 46.0 → 0.1 mM.

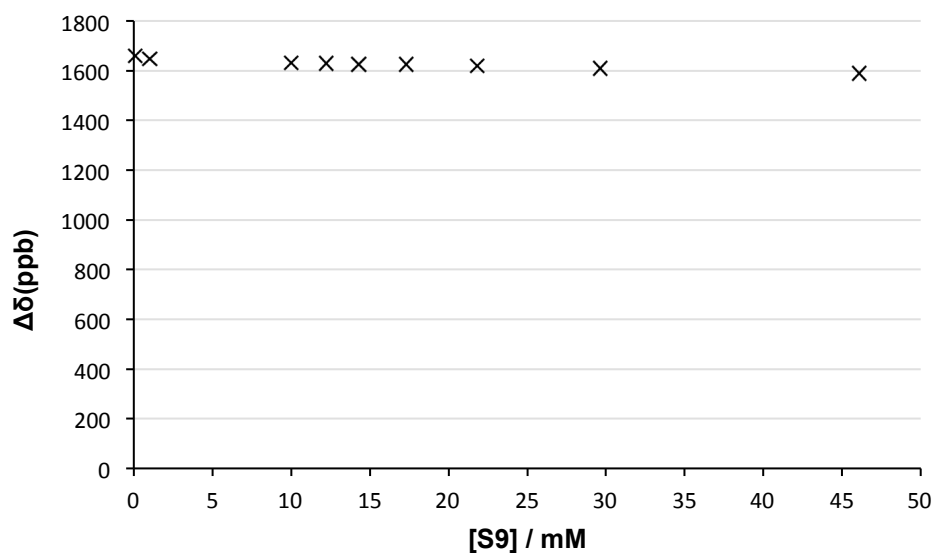


Figure S25. Plot the anisochronicity ($\Delta\delta$, ppb) of the two diastereotopic ¹³CH₃ signals of the NMR probe in foldamer **S9** vs [S9] (mM) recorded in CDCl₃ at 296 K.

• Variable temperature experiments of foldamer **S10** in CDCl₃ at different concentrations

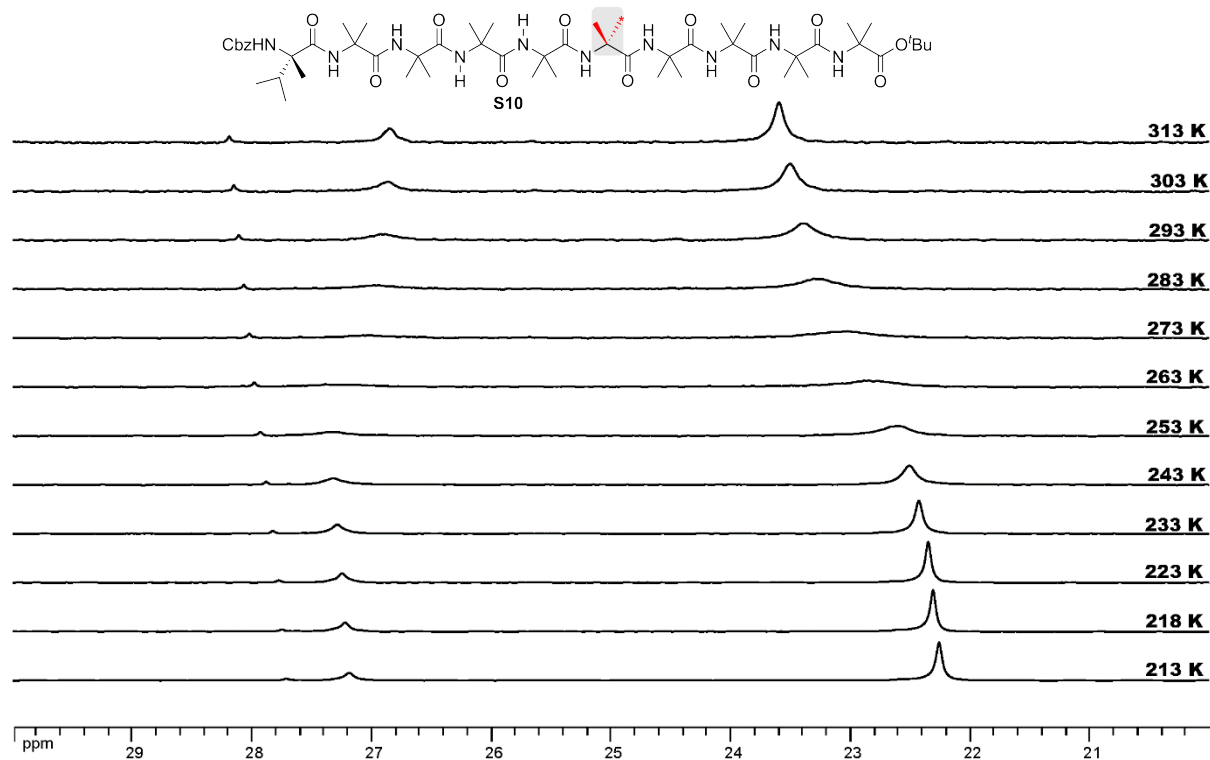


Figure S26. Variable temperature experiment: portions of the ¹³C NMR (125 MHz, CDCl₃) spectra of foldamer **S10**; [**S10**] = 10 mM.

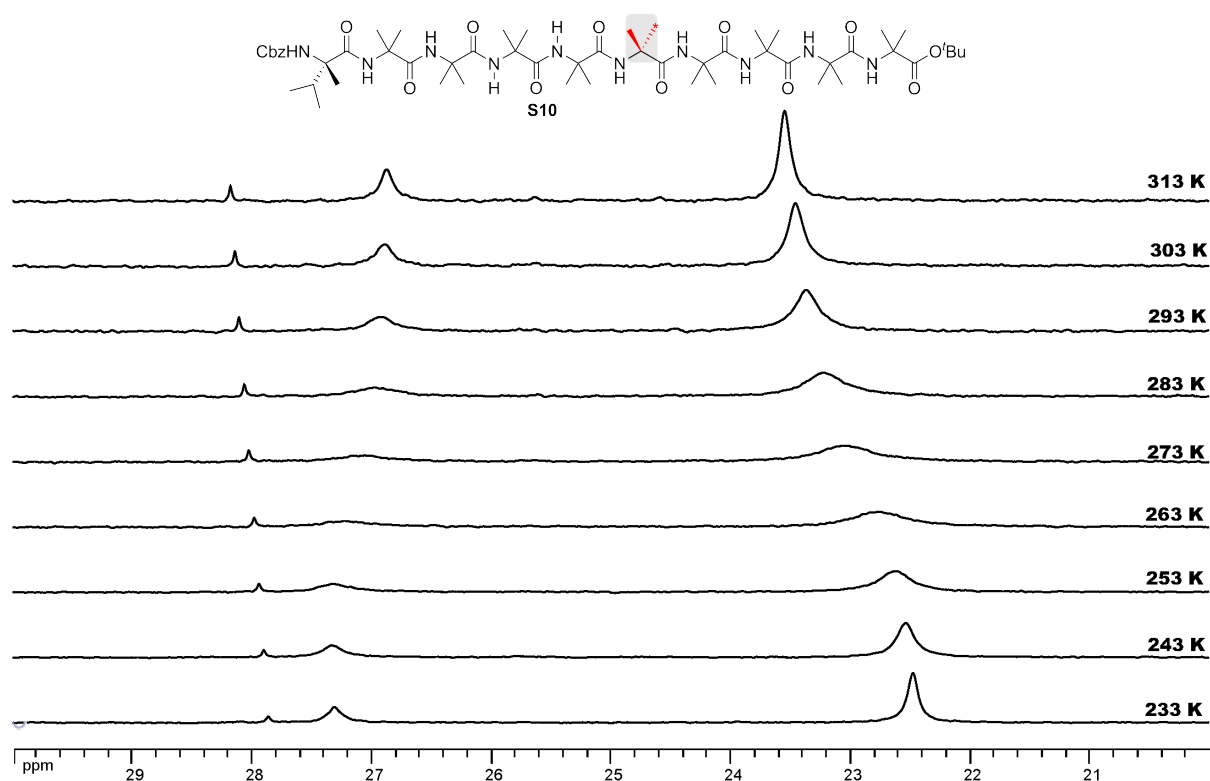


Figure S27. Variable temperature experiment: portions of the ¹³C NMR (125 MHz, CDCl₃) spectra of foldamer **S10**; [**S10**] = 2.5 mM.

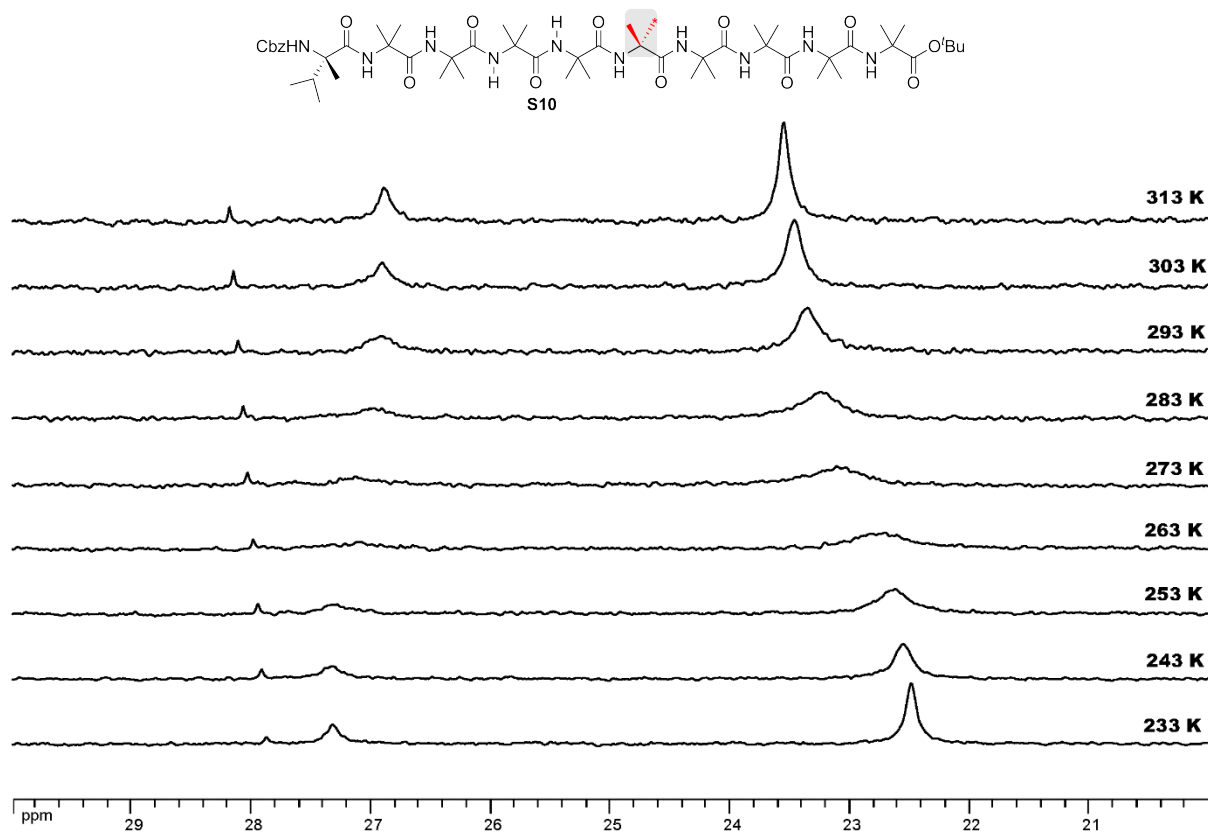


Figure S28. Variable temperature experiment: portions of the ^{13}C NMR (125 MHz, CDCl_3) spectra of foldamer **S10**; $[\text{S10}] = 0.5 \text{ mM}$.

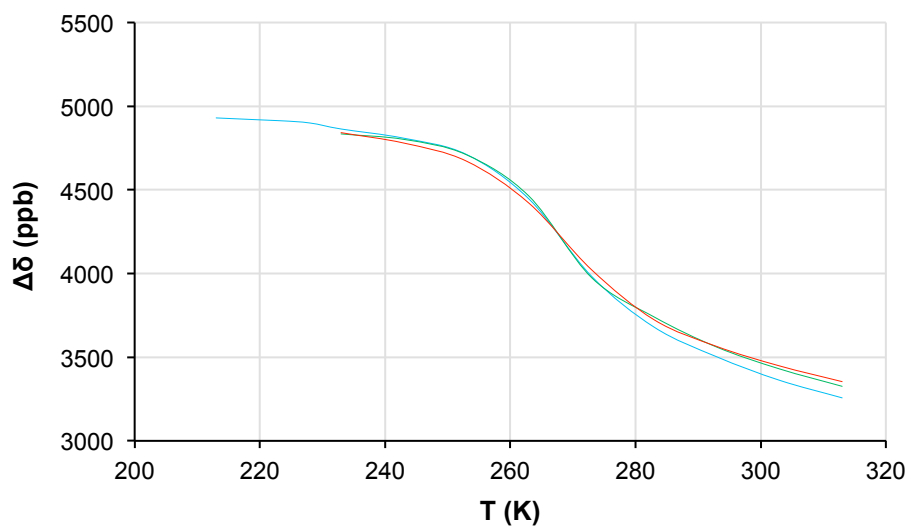


Figure S29. Plot of the anisochronicity ($\Delta\delta$, ppb) of the two diastereotopic $^{13}\text{CH}_3$ signals of the NMR probe in foldamer **S10** vs the temperature (T , K) recorded in CDCl_3 at 296 K; (—) $[\text{S10}] = 10 \text{ mM}$; (—) $[\text{S10}] = 2.5 \text{ mM}$; (—) $[\text{S10}] = 0.5 \text{ mM}$.

Coalescence was observed between 260 and 280 K (Figures S25, S26 and S27) and the helical excess at 293 K was determined in each case using the formula $\text{h.e.} = (\Delta\delta_{\text{fast}} \text{ at } 293 \text{ K} / \Delta\delta_{\text{slow}} \text{ at } 233 \text{ K}) \times 100$.⁶ The values are summarized in Table S6 and were found to be constant over the range of concentrations of foldamer **S10**.

Entry	[S10] (mM)	$\Delta\delta_{\text{fast}}$ (ppb) at 293 K	$\Delta\delta_{\text{slow}}$ (ppb) at 233 K	h.e. (%)
1	10	3502	4864	72
2	2.5	3564	4834	73
3	0.5	3564	4841	73

Table S6. Helical excess of foldamer **S10** determined at 293 K

• **Determination of an estimated value of $\Delta\delta_{\text{slow}}$ for ^{13}C NMR reporter in foldamer **S9****

(a) The variable temperature ^{13}C NMR experiments carried out with foldamer **S10** allowed the determination of $\Delta\delta_{\text{slow}}$ (4864 ppb) in CDCl_3 for foldamers having a ^{13}C NMR probe inserted in the middle of the Aib backbone (Figure S30, eq. 1).

(b) Irrespective of the difference in their chiral inducers ($Z\alpha\text{MeVal-}$ and $Z\alpha\text{MeVal}_2^-$), both foldamers **S10** and **S11** have an identical ^{13}C NMR helicity probe located in the same position in their Aib chain. Therefore, the previous value of $\Delta\delta_{\text{slow}}$ (4864 ppb) was used to calculate the helical excess of foldamer **S11** in CDCl_3 . The value obtained (92%) was found to be in agreement with the value of the helical excess obtained for foldamer **S11** in THF (Figure S30, eq. 2).⁷

(c) Since both foldamers **S9** and **S11** have the same chiral controller ($Z\alpha\text{MeVal}_2^-$) covalently attached to their *N*-terminus positions and a similar ^{13}C NMR probe located four Aib residues after the chiral controller, the probes in foldamers **S9** and **S11** should experience approximately equal local helical excess. Using this assumption in conjunction with the formula previously described, the value of $\Delta\delta_{\text{slow}}$ in CDCl_3 for foldamers having a ^{13}C -labelled Aib methyl ester probe located at their *C*-terminal position is estimated to be 1771 ppb (Figure S30, eq. 3). This value was used to calculate the helical excess reported in Table 1.

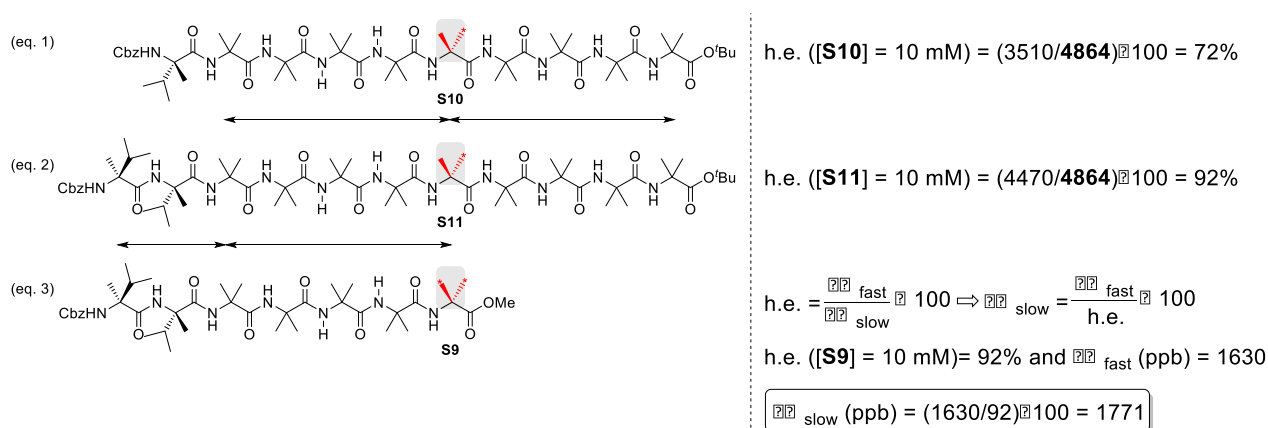


Figure S30. Determination of an estimated value of $\Delta\delta_{\text{slow}}$ for ^{13}C -AibOMe NMR reporter in CDCl_3 at 296 K

[6] Solà, J.; Morris, G. M.; Clayden, J. *J. Am. Chem. Soc.* **2011**, *133*, 3712–3715.

[7] Byrne, L.; Solà, J.; Boddart, T.; Marcelli, T.; Adams, R. W.; Morris, G. M.; Clayden, J. *Angew. Chem. Int. Ed.* **2014**, *53*, 151–155.

V. Titration studies of F with HA

Procedure for the titration of F2 with HA4: foldamer **F2** (0.005 mmol, 2.6 mg) was directly weighed in an NMR tube to which CDCl₃ (0.5 mL) was added. Portions of **HA4** (0.0015 mmol, 1.1 mg) were added to the NMR tube containing the solution of **F2**. After each addition of **HA4**, the NMR tube was shaken vigorously for 1 min and ¹H and ¹³C spectra of the resultant solution were recorded at 296 K. The portions of ¹H and ¹³C spectra of **F2** in the presence of **HA4** are shown in Figure S31-33. The plot of the anisochronicity ($\Delta\delta$, ppb) of the two diastereotopic ¹³CH₃ signals of the NMR probe in **F2** vs the ratio **HA4:F2** is shown in Figure S34. **NB:** broadening in the ¹H NMR spectra did not allow accurate integrations of diagnostic signals of **HA4** and **F2**, therefore the ratios **HA4:F2** were uncorrected.

Procedure for the titration of F4 with HA1: foldamer **F4** (0.005 mmol, 2.9 mg) was directly weighed in an NMR tube to which CDCl₃ (0.5 mL) was added. Portions of **HA1** in CDCl₃ (0.0015 mmol, 5 μ L, 0.3 M) were added to the NMR tube containing the solution of **F4**. After each addition of **HA1**, the NMR tube was vigorously shaken for 1 min then ¹H and ¹³C spectra of the resultant solution were recorded at 296 K. The portions of the ¹H and ¹³C spectra of **F4** in the presence of **HA1** are shown in Figures S35-37. The plot of the anisochronicity ($\Delta\delta$, ppb) of the two diastereotopic ¹³CH₃ signals of the NMR probe in **F4** vs the ratio **HA1:F4** is shown in Figure S38. **NB:** ratios **HA1:F4** were corrected by integrating diagnostic signals of **HA1** and **F4** in the ¹H NMR spectra.

Procedure for the titration of F4 with HA4: foldamer **F4** (0.005 mmol, 2.9 mg) was directly weighed in an NMR tube to which CDCl₃ (0.5 mL) was added. Portions of **HA4** (0.0015 mmol, 1.1 mg) were added to the NMR tube containing the solution of **F4**. After each addition of **HA4**, the NMR tube was vigorously shaken for 1 min then ¹H and ¹³C spectra of the resultant solution were recorded at 296 K. The portions of the ¹H and ¹³C spectra of **F4** in the presence of **HA4** are shown in Figures S39-41. The plot of the anisochronicity ($\Delta\delta$, ppb) of the two diastereotopic ¹³CH₃ signals of the NMR probe in **F4** vs the ratio **HA4:F4** is shown in Figure S42. **NB:** ratios **HA4:F4** were corrected by integrating diagnostic signals of **HA4** and **F4** in the ¹H NMR spectra.

Procedure for the titration of F4 with HA6: foldamer **F4** (0.005 mmol, 2.9 mg) was directly weighed in an NMR tube to which CDCl₃ (0.5 mL) was added. Portions of **HA6** (0.0015 mmol, 1.0 mg) were added to the NMR tube containing the solution of **F4**. After each addition of **HA6**, the NMR tube was shaken vigorously for 1 min, then ¹H and ¹³C spectra of the resultant solution were recorded at 296 K. The portions of the ¹H and ¹³C spectra of **F4** in the presence of **HA6** are shown in Figures S43-45. The plot of the anisochronicity ($\Delta\delta$, ppb) of the two diastereotopic ¹³CH₃ signals of the NMR probe in **F4** vs the ratio **HA6:F4** is shown in Figure S46. **NB:** broadening in the ¹H NMR spectra did not allow accurate integrations of diagnostic signals of **HA6** and **F4**, therefore the ratios **HA6:F4** were uncorrected.

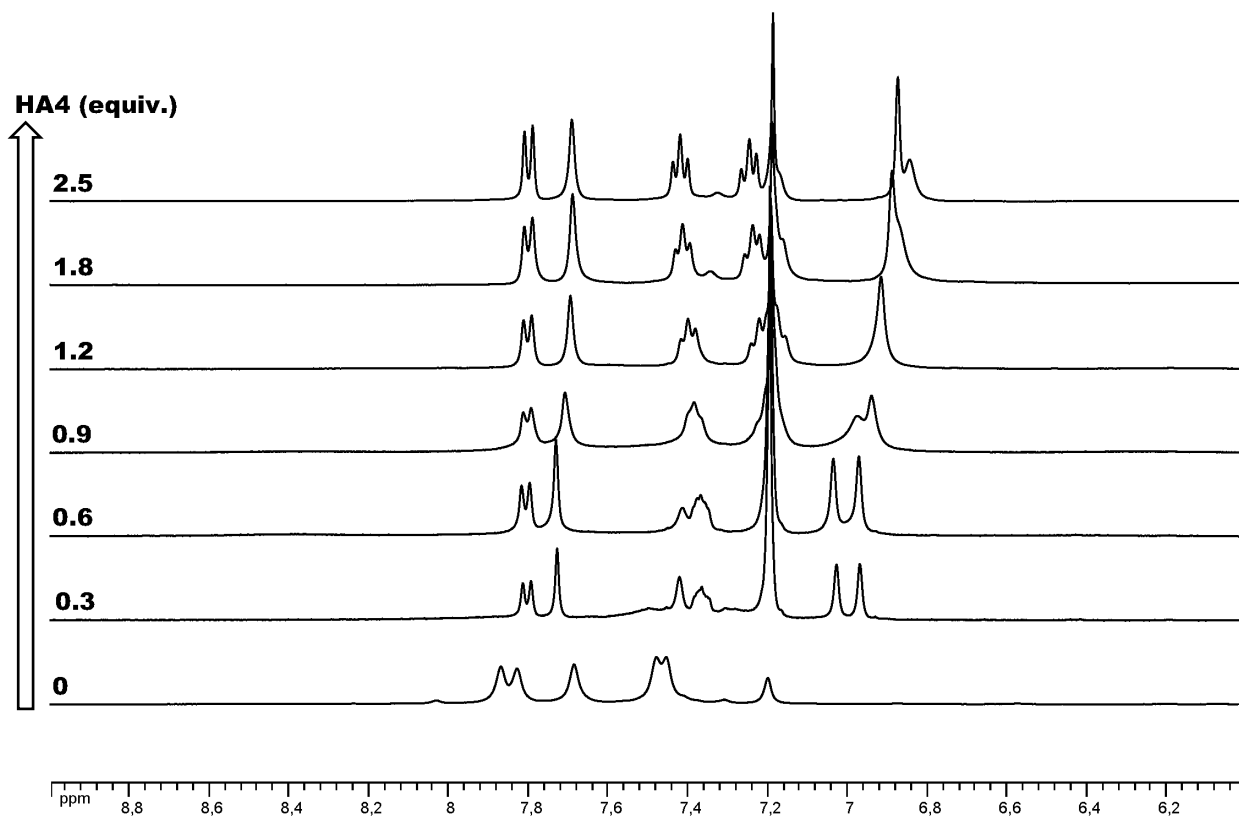


Figure S31. Titration experiment: portions of the ^1H NMR (400 MHz, CDCl_3) spectra of **F2** recorded at 296 K in the presence of different numbers of equivalents of **HA4**; $[\text{F2}] = 10$ mM.

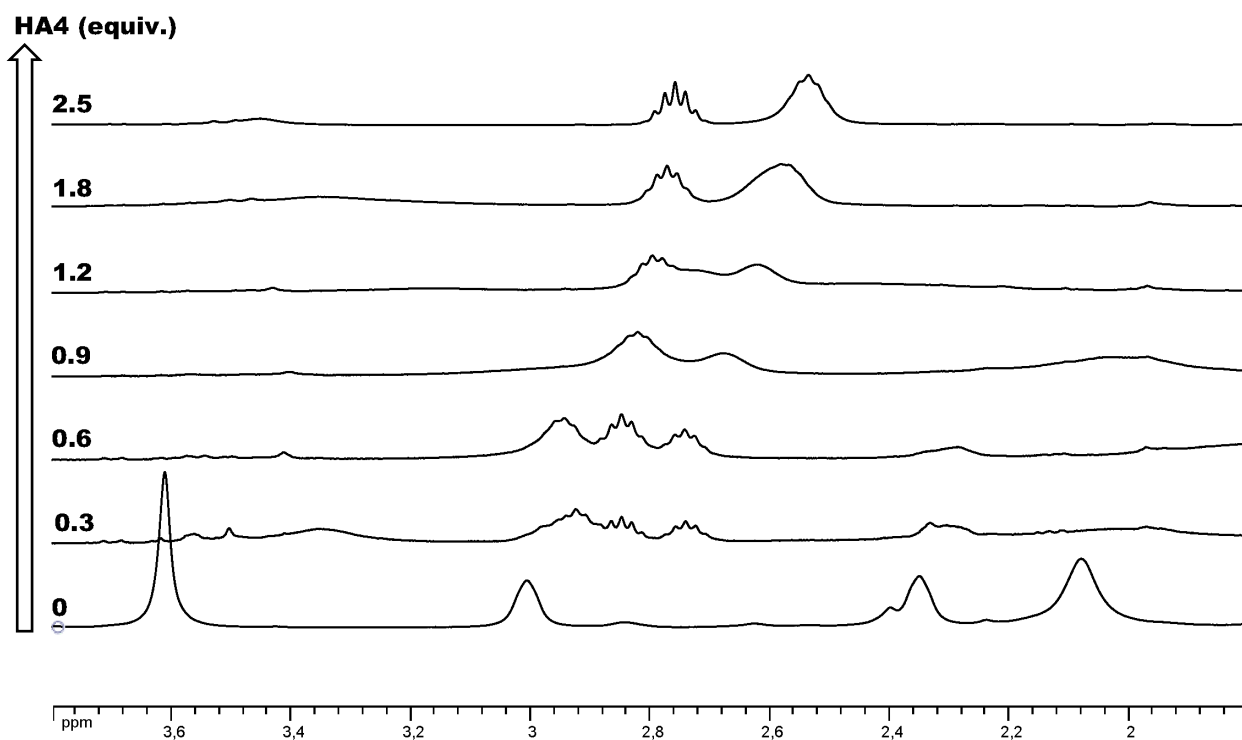


Figure S32. Titration experiment: portions of the ^1H NMR (400 MHz, CDCl_3) spectra of **F2** recorded at 296 K in the presence of different numbers of equivalents of **HA4**; $[\text{F2}] = 10$ mM.

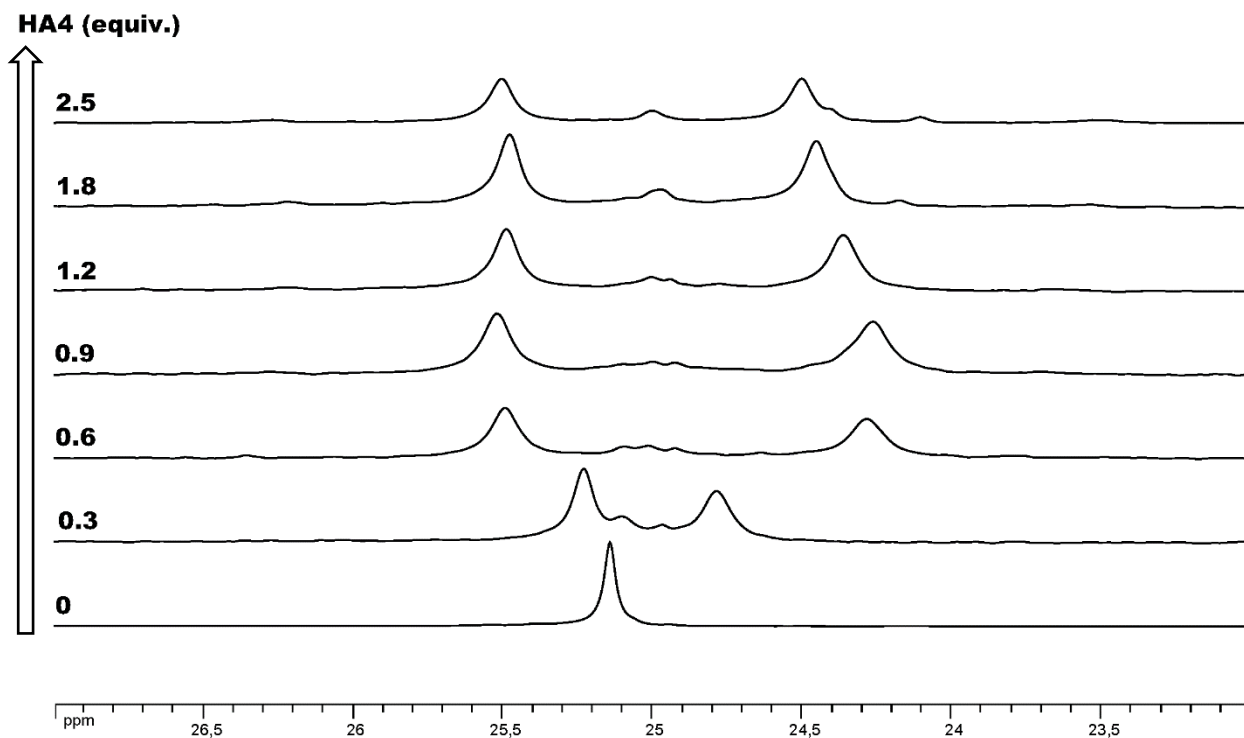


Figure S33. Titration experiment: portions of the ^{13}C NMR (100 MHz, CDCl_3) spectra of **F2** recorded at 296 K in the presence of different numbers of equivalents of **HA4**; [**F2**] = 10 mM.

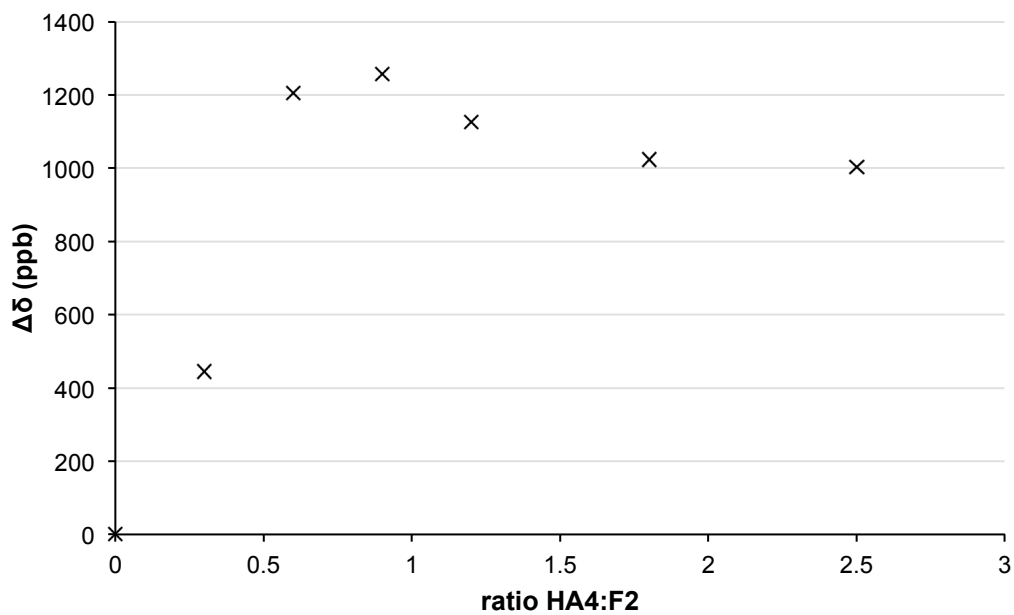


Figure S34. Plot of the anisochronicity ($\Delta\delta$, ppb) of the two diastereotopic $^{13}\text{CH}_3$ signals of the NMR probe in **F2** vs the ratio **HA4:F2** recorded in CDCl_3 at 296 K; [**F2**] = 10 mM.

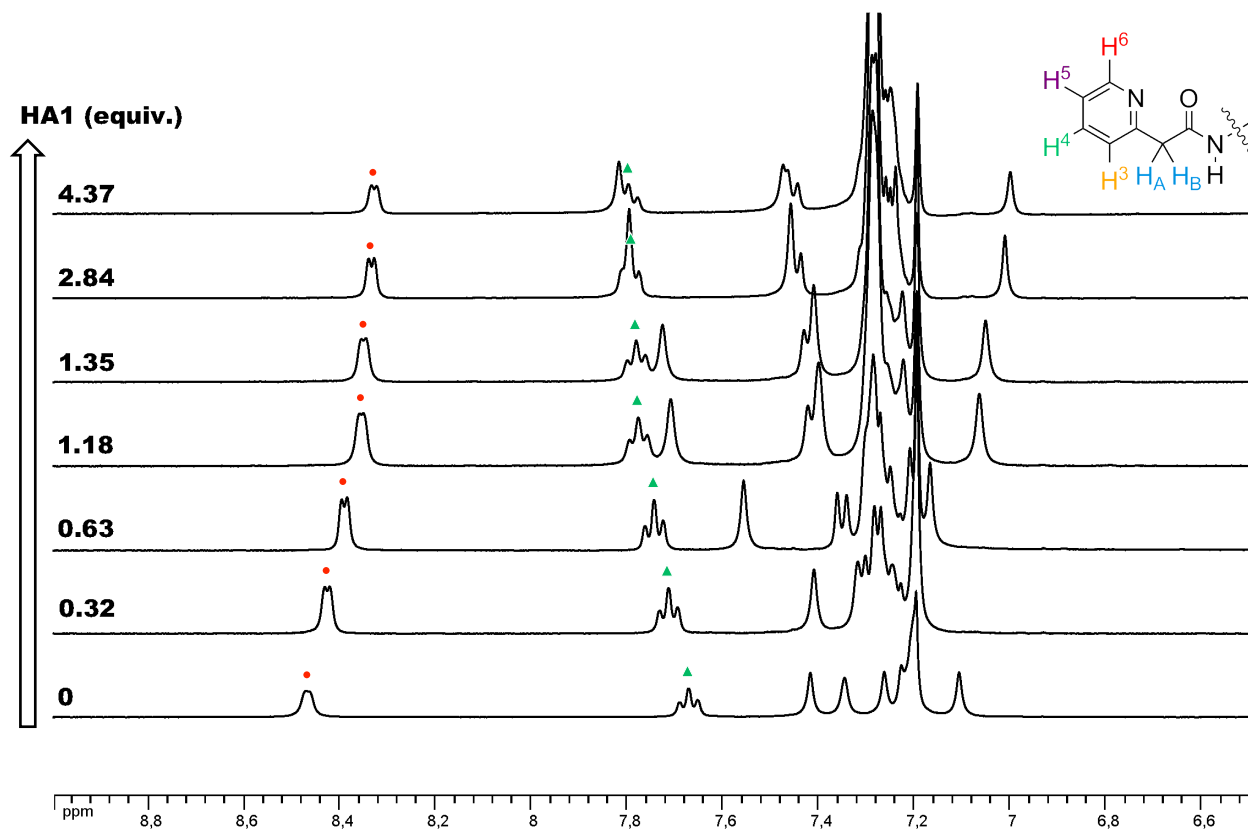


Figure S35. Titration experiment: portions of the ^1H NMR (400 MHz, CDCl_3) spectra of **F4** recorded at 296 K in the presence of different numbers of equivalents of **HA1**; $8.8 < [\text{F4}] < 10$ mM; (●) δH_6 ; (▲) δH_4 .

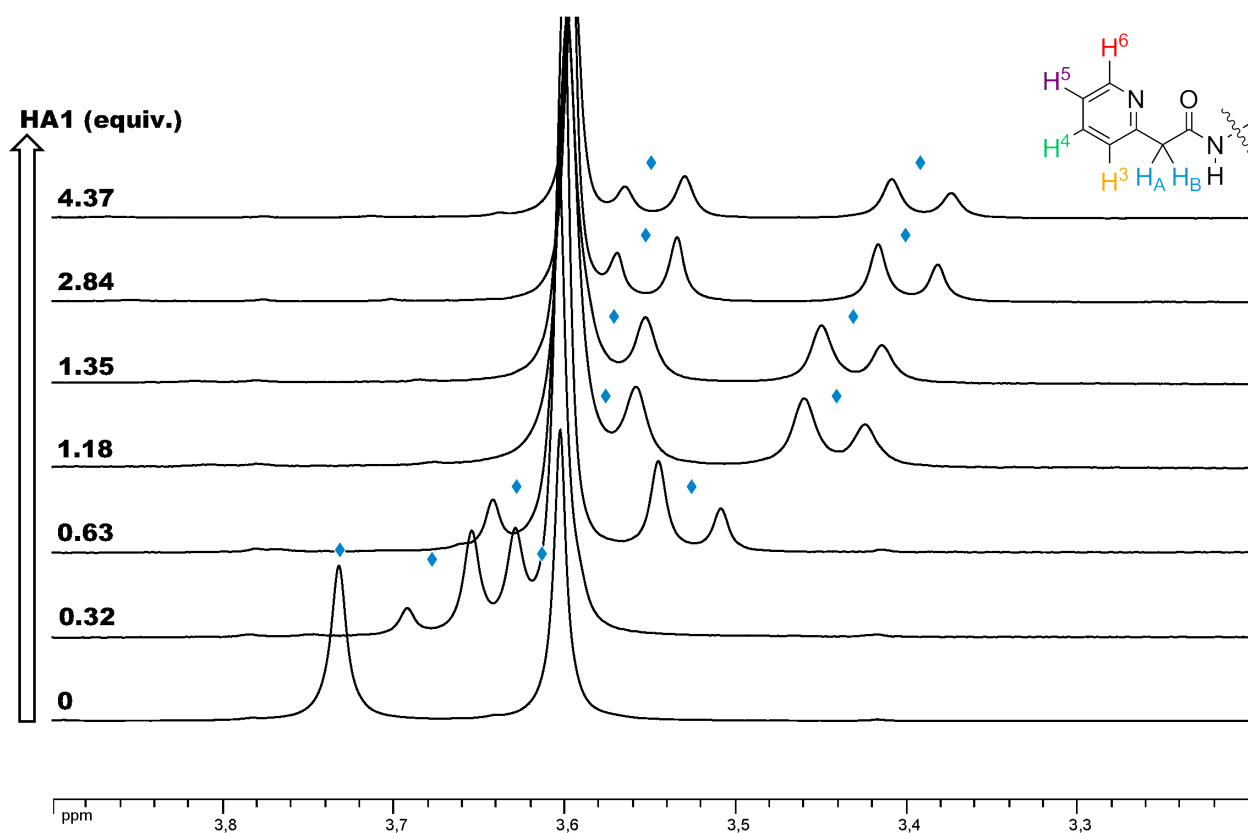


Figure S36. Titration experiment: portions of the ^1H NMR (400 MHz, CDCl_3) spectra of **F4** recorded at 296 K in the presence of different numbers of equivalents of **HA1**; $8.8 < [\text{F4}] < 10$ mM; (◆) $\delta\text{H}_{\text{AB}}$.

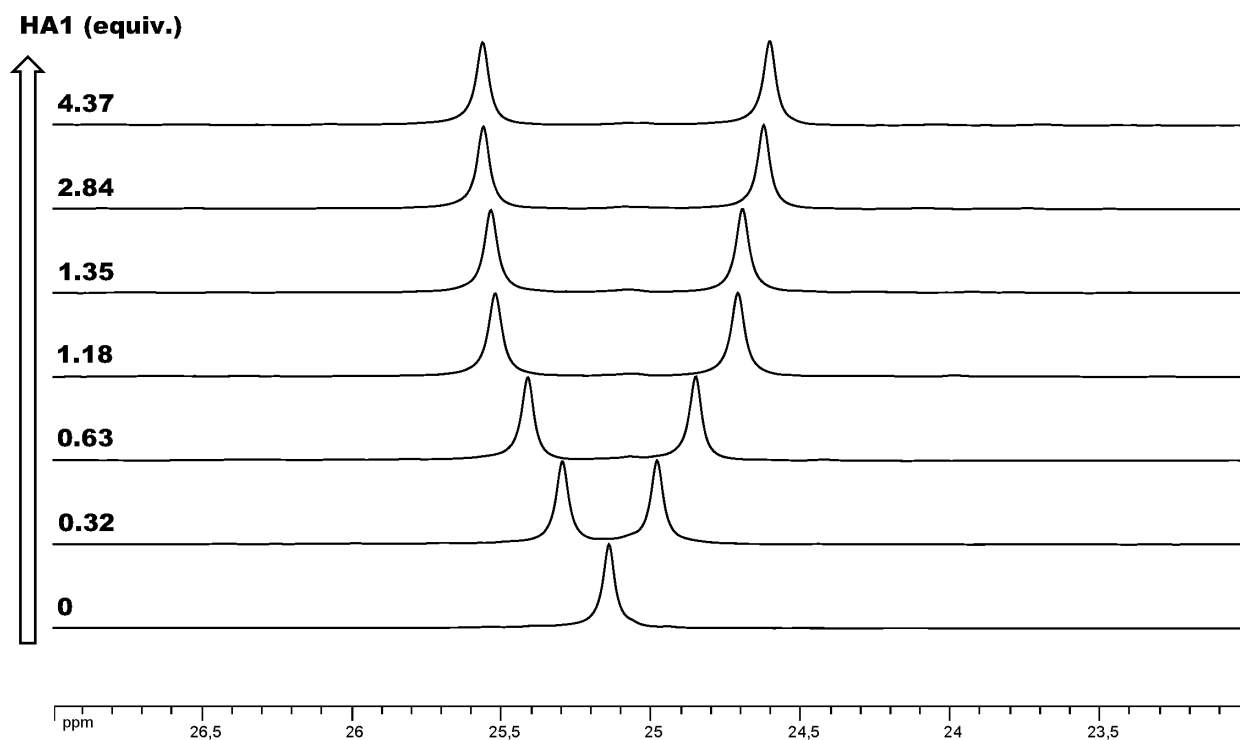


Figure S37. Titration experiment: portions of the ^{13}C NMR (100 MHz, CDCl_3) spectra of **F4** recorded at 296 K in the presence of different numbers of equivalents of **HA1**; $8.8 < [\text{F4}] < 10$ mM.

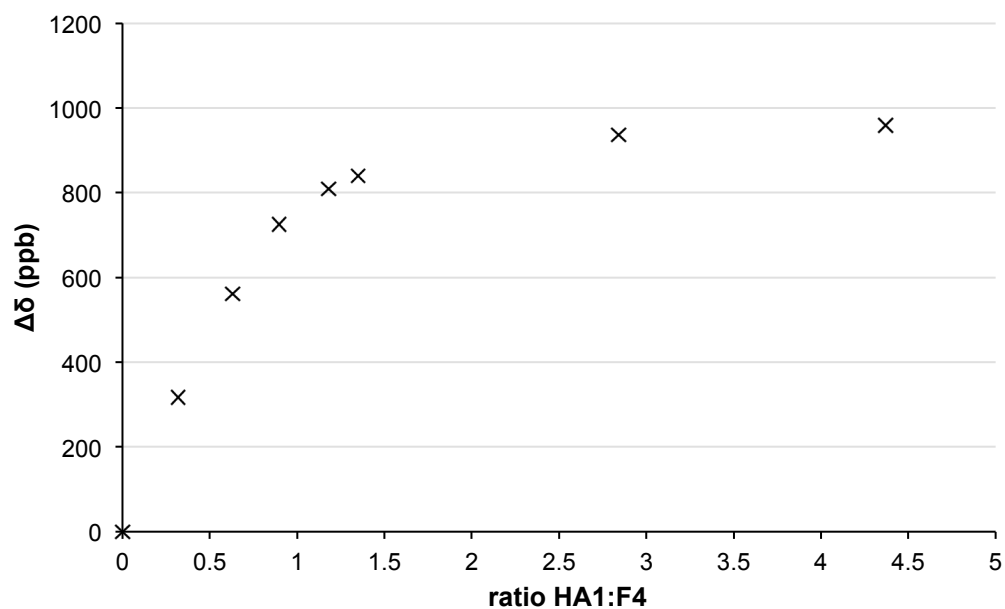


Figure S38. Plot of the anisochronicity ($\Delta\delta$, ppb) of the two diastereotopic $^{13}\text{CH}_3$ signals of the NMR probe in **F4** vs the ratio **HA1:F4** recorded in CDCl_3 at 296 K; $8.8 < [\text{F4}] < 10$ mM.

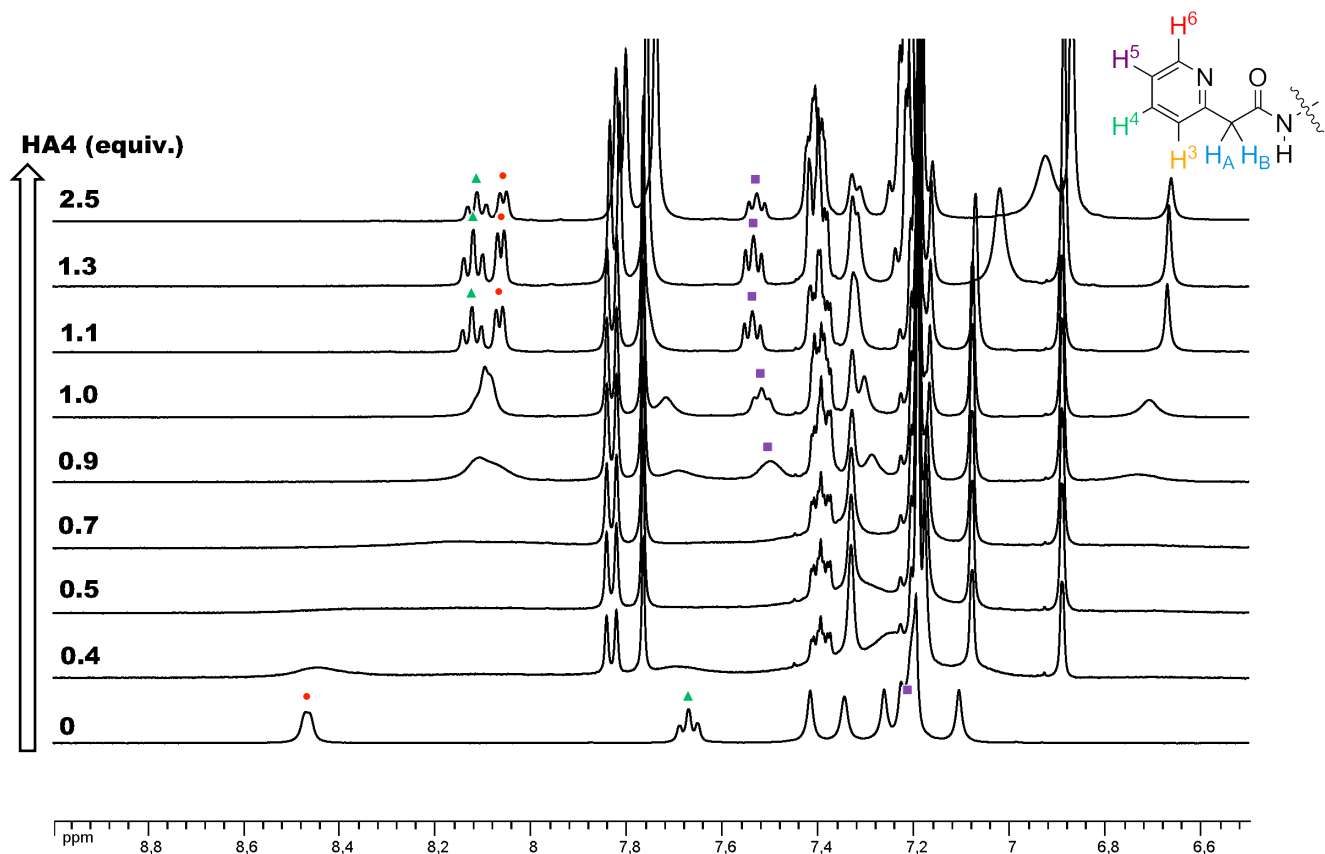


Figure S39. Titration experiment: portions of the ^1H NMR (400 MHz, CDCl_3) spectra of **F4** recorded at 296 K in the presence of different numbers of equivalents of **HA4**; [**F4**] = 10 mM; (\blacktriangle) δH_4 ; (\blacksquare) δH_5 ; (\bullet) δH_6 .

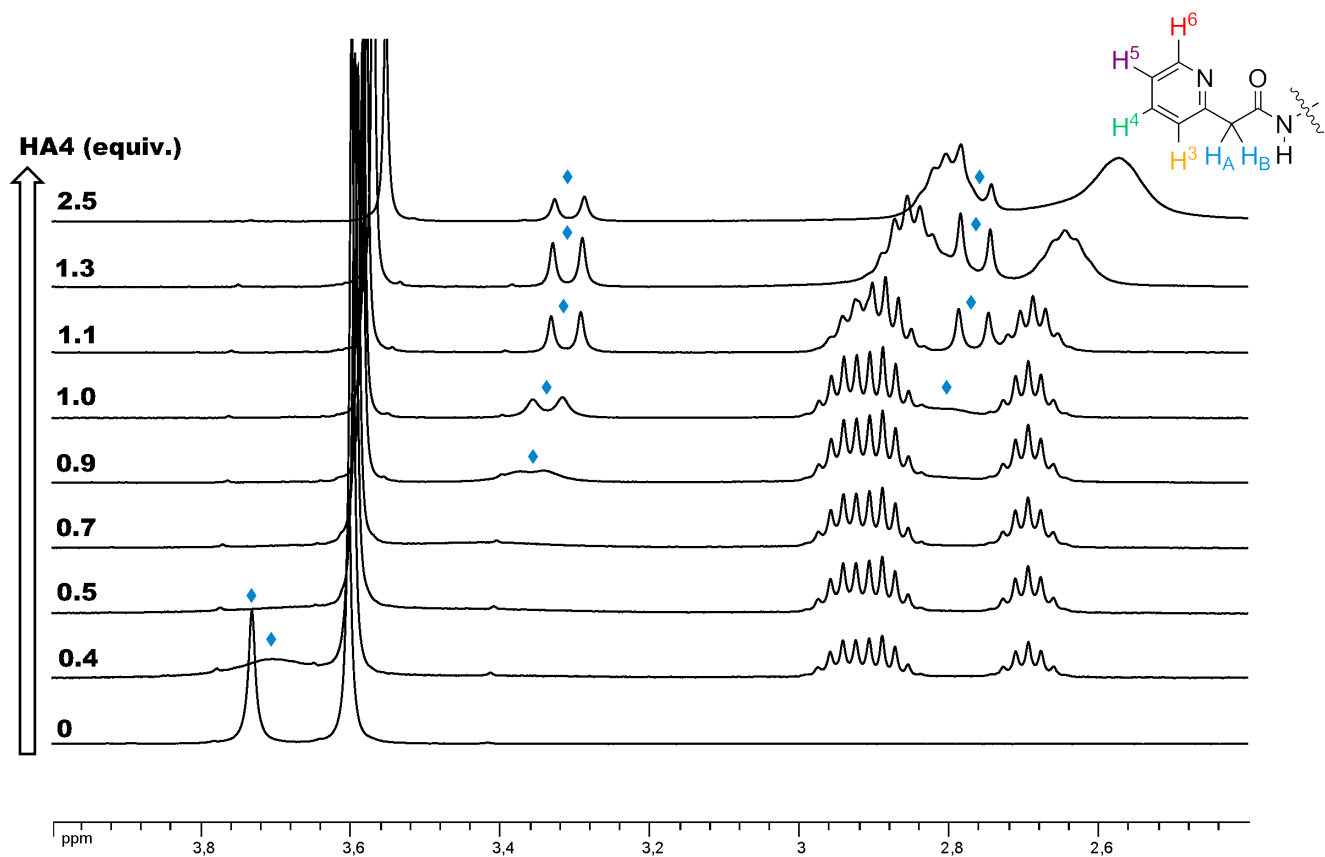


Figure S40. Titration experiment: portions of the ^1H NMR (400 MHz, CDCl_3) spectra of **F4** recorded at 296 K in the presence of different numbers of equivalents of **HA4**; [**F4**] = 10 mM; (\blacklozenge) $\delta\text{H}_{\text{AB}}$.

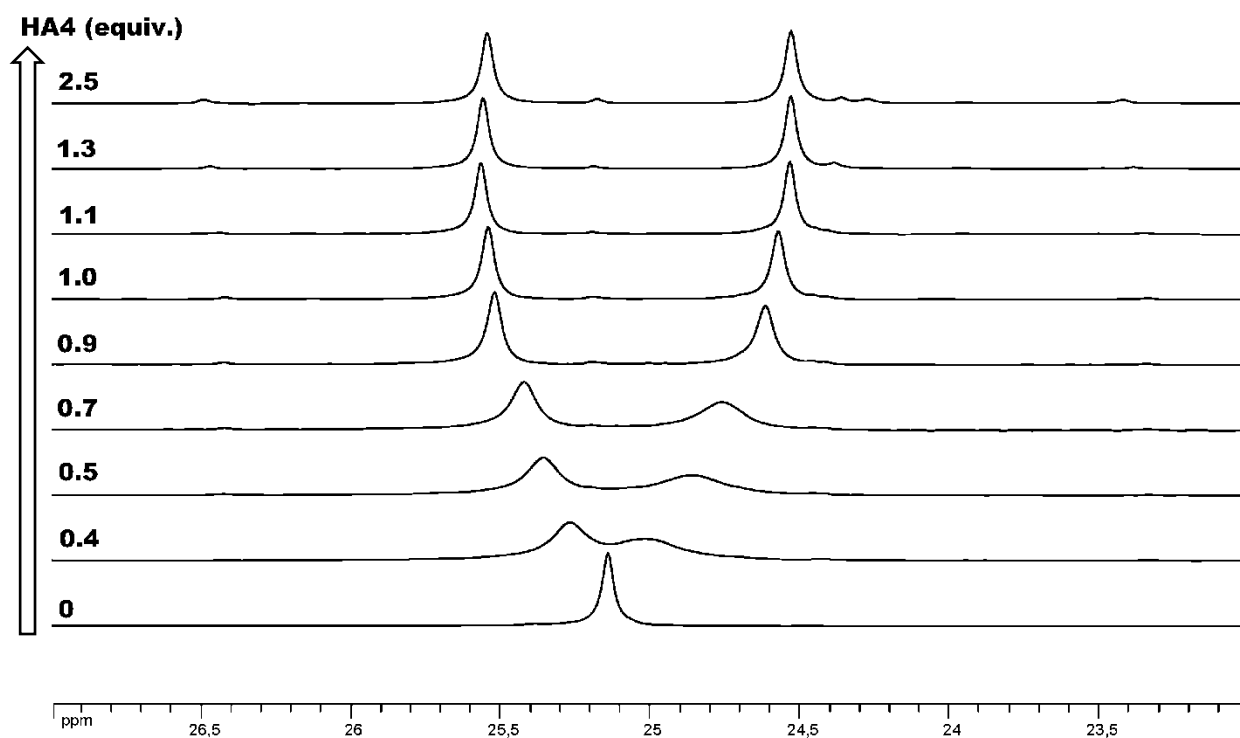


Figure S41. Titration experiment: portions of the ^{13}C NMR (100 MHz, CDCl_3) spectra of **F4** recorded at 296 K in the presence of different numbers of equivalents of **HA4**; $[\text{F4}] = 10$ mM.

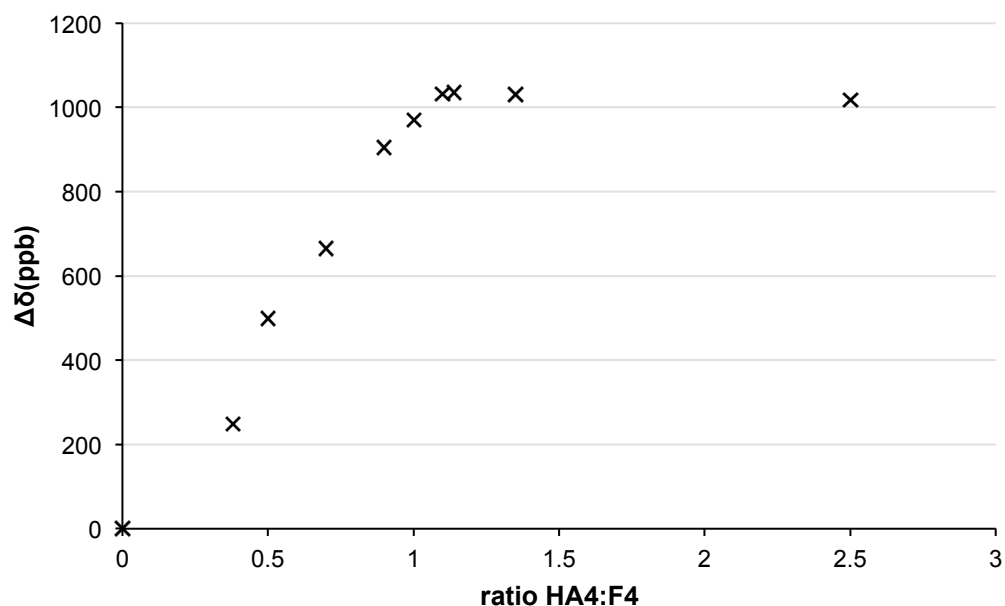


Figure S42. Plot of the anisochronicity ($\Delta\delta$, ppb) of the two diastereotopic $^{13}\text{CH}_3$ signals of the NMR probe in **F4** vs the ratio **HA4:F4** recorded in CDCl_3 at 296 K; $[\text{F4}] = 10$ mM.

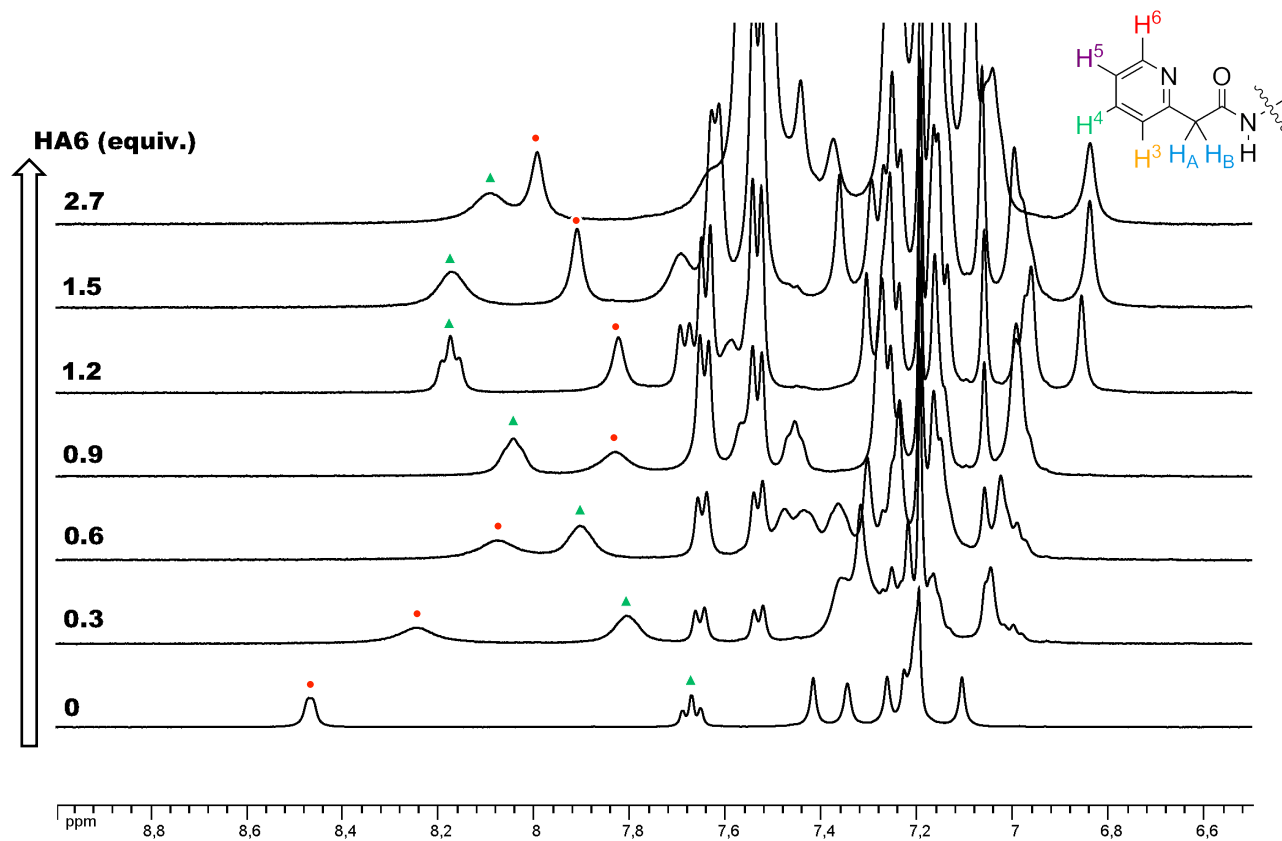


Figure S43. Titration experiment: portions of the ^1H NMR (400 MHz, CDCl_3) spectra of **F4** recorded at 296 K in the presence of different numbers of equivalents of **HA6**; [**F4**] = 10 mM; (●) δH_6 ; (▲) δH_4 .

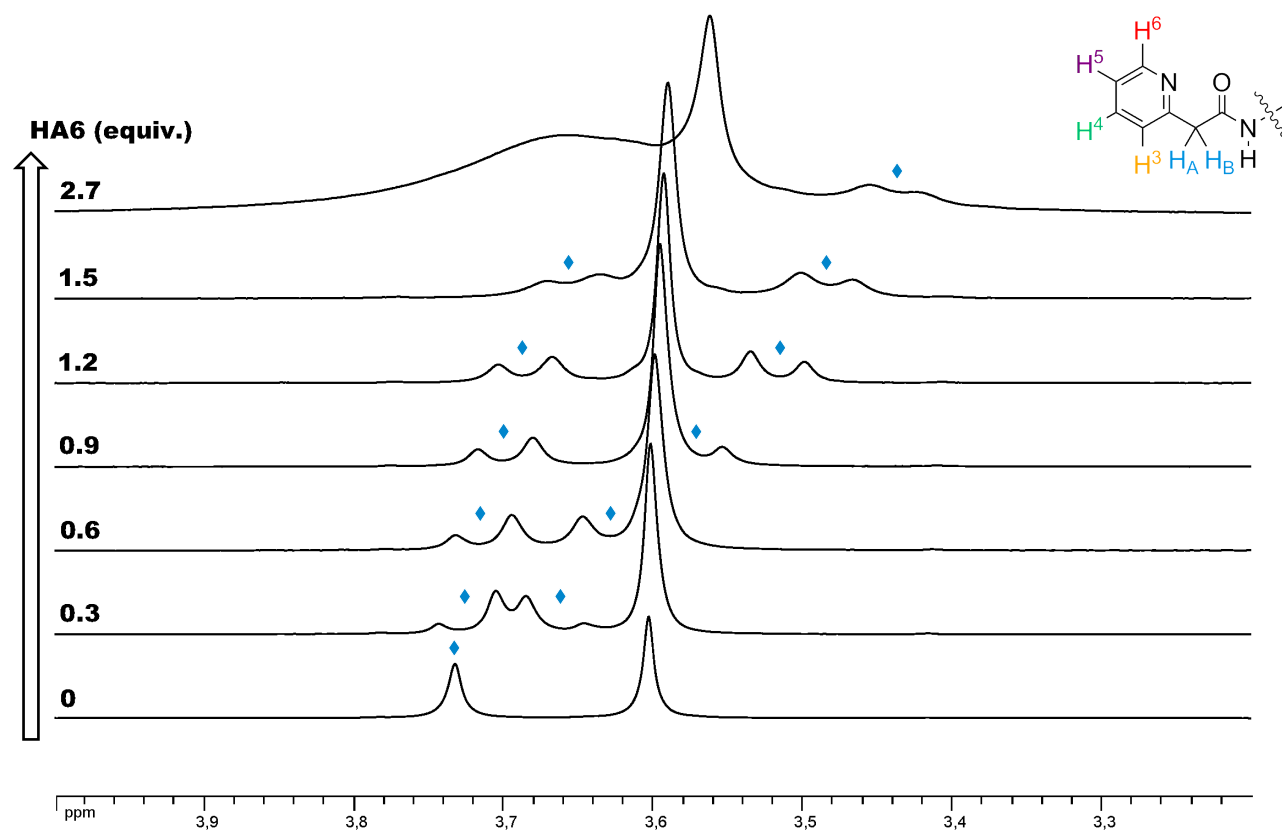


Figure S44. Titration experiment: portions of the ^1H NMR (400 MHz, CDCl_3) spectra of **F4** recorded at 296 K in the presence of different numbers of equivalents of **HA6**; [**F4**] = 10 mM; (◆) $\delta\text{H}_{\text{AB}}$.

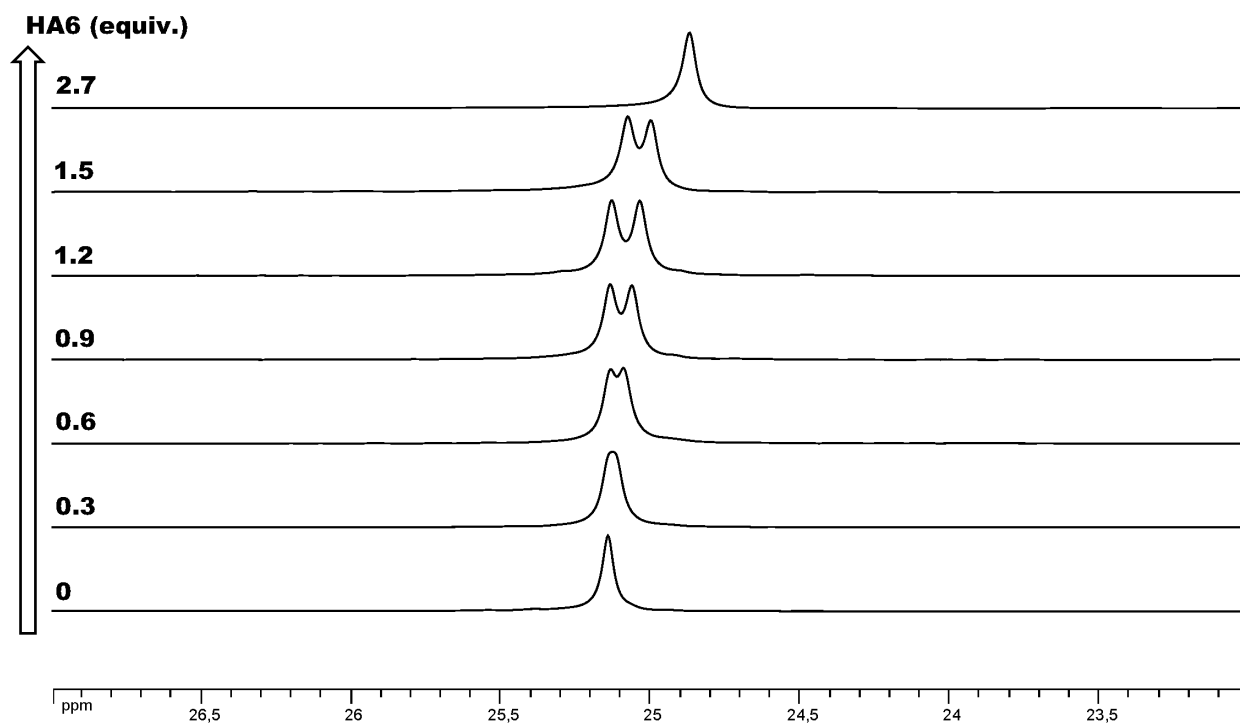


Figure S45. Titration experiment: portions of the ¹³C NMR (100 MHz, CDCl₃) spectra of **F4** recorded at 296 K in the presence of different numbers of equivalents of **HA6**; [**F4**] = 10 mM.

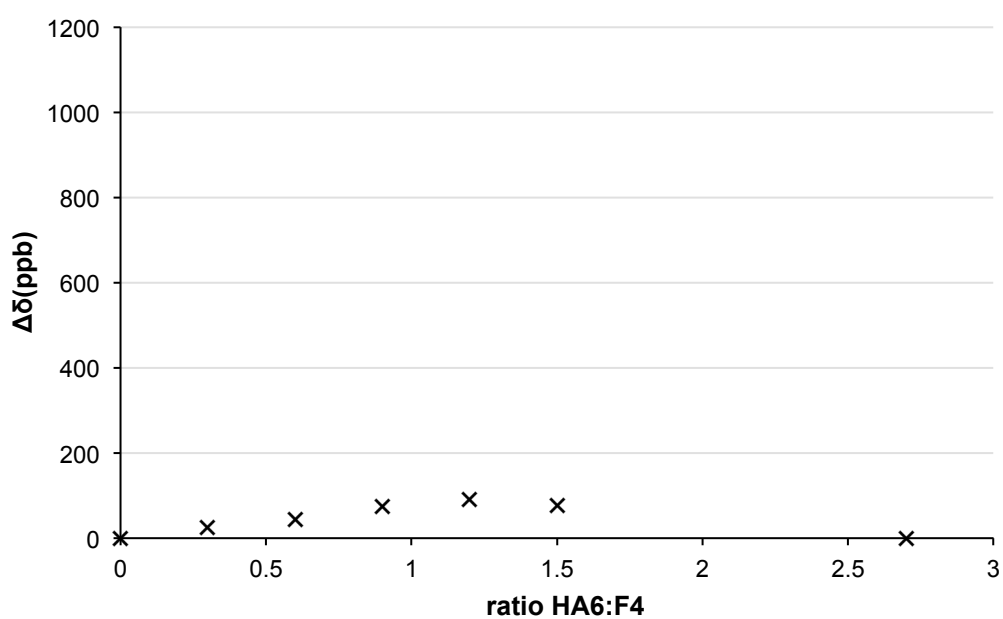


Figure S46. Plot of the anisochronicity ($\Delta\delta$, ppb) of the two diastereotopic ¹³CH₃ signals of the NMR probe in **F4** vs the ratio **HA6:F4** recorded in CDCl₃ at 296 K; [**F4**] = 10 mM.

VI. Dilution studies for systems HA↔F

Procedure for the dilution experiment of systems HA4↔F2: A NMR sample of HA4↔F2 ([F2] = 10 mM, [HA4] = 12 mM) prepared according to the procedure used to establish Table 1 was diluted with CDCl₃ until [F2] = 0.1 mM. After each dilution, the NMR tube was vigorously shaken for 1 min then ¹H and ¹³C spectra of the resultant solution were recorded at 296 K. The portions of the ¹³C spectra of F2 in the presence of HA4 are shown in Figure S47. The plot of the anisochronicity ($\Delta\delta$, ppb) of the two diastereotopic ¹³CH₃ signals of the NMR probe in F2 vs [F2] (mM) is shown in Figure S48.

Procedure for the dilution experiment of systems HA1↔F4: A NMR sample of HA1↔F4 ([F4] = 10 mM, [HA1] = 15 mM) prepared according to the procedure used to establish Table 1 was diluted with CDCl₃ until [F4] = 0.1 mM. After each dilution, the NMR tube was vigorously shaken for 1 min then ¹H and ¹³C spectra of the resultant solution were recorded at 296 K. The portions of the ¹³C spectra of F4 in the presence of HA1 are shown in Figure S49. The plot of the anisochronicity ($\Delta\delta$, ppb) of the two diastereotopic ¹³CH₃ signals of the NMR probe in F4 vs [F4] (mM) is shown in Figure S50.

Procedure for the dilution experiment of systems HA4↔F4: A NMR sample of HA4↔F4 ([F4] = 10 mM, [HA4] = 12 mM) prepared according to the procedure used to establish Table 1 was diluted with CDCl₃ until [F4] = 0.1 mM. After each dilution, the NMR tube was vigorously shaken for 1 min then ¹H and ¹³C spectra of the resultant solution were recorded at 296 K. The portions of the ¹³C spectra of F4 in the presence of HA4 are shown in Figure S51. The plot of the anisochronicity ($\Delta\delta$, ppb) of the two diastereotopic ¹³CH₃ signals of the NMR probe in F4 vs [F4] (mM) is shown in Figure S52.

Procedure for the dilution experiment of systems HA6↔F4: A NMR sample of HA6↔F4 ([F4] = 10 mM, [HA6] = 12 mM) prepared according to the procedure used to establish Table 1 was diluted with CDCl₃ until [F4] = 0.1 mM. After each dilution, the NMR tube was vigorously shaken for 1 min then ¹H and ¹³C spectra of the resultant solution were recorded at 296 K. The portions of the ¹³C spectra of F4 in the presence of HA6 are shown in Figure S53. The plot of the anisochronicity ($\Delta\delta$, ppb) of the two diastereotopic ¹³CH₃ signals of the NMR probe in F4 vs [F4] (mM) is shown in Figure S54.

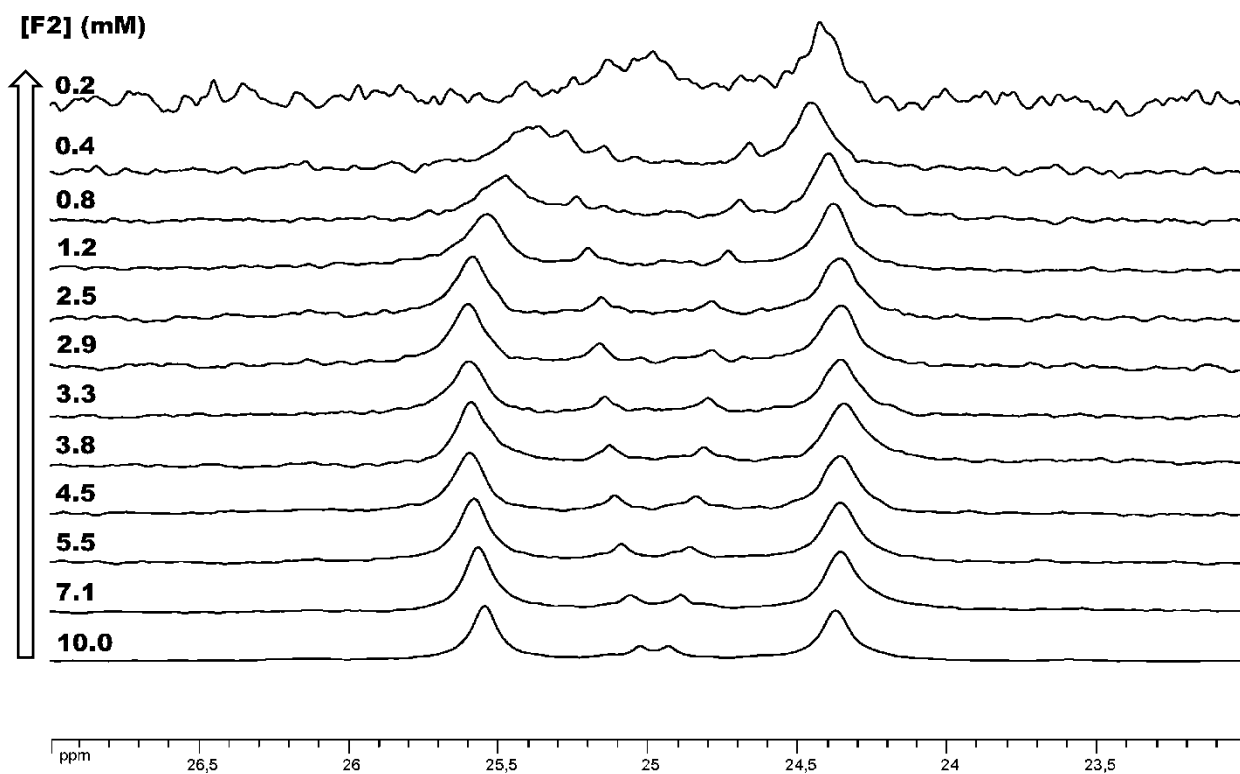


Figure S47. Dilution experiment: portions of the ^{13}C NMR (100 MHz, CDCl_3) spectra of **F2** at 296 K in the presence of **HA4**; **HA4:F2** = 1.2:1; **[F2]** = 10 \rightarrow 0.1 mM; **[HA4]** = 12 \rightarrow 0.12 mM.

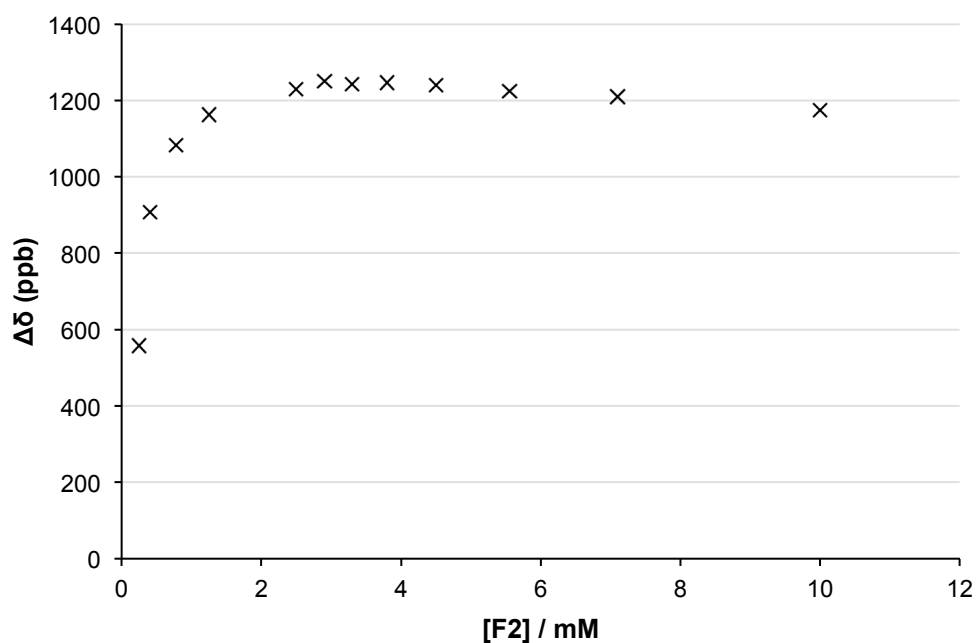


Figure S48. Plot of the anisochronicity ($\Delta\delta$, ppb) of the two diastereotopic $^{13}\text{CH}_3$ signals of the NMR probe in **F2** vs $[\text{F2}]$ (mM) recorded in CDCl_3 at 296 K; **HA4:F2** = 1.2:1.

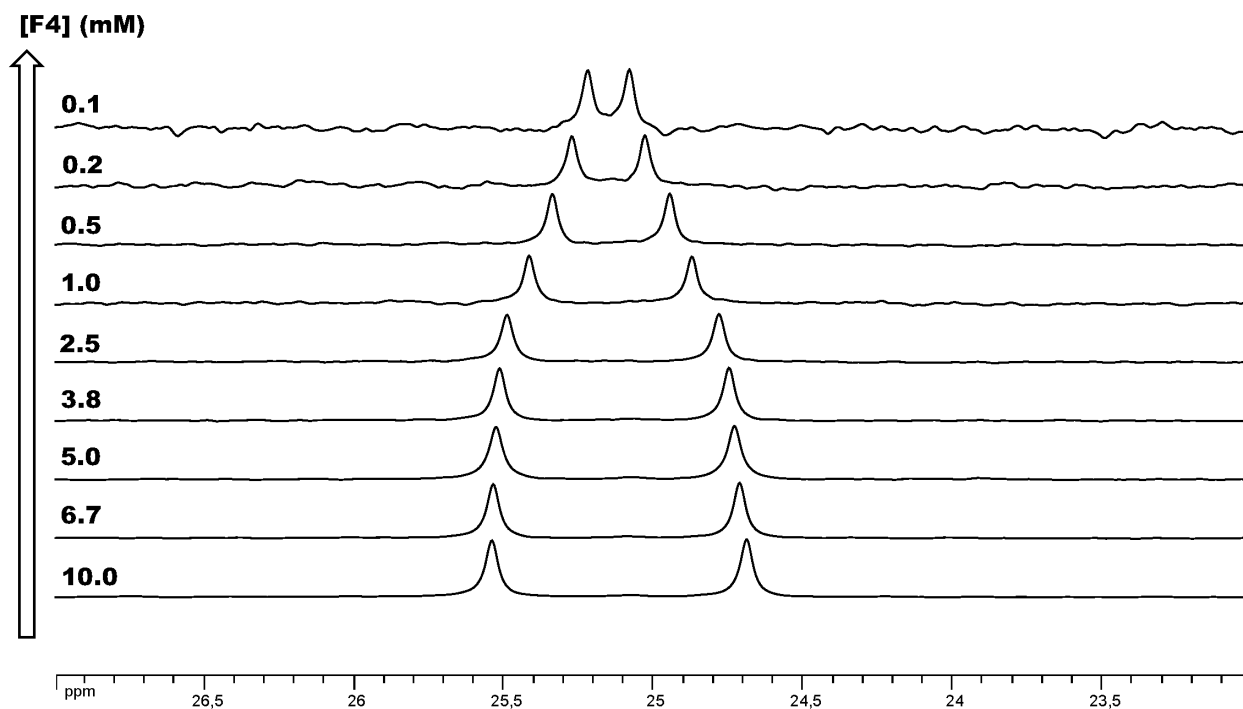


Figure S49. Dilution experiment: portions of the ^{13}C NMR (100 MHz, CDCl_3) spectra of **F4** at 296 K in the presence of **HA1**; **HA1:F4** = 1.5:1; **[F4]** = 10 \rightarrow 0.1 mM; **[HA1]** = 15 \rightarrow 0.15 mM.

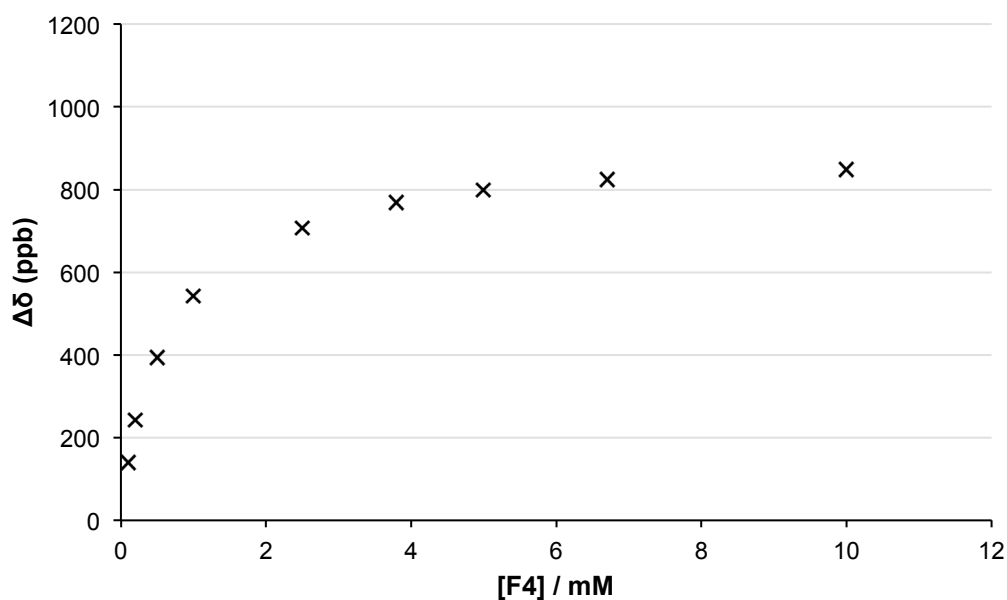


Figure S50. Plot of the anisochronicity ($\Delta\delta$, ppb) of the two diastereotopic $^{13}\text{CH}_3$ signals of the NMR probe in **F4** vs **[F4]** (mM) recorded in CDCl_3 at 296 K; **HA1:F4** = 1.5:1.

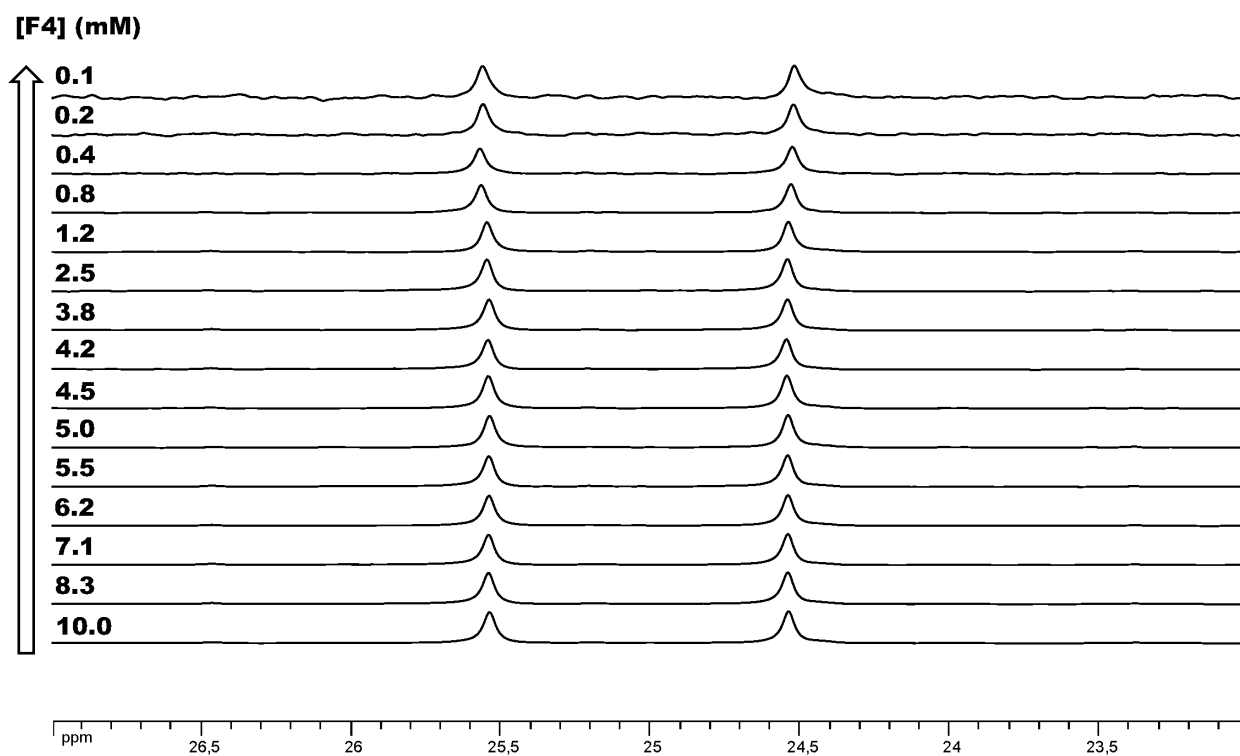


Figure S51. Dilution experiment: portions of the ^{13}C NMR (100 MHz, CDCl_3) spectra of **F4** at 296 K in the presence of **HA4**; **HA4:F4** = 1.2:1; **[F4]** = 10 \rightarrow 0.1 mM; **[HA4]** = 12 \rightarrow 0.12 mM.

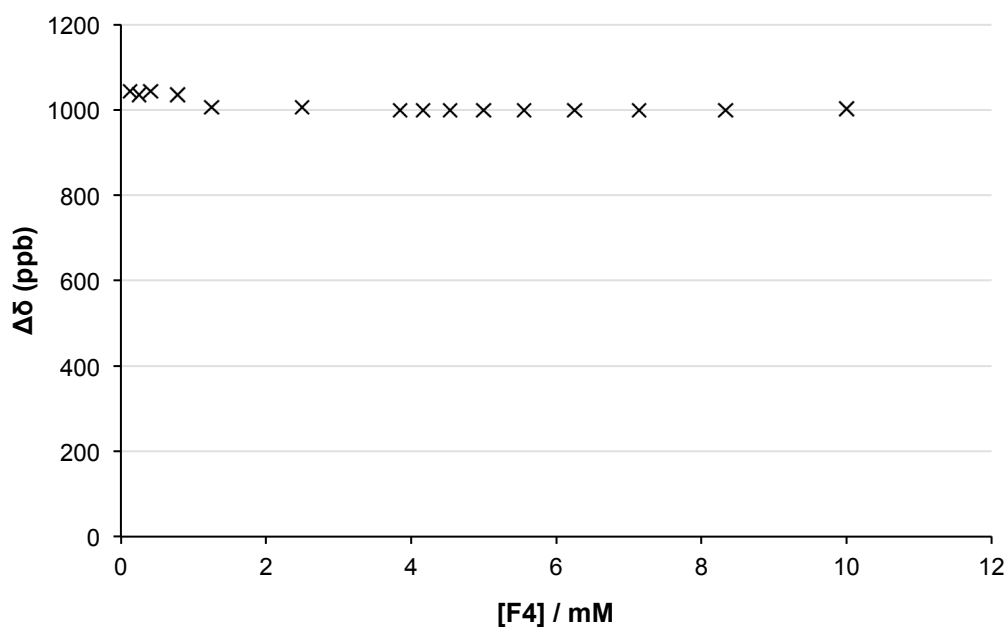


Figure S52. Plot the anisochronicity ($\Delta\delta$, ppb) of the two diastereotopic $^{13}\text{CH}_3$ signals of the NMR probe in **F4** vs **[F4]** (mM) recorded in CDCl_3 at 296 K; **HA4:F4** = 1.2:1.

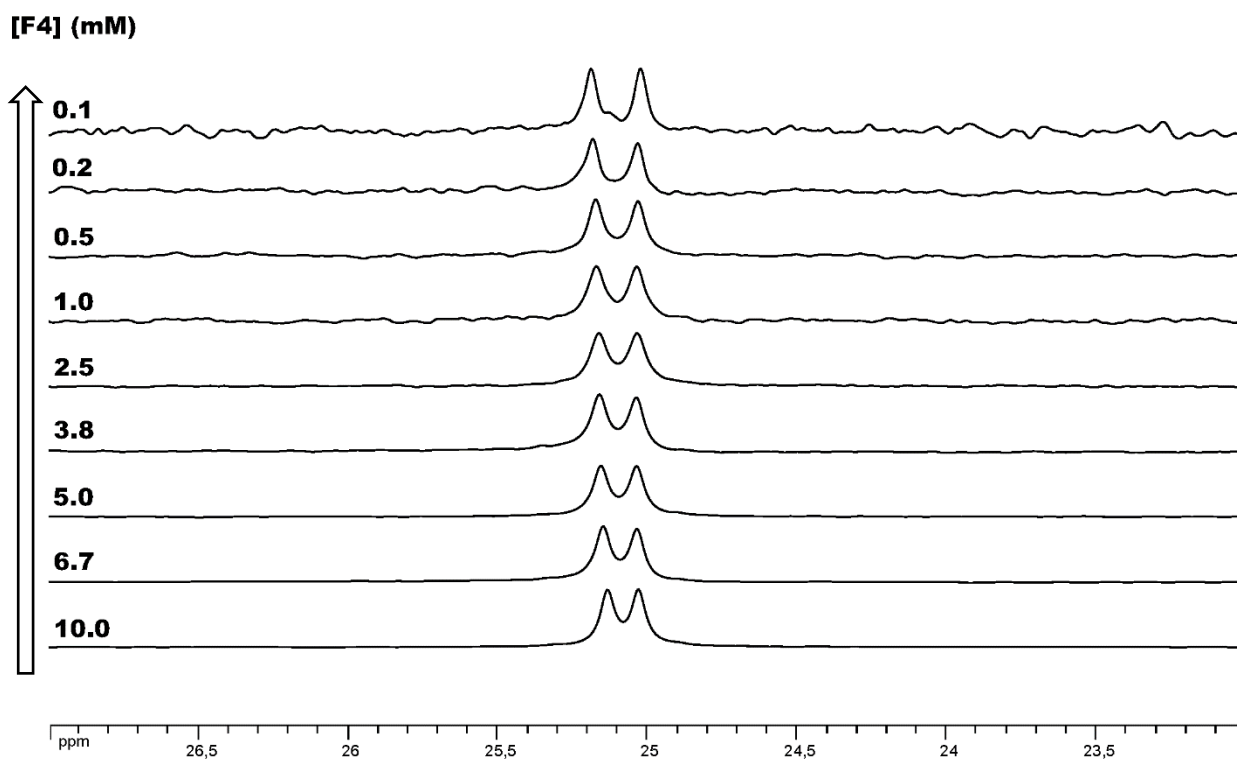


Figure S53. Dilution experiment: portions of the ^{13}C NMR (100 MHz, CDCl_3) spectra of **F4** at 296 K in the presence of **HA6**; **HA6:F4** = 1.2:1; **[F4]** = 10 \rightarrow 0.1 mM; **[HA6]** = 12 \rightarrow 0.12 mM.

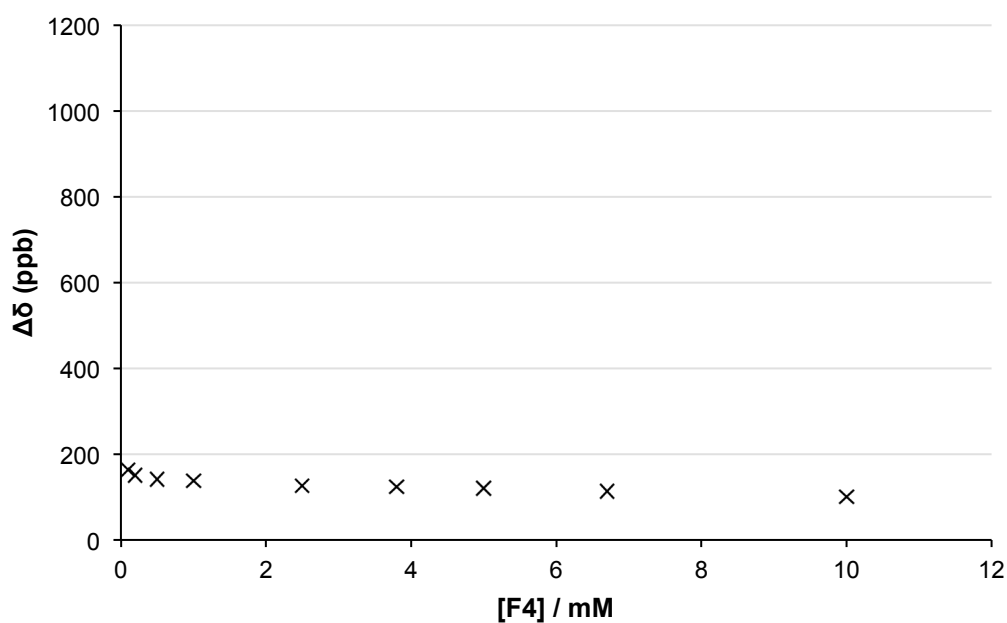


Figure S54. Plot of the anisochronicity ($\Delta\delta$, ppb) of the two diastereotopic $^{13}\text{CH}_3$ signals of the NMR probe in **F4** vs **[F4]** (mM) in CDCl_3 at 296 K; **HA6:F4** = 1.2:1.

VII. Influence of MeOH-d3 on HA4↔F4 system

MeOH-d3 was gradually added to an NMR sample containing the HA4↔F4 system which was prepared according to the procedure used to establish Table 1. After each addition of MeOH-d3, the NMR tube was vigorously shaken for 1 min then ^1H and ^{13}C spectra of the resultant solution were recorded at 296 K. The portions of the ^{13}C spectra of F4 in the presence of HA4 and MeOH-d3 are shown in Figure S55. The plot of the anisochronicity ($\Delta\delta$, ppb) of the two diastereotopic $^{13}\text{CH}_3$ signals of the NMR probe in F4 vs the percentage of MeOH-d3 (%) added to F4 is shown in Figure S56.

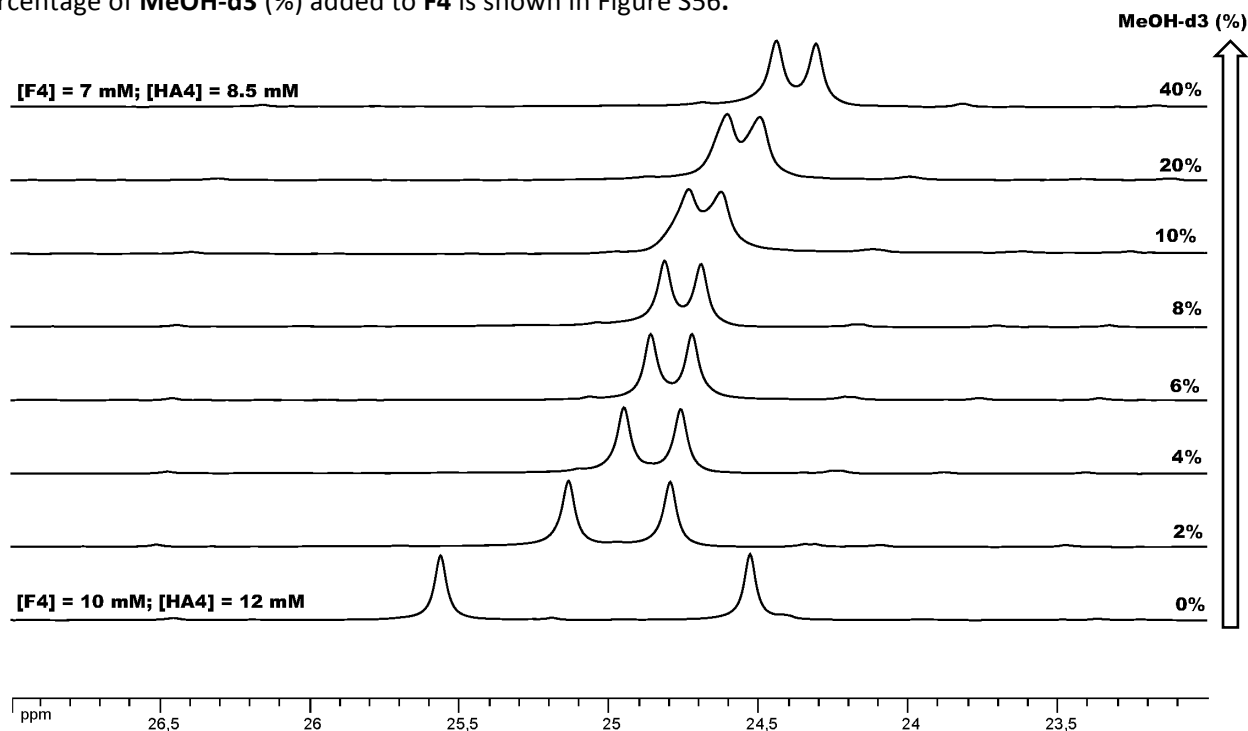


Figure S55. Portions of the ^{13}C (100 MHz, CDCl_3) spectra in F4 recorded at 296 K in the presence of HA4 and MeOH-d3; [F4] = 10 → 7 mM; [HA4] = 12 → 8.5 mM; MeOH-d3 / 0 → 40%.

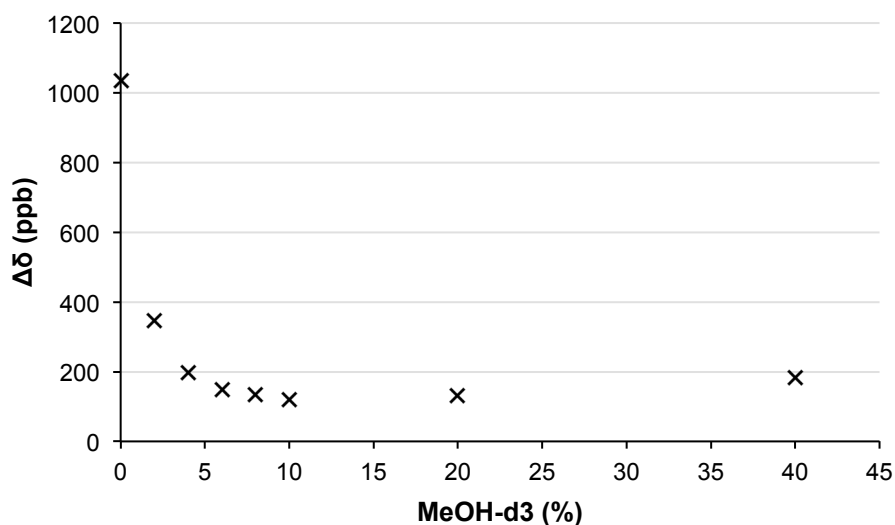


Figure S56. Plot the anisochronicity ($\Delta\delta$, ppb) of the two diastereotopic $^{13}\text{CH}_3$ signals of the NMR probe in F4 recorded at 296 K for the system HA4↔F4 vs the percentage of MeOH-d3 (%).

VIII. Influence of HCl on F4 in CDCl₃ at 296 K

Foldamer **F4** (0.005 mmol, 2.9 mg) was directly weighed in an NMR tube, to which CDCl₃ (0.5 mL) was added. A solution of HCl (0.015 mmol, 20 μ L, 0.75 M) in CDCl₃:dioxane (5.3:1), prepared from commercially available solution of HCl in dioxane (4 M), was added to the NMR tube containing the solution of **F4**. The NMR tube was shaken vigorously for 1 min and the ¹H spectrum of the resultant solution was recorded at 296 K. The portions of the ¹H spectra of **F4** and of **F4** in the presence of HCl are shown in Figure S57.

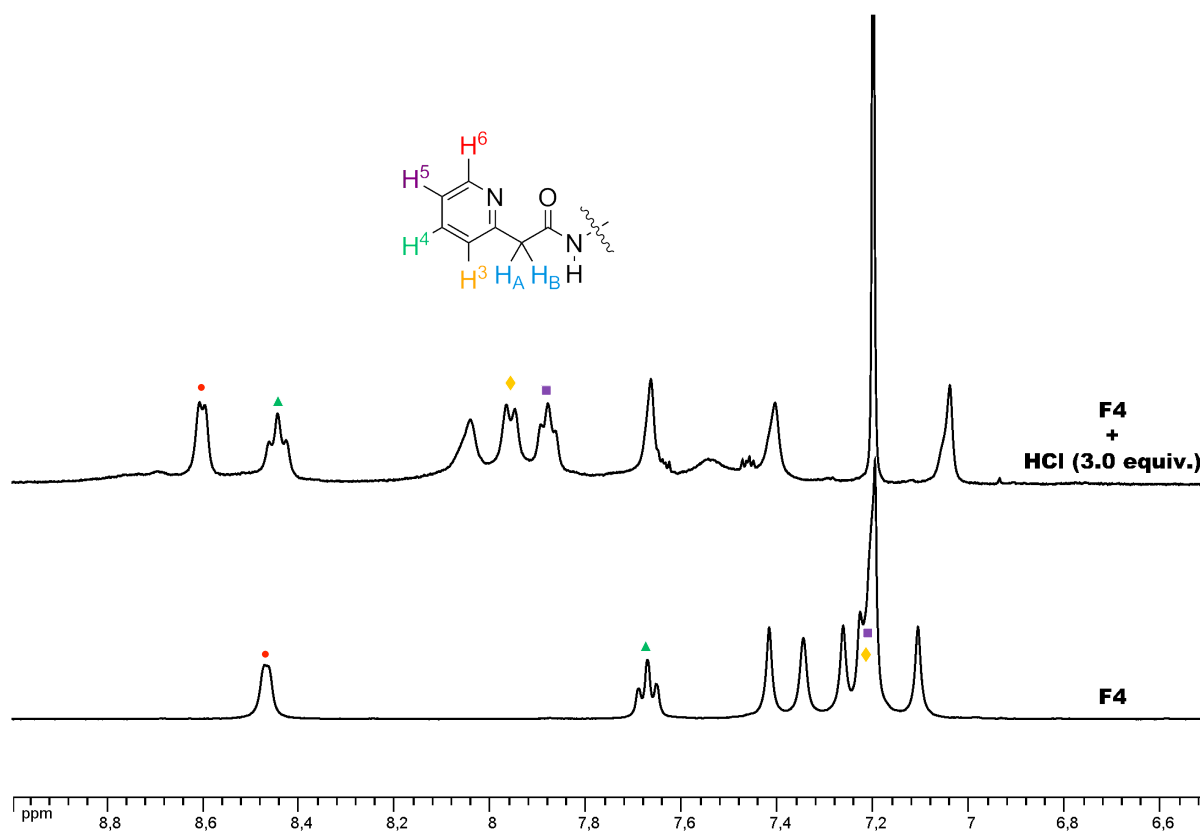


Figure S57. Portions of the ¹H NMR (400 MHz, CDCl₃) spectra of **F4**, and **F4** in the presence of HCl (3.0 equiv.) both recorded at 296 K; [**F4**] = 10 → 9.6 mM; () δ H₃; (▲) δ H₄; (■) δ H₅; (●) δ H₆.

IX. Estimation of the binding constants for the systems HA1↔F4, HA4↔F4 and HA6↔F4

The estimation of the order of magnitude of the binding constants (K) for the systems **HA1↔F4**, **HA4↔F4** and **HA6↔F4** have been obtained using the program DYNAFIT.⁸

• For the **HA1↔F4** system, a 1:1 binding model has been used to fit the experimental data from the corresponding titration experiment. Four different spectroscopic outputs were fitted:

- The anisochronicities ($\Delta\delta$) of the two diastereotopic signals ^{13}C of the NMR probe from Figure S37.
- The anisochronicities ($\Delta\delta$) of the two diastereotopic signals ^1H of the 2-pyridylacetamide motif **B4** from Figure S36.⁹
- The chemical shift difference of the aromatic proton in position 4 ($\Delta\delta\text{H4}$) of the 2-pyridylacetamide motif **B4** with respect to $\delta^0\text{H4} = 7671$ ppb (**HA1** = 0 equiv.) of **F4** from Figure S35.
- The chemical shift of the aromatic proton in position 6 ($\Delta\delta\text{H6}$) of the 2-pyridylacetamide motif **B4** with respect to $\delta^0\text{H6} = 8468$ ppb (**HA1** = 0 equiv.) of **F4** from Figure S35.

In each cases, three binding constants ($K = 10^3$, 10^4 and 10^5 M^{-1}) have been simulated and plotted alongside the experimental data. The results are shown Figures S58-61.

• For the **HA1↔F4** system, a 1:1 binding model has been used to fit the experimental data from the corresponding titration experiment (Figure 41). The anisochronicities ($\Delta\delta$) of the two diastereotopic signals ^{13}C of the NMR probe have been simulated and plotted alongside the experimental data using three binding constants ($K = 10^3$, 10^4 and 10^5 M^{-1}). The results are shown Figure S62.

• For the **HA6↔F4** system, a 2:1 binding model have been used in order to fit the experimental data of the corresponding titration experiment (Figure S45). The anisochronicities ($\Delta\delta$) of the two diastereotopic signals ^{13}C of the NMR probe have been simulated and plotted alongside the experimental data. In this case, two sets of fitting have been performed: a) $K = 10^5$, 10^6 , 10^7 and 10^8 M^{-1} with $K' = 10^4 \text{ M}^{-1}$; b) $K = 10^7 \text{ M}^{-1}$ with $K' = 10^3$, 10^4 , 10^5 and 10^6 M^{-1} . The results are shown Figures S63 and S64.

[8] Kuzmic, P. *Anal. Biochem.* **1996**, *237*, 260–273.

[9] Anisochronicity ($\Delta\delta$) in this AB systems was calculated from the formula: $\Delta\delta = [(v_1 - v_4) \times (v_2 - v_3)]^{1/2}$

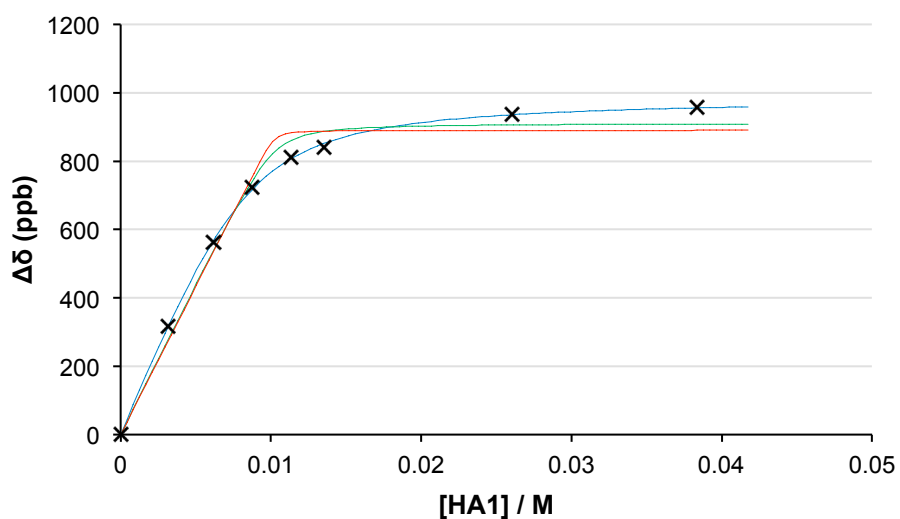


Figure S58. Anisochronicity ($\Delta\delta$, ppb) of the two diastereotopic $^{13}\text{CH}_3$ signals of the NMR probe in **F4** vs $[\text{HA1}]$ (M): (X) Plot of the experimental data recorded in CDCl_3 at 296 K; $0.088 < [\text{F4}] < 0.010$ M. Curves fits shown for a 1:1 binding model using the program DynaFit: $K = 10^3 \text{ M}^{-1}$ (—), $K = 10^4 \text{ M}^{-1}$ (—), $K = 10^5 \text{ M}^{-1}$ (—).

Optimized Parameters for $K = 10^3 \text{ M}^{-1}$

No.	Par#Set	Initial	Final	Std. Error	CV (%)
#1	[F4] (M)	0.01	0.00840965	0.000132323	1.57
#2	$r(\text{HA1.F4}) (\Delta\delta/\text{M})$	100000	117441	1558.63	1.33

Optimized Parameters for $K = 10^4 \text{ M}^{-1}$

No.	Par#Set	Initial	Final	Std. Error	CV (%)
#1	[F4] (M)	0.01	0.0102202	0.000630884	6.17
#2	$r(\text{HA1.F4}) (\Delta\delta/\text{M})$	100000	89216.2	4532.79	5.08

Optimized Parameters for $K = 10^5 \text{ M}^{-1}$

No.	Par#Set	Initial	Final	Std. Error	CV (%)
#1	[F4] (M)	0.01	0.010253	0.000691109	6.74
#2	$r(\text{HA1.F4}) (\Delta\delta/\text{M})$	100000	86858.2	5048.47	5.81

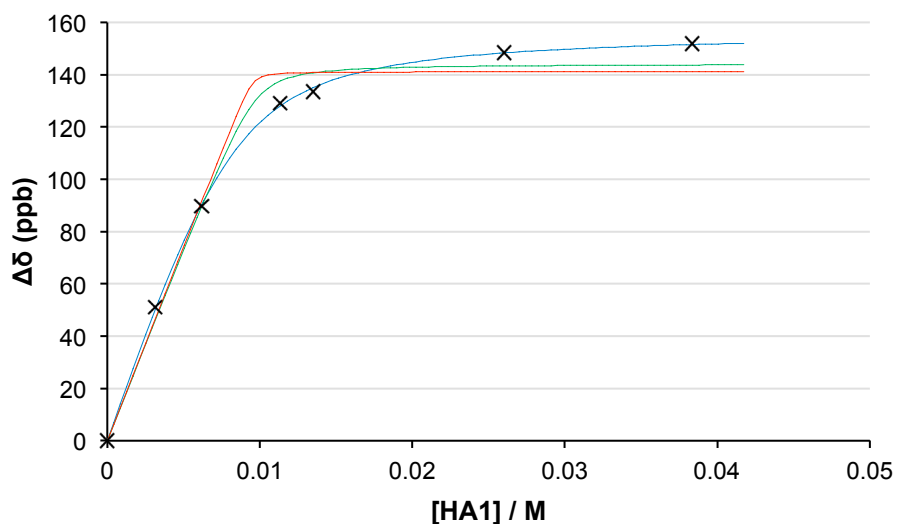


Figure 59. Anisochronicity ($\Delta\delta$, ppb) of the two diastereotopic ^1H signals of the NMR probe in **F4** vs **[HA1]** (M): (X) Plot of the experimental data recorded in CDCl_3 at 296 K; $0.088 < [\text{F4}] < 0.010$ M. Curves fits shown for a 1:1 binding model using the program DynaFit: $K = 10^3 \text{ M}^{-1}$ (—), $K = 10^4 \text{ M}^{-1}$ (—), $K = 10^5 \text{ M}^{-1}$ (—).

Optimized Parameters for $K = 10^3 \text{ M}^{-1}$

No.	Par#Set	Initial	Final	Std. Error	CV (%)
#1	[F4] (M)	0.01	0.00837463	0.000129025	1.54
#2	r(HA1.F4) ($\Delta\delta/\text{M}$)	10000	18696.2	251.208	1.34

Optimized Parameters for $K = 10^4 \text{ M}^{-1}$

No.	Par#Set	Initial	Final	Std. Error	CV (%)
#1	[F4] (M)	0.01	0.00972676	0.000785506	8.08
#2	r(HA1.F4) ($\Delta\delta/\text{M}$)	10000	14829.8	1069.09	7.21

Optimized Parameters for $K = 10^5 \text{ M}^{-1}$

No.	Par#Set	Initial	Final	Std. Error	CV (%)
#1	[F4] (M)	0.01	0.00952711	0.000870217	9.13
#2	r(HA1.F4) ($\Delta\delta/\text{M}$)	10000	14820.1	1261.74	8.51

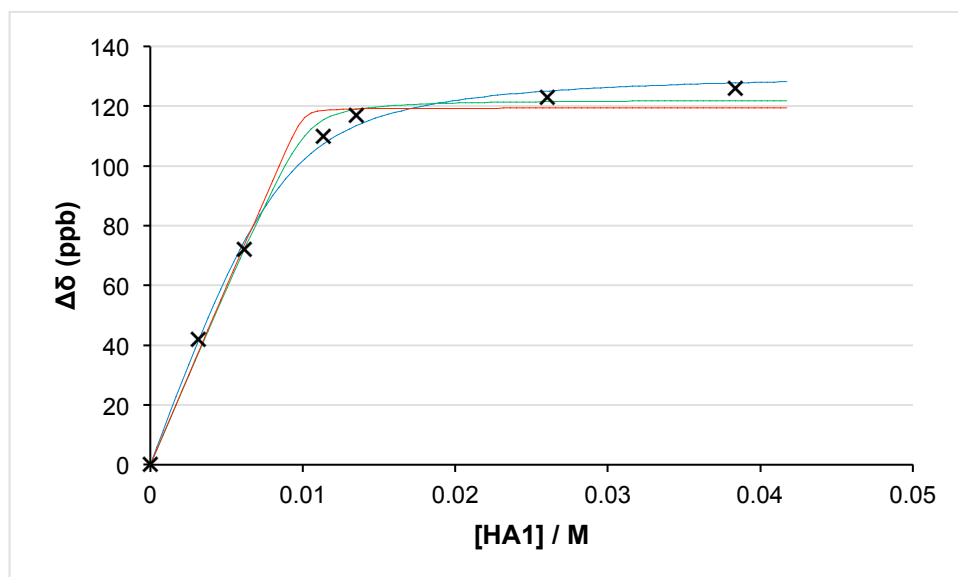


Figure 60. Chemical shift difference ($\Delta\delta$, ppb) of the aromatic proton in position 4 in **F4** vs **[HA1]** (M): (X) Plot of the experimental data recorded in CDCl_3 at 296 K; $0.088 < [\text{F4}] < 0.010$ M. Curves fits shown for a 1:1 binding model using the program DynaFit: $K = 10^3 \text{ M}^{-1}$ (—), $K = 10^4 \text{ M}^{-1}$ (—), $K = 10^5 \text{ M}^{-1}$ (—).

Optimized Parameters for $K = 10^3 \text{ M}^{-1}$

No.	Par#Set	Initial	Final	Std. Error	CV (%)
#1	[F4] (M)	0.01	0.00860129	0.000443531	5.16
#2	r(HA1.F4) ($\Delta\delta/\text{M}$)	10000	15353.3	687.709	4.48

Optimized Parameters for $K = 10^4 \text{ M}^{-1}$

No.	Par#Set	Initial	Final	Std. Error	CV (%)
#1	[F4] (M)	0.01	0.0102394	0.000554792	5.42
#2	r(HA1.F4) ($\Delta\delta/\text{M}$)	10000	11942.9	569.319	4.77

Optimized Parameters for $K = 10^5 \text{ M}^{-1}$

No.	Par#Set	Initial	Final	Std. Error	CV (%)
#1	[F4] (M)	0.01	0.0100106	0.000727985	7.27
#2	r(HA1.F4) ($\Delta\delta/\text{M}$)	100000	11931.8	808.548	6.78

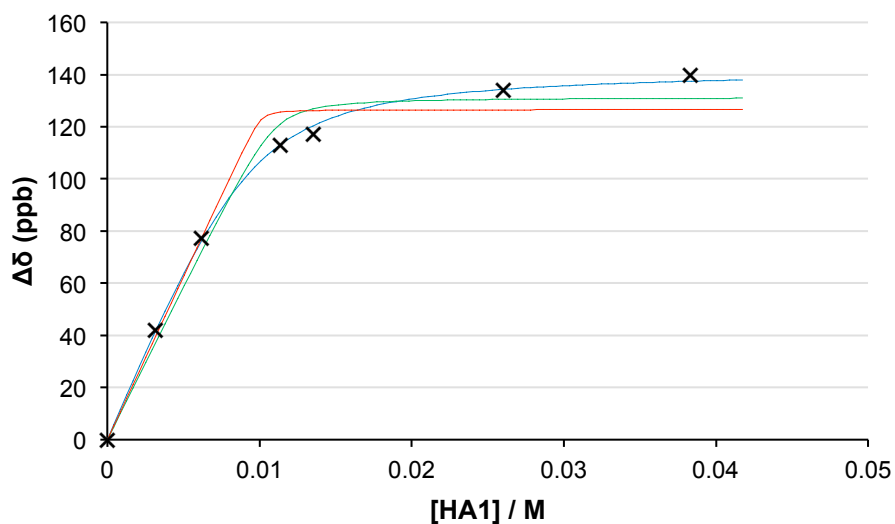


Figure 61. Chemical shift difference ($\Delta\delta$, ppb) of the aromatic proton in position 6 in **F4** vs **[HA1]** (M): (X) Plot of the experimental data recorded in CDCl_3 at 296 K; $0.088 < [\text{F4}] < 0.010$ M. Curves fits shown for a 1:1 binding model using the program DynaFit: $K = 10^3 \text{ M}^{-1}$ (—), $K = 10^4 \text{ M}^{-1}$ (—), $K = 10^5 \text{ M}^{-1}$ (—).

Optimized Parameters for $K = 10^3 \text{ M}^{-1}$

No.	Par#Set	Initial	Final	Std. Error	CV (%)
#1	[F4] (M)	0.01	0.00942117	0.000326581	3.47
#2	r(HA1.F4) ($\Delta\delta/\text{M}$)	100000	15091.4	447.622	2.97

Optimized Parameters for $K = 10^4 \text{ M}^{-1}$

No.	Par#Set	Initial	Final	Std. Error	CV (%)
#1	[F4] (M)	0.01	0.0110802	0.00112555	10.16
#2	r(HA1.F4) ($\Delta\delta/\text{M}$)	100000	11856.9	1023.3	8.63

Optimized Parameters for $K = 10^5 \text{ M}^{-1}$

No.	Par#Set	Initial	Final	Std. Error	CV (%)
#1	[F4] (M)	0.01	0.0101312	0.00124573	12.30
#2	r(HA1.F4) ($\Delta\delta/\text{M}$)	100000	12495.1	1430.16	11.45

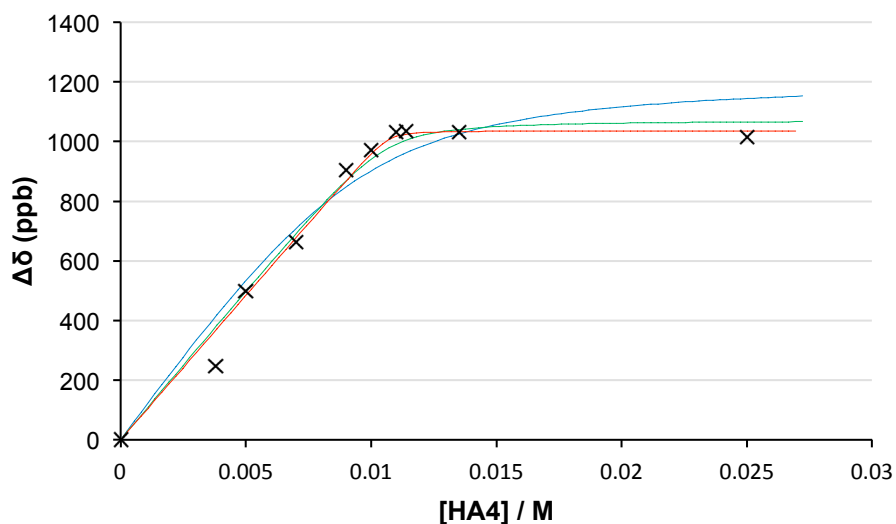


Figure S62. Anisochronicity ($\Delta\delta$, ppb) of the two diastereotopic $^{13}\text{CH}_3$ signals of the NMR probe in **F4** vs $[\text{HA4}]$ (M): (X) Plot of the experimental data recorded in CDCl_3 at 296 K; $[\text{F4}] = 0.010$ M. Curves fits shown for a 1:1 binding model using the program DynaFit: $K = 10^3 \text{ M}^{-1}$ (—), $K = 10^4 \text{ M}^{-1}$ (—), $K = 10^5 \text{ M}^{-1}$ (—)

Optimized Parameters for $K = 10^3 \text{ M}^{-1}$

No.	Par#Set	Initial	Final	Std. Error	CV (%)
#1	$[\text{F4}]$ (M)	0.01	0.00962265	0.00165074	17.15
#2	$r(\text{HA4.F4})$ ($\Delta\delta/\text{M}$)	101700	126414	15442.6	12.22

Optimized Parameters for $K = 10^4 \text{ M}^{-1}$

No.	Par#Set	Initial	Final	Std. Error	CV (%)
#1	$[\text{F4}]$ (M)	0.01	0.0105973	0.000702324	6.63
#2	$r(\text{HA4.F4})$ ($\Delta\delta/\text{M}$)	101700	101255	4530.43	4.47

Optimized Parameters for $K = 10^5 \text{ M}^{-1}$

No.	Par#Set	Initial	Final	Std. Error	CV (%)
#1	$[\text{F4}]$ (M)	0.01	0.0106926	0.000458916	4.29
#2	$r(\text{HA4.F4})$ ($\Delta\delta/\text{M}$)	101700	96986.6	2985.36	3.08

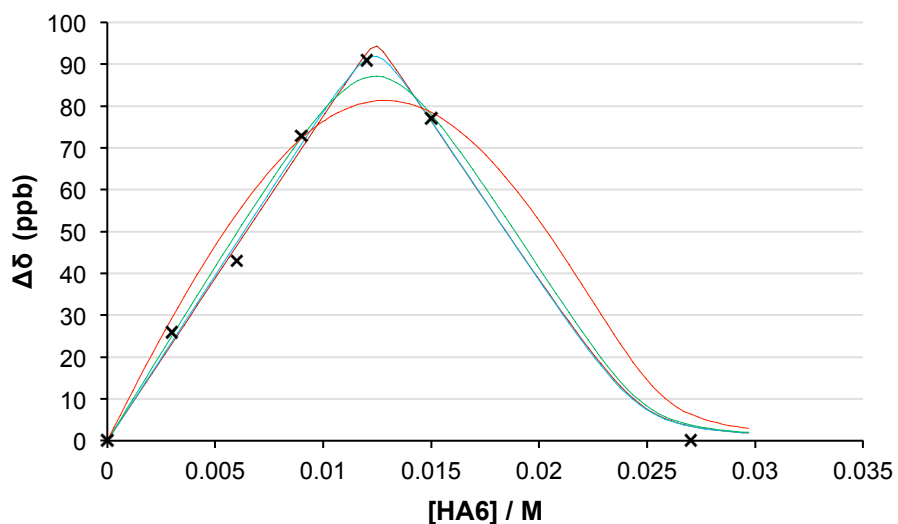


Figure S63. Anisochronicity ($\Delta\delta$, ppb) of the two diastereotopic $^{13}\text{CH}_3$ signals of the NMR probe in **F4** vs **[HA6]** (M): (X) Plot of the experimental data recorded in CDCl_3 at 296 K; **[F4]** = 0.010 M. Curves fits shown for a 2:1 binding model using the program DynaFit: $K = 10^5 \text{ M}^{-1}$ and $K' = 10^4 \text{ M}^{-1}$ (—), $K = 10^6 \text{ M}^{-1}$ and $K' = 10^4 \text{ M}^{-1}$ (—), $K = 10^7 \text{ M}^{-1}$ and $K' = 10^4 \text{ M}^{-1}$ (—), $K = 10^8 \text{ M}^{-1}$ and $K' = 10^4 \text{ M}^{-1}$ (—).

Optimized Parameters for $K_1 = 10^5 \text{ M}^{-1}$ and $K_2 = 10^4 \text{ M}^{-1}$

No.	Par#Set	Initial	Final	Std. Error	CV (%)
#1	[F4] (M)	0.01	0.0128113	0.00102255	7.98
#2	r(HA6.F4) ($\Delta\delta/\text{M}$)	1000	10368.7	866.497	8.36

Optimized Parameters for $K_1 = 10^6 \text{ M}^{-1}$ and $K_2 = 10^4 \text{ M}^{-1}$

No.	Par#Set	Initial	Final	Std. Error	CV (%)
#1	[F4] (M)	0.01	0.0124041	0.000387968	3.13
#2	r(HA6.F4) ($\Delta\delta/\text{M}$)	1000	8433.23	330.68	3.92

Optimized Parameters for $K_1 = 10^7 \text{ M}^{-1}$ and $K_2 = 10^4 \text{ M}^{-1}$

No.	Par#Set	Initial	Final	Std. Error	CV (%)
#1	[F4] (M)	0.01	0.0123462	0.0002391	1.94
#2	r(HA6.F4) ($\Delta\delta/\text{M}$)	1000	7916.27	204.668	2.59

Optimized Parameters for $K_1 = 10^8 \text{ M}^{-1}$ and $K_2 = 10^4 \text{ M}^{-1}$

No.	Par#Set	Initial	Final	Std. Error	CV (%)
#1	[F4] (M)	0.01	0.0124054	0.000232729	1.88
#2	r(HA6.F4) ($\Delta\delta/\text{M}$)	1000	7765.17	189.937	2.45

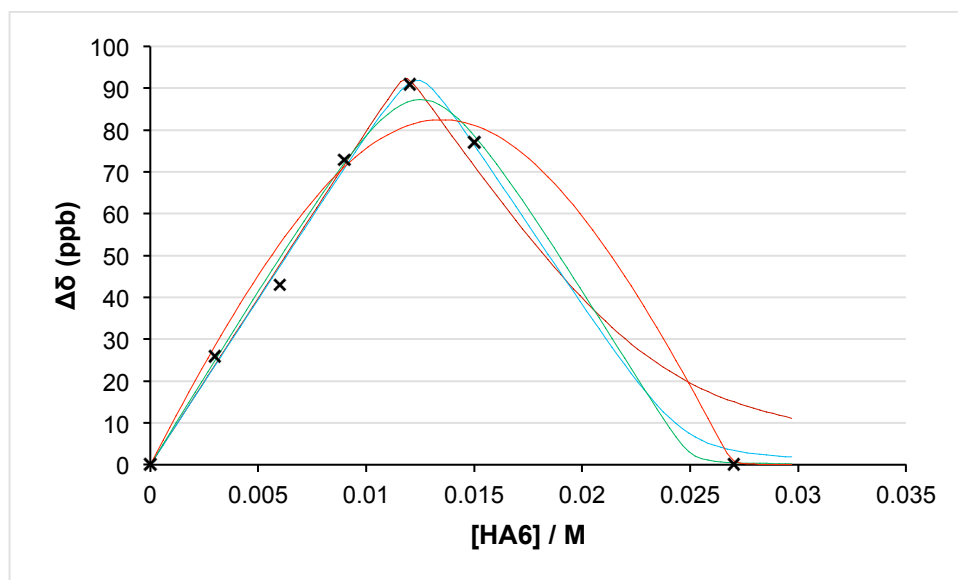


Figure 64. Anisochronicity ($\Delta\delta$, ppb) of the two diastereotopic $^{13}\text{CH}_3$ signals of the NMR probe in **F4** vs **[HA6]** (M): (X) Plot of the experimental data recorded in CDCl_3 at 296 K; **[F4]** = 0.010 M. Curves fits shown for a 2:1 binding model using the program DynaFit: $K = 10^7 \text{ M}^{-1}$ and $K' = 10^3 \text{ M}^{-1}$ (—), $K = 10^7 \text{ M}^{-1}$ and $K' = 10^4 \text{ M}^{-1}$ (—), $K = 10^7 \text{ M}^{-1}$ and $K' = 10^5 \text{ M}^{-1}$ (—), $K = 10^7 \text{ M}^{-1}$ and $K' = 10^6 \text{ M}^{-1}$ (—).

Optimized Parameters for $K_1 = 10^7 \text{ M}^{-1}$ and $K_2 = 10^3 \text{ M}^{-1}$

No.	Par#Set	Initial	Final	Std. Error	CV (%)
#1	[F4] (M)	0.01	0.0118217	0.000613102	5.19
#2	r(HA6.F4) ($\Delta\delta/\text{M}$)	1000	7968.98	645.66	8.10

Optimized Parameters for $K_1 = 10^7 \text{ M}^{-1}$ and $K_2 = 10^4 \text{ M}^{-1}$

No.	Par#Set	Initial	Final	Std. Error	CV (%)
#1	[F4] (M)	0.01	0.0123462	0.0002391	1.94
#2	r(HA6.F4) ($\Delta\delta/\text{M}$)	1000	7916.27	204.668	2.59

Optimized Parameters for $K_1 = 10^7 \text{ M}^{-1}$ and $K_2 = 10^5 \text{ M}^{-1}$

No.	Par#Set	Initial	Final	Std. Error	CV (%)
#1	[F4] (M)	0.01	0.0124978	0.000360341	2.88
#2	r(HA6.F4) ($\Delta\delta/\text{M}$)	1000	8385.48	296.071	3.53

Optimized Parameters for $K_1 = 10^7 \text{ M}^{-1}$ and $K_2 = 10^6 \text{ M}^{-1}$

No.	Par#Set	Initial	Final	Std. Error	CV (%)
#1	[F4] (M)	0.01	0.0134769	0.000712328	5.29
#2	r(HA6.F4) ($\Delta\delta/\text{M}$)	1000	9991.32	595.802	5.96

X. Estimation of relative pK_a values of acids in 1,2-dichloroethane

The pK_a values of acids **HA1**, **HA4** and **HA6** in 1,2-dichloroethane (DCE) relative to 2,4,6-trinitrophenol were estimated by linear regression method. For **HA4** and **HA6**, absolute pK_a values of a set of acids in acetonitrile^{10,11,12,13} were correlated with corresponding relative pK_a values in 1,2-dichloroethane.^{10,14} Separate correlations were built for OH and NH acids. The numerical data are shown in Table S7.

As there were no suitable acidity data reported for **HA1**, the dissociation energies of 8 OH acids were calculated using COSMO-RS method¹⁵ and correlated with their relative pK_a values in DCE. Calculations were carried out with software packages Turbomole V6.2¹⁶ and COSMOtherm Version C3.0 release 14.01¹⁷ (with default parametrization). The BP functional with TZVP basis set and RI approximation were used.¹⁸ Calculated dissociation energy values are shown in Table S7.

Parameters of linear regressions:

HA1: 8 OH acids, R²=0.9915

HA4: 7 OH acids, R²=0.9941

HA6: 7 NH acids, R²=0.9967

In order to confirm the usability of DCE as model for chloroform the Gibbs free energy differences between acids and their anions were calculated in chloroform using COSMO-RS, and the results correlated with pK_a data in 1,2-dichloroethane. The obtained R² values, 0.97 for OH acids and 0.96 for NH acids, confirm the validity of DCE as a model for chloroform.

-
- [10] Kütt, A.; Rodima, T.; Saame, J.; Raamat, E.; Mäemets, V.; Kaljurand, I.; Koppel, I. A.; Garlyauskayte, R. Yu.; Yagupolskii, Yu. L.; Yagupolskii, L. M.; Bernhardt, E.; Willner, H.; Leito, I. *J. Org. Chem.* **2011**, *76*, 391–395.
- [11] Kütt, A.; Leito, I.; Kaljurand, I.; Sooväli, L.; Vlasov, V. M.; Yagupolskii, L. M.; Koppel, I. A. *J. Org. Chem.* **2006**, *71*, 2829–2838.
- [12] Kaupmees, K.; Tolstoluzhsky, N.; Raja, S.; Rueping, M.; Leito, I. *Angew. Chem. Int. Ed.* **2013**, *52*, 11569–11572.
- [13] Kütt, A.; Movchun, V.; Rodima, T.; Dansauer, T.; Rusanov, E. B.; Leito, I.; Kaljurand, I.; Koppel, J.; Pihl, V.; Koppel, I.; Ovsjannikov, G.; Toom, L.; Mishima, M.; Medebielle, M.; Lork, E.; Röschenthaler, G.-V.; Koppel, I. A.; Kolomeitsev, A. A. *J. Org. Chem.* **2008**, *73*, 2607–2620.
- [14] Raamat, E.; Kaupmees, K.; Ovsjannikov, G.; Trummal, A.; Kütt, A.; Saame, J.; Koppel, I.; Kaljurand, I.; Lipping, L.; Rodima, T.; Pihl, V.; Koppel, I. A.; Leito, I. *J. Phys. Org. Chem.* **2013**, *26*, 162–170.
- [15] Eckert, F.; Klamt, A. *AIChE J.* **2002**, *48*, 369–385.
- [16] Ahlrichs, R.; Bär, M.; Baron, H.-P.; Bauernschmitt, R.; Böcker, S.; Ehrig, M.; Eichkorn, K.; Elliott, S.; Furche, F.; Haase, F.; Häser, M.; Horn, H.; Hattig, C.; Huber, C.; Huniar, U.; Kattannek, M.; Köhn, M.; Kölmel, C.; Kollwitz, M.; May, K.; Ochsenfeld, C.; Öhm, H.; Schäfer, A.; Schneider, U.; Treutler, O.; Arnim, M. Von; Weigend, F.; Weis, P.; Weiss, H.; TURBOMOLE V6.2, **2010**.
- [17] F. Eckert and A. Klamt, COSMOtherm, Version C3.0, Release 14.01; COSMOlogic GmbH & Co. KG, Leverkusen, Germany, 2013.
- [18] For more details on the computational procedure, see: Eckert, F.; Leito, I.; Kaljurand, I.; Kütt, A.; Klamt, A.; Diedenhofen, M. *J. Comput. Chem.* **2009**, *30*, 799–810.

Acid	Type	pK _a		ΔG _{diss} (kcal/mol)
		in MeCN (abs) ^a	in DCE (rel) ^b	in DCE
Phenol	OH	29.14 [ref 13]	19.6 [ref 14]	81.8
Acetic acid	OH	23.51[ref 11]	15.5 [ref 14]	75.8
(CF ₃) ₃ COH	OH	20.55 [ref 11]	9.2 [ref 14]	67.3
2,4,6-trinitrophenol	OH	11.0	0	56.3
2,4,6-(SO ₂ F) ₃ -phenol	OH	5.53	-5.9	47.1
2,4,6-Tf ₃ -phenol	OH	4.80	-6.4	49.5
TfOH	OH	0.70 [ref 10]	-11.4	41.6
C(CN) ₂ =C(CN)OH	OH		-8.8	41.4
4-NO ₂ -C ₆ H ₄ SO ₂ NHTos	NH	10.04	-1.5	59.8
4-NO ₂ -C ₆ H ₄ SO ₂ -NH-SO ₂ -C ₆ H ₄ -4-Cl	NH	9.17	-2.4	58.6
(4-NO ₂ -C ₆ H ₄ -SO ₂) ₂ -NH	NH	8.19	-3.7	56.6
4-Cl-C ₆ H ₄ SO(=NTf)-NH-Tos	NH	5.14	-6.8	53.9
4-Cl-C ₆ H ₄ SO(=NTf)-NH-SO ₂ -C ₆ H ₄ -4-Cl	NH	4.34	-7.6	52.7
4-NO ₂ -C ₆ H ₄ SO ₂ NHTf	NH	4.39	-7.8	50.8
4-Cl-C ₆ H ₄ SO(=NTf)-NH-SO ₂ -C ₆ H ₄ -4-NO ₂	NH	3.62	-8.9	48.7
HA1	OH			70.9
HA4	OH	13.6 [ref 12]		59.5
HA6	NH	6.7 [ref 12]		55.1

Table S7. Acidity data used for pK_a estimation: ^aAbsolute pK_a values, experimental data from reference 18, if not stated otherwise; ^brelative pK_a values, experimental data from reference 10, if not stated otherwise.

XI. VT ^{13}C NMR experiments of F4 with 0.5 equiv. of HA1 and F4 with 0.5 equiv. of HA4

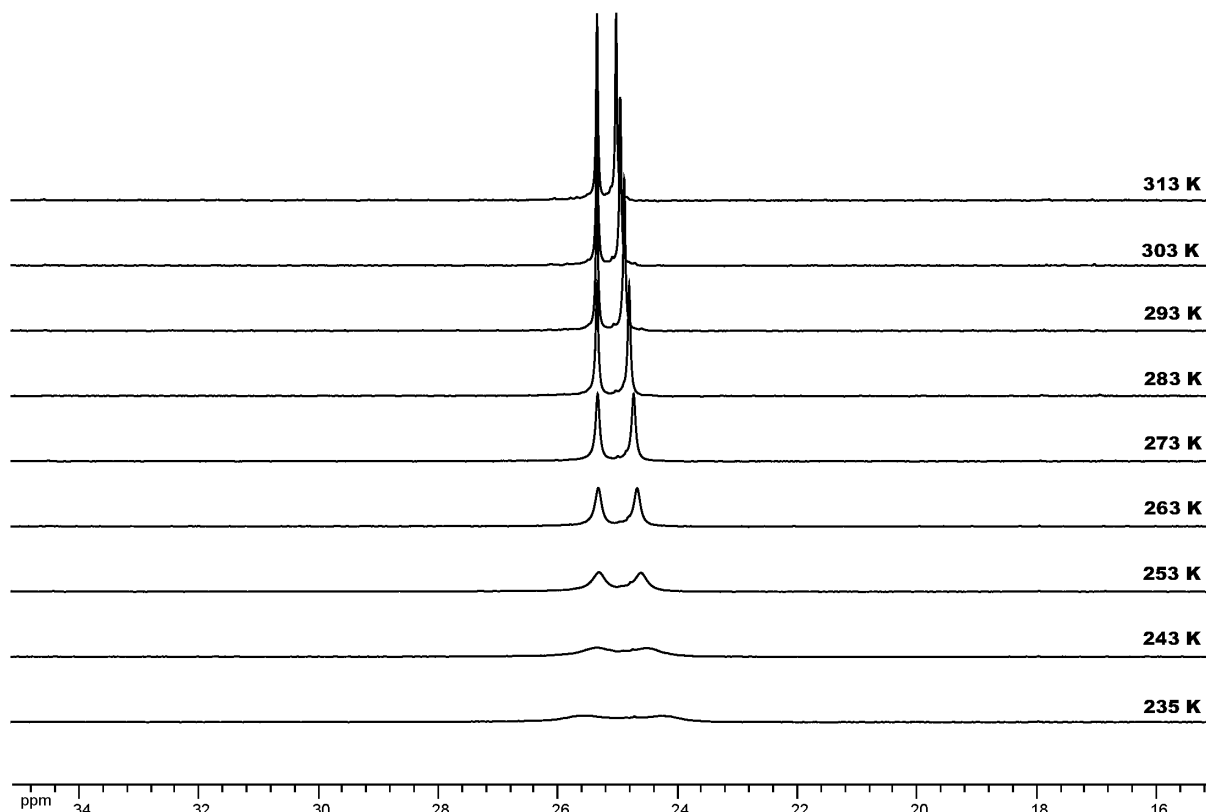


Figure S65. Variable temperature experiment: portions of the ^{13}C NMR (125 MHz, CDCl_3) spectra of F4 in the presence of HA1; [F4] = 10 mM, [HA1] = 5 mM

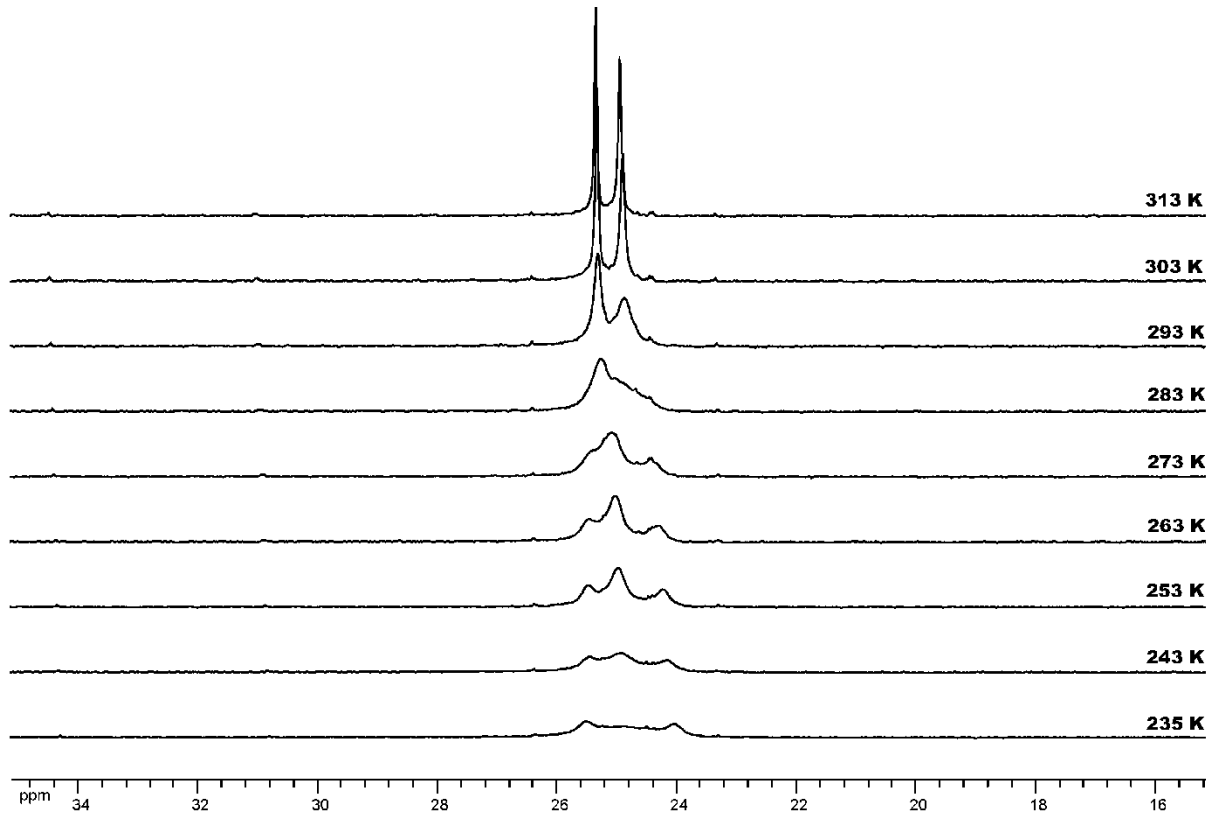


Figure S66. Variable temperature experiment: portions of the ^{13}C NMR (125 MHz, CDCl_3) spectra of F4 in the presence of HA4; [F4] = 10 mM, [HA4] = 5 mM

XII. Line shapes simulation of the ^{13}C NMR spectra

Experimental methyl region ^{13}C NMR spectra for the titration of **F4** with **HA4** from 0 to 0.9 equivalents at +22 °C, and for a mixture of 0.5 equivalents of **HA4** with **F4** as a function of temperature from -38 to +40 °C, were fitted as a single combined dataset to a basic analytical 4+4 site model for the spectral bandshape of the two **F4** methyl signals, using the program Mathematica. (Titration data beyond 0.9 equivalents were discarded because of evidence for multiple binding). The model is summarised in Fig. S67, and involves exchange between the left- and right-handed forms of bound and unbound **F4**. To keep the number of variable parameters within bounds it makes a number of simplifying assumptions, including that there is no direct exchange between bound and unbound **F4** of opposite chirality (i.e. dissociation and inversion are not concerted), that the rate constants for binding are independent of chirality (i.e. that the bound chiral preference is reflected solely in the dissociation rate constants), and that the chemical shifts of the two methyls in bound **F4** are exchanged by inversion (i.e. that the effect of the distant bound **HA4** on the chemical shift difference between the two methyls is negligible). The two-bond coupling between the labelled methyl carbons is unresolved under the conditions used and so is neglected.

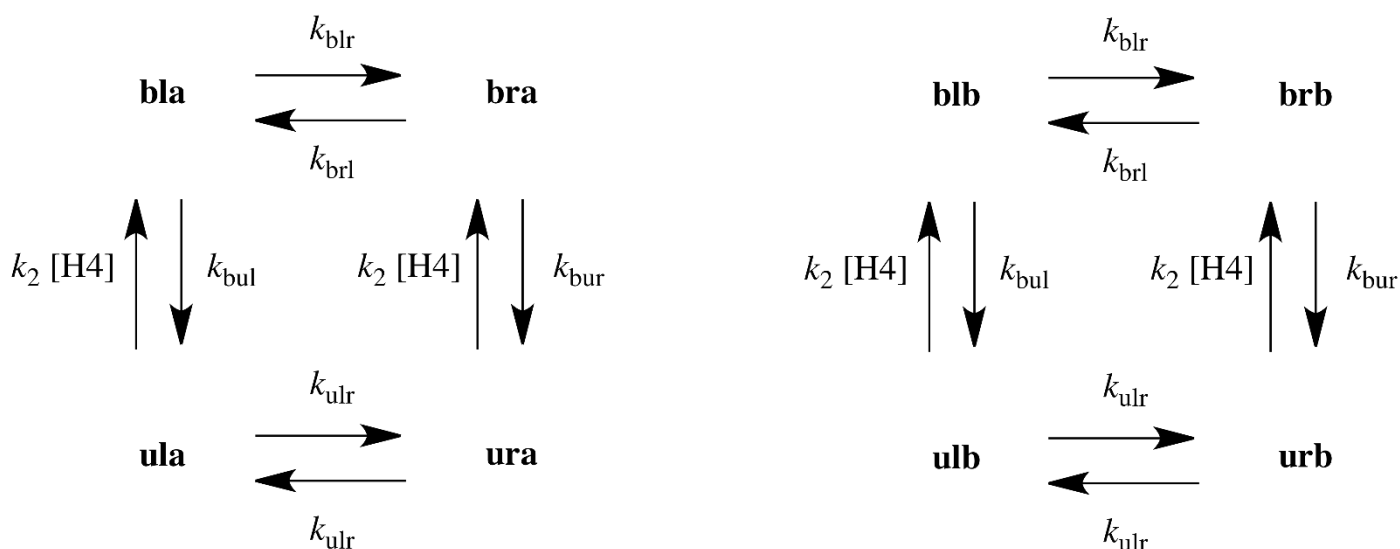


Figure S67. Exchange processes for the 4+4 site exchange model for the two methyl resonances of **F4** binding reversibly to **HA4**. The two methyls (**a** and **b**) are found in left- and right-handed forms (**l** and **r**) bound and unbound (**b** and **u**) to **HA4**.

The calculation is simplified by the requirements that the concentrations of left- and right-handed free **F4** be equal, and that the chemical shifts of the two methyl resonances exchange on helix inversion. Since there is no direct exchange between the two methyl groups in a given **F4** molecule, the final bandshape for the reporter methyl region reduces to the result of adding together the independent results of calculating the 4-site exchange spectra for the two different methyl resonances. The 4-site bandshape is calculated analytically by solving four coupled sets of the complex Bloch equations for transverse magnetization in the steady state.

The principal uncertainty in the calculation is the true difference in chemical shift $\Delta\delta$ between the reporter methyl signals; iteration including this as a parameter tends to diverge, so a series of iterative fits were performed for different estimated values and the best fit by eye selected. The complete set of species and processes in Fig. S67 involves far too many parameters for reliable fitting, so some fairly drastic assumptions are necessary. Enthalpy differences between species are neglected, except in the case of helicity preference. Binding of **HA4** to **F4** is tight under all the conditions studied, so it is not possible to differentiate between the activation energies of the association and dissociation processes and a value has to be assumed for one or other. The activation energy is assumed to be the same for left- and right-handed **HA4-F4** dissociation, and the same for left-right interconversion in bound and unbound **F4**.

The fitting process finds the lowest sum of squares of differences between experimental and calculated data by varying the rate constants at 295 K and the activation energies for each of the processes shown in Fig S67, the enthalpy difference ΔH_b between the left- and right-handed bound forms of bound **F4**, the average change $\Delta\delta_b$ in the two methyl signal chemical shifts between bound and unbound **F4**, the chemical shift difference $\Delta\delta_{lim}$ between the two bound methyl signals in the limit of fast exchange (which is directly linked to the equilibrium constant between left- and right-handed bound forms of **F4** and to the helicity excess), and the vertical scale factor for the spectral data. The activation energy for the association process was, as noted above, arbitrarily fixed at 40 kJ mol⁻¹.

The results of fitting are summarised in Fig. S68, which compares experimental data (filled circles) with simulated spectra (solid lines) for the titration and variable temperature datasets. The parameter values used for Fig. S68 were as follows, with assumed values in italics and iterated values in Roman type. The rate constants at 295 K were $k_{ulr} = 2.7 \times 10^6 \text{ s}^{-1}$, $k_{bul} = 1080 \text{ s}^{-1}$ and $k_2 = 6.8 \times 10^6 \text{ dm}^3 \text{ mol}^{-1} \text{ s}^{-1}$, with corresponding activation energies of 81, 6 and 40 kJ mol⁻¹; the bound left-right exchange rate constants at 295 K k_{blr} and k_{brl} were $5.5 \times 10^5 \text{ s}^{-1}$ and $3.1 \times 10^6 \text{ s}^{-1}$ respectively. The enthalpy difference ΔH_b between left- and right-handed bound **F4** was -19 kJ mol⁻¹. The difference in chemical shift between the reporter methyl signals in the limit of slow exchange, $\Delta\delta$, was 1.5 ppm, the limiting difference in fast exchange, $\Delta\delta_{lim}$, was 1.042 ppm, and the average chemical shift change on dissociation, $\Delta\delta_b$, was +0.083 ppm, corresponding to a helicity at 295 K of 69%.

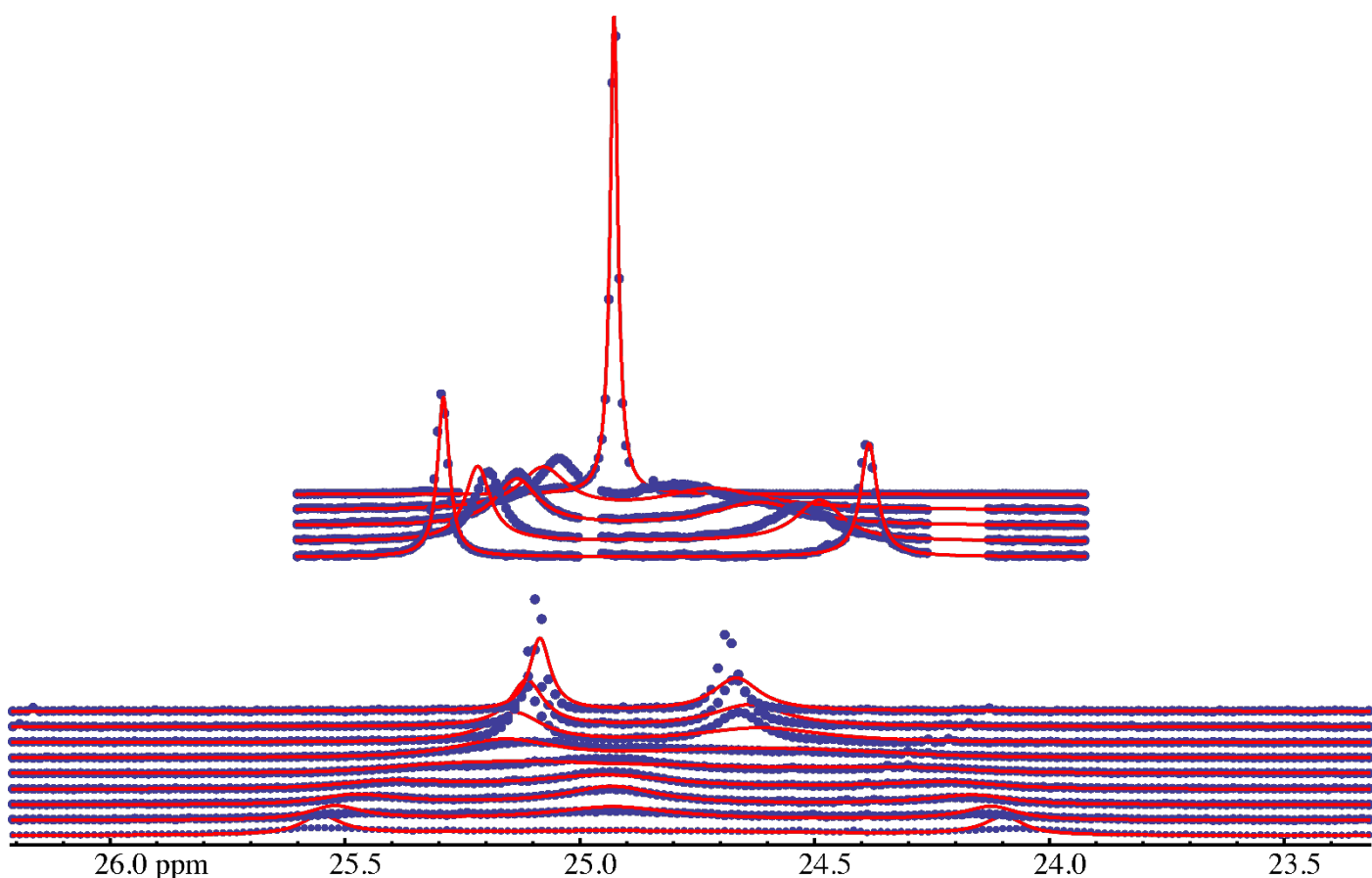


Figure S68. Experimental (filled circles) and simulated (solid lines) ^{13}C spectra for (bottom) a mixture of 5 mM HA4 and 10 mM **F4** at temperatures of (bottom to top) -38 , -30 , -20 , -10 , 0 , 10 , 20 , 30 and 40 $^{\circ}\text{C}$, and (top) a 10 mM solution of **F4** at 22 $^{\circ}\text{C}$ containing (bottom to top) 9, 7, 5, 3.8 and 0 mM **HA4**.

It should be emphasised that the values of the parameters provided by this fitting vary greatly in their significance. While the average chemical shifts are returned with very good confidence, many of the kinetic parameters are much less reliable, and a wide range of parameter sets exists that will give a good fit between theory and experiment. Even without the uncertainties introduced by fitting such a large number of parameters, the kinetic model will be incomplete at low temperatures, where other conformational processes will begin to slow down to the point where they cause significant line broadening. This biases the results of the fitting and, for example, exaggerates the difference in enthalpy between left- and right-handed bound **F4**. The purpose of the fitting exercise is not to try to obtain physically realistic parameters for the many different processes of Fig S67, but rather to provide convincing evidence for the overall form of the network of exchange processes shown there.

XIII. Switching induction ON and OFF experiment by the use of acid or base (Figure 4)

● Switching induction ON and OFF in system HA1↔F4

1. A solution of **HA1** (0.0075 mmol, 0.5 mL, 15 mM) was added to foldamer **F4** (0.005 mmol, 2.9 mg) which was directly weighed in an NMR tube. After vigorous shaking of the NMR tube for 1 min, ^1H and ^{13}C spectra of the resultant solution were recorded at 296 K. A portion of the ^{13}C NMR (100 MHz, CDCl_3) spectrum of **F4** in the presence of **HA1** is shown in Figure 4b.

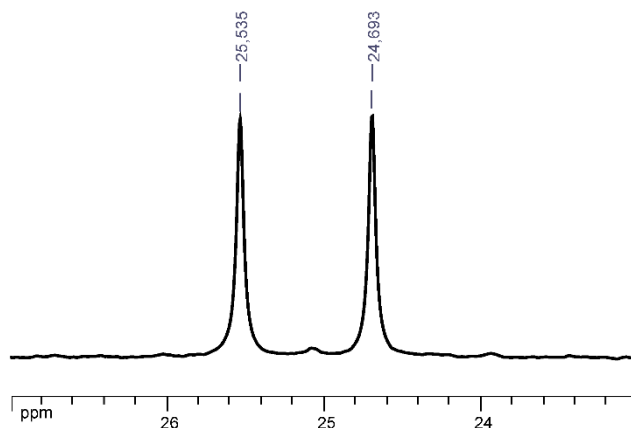


Figure 4b

2. A commercially available solution of **NH₃** in dioxane (15 μL , 0.0075 mmol, 0.5 M) was directly added in the NMR tube of the NMR sample from Fig. 4b. After vigorous shaking of the NMR tube for 1 min, ^1H and ^{13}C spectra of the resultant solution were recorded at 296 K. A portion of the ^{13}C NMR (100 MHz, CDCl_3) spectrum of **F4** in the presence of **HA1** and **NH₃** is shown in Figure 4c.

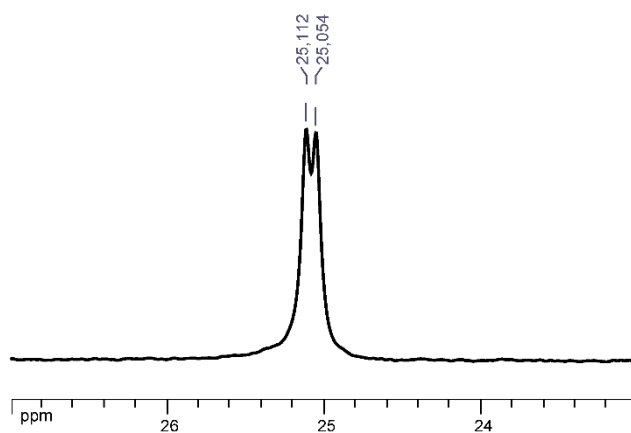


Figure 4c

3. A solution of **HCl** in CDCl_3 :dioxane / 5.3:1 (0.0075 mmol, 10 μL , 0.75 M), prepared from commercially available solution of HCl in dioxane (4 M) was directly added in the NMR tube of the NMR sample from Fig. 4c. After vigorous shaking of the NMR tube for 1 min, ^1H and ^{13}C spectra of the resultant solution were recorded at 296 K. A portion of the ^{13}C NMR (100 MHz, CDCl_3) spectrum of **F4** in the presence of **HA1**, **NH₃** and **HCl** is shown in Figure 4d.

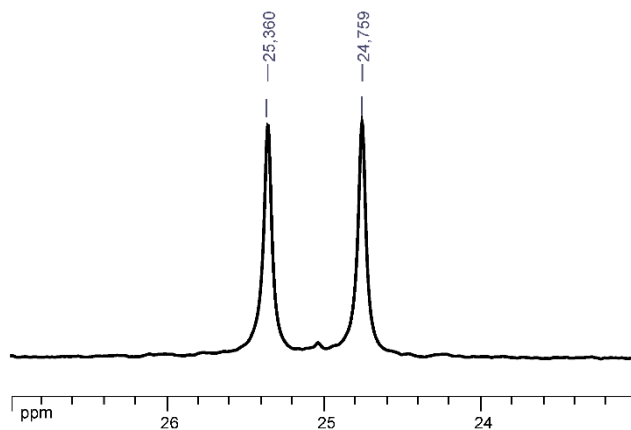


Figure 4d

● Switching induction ON and OFF in system HA4↔F4

1. HA4 (0.0075 mmol, 5.6 mg) and foldamer F4 (2.9 mg, 0.005 mmol) were directly weighed in an NMR tube to which CDCl₃ (0.5 mL) was added. After vigorous shaking of the NMR tube for 1 min, ¹H and ¹³C spectra of the resultant solution were recorded at 296 K. A portion of the ¹³C NMR (100 MHz, CDCl₃) spectrum of F4 in the presence of HA4 is shown in Figure 4f.

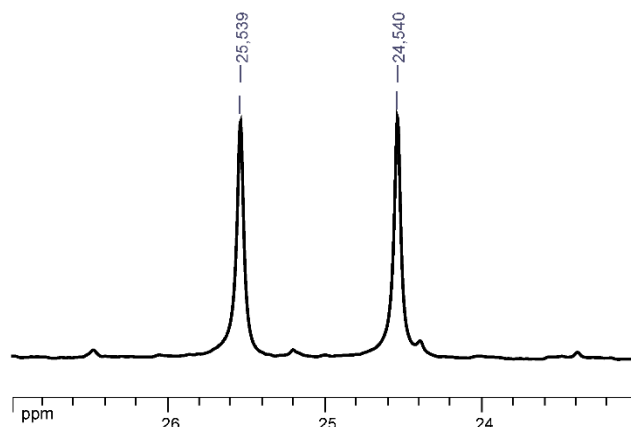


Figure 4f

2. A commercially available solution of NH₃ in dioxane (15 μL, 0.0075 mmol, 0.5 M) was directly added in the NMR tube of the NMR sample from Fig. 4f. After vigorous shaking of the NMR tube for 1 min, ¹H and ¹³C spectra of the resultant solution were recorded at 296 K. A portion of the ¹³C NMR (100 MHz, CDCl₃) spectrum of F4 in the presence of HA1 and NH₃ is shown in Figure 4g.

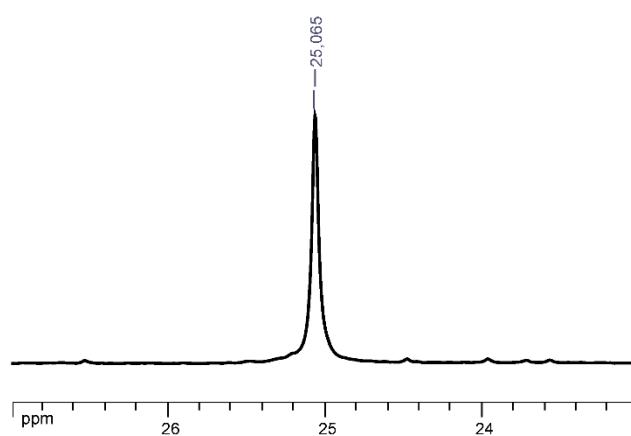


Figure 4g

3. A solution of HCl in CDCl₃:dioxane / 5.3:1 (0.0075 mmol, 10 μL, 0.75 M), prepared from commercially available solution of HCl in dioxane (4 M) was directly added in the NMR tube of the NMR sample from Fig. 4g. After vigorous shaking of the NMR tube for 1 min, ¹H and ¹³C spectra of the resultant solution were recorded at 296 K. A portion of the ¹³C NMR (100 MHz, CDCl₃) spectrum of F4 in the presence of HA4, NH₃ and HCl is shown in Figure 4h.

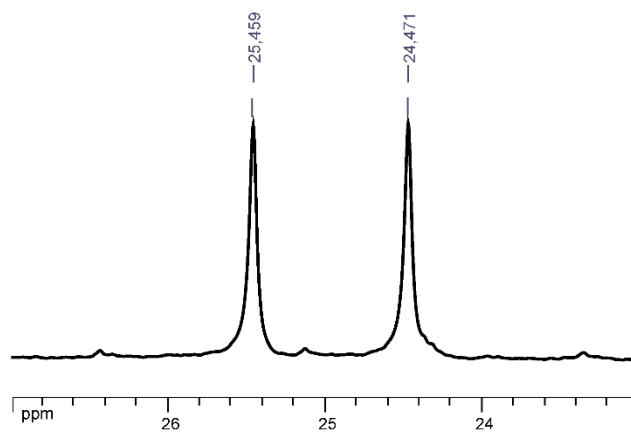
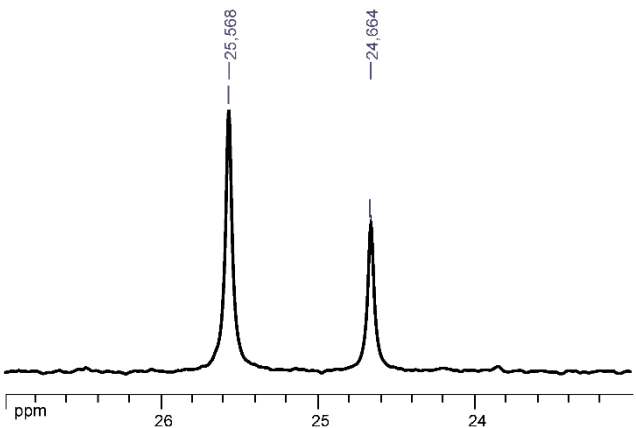
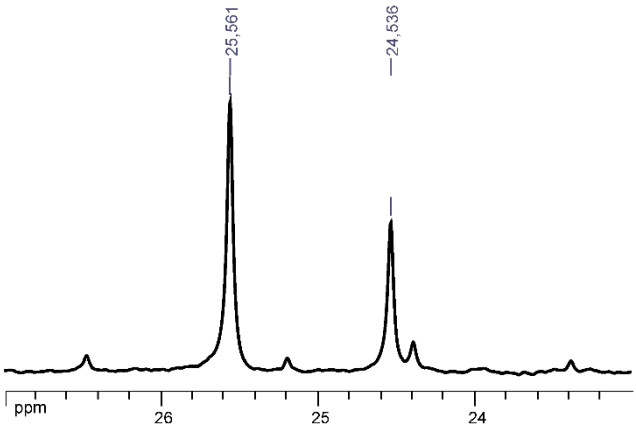
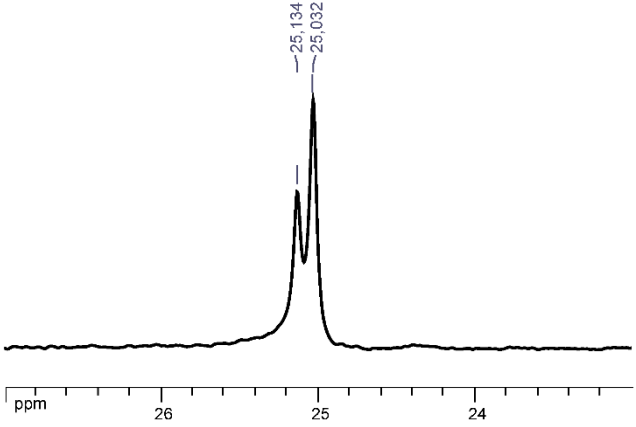


Figure 4h

XIV. Absolute screw sense induction in **F4*** induced by (*S*)-**HA1**, (*S*)-**HA4** and (*S*)-**HA6** (Figure 5a-c)

<p>A solution of (<i>S</i>)-HA1 (0.0075 mmol, 0.5 mL, 15 mM) was added to foldamer F4* (2.9 mg, 0.005 mmol) which was directly weighed in an NMR tube. After vigorous shaking of the NMR tube for 1 min, ^1H and ^{13}C spectra of the resultant solution were recorded at 296 K. A portion of the ^{13}C NMR (100 MHz, CDCl_3) spectrum of F4* in the presence of (<i>S</i>)-HA1 are shown in Figure 5a.</p>	 <p>The ^{13}C NMR spectrum shows two sharp peaks. The first peak is at 25.568 ppm and the second peak is at 24.664 ppm. The x-axis is labeled 'ppm' and ranges from 26 to 24.</p> <p style="text-align: center;">Figure 5a</p>
<p>(<i>S</i>)-HA4 (0.0075 mmol, 5.6 mg) and foldamer F4* (2.9 mg, 0.005 mmol) were directly weighed in an NMR tube to which CDCl_3 (0.5 mL) was added. After vigorous shaking of the NMR tube for 1 min, ^1H and ^{13}C spectra of the resultant solution were recorded at 296 K. A portion of the ^{13}C NMR (100 MHz, CDCl_3) spectrum of F4* in the presence of (<i>S</i>)-HA4 is shown in Figure 5b.</p>	 <p>The ^{13}C NMR spectrum shows two sharp peaks. The first peak is at 25.561 ppm and the second peak is at 24.536 ppm. The x-axis is labeled 'ppm' and ranges from 26 to 24.</p> <p style="text-align: center;">Figure 5b</p>
<p>(<i>S</i>)-HA6 (0.0075 mmol, 4.8 mg) and foldamer F4* (2.9 mg, 0.005 mmol) were directly weighed in an NMR tube to which CDCl_3 (0.5 mL) was added. After vigorous shaking of the NMR tube for 1 min, ^1H and ^{13}C spectra of the resultant solution were recorded at 296 K. A portion of the ^{13}C NMR (100 MHz, CDCl_3) spectrum of F4* in the presence of (<i>S</i>)-HA6 is shown in Figure 5c.</p>	 <p>The ^{13}C NMR spectrum shows two sharp peaks. The first peak is at 25.134 ppm and the second peak is at 25.032 ppm. The x-axis is labeled 'ppm' and ranges from 26 to 24.</p> <p style="text-align: center;">Figure 5c</p>

XV. Conformational switching experiments of foldamer F4* (Three-component system: Figure 6)

1. A solution of (*S*)-**HA1** (0.0075 mmol, 0.5 mL, 15 mM) was added to foldamer **F4*** (0.005 mmol, 2.9 mg) which was directly weighed in an NMR tube. After vigorous shaking of the NMR tube for 1 min, ^1H and ^{13}C spectra of the resultant solution were recorded at 296 K. A portion of the ^{13}C NMR (100 MHz, CDCl_3) spectrum of **F4*** in the presence of (*S*)-**HA1** is shown in Figure 6b.

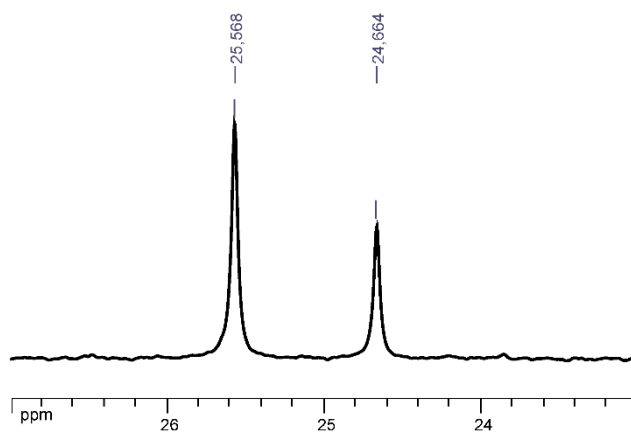


Figure 6b

2. (*R*)-**HA4** (0.0075 mmol, 5.6 mg) was directly added to the NMR tube of the NMR sample from Fig. 6b. After vigorous shaking of the NMR tube for 1 min, ^1H and ^{13}C spectra of the resultant solution were recorded at 296 K. A portion of the ^{13}C NMR (100 MHz, CDCl_3) spectrum of (*S*)-**HA1** and (*R*)-**HA4** is shown in Figure 6c.

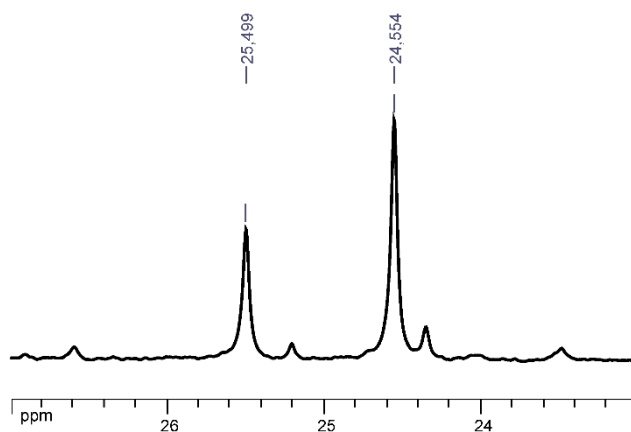


Figure 6c

3. A commercially available solution of NH_3 in dioxane (15 μL , 0.0075 mmol, 0.5 M) was directly added to the NMR tube of the NMR sample from Fig. 6c. After vigorous shaking of the NMR tube for 1 min, ^1H and ^{13}C spectra of the resultant solution were recorded at 296 K. A portion of the ^{13}C NMR (100 MHz, CDCl_3) spectrum of **F4*** in the presence of (*S*)-**HA1**, (*R*)-**HA4** and NH_3 is shown in Figure 6d.

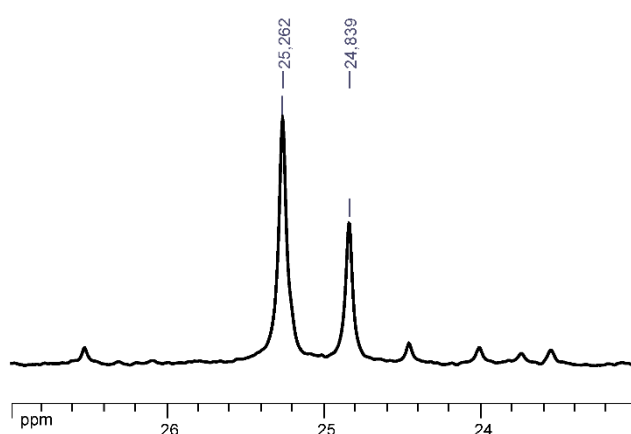


Figure 6d

4. A solution of **HCl** in CDCl_3 :dioxane / 5.3:1 (0.0075 mmol, 10 μL , 0.75 M), prepared from commercially available solution of **HCl** in dioxane (4 M) was directly added to the NMR tube of the NMR sample from Fig. 6d. After vigorous shaking of the NMR tube for 1 min, ^1H and ^{13}C spectra of the resultant solution were recorded at 296 K. A portion of the ^{13}C NMR (100 MHz, CDCl_3) spectrum of **F4*** in the presence of (*S*)-**HA1**, (*R*)-**HA4**, NH_3 and **HCl** is shown in Figure 6e.

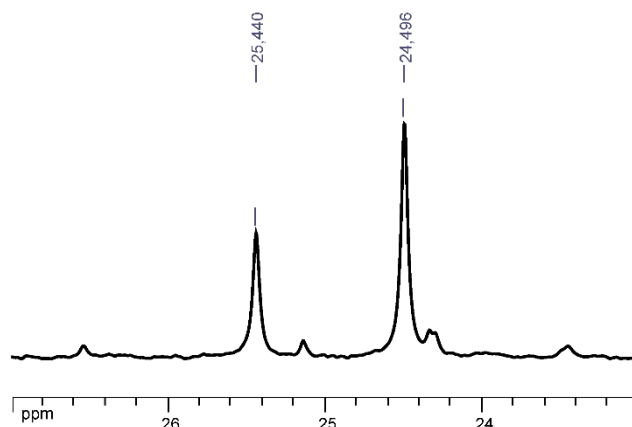


Figure 6e

5. A commercially available solution of NH_3 in dioxane (15 μL , 0.0075 mmol, 0.5 M) was directly added to the NMR tube of the NMR sample from Fig. 6e. After vigorous shaking of the NMR tube for 1 min, ^1H and ^{13}C spectra of the resultant solution were recorded at 296 K. A portion of the ^{13}C NMR (100 MHz, CDCl_3) spectrum of **F4*** in the presence of (*S*)-**HA1**, (*R*)-**HA4** and 2^*NH_3 is shown in Figure 6f.

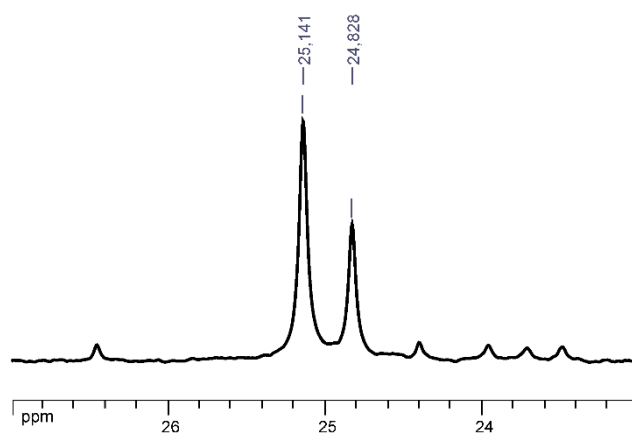


Figure 6f

6. A commercially available solution of NH_3 in dioxane (15 μL , 0.0075 mmol, 0.5 M) was directly added to the NMR tube of the NMR sample from Fig. 6f. After vigorous shaking of the NMR tube for 1 min, ^1H and ^{13}C spectra of the resultant solution were recorded at 296 K. A portion of the ^{13}C NMR (100 MHz, CDCl_3) spectrum of **F4*** in the presence of (*S*)-**HA1**, (*R*)-**HA4** and 3^*NH_3 is shown in Figure 6g.

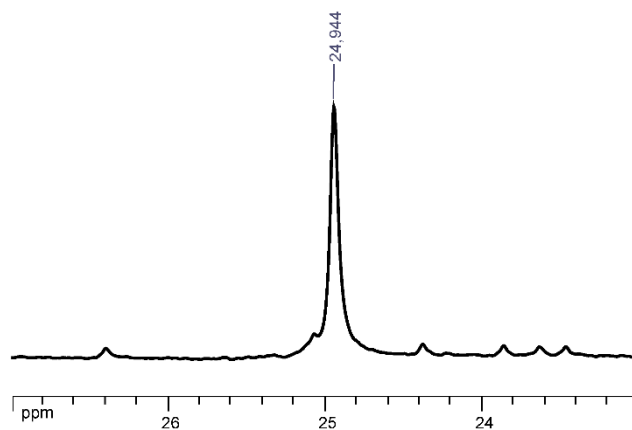


Figure 6g

7. A solution of **HCl** in CDCl_3 :dioxane / 5.3:1 (0.0225 mmol, 30 μL , 0.75 M), prepared from commercially available solution of HCl in dioxane (4 M) was directly added in the NMR tube of the NMR sample from Fig. 6g. After vigorous shaking of the NMR tube for 1 min, ^1H and ^{13}C spectra of the resultant solution were recorded at 296 K. A portion of the ^{13}C NMR (100 MHz, CDCl_3) spectrum of **F4*** in the presence of (*S*)-**HA1**, (*R*)-**HA4**, **3*NH₃** and **3*HCl** is shown in Figure 6h.

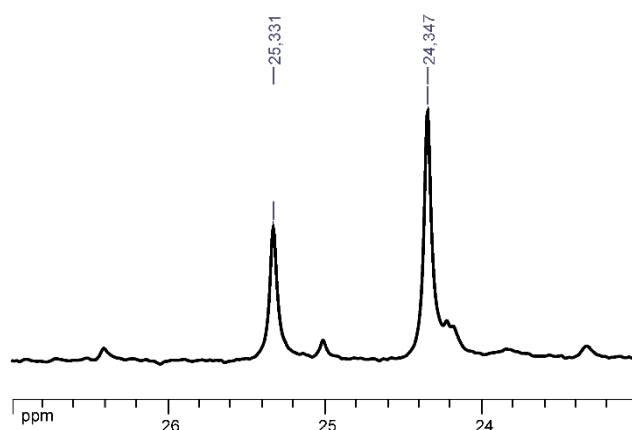


Figure 6h

XVI. Conformational switching experiments of foldamer **F4*** (Four-component system: Figure 7)

1. A solution of (*R*)-**HA1** (0.0075 mmol, 0.5 mL, 15 mM) was added to foldamer **F4*** (0.005 mmol, 2.9 mg) which was directly weighed in an NMR tube. After vigorous shaking of the NMR tube for 1 min, ^1H and ^{13}C spectra of the resultant solution were recorded at 296 K. A portion of the ^{13}C NMR (100 MHz, CDCl_3) spectrum of **F4** in the presence of (*R*)-**HA1** is shown in Figure 7b.

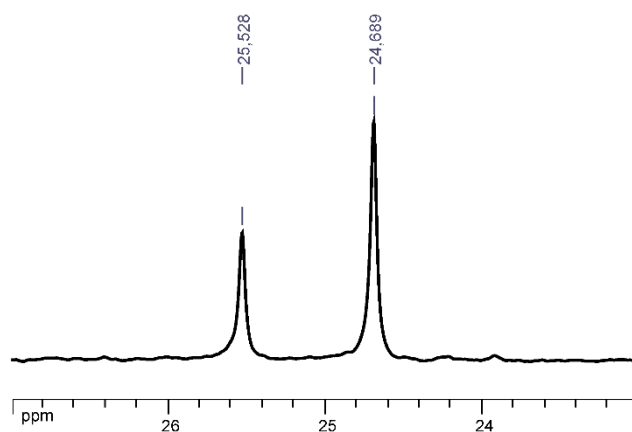


Figure 7b

2. (*S*)-**HA4** (0.0075 mmol, 5.6 mg) was directly added in the NMR tube of the NMR sample from Fig. 7b. After vigorous shaking of the NMR tube for 1 min, ^1H and ^{13}C spectra of the resultant solution were recorded at 296 K. A portion of the ^{13}C NMR (100 MHz, CDCl_3) spectrum of **F4*** in the presence of (*R*)-**HA1** and (*S*)-**HA4** is shown in Figure 7c.

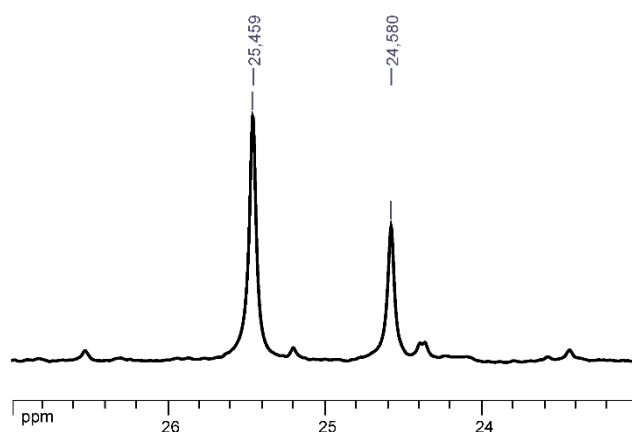


Figure 7c

3. (*S*)-**HA6** (0.0075 mmol, 4.8 mg) was directly added in the NMR tube of the NMR sample from Fig. 7c. After vigorous shaking of the NMR tube for 1 min, ^1H and ^{13}C spectra of the resultant solution were recorded at 296 K. A portion of the ^{13}C NMR (100 MHz, CDCl_3) spectrum of **F4*** in the presence of (*R*)-**HA1**, (*S*)-**HA4** and (*S*)-**HA6** is shown in Figure 7d.

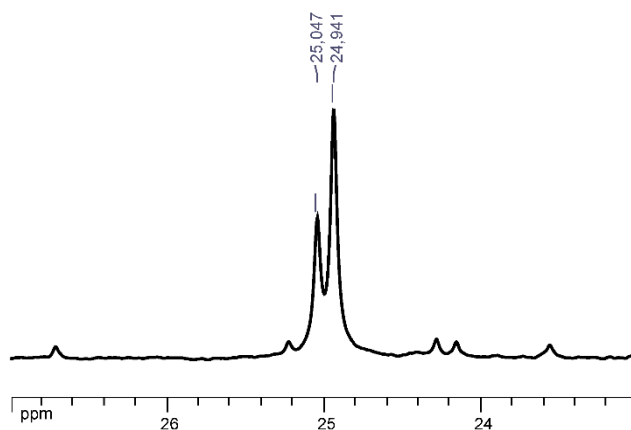


Figure 7d

4. A commercially available solution of NH_3 in dioxane (15 μL , 0.0075 mmol, 0.5 M) was directly added in the NMR tube of the NMR sample from Fig. 7d. After vigorous shaking of the NMR tube for 1 min, ^1H and ^{13}C spectra of the resultant solution were recorded at 296 K. A portion of the ^{13}C NMR (100 MHz, CDCl_3) spectrum of **F4*** in the presence of (*R*)-**HA1**, (*S*)-**HA4**, (*S*)-**HA6** and NH_3 is shown in Figure 7e.

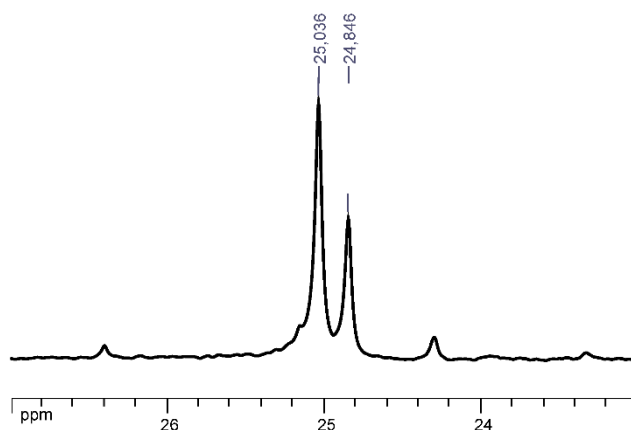


Figure 7e

5. A commercially available solution of NH_3 in dioxane (15 μL , 0.0075 mmol, 0.5 M) was directly added in the NMR tube of the NMR sample from Fig. 7e. After vigorous shaking of the NMR tube for 1 min, ^1H and ^{13}C spectra of the resultant solution were recorded at 296 K. A portion of the ^{13}C NMR (100 MHz, CDCl_3) spectrum of **F4*** in the presence of (*R*)-**HA1**, (*S*)-**HA4**, (*S*)-**HA6** and 2^*NH_3 is shown in Figure 7f

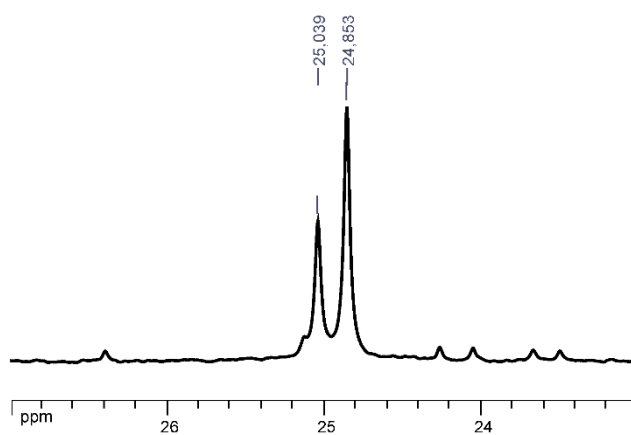


Figure 7f

6. A commercially available solution of NH_3 in dioxane (15 μL , 0.0075 mmol, 0.5 M) was directly added in the NMR tube of the NMR sample from Fig. 7f. After vigorous shaking of the NMR tube for 1 min, ^1H and ^{13}C spectra of the resultant solution were recorded at 296 K. A portion of the ^{13}C NMR (100 MHz, CDCl_3) spectrum of **F4*** in the presence of (*R*)-**HA1**, (*S*)-**HA4**, (*S*)-**HA6** and **3*NH₃** is shown in Figure 7g.

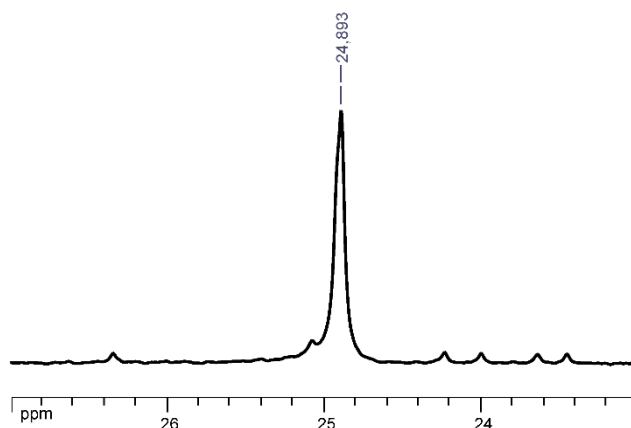


Figure 7g

7. A solution of **HCl** in CDCl_3 :dioxane / 5.3:1 (0.0225 mmol, 30 μL , 0.75 M), prepared from commercially available solution of HCl in dioxane (4 M) was directly added in the NMR tube of the NMR sample from Fig. 7g. After vigorous shaking of the NMR tube for 1 min, ^1H and ^{13}C spectra of the resultant solution were recorded at 296 K. A portion of the ^{13}C NMR (100 MHz, CDCl_3) spectrum of **F4*** in the presence of (*R*)-**HA1**, (*S*)-**HA4**, (*S*)-**HA6**, **3*NH₃** and **3*HCl** is shown in Figure 7h.

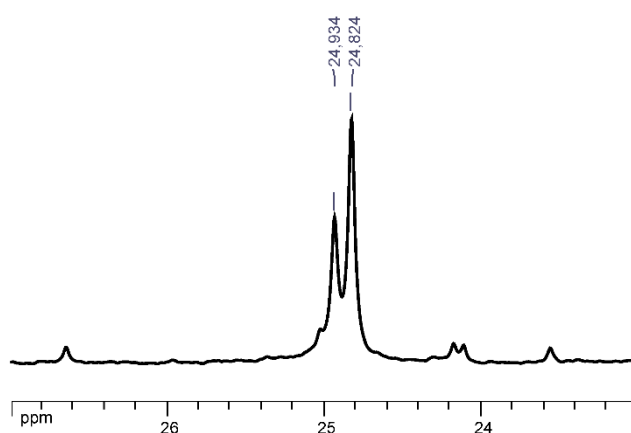


Figure 7h

XVII. Conformational switching experiment of foldamer **F4*** (Four-component system: Figure 8)

1. A solution of (*R*)-**HA1** (0.0075 mmol, 0.5 mL, 15 mM) was added to foldamer **F4** (0.005 mmol, 2.9 mg) which was directly weighed in an NMR tube. After vigorous shaking of the NMR tube for 1 min, ^1H and ^{13}C spectra of the resultant solution were recorded at 296 K. A portion of the ^{13}C NMR (100 MHz, CDCl_3) spectrum of **F4*** in the presence of (*R*)-**HA1** is shown in Figure 8b.

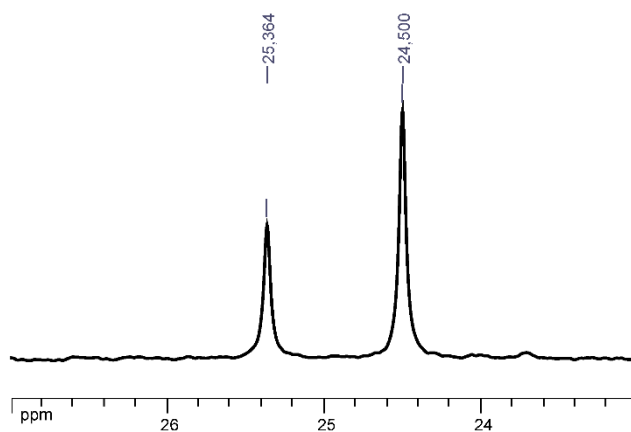


Figure 8b

2. (*S*)-**HA4** (0.0075 mmol, 5.6 mg) was directly added in the NMR tube of the NMR sample from Fig. 8b. After vigorous shaking of the NMR tube for 1 min, ^1H and ^{13}C spectra of the resultant solution were recorded at 296 K. A portion of the ^{13}C NMR (100 MHz, CDCl_3) spectrum of **F4*** in the presence of (*R*)-**HA1** and (*S*)-**HA4** is shown in Figure 8c.

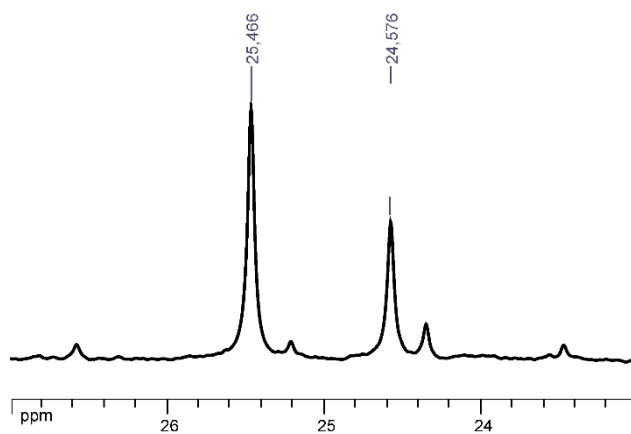


Figure 8c

3. (*S*)-**HA6** (0.0075 mmol, 4.8 mg) was directly added in the NMR tube of the NMR sample from Fig. 8c. After vigorous shaking of the NMR tube for 1 min, ^1H and ^{13}C spectra of the resultant solution were recorded at 296 K. A portion of the ^{13}C NMR (100 MHz, CDCl_3) spectrum of **F4*** in the presence of (*R*)-**HA1**, (*S*)-**HA4** and (*S*)-**HA6** is shown in Figure 8d.

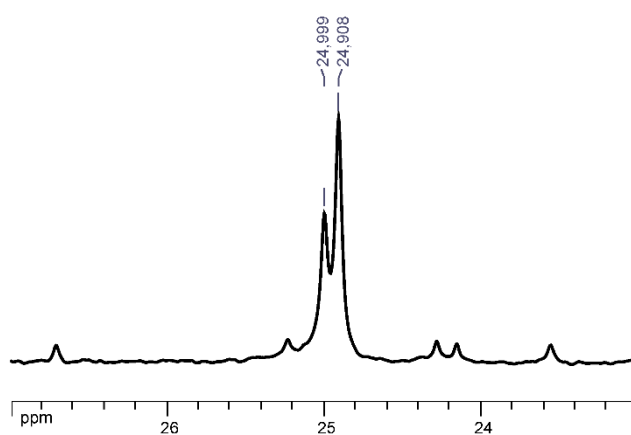


Figure 8d

4. A solution of proton sponge (**PS**) in CDCl_3 (25 μL , 0.0075 mmol, 0.3 M) was directly added in the NMR tube of the NMR sample from Fig. 8d. After vigorous shaking of the NMR tube for 1 min, ^1H and ^{13}C spectra of the resultant solution were recorded at 296 K. A portion of the ^{13}C NMR (100 MHz, CDCl_3) spectrum of **F4*** in the presence of (*R*)-**HA1**, (*S*)-**HA4**, (*S*)-**HA6** and **PS** is shown in Figure 8e.

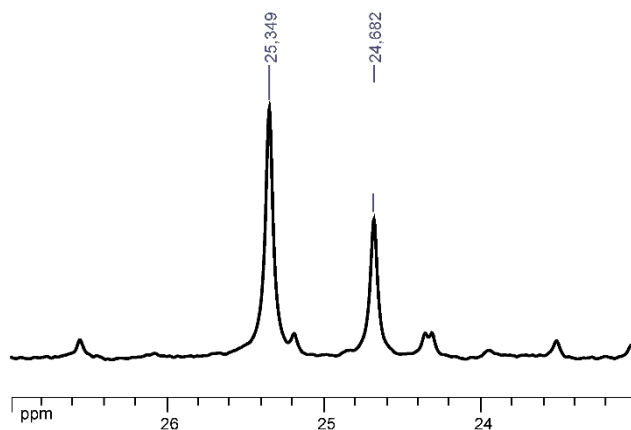


Figure 8e

5. A solution of proton sponge (**PS**) in CDCl_3 (25 μL , 0.0075 mmol, 0.3 M) was directly added in the NMR tube of the NMR sample from Fig. 8e. After vigorous shaking of the NMR tube for 1 min, ^1H and ^{13}C spectra of the resultant solution were recorded at 296 K. A portion of the ^{13}C NMR (100 MHz, CDCl_3) spectrum of **F4*** in the presence of (*R*)-**HA1**, (*S*)-**HA4**, (*S*)-**HA6** and **2*PS** is shown in Figure 8f.

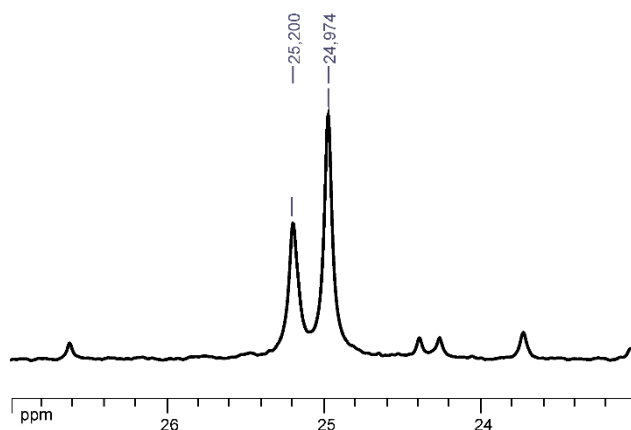


Figure 8f

6. A solution of proton sponge (**PS**) in CDCl_3 (25 μL , 0.0075 mmol, 0.3 M) was directly added in the NMR tube of the NMR sample from Fig. 8f. After vigorous shaking of the NMR tube for 1 min, ^1H and ^{13}C spectra of the resultant solution were recorded at 296 K. A portion of the ^{13}C NMR (100 MHz, CDCl_3) spectrum of **F4*** in the presence of (*R*)-**HA1**, (*S*)-**HA4**, (*S*)-**HA6** and **3*PS** is shown in Figure 8g.

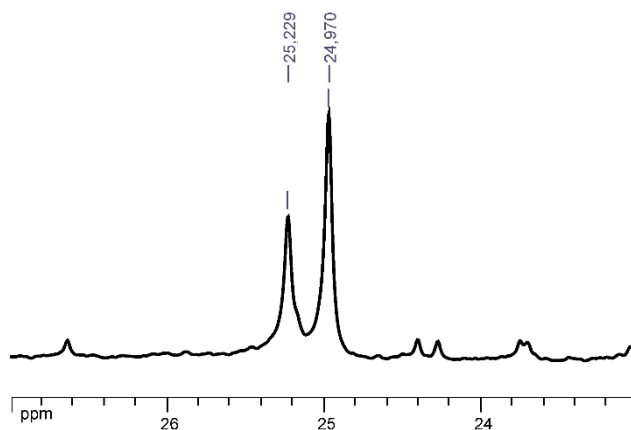


Figure 8g

7. A solution of **HCl** in CDCl_3 :dioxane / 5.3:1 (0.0075 mmol, 10 μL , 0.75 M), prepared from commercially available solution of HCl in dioxane (4 M) was directly added in the NMR tube of the NMR sample from Fig. 8g. After vigorous shaking of the NMR tube for 1 min, ^1H and ^{13}C spectra of the resultant solution were recorded at 296 K. A portion of the ^{13}C NMR (100 MHz, CDCl_3) spectrum of **F4*** in the presence of (*R*)-**HA1**, (*S*)-**HA4**, (*S*)-**HA6**, **3*PS** and **HCl** is shown in Figure 8h.

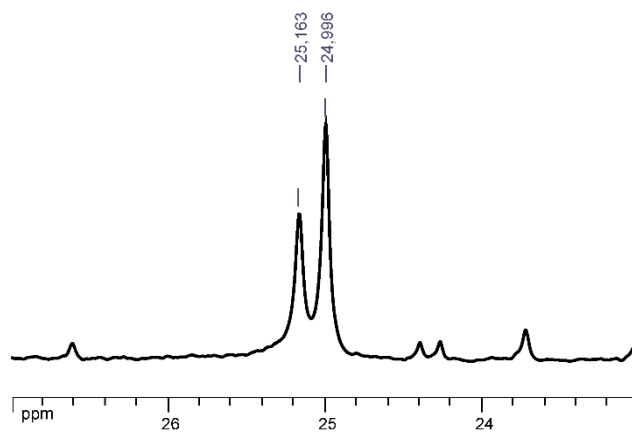


Figure 8h

8. A solution of **HCl** in CDCl_3 :dioxane / 5.3:1 (0.0075 mmol, 10 μL , 0.75 M), prepared from commercially available solution of HCl in dioxane (4 M) was directly added in the NMR tube of the NMR sample from Fig. 8h. After vigorous shaking of the NMR tube for 1 min, ^1H and ^{13}C spectra of the resultant solution were recorded at 296 K. A portion of the ^{13}C NMR (100 MHz, CDCl_3) spectrum of **F4*** in the presence of (*R*)-**HA1**, (*S*)-**HA4**, (*S*)-**HA6**, **3*PS** and **2*HCl** is shown in Figure 8i.

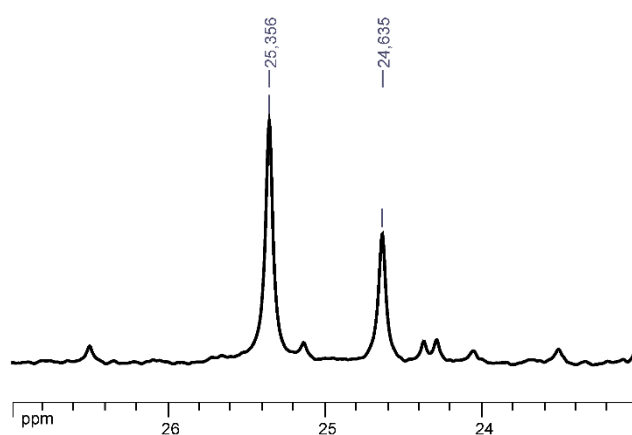


Figure 8i

9. A solution of **HCl** in CDCl_3 :dioxane / 5.3:1 (0.0075 mmol, 10 μL , 0.75 M), prepared from commercially available solution of HCl in dioxane (4 M) was directly added in the NMR tube of the NMR sample from Fig. 8i. After vigorous shaking of the NMR tube for 1 min, ^1H and ^{13}C spectra of the resultant solution were recorded at 296 K. A portion of the ^{13}C NMR (100 MHz, CDCl_3) spectrum of **F4*** in the presence of (*R*)-**HA1**, (*S*)-**HA4**, (*S*)-**HA6**, **3*PS** and **3*HCl** is shown in Figure 8j.

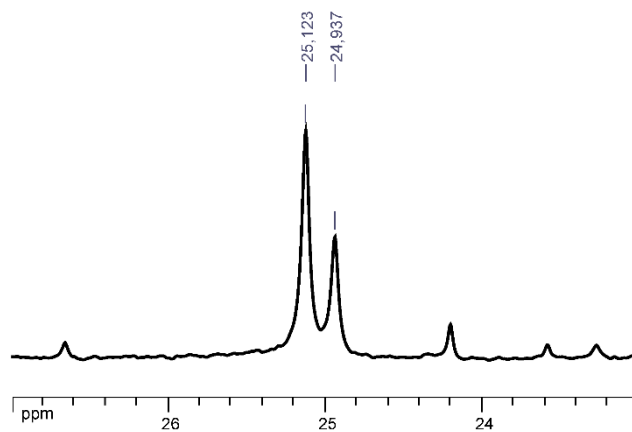
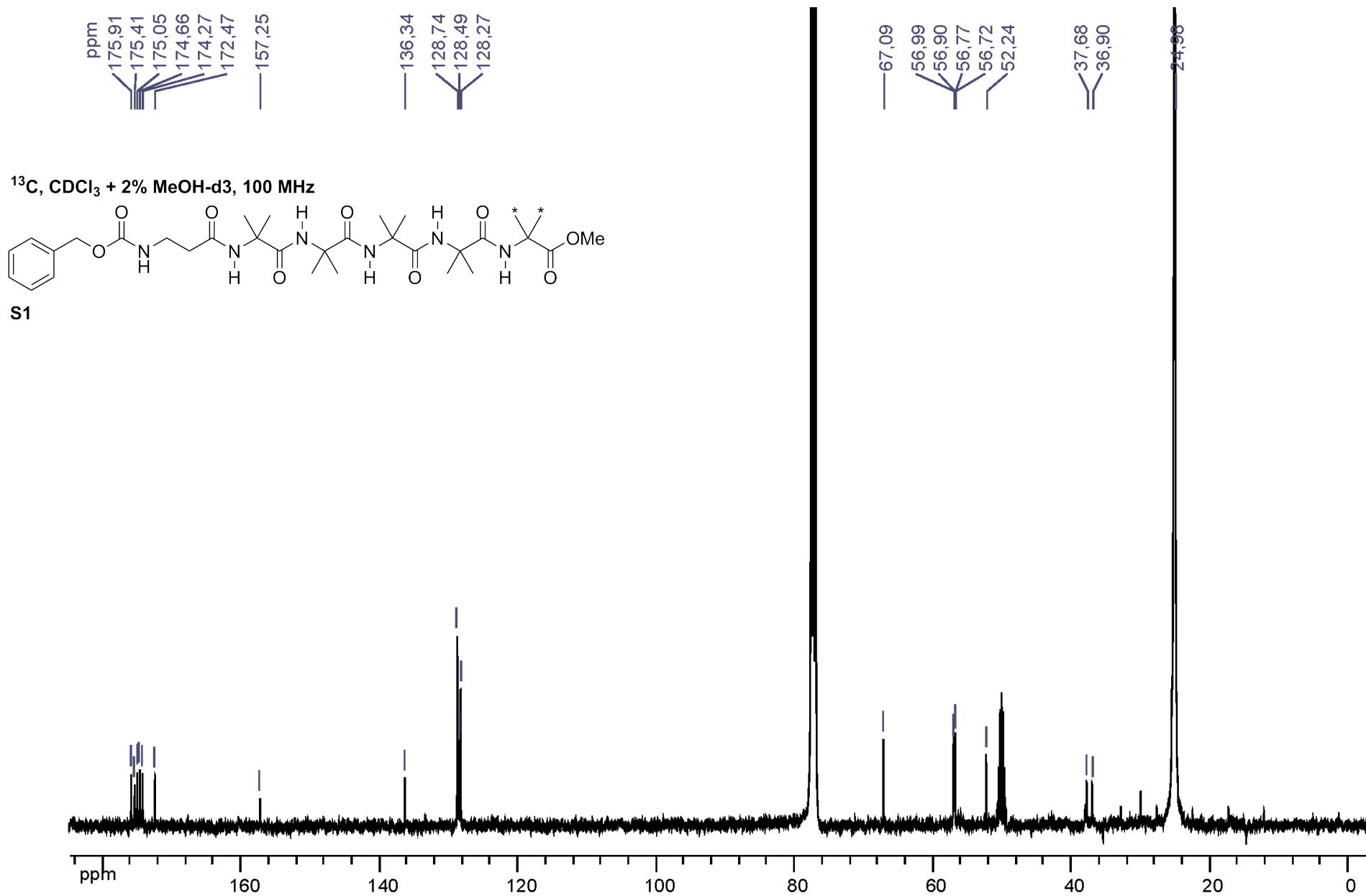
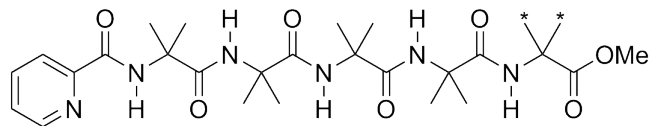


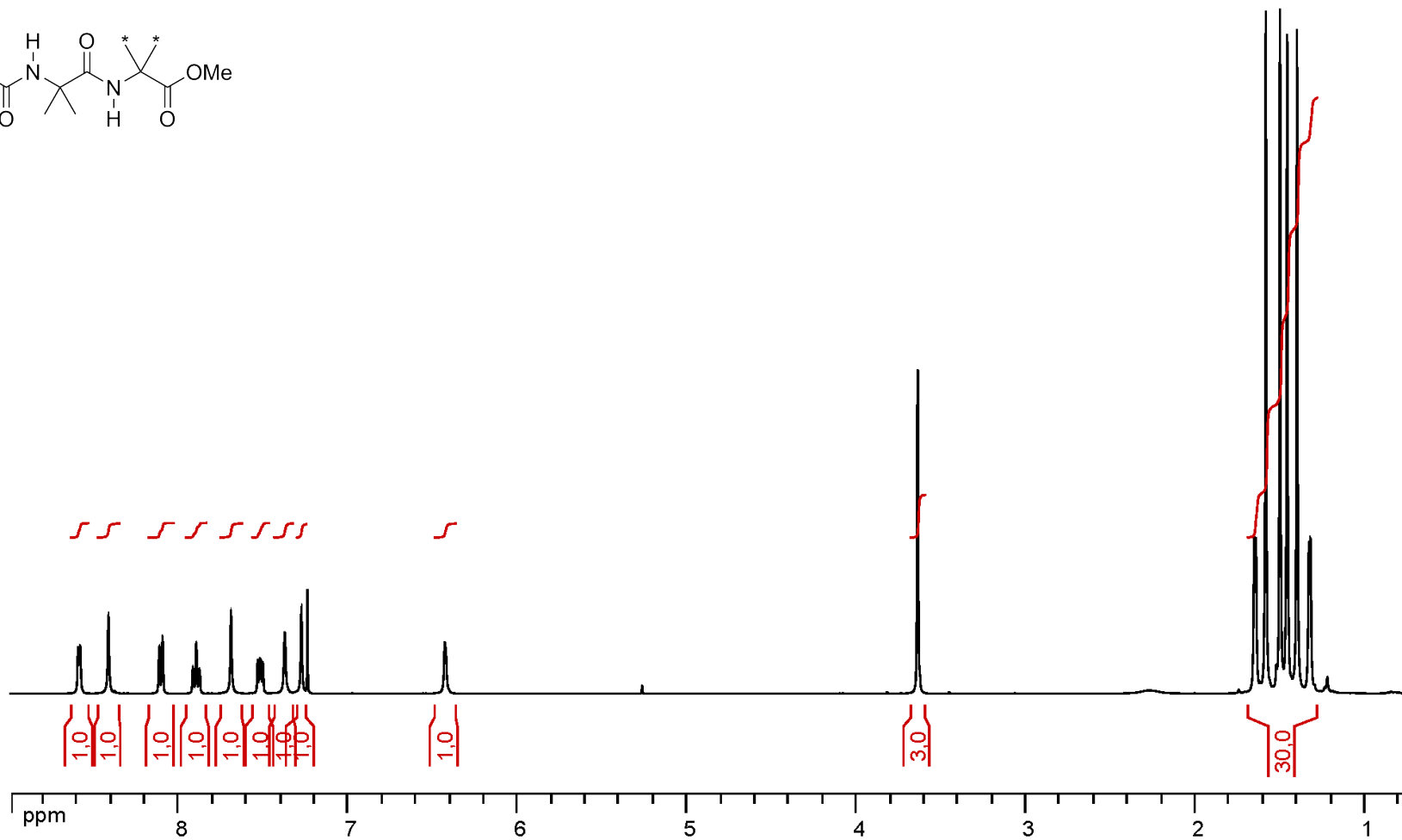
Figure 8j



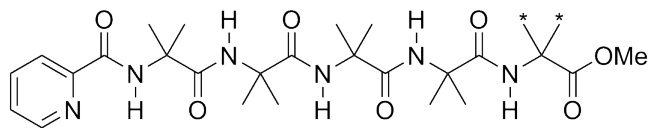
^1H , CDCl_3 , 400 MHz



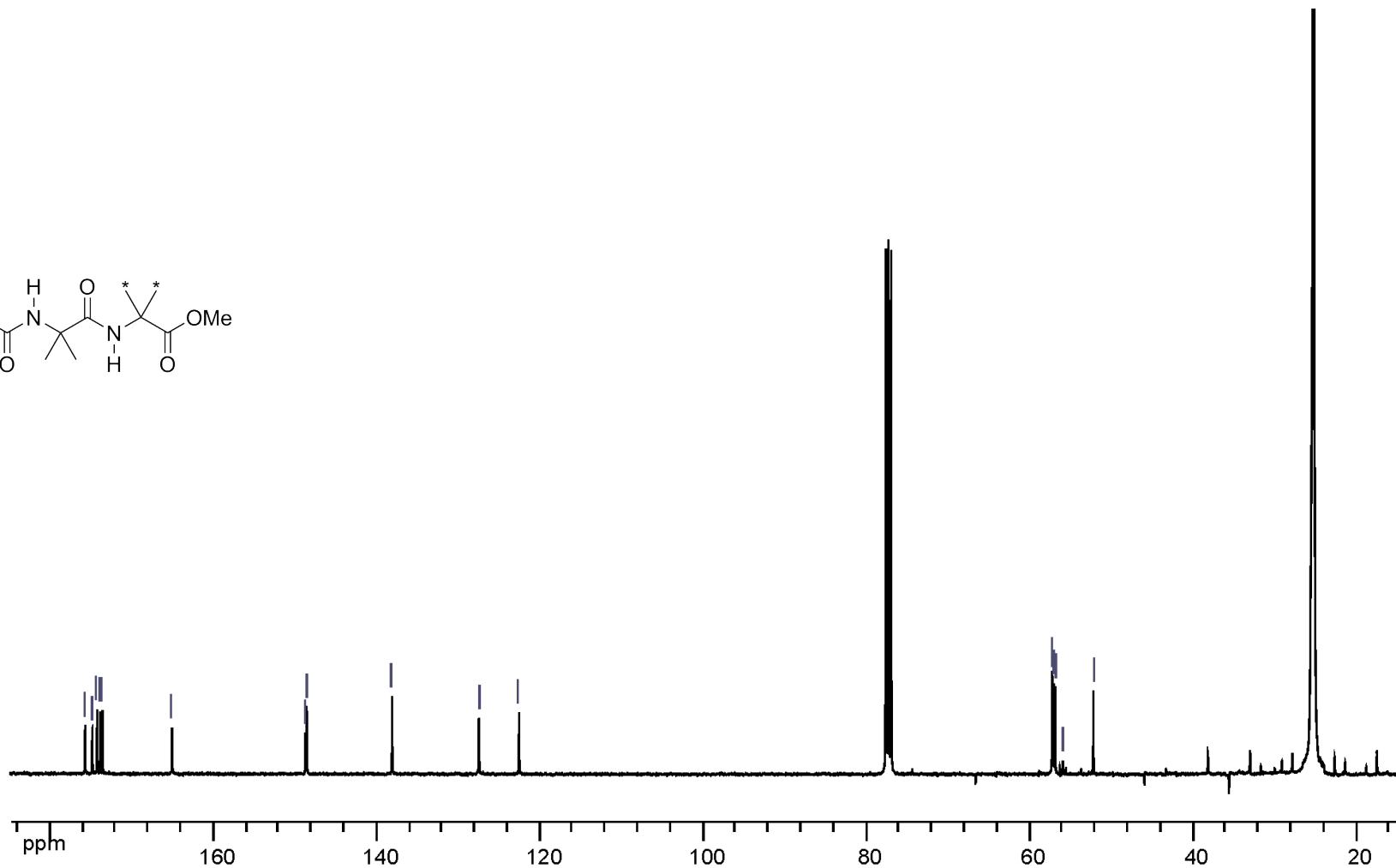
F3



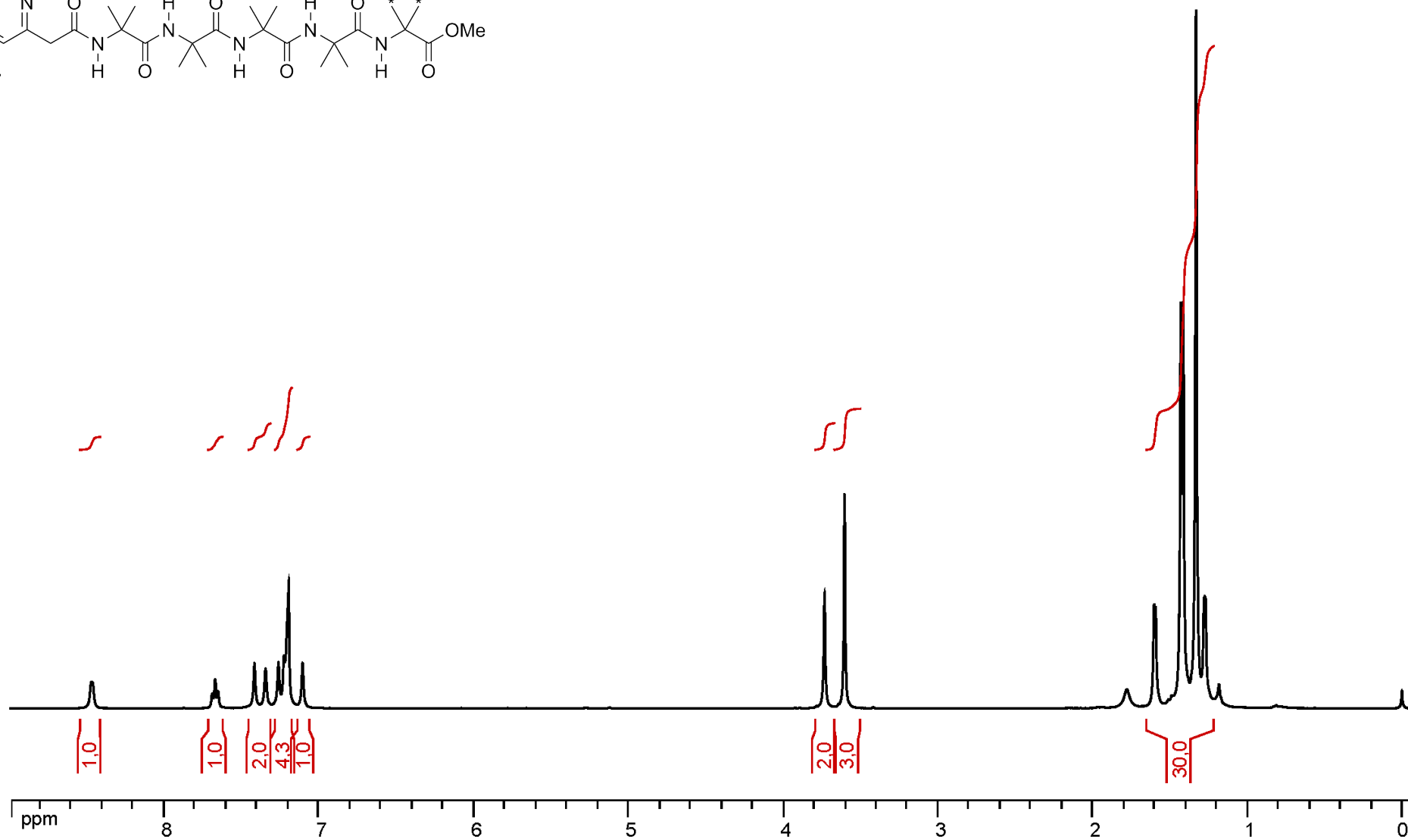
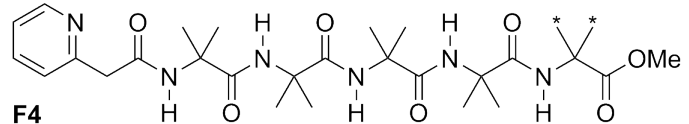
^{13}C , CDCl_3 , 100 MHz



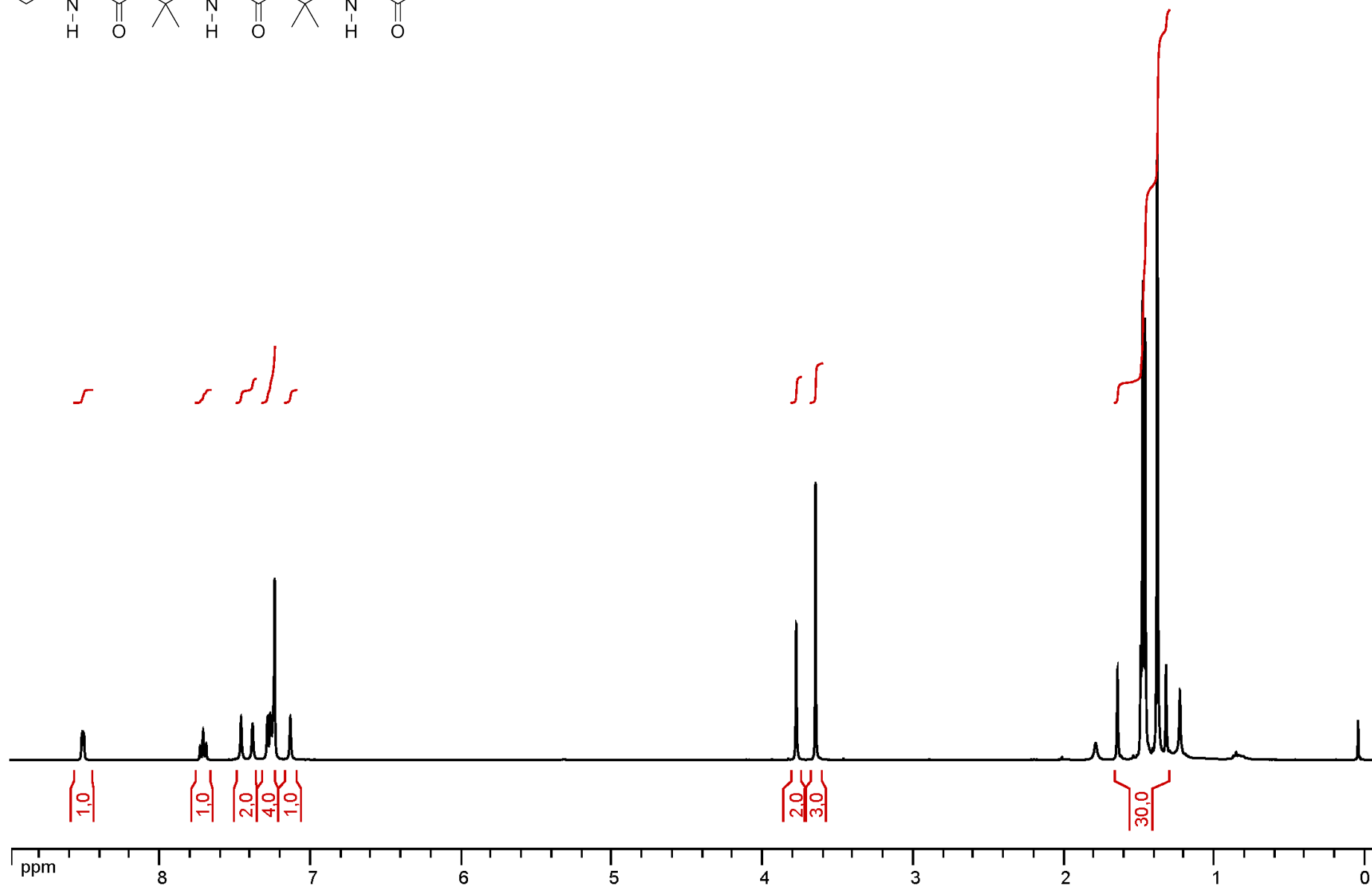
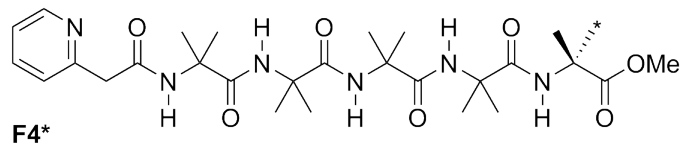
F3



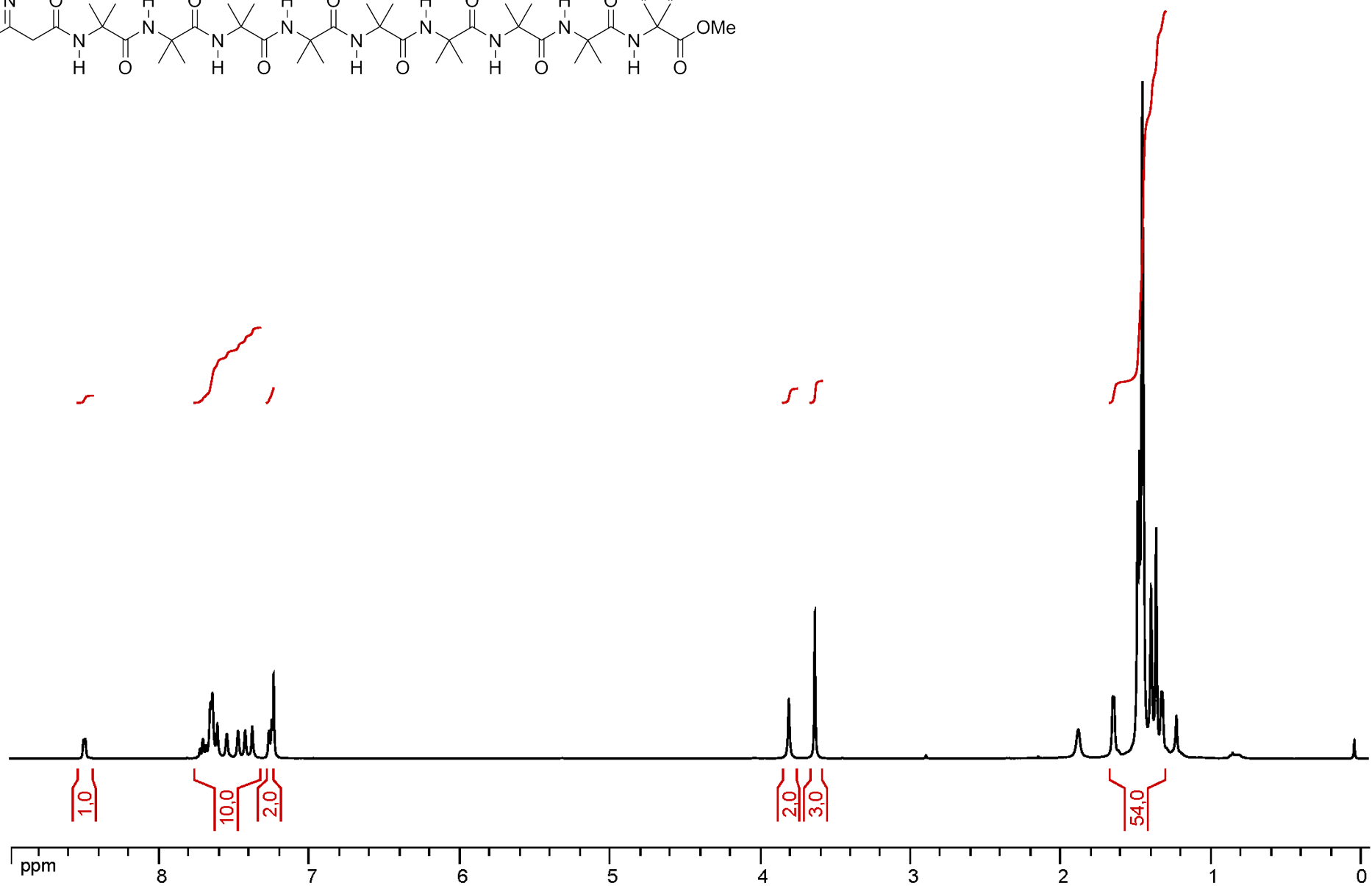
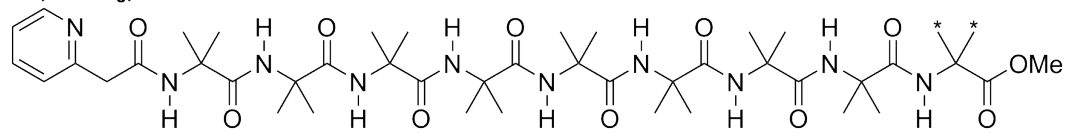
¹H, CDCl₃, 400 MHz

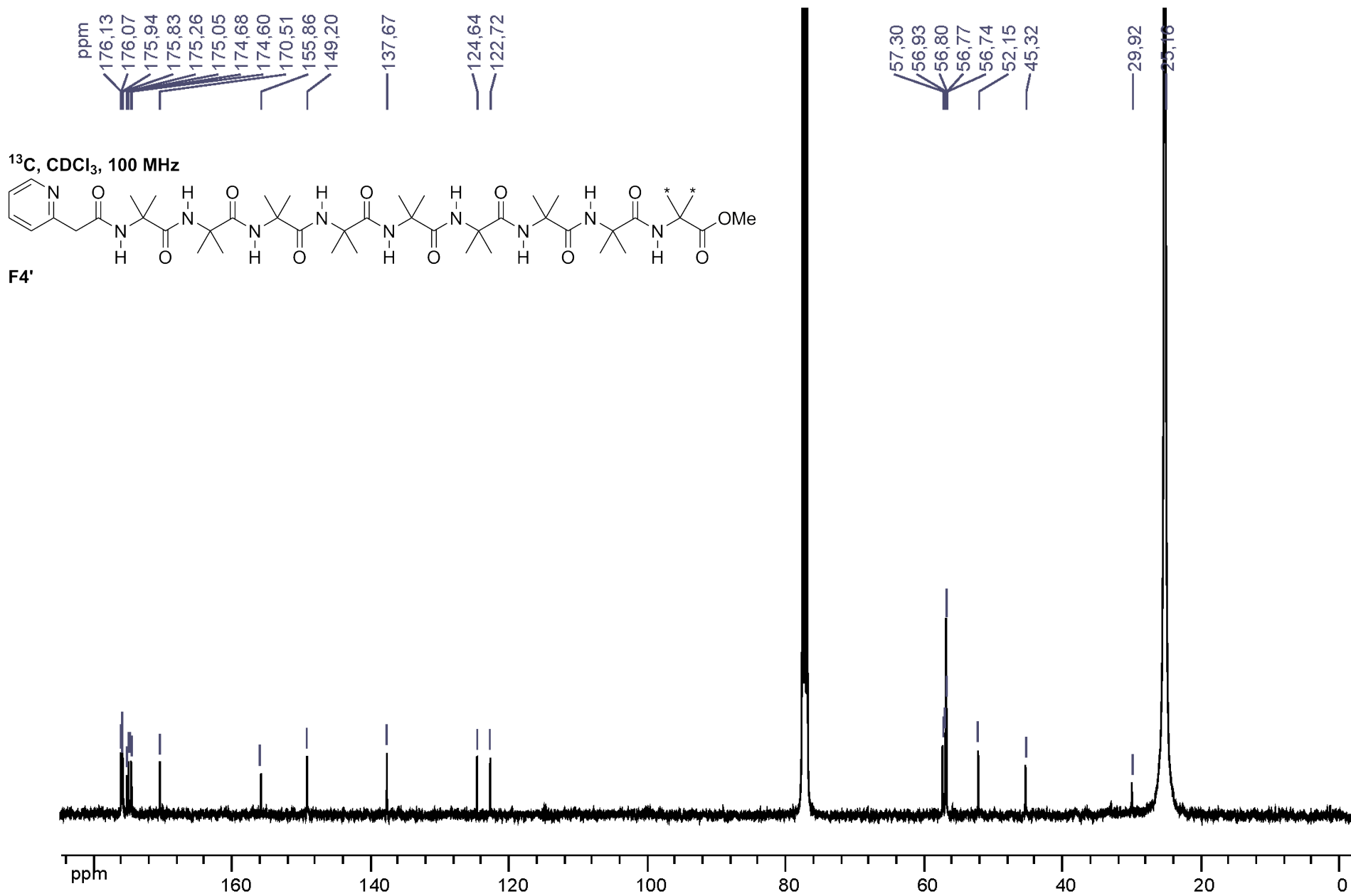


^1H , CDCl_3 , 400 MHz

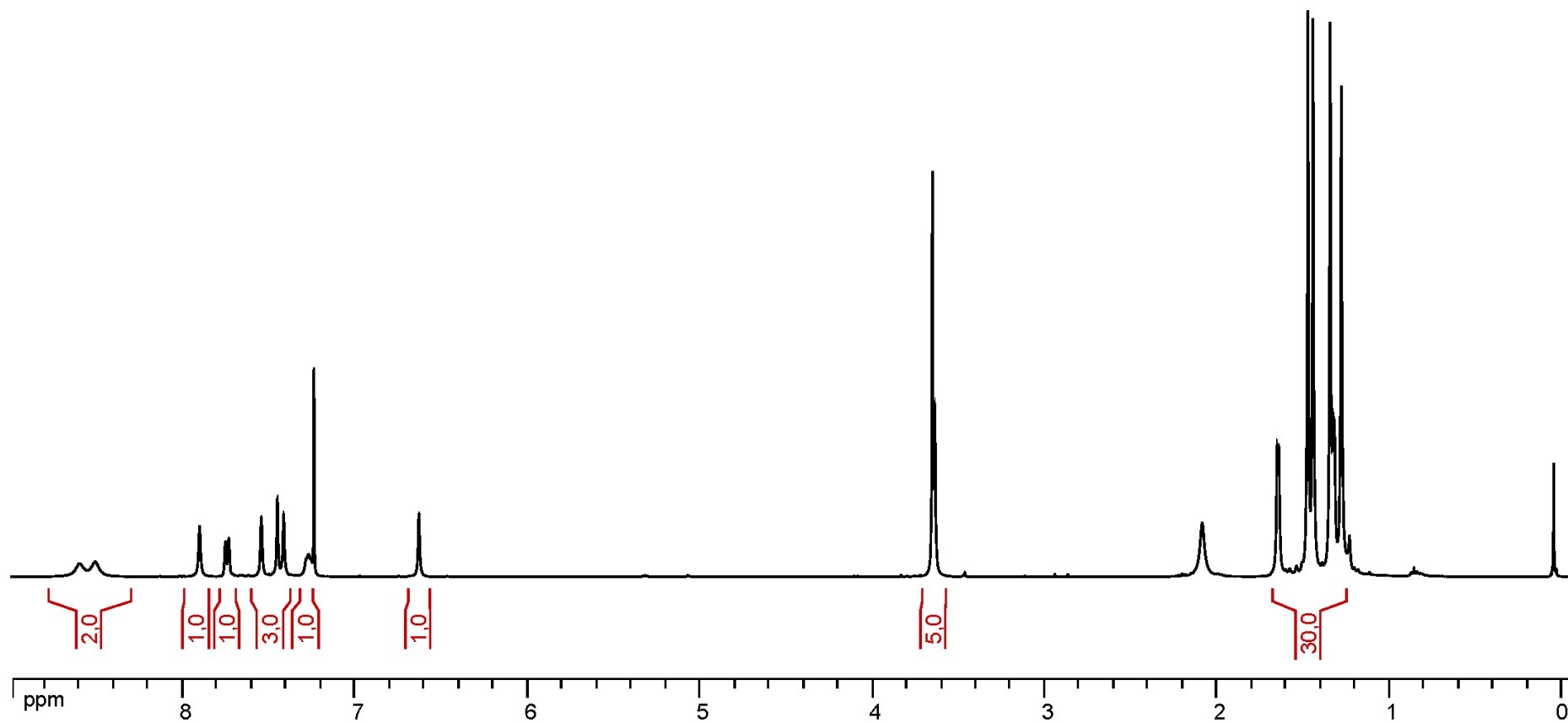
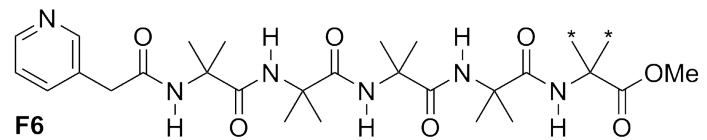


^1H , CDCl_3 , 400 MHz

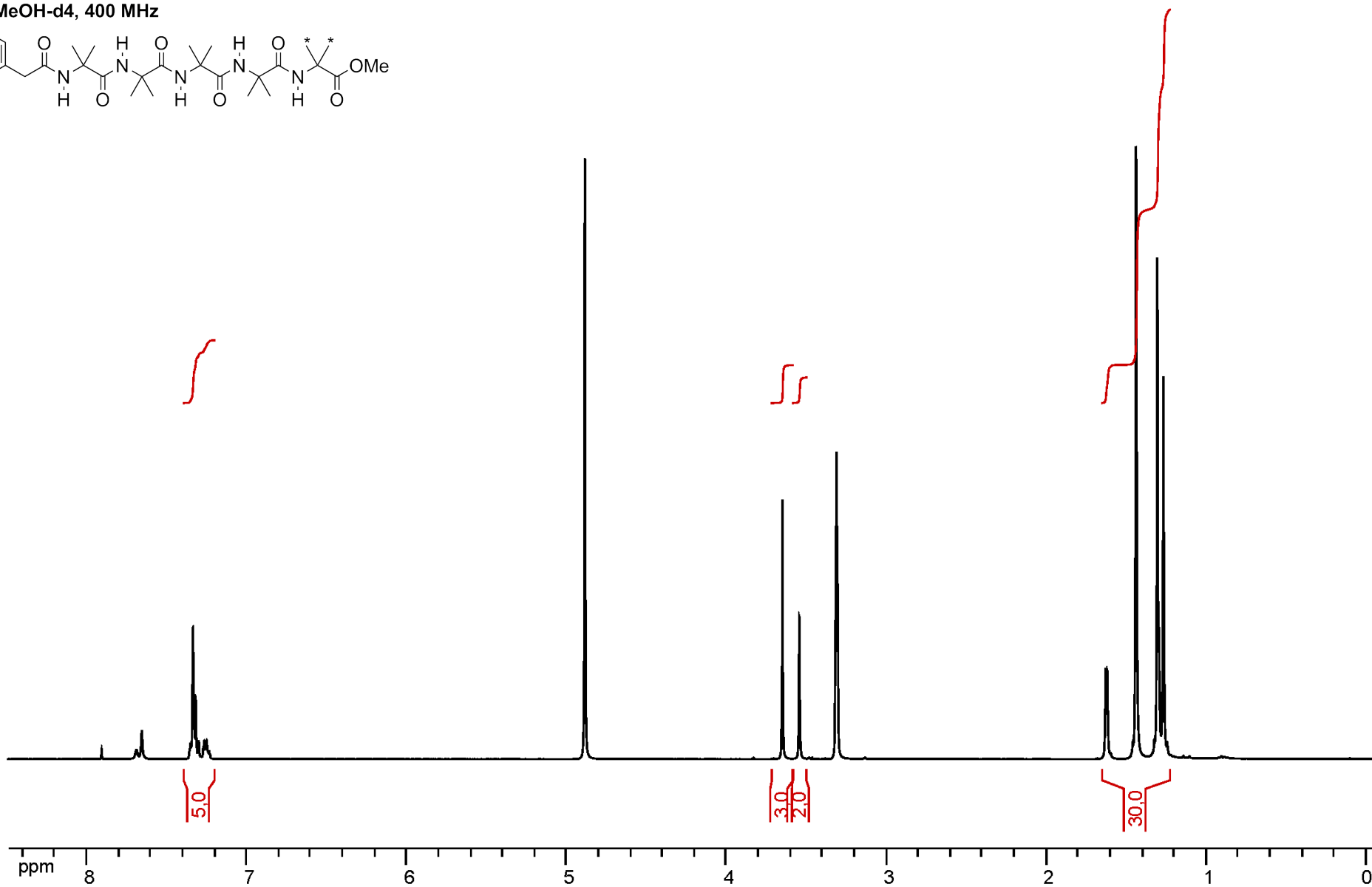
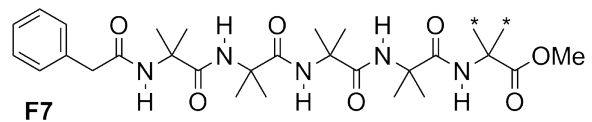


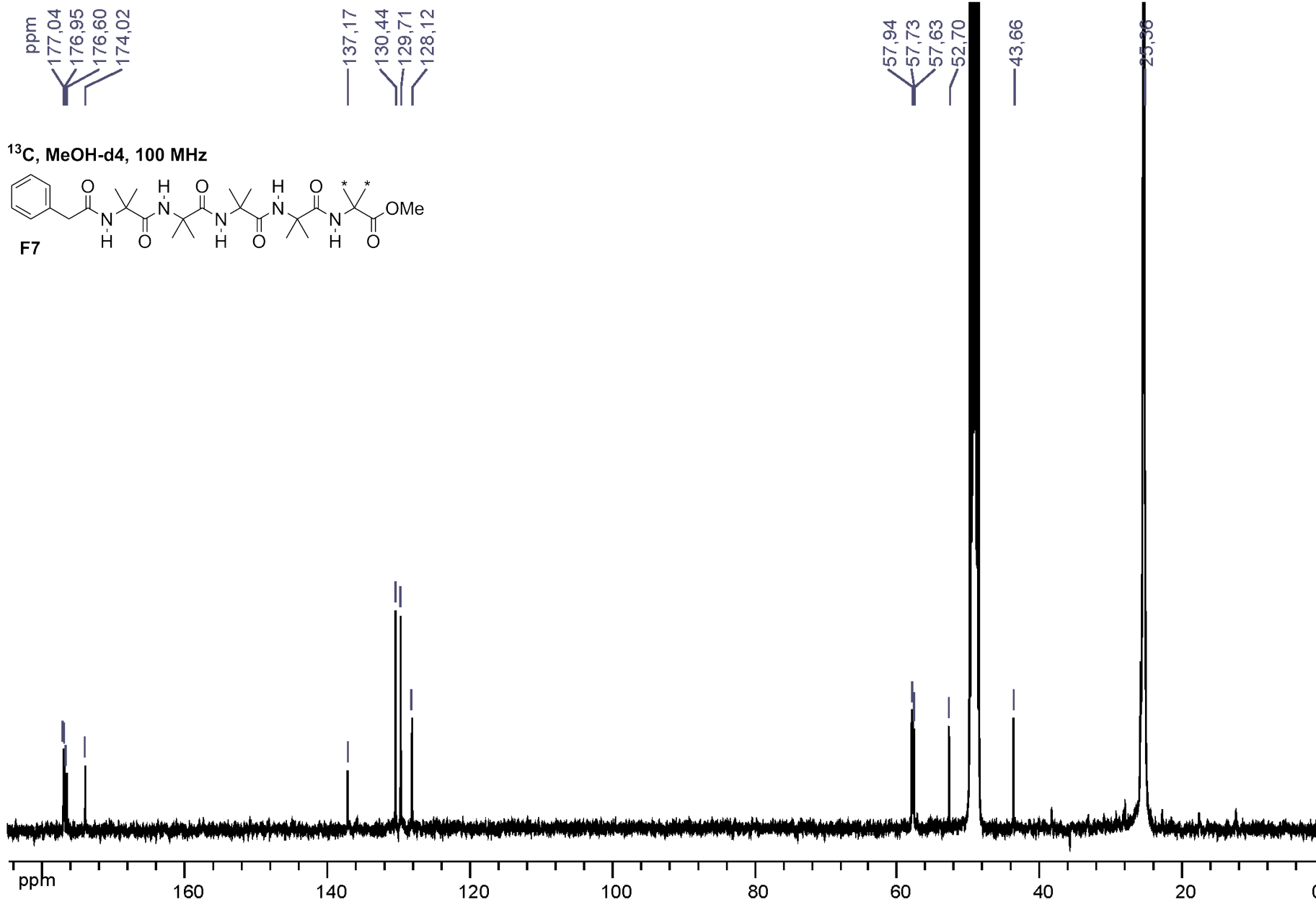


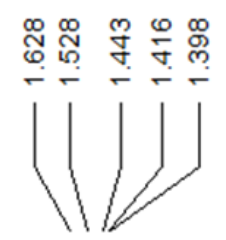
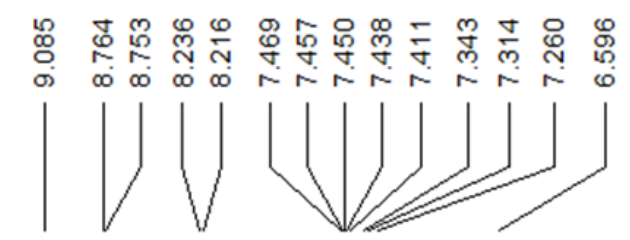
^1H , CDCl_3 , 400 MHz



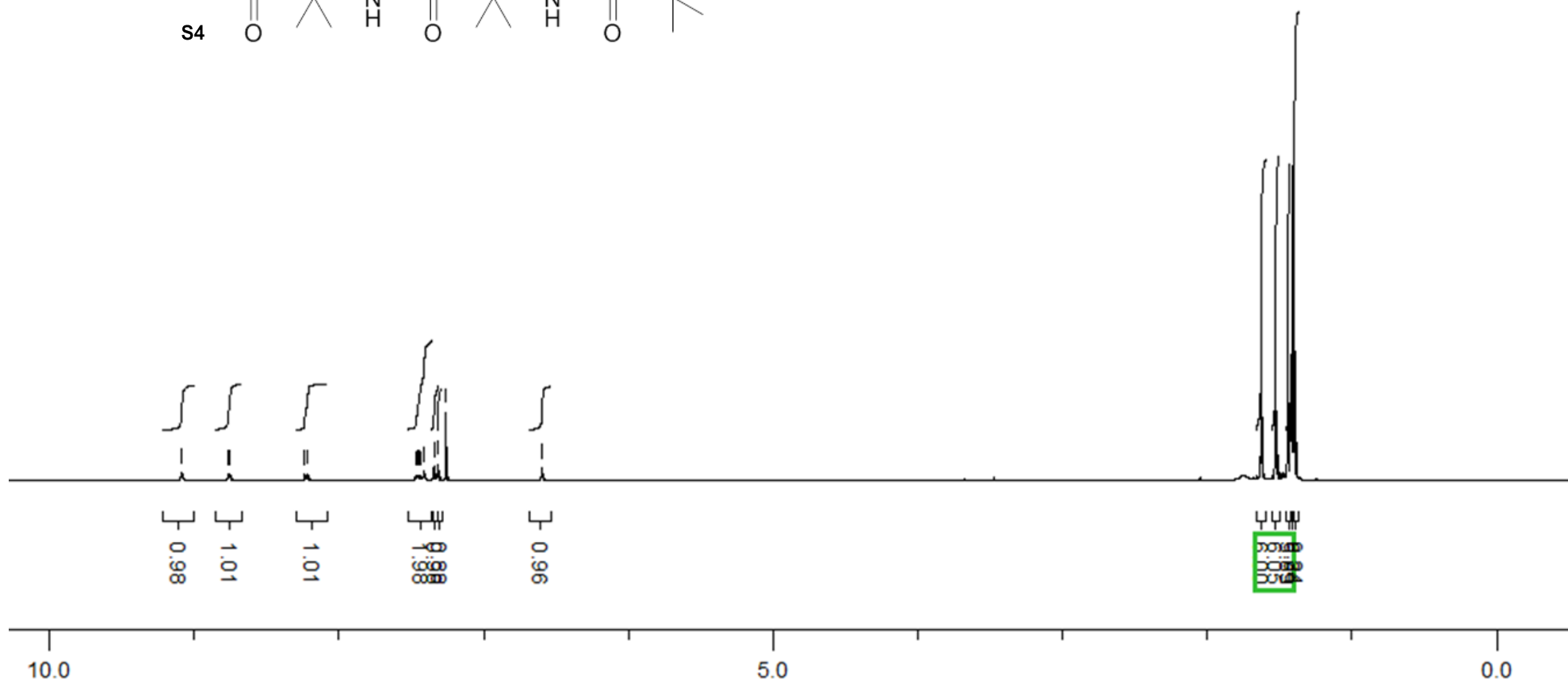
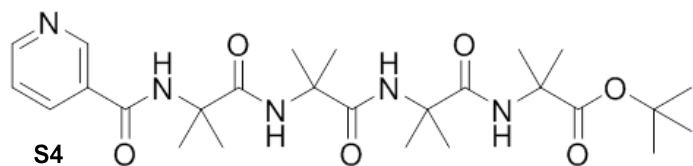
¹H, MeOH-d₄, 400 MHz

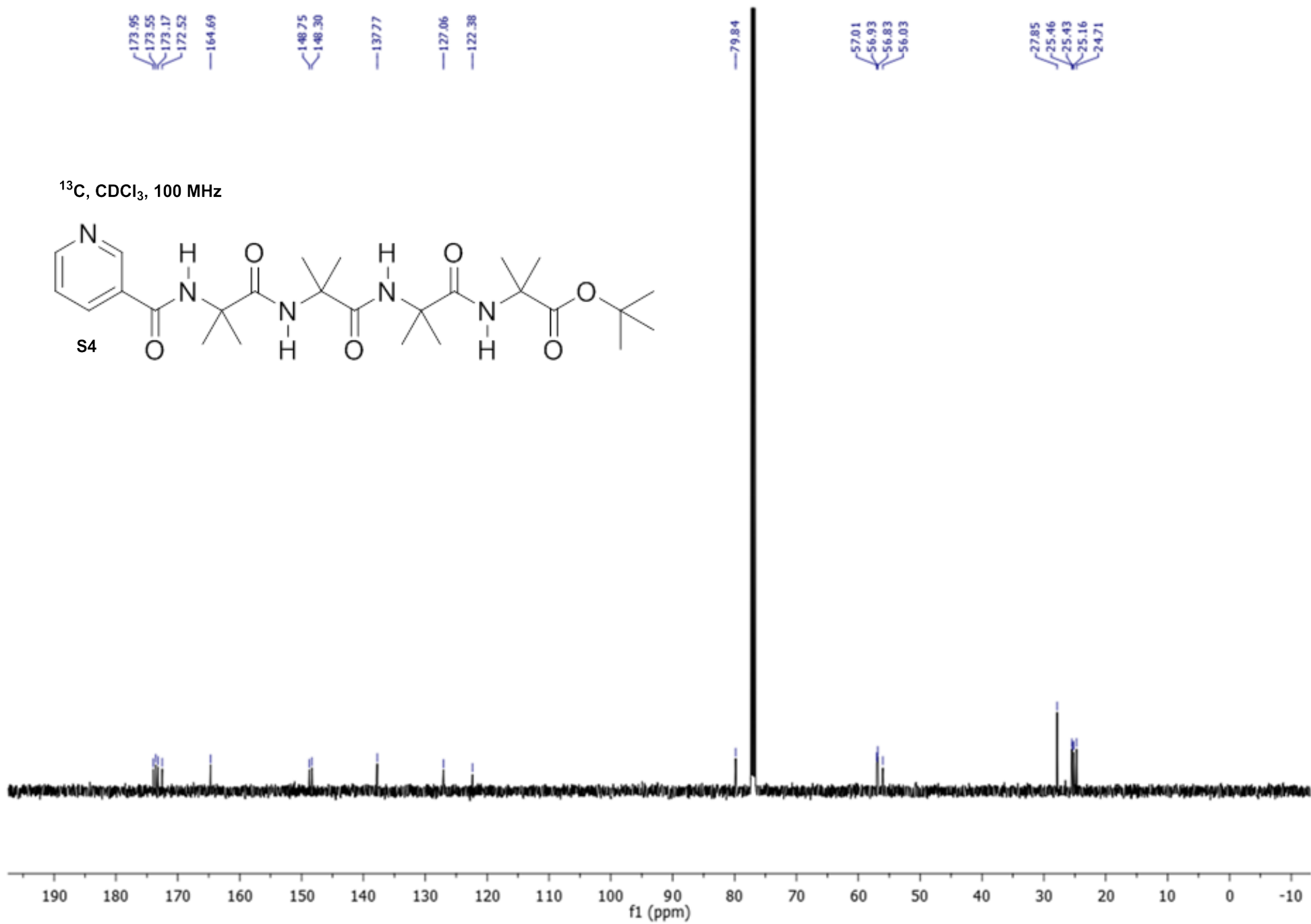


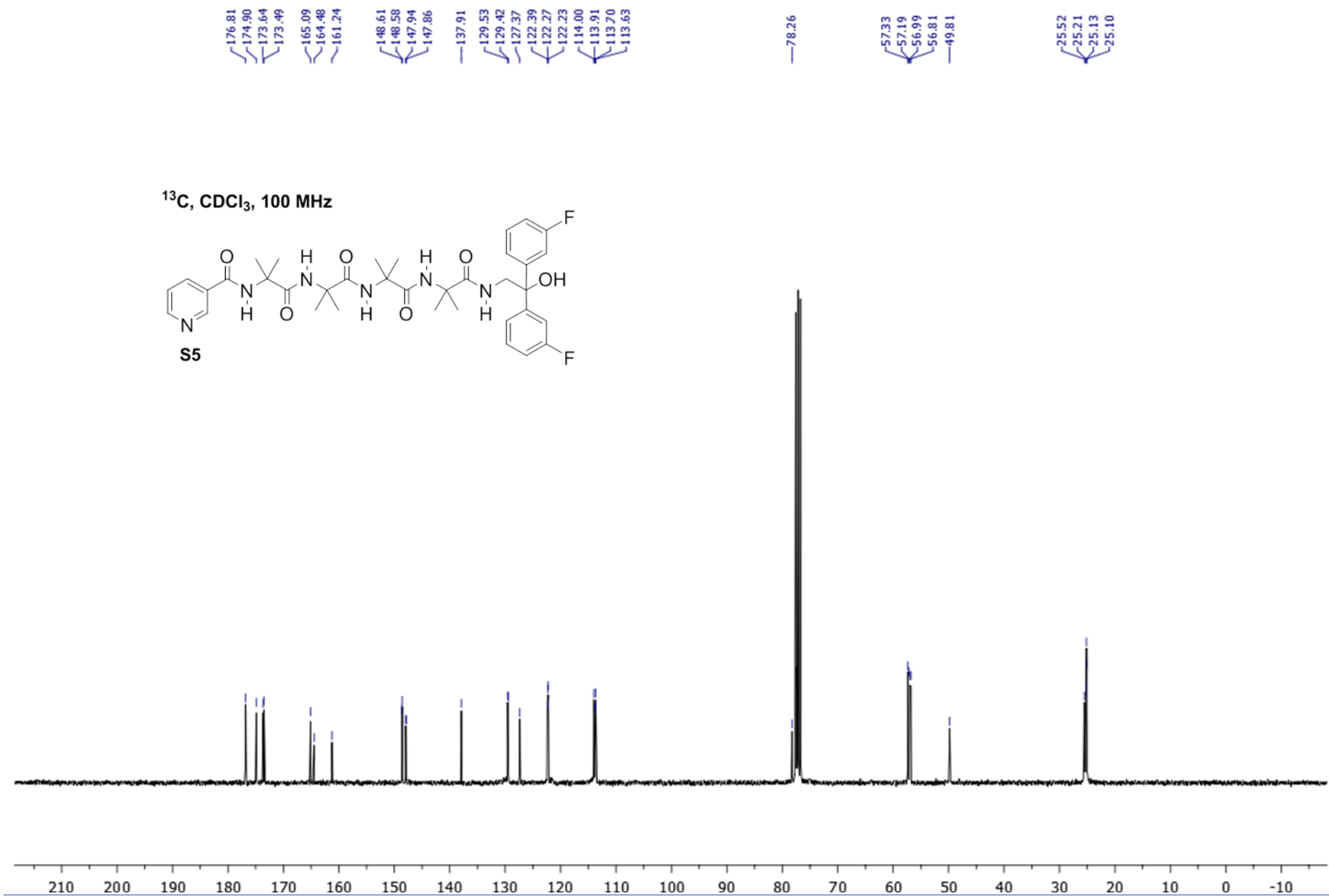




¹H, CDCl₃, 300 MHz

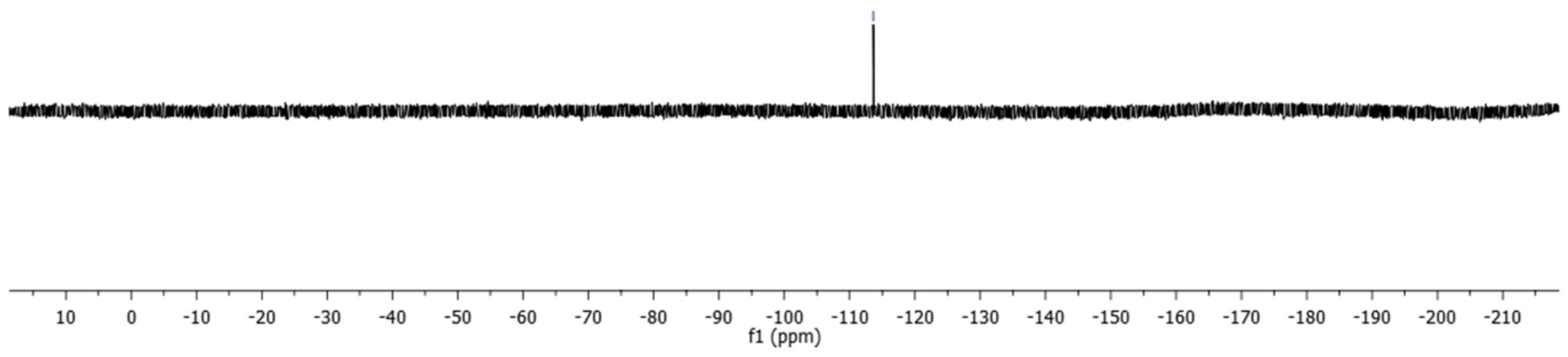
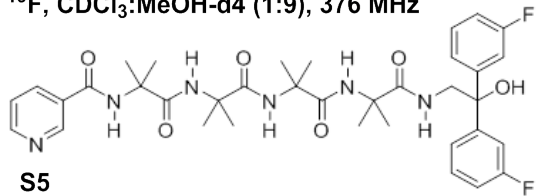






113.63

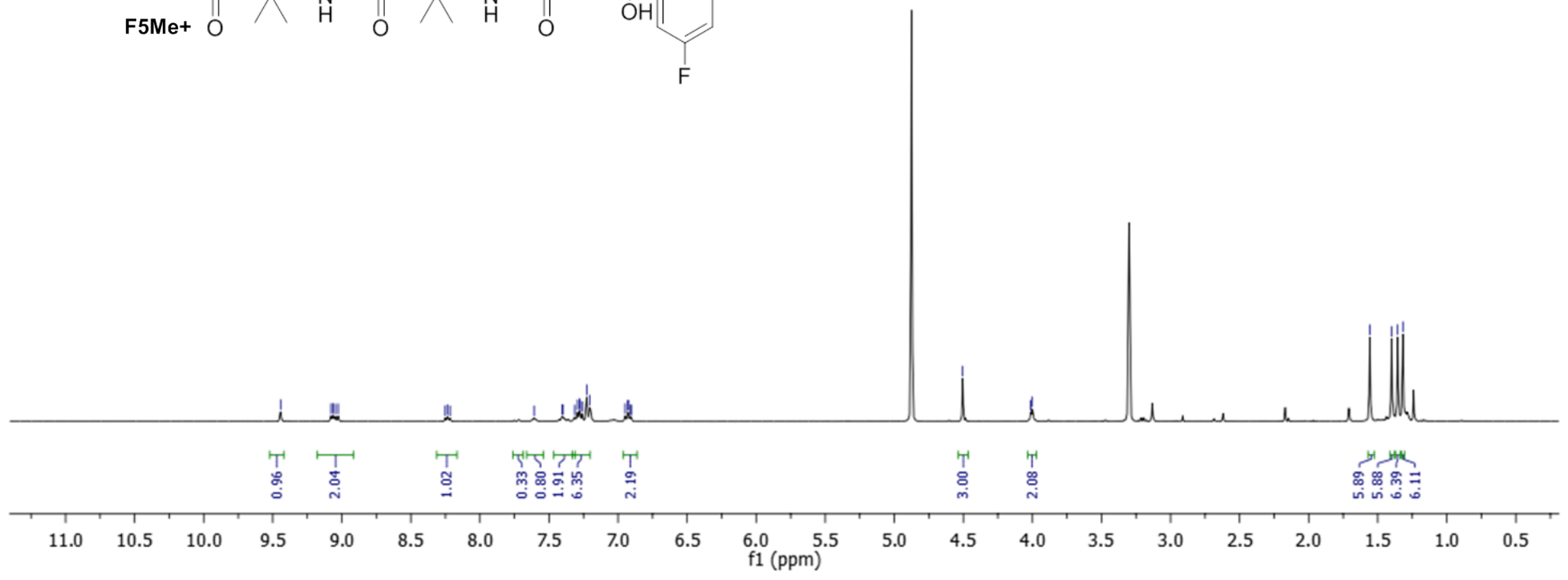
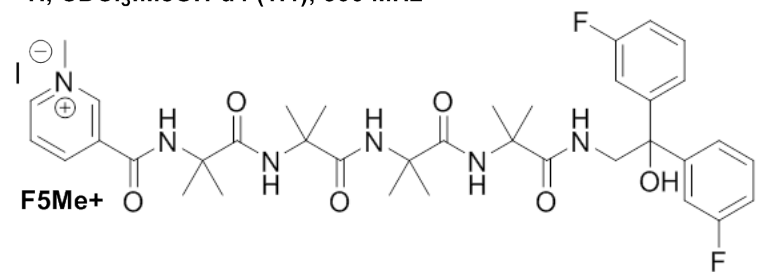
^{19}F , $\text{CDCl}_3:\text{MeOH-d}_4$ (1:9), 376 MHz

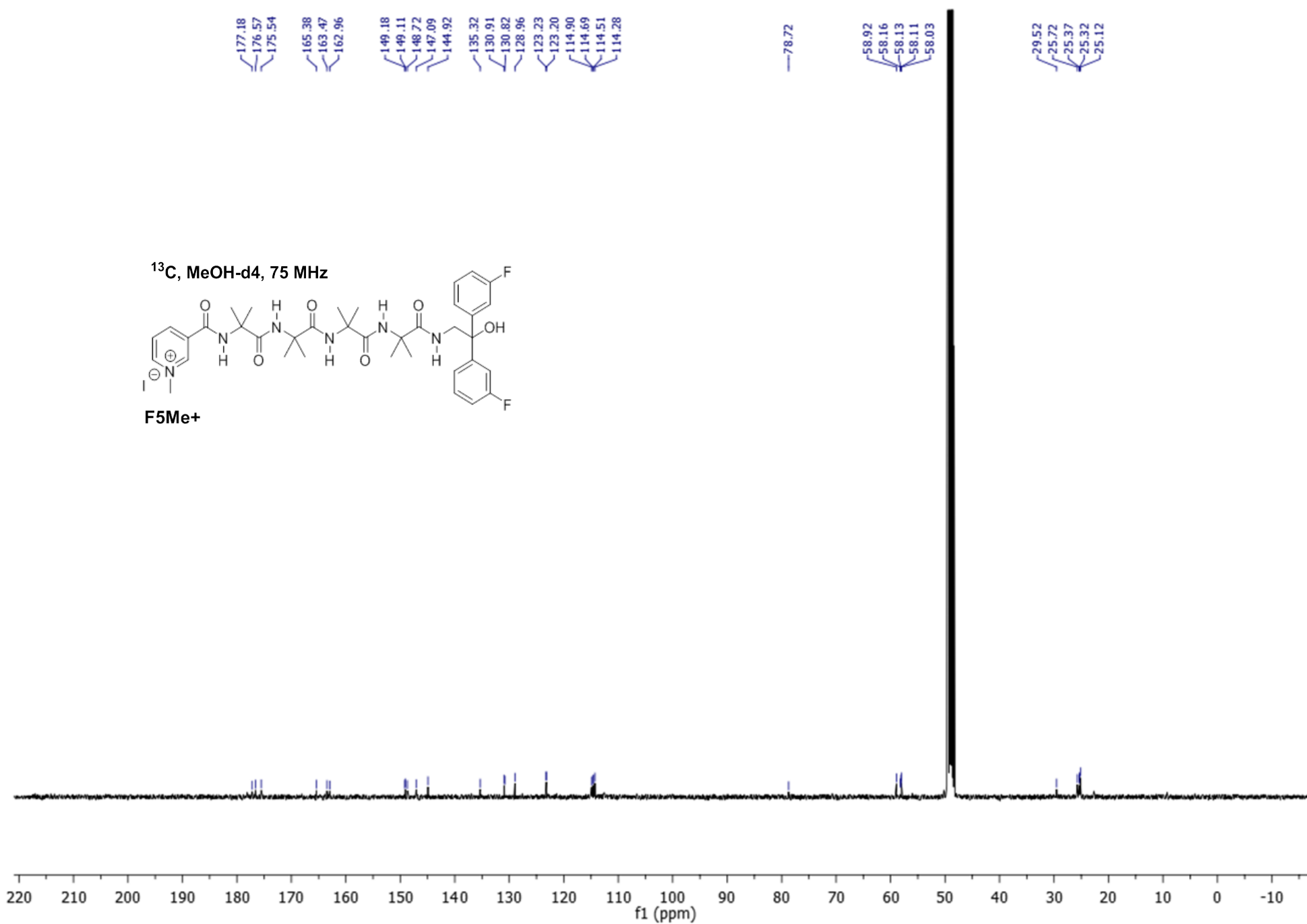


9.44, 9.08, 9.06, 9.05, 9.03, 8.25, 8.24, 8.22, 7.61, 7.41, 7.40, 7.31, 7.29, 7.28, 7.27, 7.26, 7.23, 7.20, 6.95, 6.93, 6.91, 6.90, 4.50, 4.01, 4.00, 1.56, 1.40, 1.36, 1.32

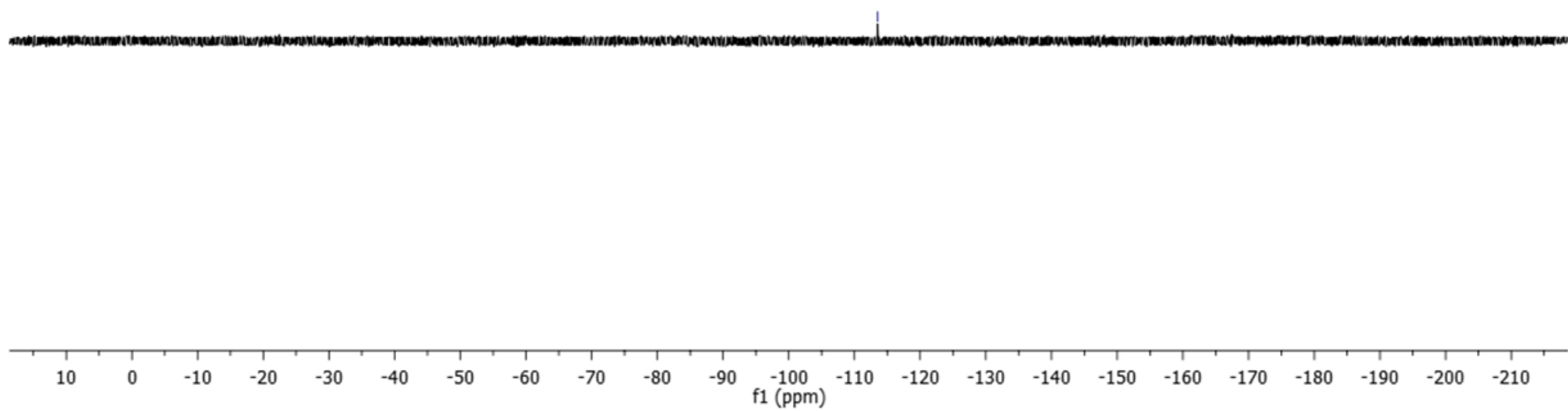
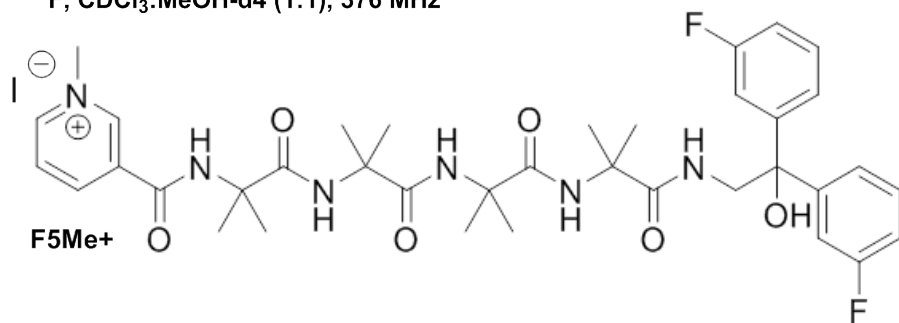


¹H, CDCl₃:MeOH-d₄ (1:1), 300 MHz





¹⁹F, CDCl₃:MeOH-d₄ (1:1), 376 MHz



8.5214
8.5110
7.7407
7.7363
7.7214
7.7171
7.7023
7.6979
7.3811
7.2882
7.2778
7.2693
7.2599
7.2445
7.1363
7.1142

3.7776

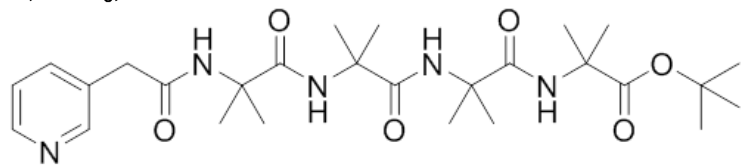
1.4880
1.4391
1.4058
1.3593

s s s/s

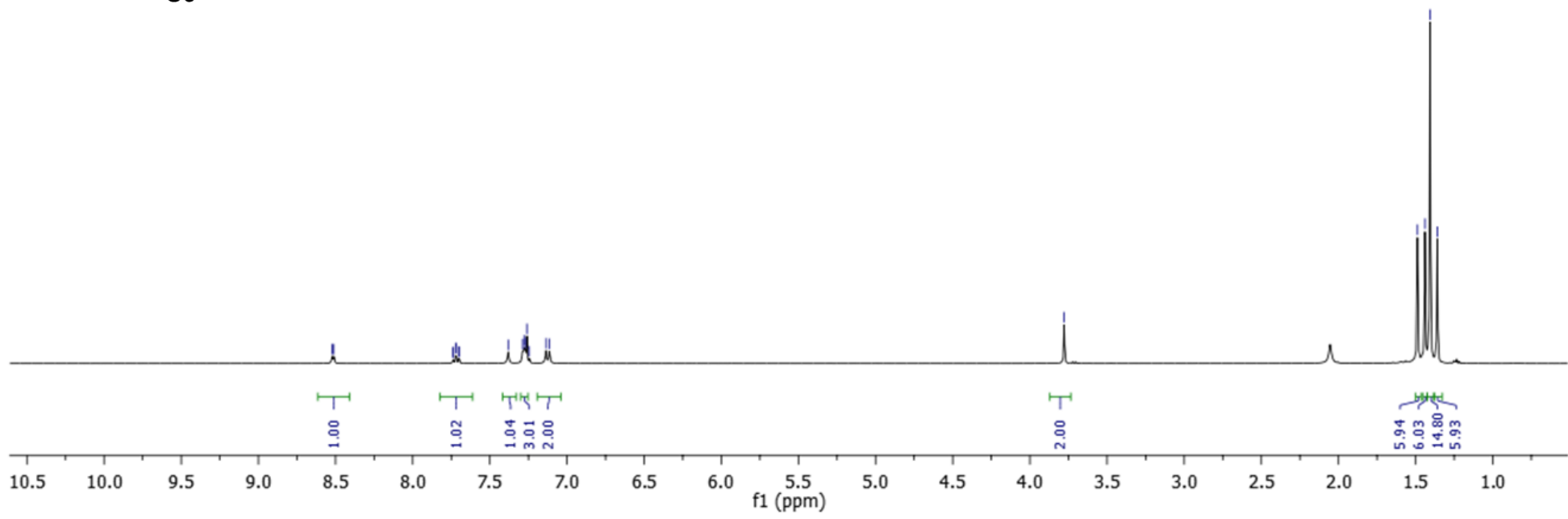
s

s

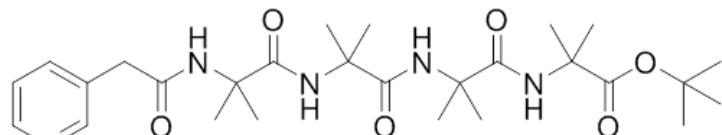
¹H, CDCl₃, 300 MHz



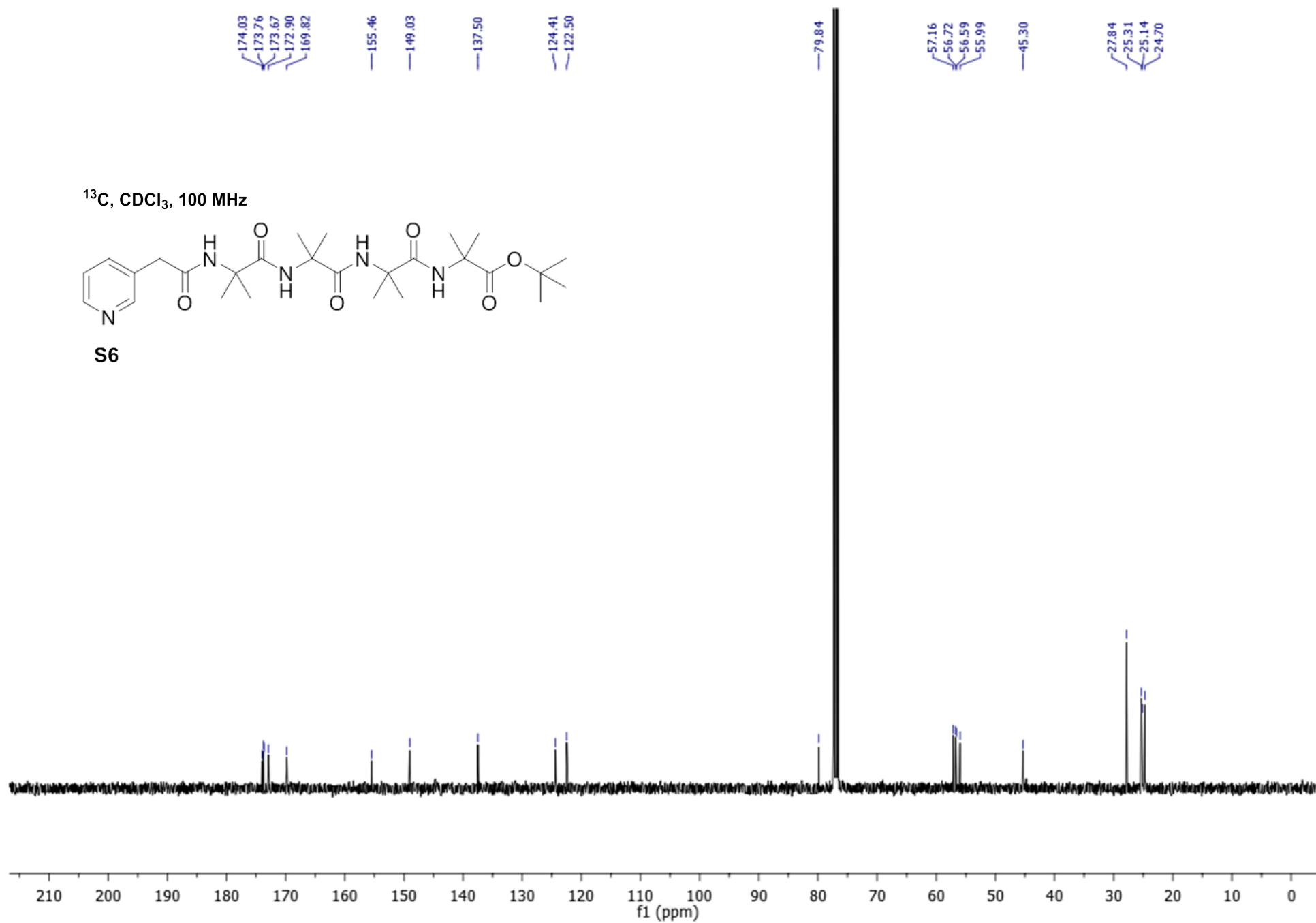
S6

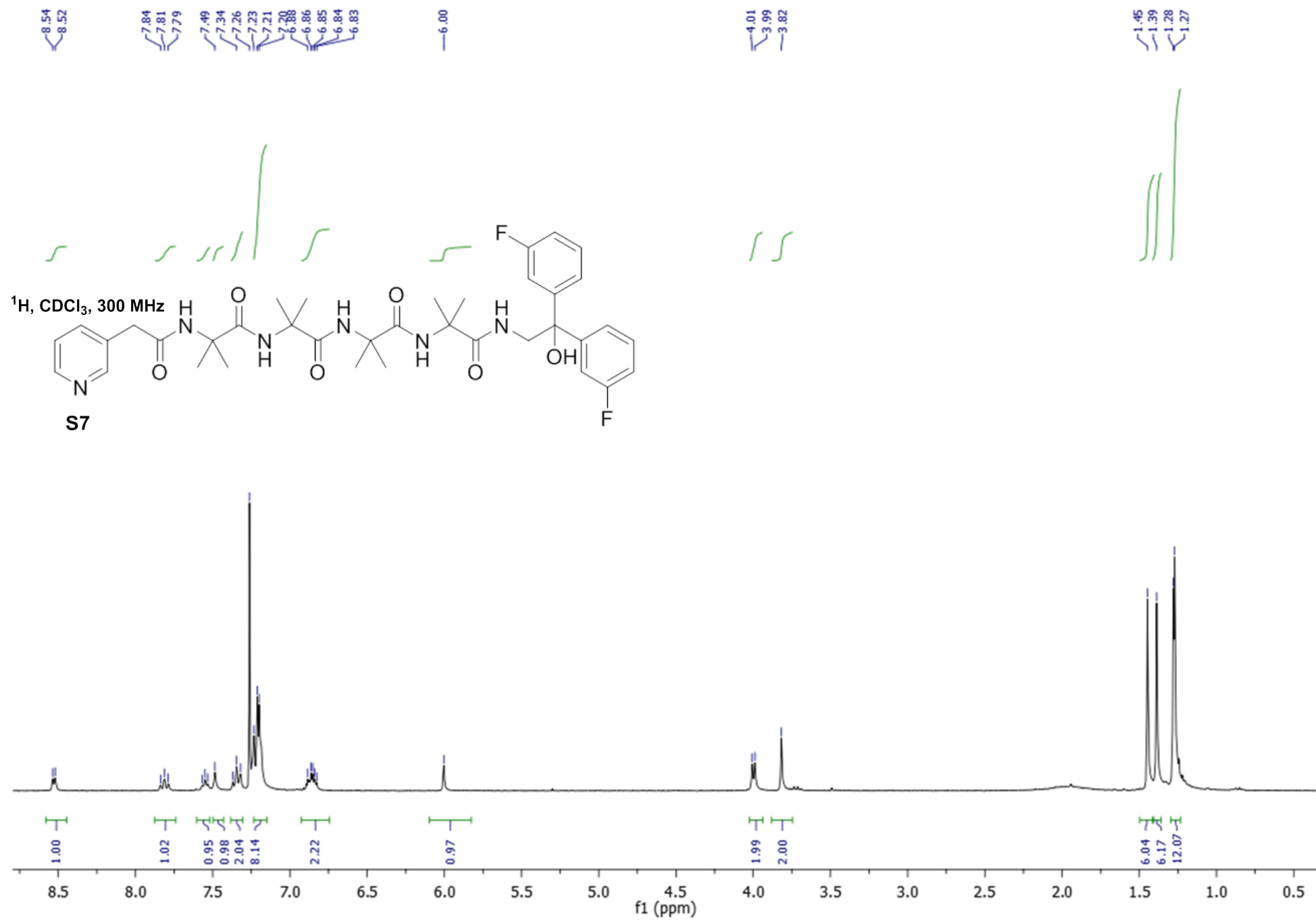


^{13}C , CDCl_3 , 100 MHz

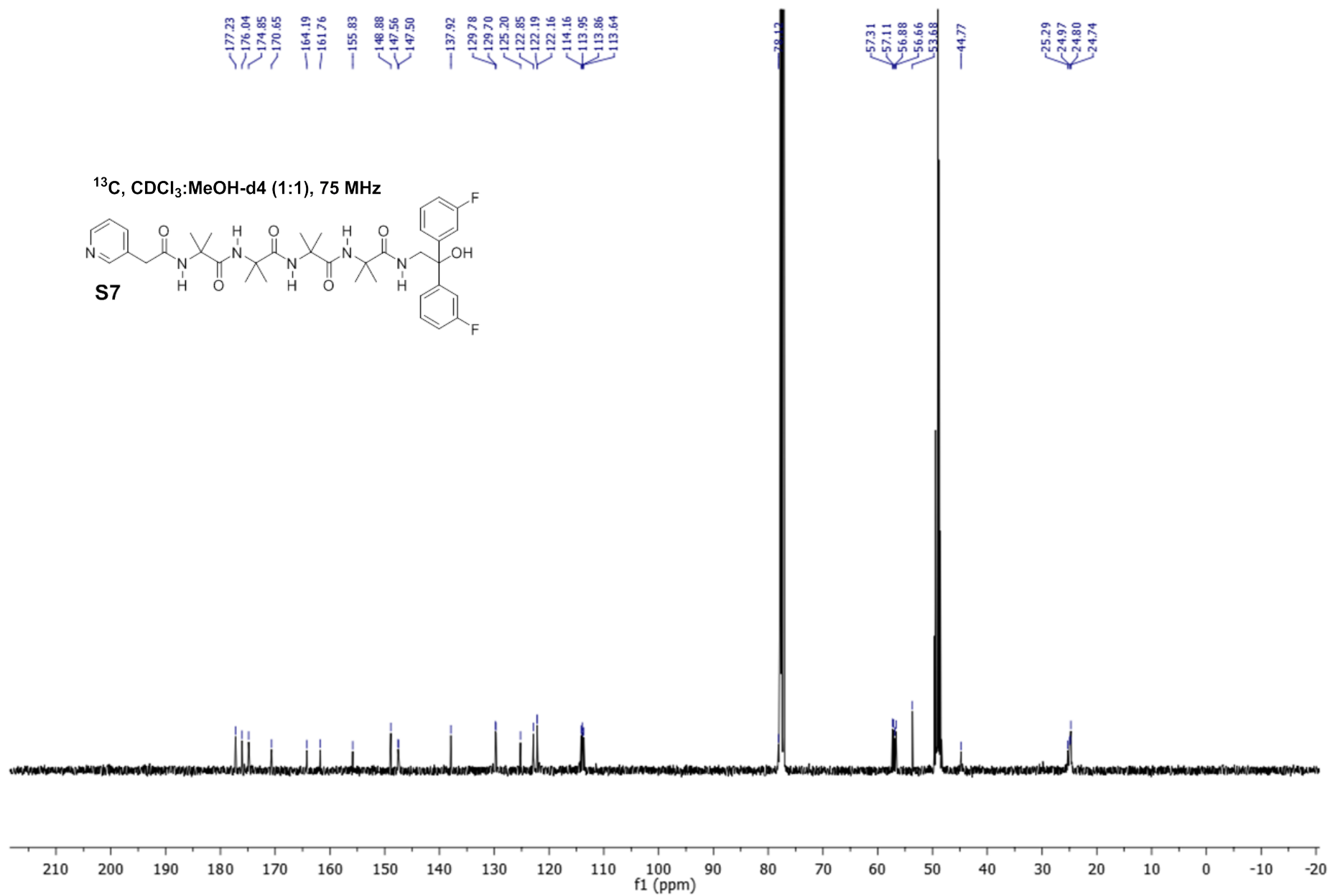
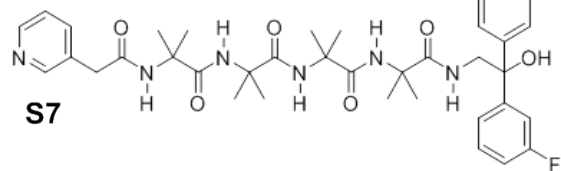


S6

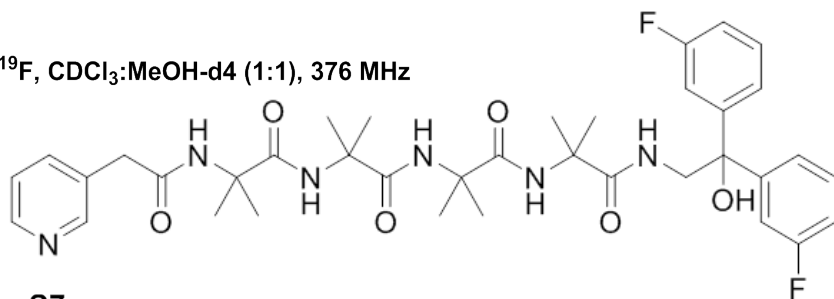




¹³C, CDCl₃:MeOH-d₄ (1:1), 75 MHz

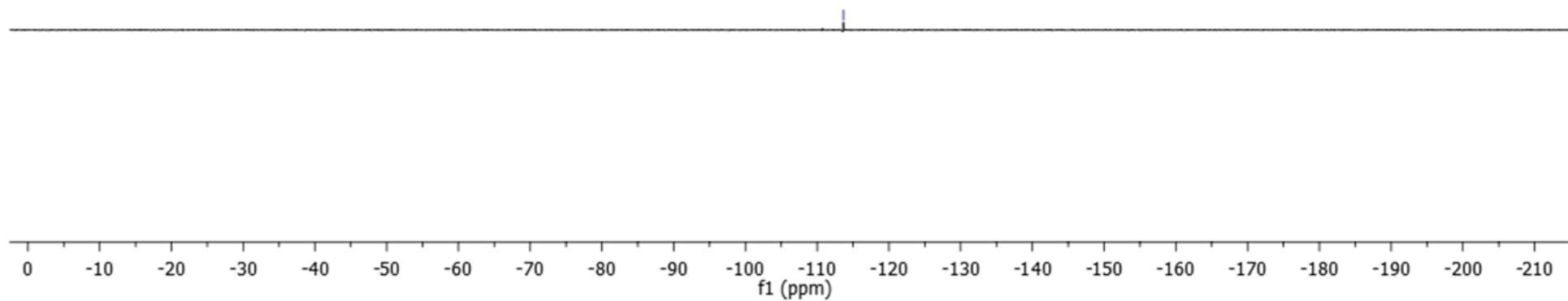


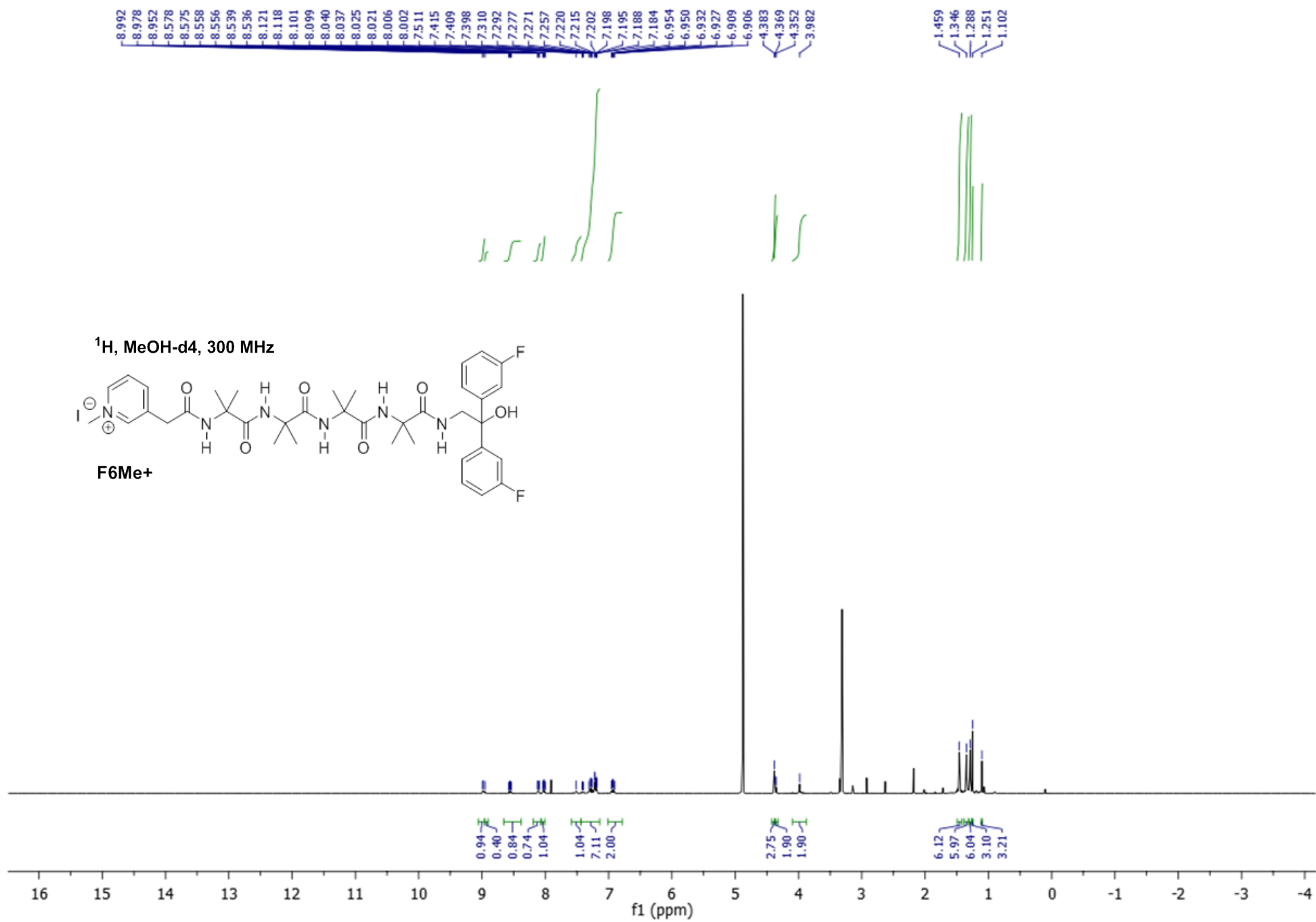
¹⁹F, CDCl₃:MeOH-d₄ (1:1), 376 MHz

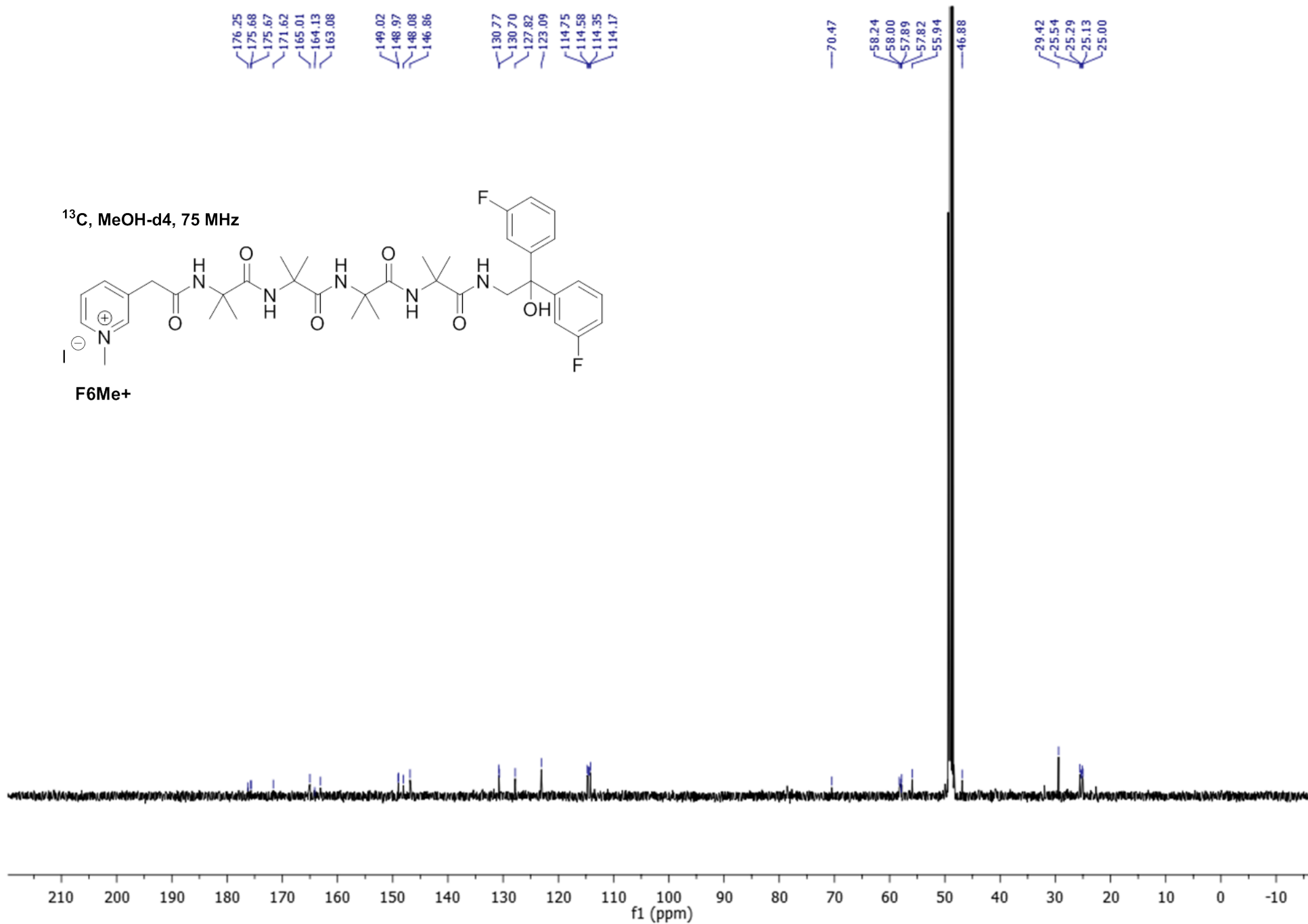


S7

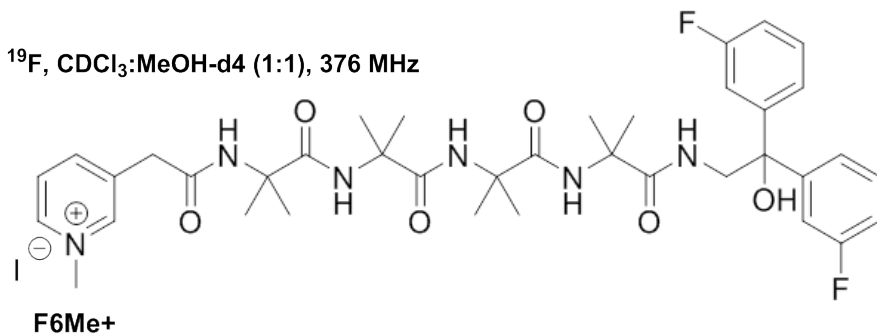
113.67



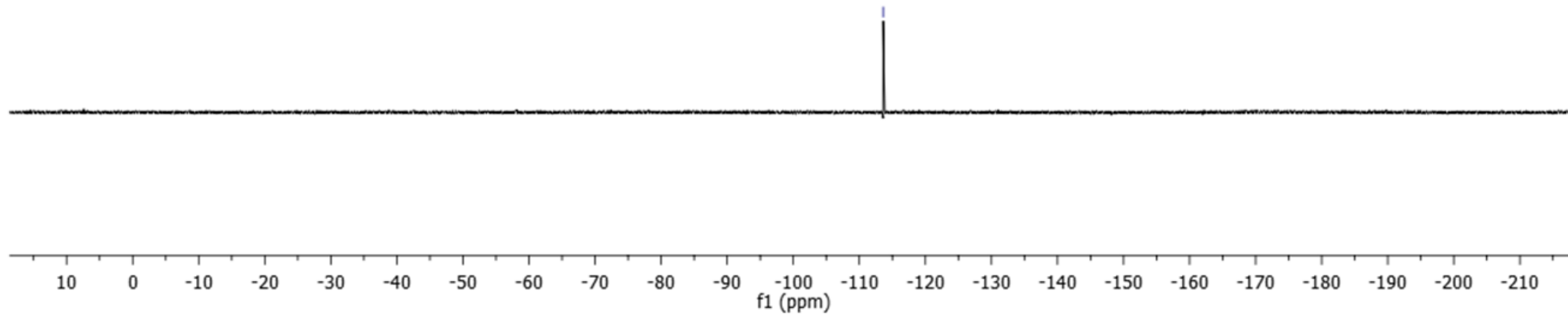




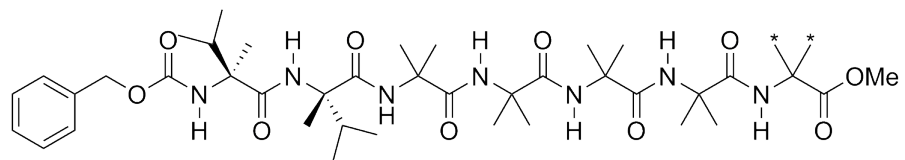
¹⁹F, CDCl₃:MeOH-d₄ (1:1), 376 MHz



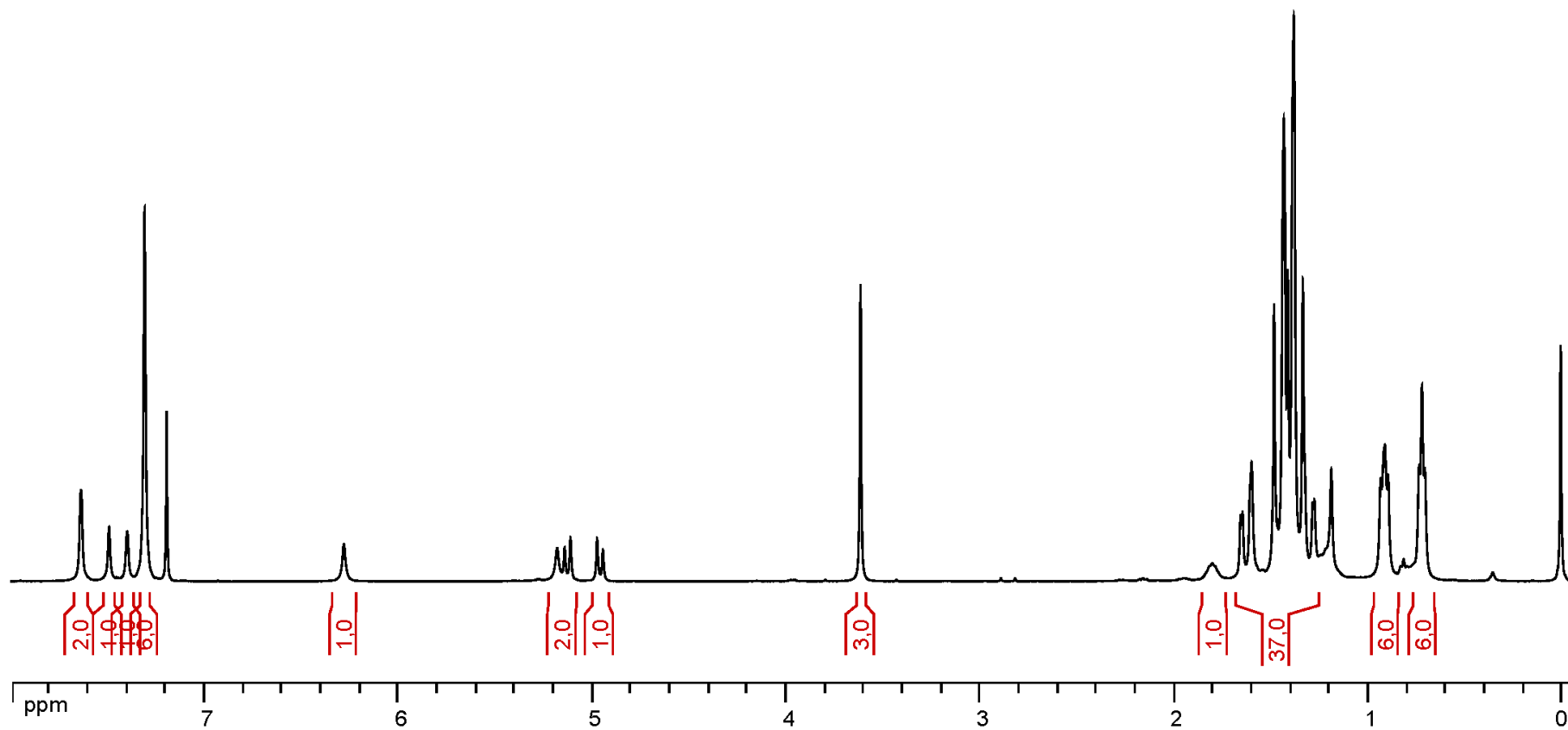
113.62



^1H , CDCl_3 , 400 MHz



S9



¹³C, CDCl₃, 100 MHz

